Physiology in Health and Disease
Published on behalf of the American Physiological Society by Springer

L. Britt Wilson
Richard A. Hoppmann
Floyd E. Bell
Victor V. Rao *Editors*

Understanding Physiology with Ultrasound

american physiological society

MOREMEDIA

Springer

Physiology in Health and Disease

Published on behalf of The American Physiological Society by Springer

This book series is published on behalf of the American Physiological Society (APS) by Springer. Access to APS books published with Springer is free to APS members.

APS publishes three book series in partnership with Springer: *Physiology in Health and Disease* (formerly *Clinical Physiology*), *Methods in Physiology*, and *Perspectives in Physiology* (formerly *People and Ideas*), as well as general titles.

Springer Nature More Media App

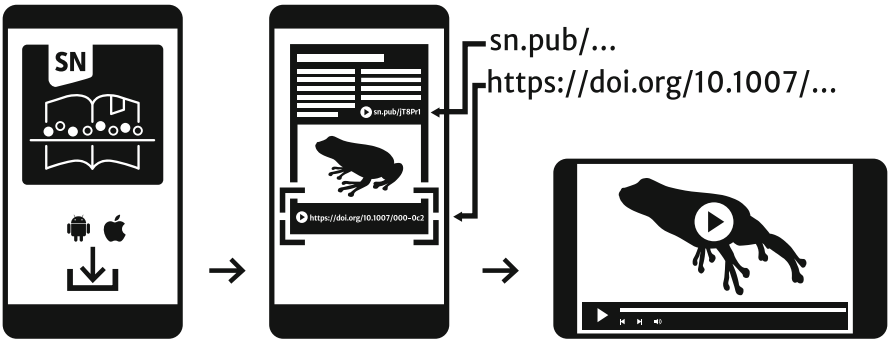

Support: customerservice@springernature.com

L. Britt Wilson • Richard A. Hoppmann •
Floyd E. Bell • Victor V. Rao
Editors

Understanding Physiology with Ultrasound

Springer

american physiological society

Editors
L. Britt Wilson
Department of Pharmacology, Physiology, and Neuroscience
University of South Carolina School of Medicine
Columbia, SC, USA

Richard A. Hoppmann
Ultrasound Institute
University of South Carolina School of Medicine
Columbia, SC, USA

Floyd E. Bell
Department of Radiology
Ultrasound Institute, University of South Carolina School of Medicine
Columbia, SC, USA

Victor V. Rao
Point-of-Care Ultrasound Certification Academy, Inteleos
Rockville, MD, USA

This work contains media enhancements, which are displayed with a "play" icon. Material in the print book can be viewed on a mobile device by downloading the Springer Nature "More Media" app available in the major app stores. The media enhancements in the online version of the work can be accessed directly by authorized users.

ISSN 2625-252X ISSN 2625-2538 (electronic)
Physiology in Health and Disease
ISBN 978-1-0716-1862-2 ISBN 978-1-0716-1863-9 (eBook)
https://doi.org/10.1007/978-1-0716-1863-9

Published on behalf of The American Physiological Society by Springer

This Springer imprint is published by the registered company Springer Science+Business Media, LLC, part of Springer Nature.
The registered company address is: 1 New York Plaza, New York, NY 10004, U.S.A.

To Lizzie and all the wonderful students I've had the privilege to interact with.
—From L. Britt Wilson
To Anne, my wife, and to all those who were called to be teachers.
—From Richard A. Hoppmann
To Melissa, Barrett, Bridget, my parents, my sisters, and my teachers.
—From Floyd E. Bell, III
To my parents, my friends, and my students.
—From Victor V. Rao

Contents

Chapter 1
Using Ultrasound to Teach Physiology: An Introduction

Richard Hoppmann, L. Britt Wilson, and Jeanette Mladenovic

Physiology forms the foundation for understanding the life sciences and for the practice of medicine. An understanding of physiological concepts and principles is essential for knowing how the body works and how it responds when disease or injury adversely affects normal function. Ultrasound can be a safe and effective visual and interactive learning tool to teach physiology and pathophysiology. For those entering healthcare professions, ultrasound can eventually serve as a valuable clinical tool in medical practice to improve patient care.

The ability to look inside the living body with ultrasound is proving to be a learning experience that captivates and motivates learners at all levels of education to better understand the physiology of human life. An estimate of the rising level of interest in ultrasound education in general and in physiology education in particular can be appreciated from the number of publications reported in PubMed by year shown in Fig. 1.1. A gradual rise in publications in the 1990s and early 2000s has reached exponential growth in recent years. The interest in ultrasound as a teaching tool will likely continue to rise as the technology of ultrasound continues to advance and the number of educational and medical applications of ultrasound continues to increase.

This introductory chapter will briefly review the evolution of ultrasound technology, the emergence of point-of-care ultrasound, and the introduction of ultrasound

R. Hoppmann (✉)
University of South Carolina School of Medicine, Columbia, SC, USA
e-mail: Richard.Hoppmann@uscmed.sc.edu

L. B. Wilson
Department of Pharmacology, Physiology, and Neuroscience, University of South Carolina School of Medicine, Columbia, SC, USA
e-mail: Britt.Wilson@uscmed.sc.edu

J. Mladenovic
Foundation for International Medical Education and Research, Philadelphia, PA, USA
e-mail: JMladenovic@faimer.org

L. B. Wilson et al. (eds.), *Understanding Physiology with Ultrasound*, Physiology in Health and Disease, https://doi.org/10.1007/978-1-0716-1863-9_1

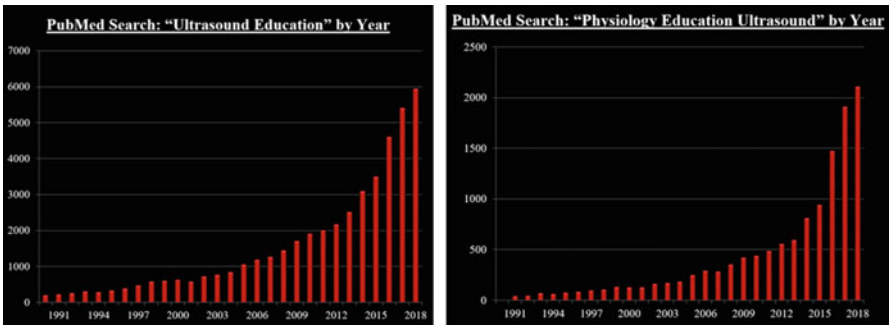

Fig. 1.1 Left panel: Pubmed search by year for Ultrasound Education. Right panel: Pubmed search by year for Physiology Education Ultrasound

into life science education. The primary advantages of using ultrasound as a tool for teaching physiology will also be discussed.

1.1 Ultrasound Technology, Point-of-Care Ultrasound, and Ultrasound in Education

Real-time diagnostic ultrasound was introduced into medical practice in the mid-1960s. At that time machines were large, relatively difficult to maneuver and use, and produced images of much inferior quality compared to today's high-resolution digital images. Over the next three decades there have been significant improvements in image quality, processing speed, ease of use, and functionality such as color and spectral Doppler. During this period, ultrasound was primarily used by radiologists, cardiologists, obstetricians and gynecologists, and sonographers.

In the late 1990s, portable hand-carried ultrasound systems were developed that ushered in the era of point-of-care ultrasound or POCUS. Point-of-care ultrasound can be defined as ultrasonography performed and interpreted by the clinician at the bedside. In general, these examinations are not comprehensive ultrasound examinations as typically performed by a department of radiology. Rather, they are examinations focused or limited to answering specific questions at the point of care, where the clinical information is needed to make diagnostic or treatment decisions such as trying to determine whether a patient with shortness of breath has heart failure or a patient with abdominal pain has gallstones.

As can be seen in Fig. 1.2, similar to the PubMed graphs of ultrasound education, POCUS publications have also risen exponentially.

The specialties of emergency medicine and surgery have led the way in developing point-of-care ultrasound applications, conducting point-of-care ultrasound research, developing educational material and training guidelines, and establishing best medical practices for physicians using point-of-care ultrasound.

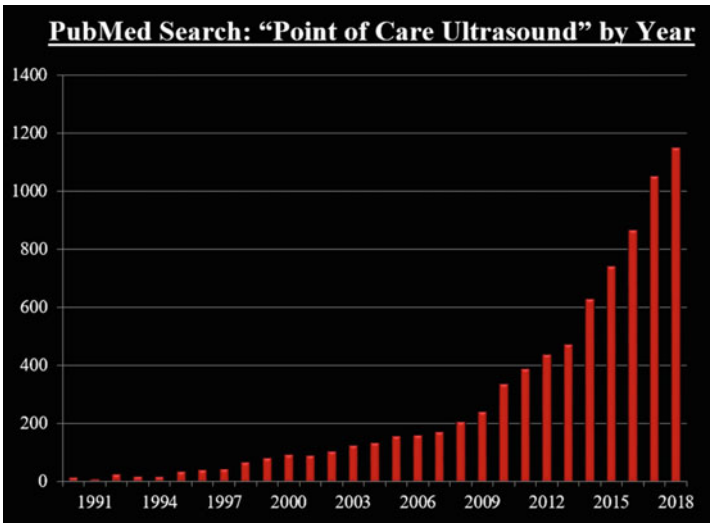

Fig. 1.2 Pubmed search by year for Point-of-care Ultrasound

In the mid-1990s, articles began to appear in the medical literature on using ultrasound to teach medical students anatomy, physiology, and physical diagnosis. In 2006, the University of South Carolina School of Medicine introduced an integrated ultrasound curriculum (iUSC) across all 4 years of medical school. Since that time, a number of other medical schools have initiated integrated ultrasound curricula and many others have introduced ultrasound into basic science education and clinical rotations, most frequently in anatomy courses and emergency medicine clerkships.

Interest in ultrasound as a teaching tool can now be seen in life science education at all levels and across a broad spectrum of the health professions. Ultrasound has been introduced into middle and high school science education, university undergraduate and graduate education, nursing and physician assistant education, medical resident postgraduate education, and practicing healthcare provider continuing medical education (CME). Figure 1.3 captures the sense of excitement and wonder of new medical students scanning for the first time.

1.2 Advantages of Using Ultrasound to Teach Physiology

Below is a list of some of the primary advantages of using ultrasound to teach physiology. Each of these will be discussed.

1. Ultrasound is a safe and relatively easy to learn imaging modality to visualize anatomy and see dynamic changes within the body illustrating the physiology of the human body.

Fig. 1.3 A medical student ultrasound scanning laboratory session during orientation week of medical school

2. Ultrasound can be used in multiple teaching formats from enhancing lectures with ultrasound images to hands-on, interactive, self-directed learning exercises.
3. Ultrasound is well-suited for a competency-based medical education model.
4. Ultrasound facilitates integration across life science and medical curricula.
5. Ultrasound introduces the healthcare learner to a future clinical practice tool.

1.2.1 Safety and Ease of Learning Ultrasound to Visualize Anatomy and Assess Physiology/Function

As an imaging modality, ultrasound is very safe. In creating images, ultrasound does not use the ionizing radiation of x-rays or computed tomography (CT) and thus avoids their toxicity, especially the increased risk of cancer. Because of its safety and clinical value, the American Institute of Ultrasound in Medicine has encouraged medical practitioners to consider ultrasound as their "First" choice of imaging across a wide range of clinical situations. The safety profile of ultrasound extends to users, models, and standardized patients during ultrasound teaching sessions. Thus, learners are able to look inside the body beneath the skin to study "living physiology" with virtually no risk to themselves or those being scanned.

Modern day digital technology and artificial intelligence applications have allowed even novice learners and instructors to capture quality ultrasound images early in their exposure to ultrasound scanning. In real-time scanning, artificial intelligence software can label anatomical structures, as well as display probe instructions on the ultrasound monitor such as rotate the probe in a specific direction to help the learner capture quality images (Fig. 1.4).

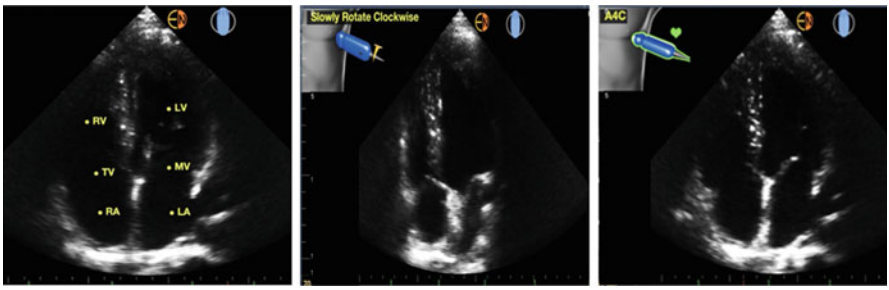

Fig. 1.4 Apical 4 chamber views of the heart with artificial intelligence assistance. Left panel: anatomical structures labeled—left ventricle (LV), mitral valve (MV), left atrium (LA), right ventricle (RV), tricuspid valve (TV), and right atrium (RA). Middle panel: instructions to rotate the probe clockwise for a better image. Right panel: the result of rotating the probe clockwise

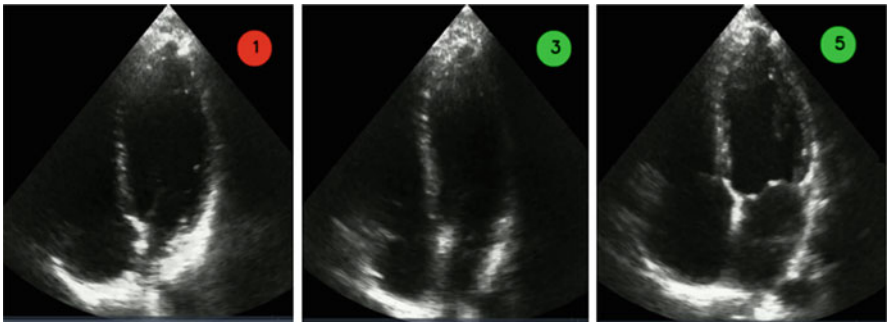

Fig. 1.5 Apical 4 chamber view evaluated by artificial intelligence. Left panel: a poor image with a score of 1. Middle panel: an acceptable image with a score of 3. Right panel: an excellent image with a score of 5

In real time, the quality of the image as determined by artificial intelligence can be displayed on the screen using an image scale such as 1 for a poor image, 3 for an acceptable image, and 5 for excellent image (Fig. 1.5). Any image rated 3 or higher would be considered acceptable for accurate image interpretation and physiological measurements.

Laptop and even hand-held ultrasound devices are now able to compute a number of physiological measurements such as the volume of blood ejected from the left ventricle of the heart with each heartbeat, i.e. the stroke volume. In addition, the percentage of blood ejected from the left ventricle with each heartbeat, called ejection fraction, can be determined. The stroke volume and the heart rate can be used to calculate the volume of blood pumped by the heart in a unit of time or the cardiac output (Fig. 1.6).

This ease of capturing quality ultrasound images and calculating accurate cardiac hemodynamic measurements with artificial intelligence allow teachers and students to focus more on the physiological principles revealed by ultrasound than the task of capturing acceptable images. This represents a tremendous advance in ultrasound

Fig. 1.6 Display of hand-held ultrasound computation of ejection fraction (EF), stroke volume (SV), cardiac output (CO), and heart rate (HR). Computations were made based on the left ventricular end diastolic volume (EDV) and the end systolic volume (ESV) from an ultrasound apical 4 chamber view (A4C) and an ultrasound apical 2 chamber view (A2C) and a single lead electrocardiogram

technology applied to education that should accelerate adoption of ultrasound in physiology education at all levels and spur educational research in this area. Much of the work with AI and ultrasound has focused on the cardiovascular system, but the advances are now being applied to other organ systems such as the respiratory, genitourinary, and reproductive systems.

It should be noted that because of its safety profile, portability, low cost, and clinical value, ultrasound has become the most common imaging modality in the world. Thus, a familiarity with ultrasound and basic image interpretation, even if one is not performing ultrasound scans, will likely serve teachers and students of the life sciences and health professions very well into the foreseeable future.

1.2.2 Ultrasound Use in Multiple Teaching Formats

Ultrasound can be readily adapted to teaching physiology in many formats and settings. Ultrasound images and loops can be used as lecture material to help students better visualize and understand the dynamic aspects of physiology, such as the cardiac cycle, vascular flow, lung movement, joint movement, and even the neuro-muscular components of the knee jerk reflex from stimulation with a reflex hammer. In addition, brief live ultrasound demonstrations projected onto a large screen can be included at the start or end of a lecture to bring physiology principles to life and stimulate discussion.

These ultrasound examples as well as many others can be used for small group hands-on ultrasound scanning laboratory sessions. Student laboratory sessions can be

taught by faculty, sonographers, and others with basic skills in ultrasound such as upper level students and medical residents. In addition, both team teaching and peer-peer teaching have been successfully incorporated into small group ultrasound instruction.

Ultrasound scanning is a visual, hands-on, interactive learning experience. The education literature has consistently reported high degrees of student engagement and student satisfaction when ultrasound scanning is incorporated into courses and curricula. Studies that have objectively assessed learning with ultrasound show that students acquire very good levels of ultrasound knowledge and skill, while learning subject content very well across a variety of basic science and clinical topics, including physiology.

In recent years, education accrediting bodies, especially those in the health sciences, have incorporated in their accreditation standards the need for student self-directed learning opportunities in order to encourage the development of life-long learning habits. Ultrasound offers a number of opportunities for self-directed learning such as online learning modules and videos, ultrasound simulation, and open informal laboratory scanning sessions.

There are numerous quality ultrasound learning modules and scanning videos available online. Many of these are Open Access such as those offered on the Society of Ultrasound in Medicine Education website.

Advances in ultrasound simulation have contributed significantly to self-directed learning of ultrasound. Figure 1.7 shows a student independently working on a simulator that displays the ultrasound image being captured, the anatomical slice of the ultrasound beam, and the probe position. Scanning tips are also offered on the monitor if requested by the learner. In addition, the student's performance for both the session as well as progress across multiple sessions can be graphically displayed and recorded.

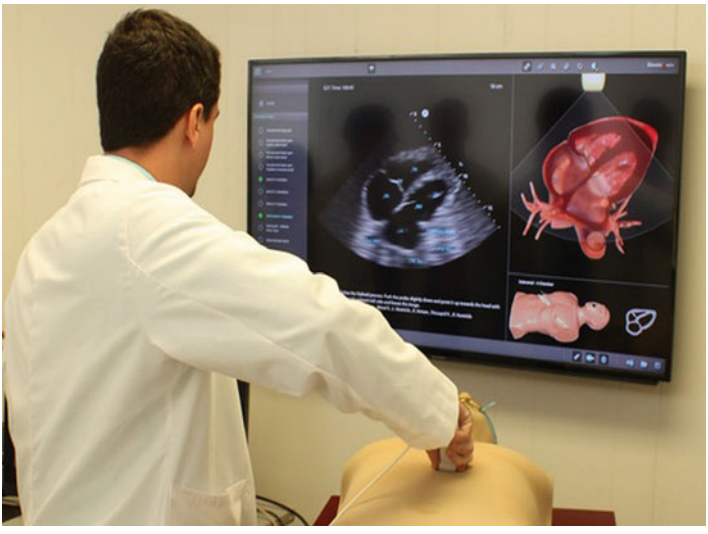

Fig. 1.7 Student using a self-directed ultrasound simulator

Open laboratory scanning sessions, which are voluntary sessions offered in addition to required scheduled laboratory sessions, add considerable flexibility of scheduling for students and provide additional hands-on scanning time for students to practice their scanning skills. In addition, ultrasound devices with artificial intelligence can assist learners in developing their ultrasound skills. Students can attempt to capture quality images, identify anatomical structures, compute physiological measurements, and subsequently activate the artificial intelligence features to compare their results to those produced by artificial intelligence. Thus, the AI augmented devices become excellent self-directed learning tools. The potential for such devices in the teaching of physiology are just beginning to be explored but hold considerable promise for independent, self-directed learning. Artificial intelligence will likely play an ever-increasing role in making ultrasound a widely accessible teaching tool for physiology.

1.2.3 Competency-Based Medical Education (CBME)

In the health professions, competency-based medical education (CBME) is becoming the preferred model of education and has been incorporated into accreditation standards across the globe. CBME uses an outcomes approach rather than a time-based approach for the design, implementation, student assessment, and evaluation of education programs based on a framework of well-defined competencies. Competency can be defined as what a health professional is qualified to do and includes the appropriate knowledge, skills, behaviors and attitudes of practice. Competencies should be observable and measurable. Competencies can be further broken down into milestones that are observable steps used to assess and document a learner's progress toward a given competency.

Physiology and ultrasound knowledge, as well as skill can be assessed using a number of objective methods such as multiple-choice examination questions, objective structured clinical exams (OSCE), and high-fidelity simulation with assessment software capabilities. In addition, cloud-based image review portals can be used for an objective assessment of a learner's knowledge and skills. Students can submit ultrasound images they have obtained either in the ultrasound laboratory or on clinical clerkships via the image portal for assessment and feedback. Student electronic portfolios of results of their assessments can be used to track a student's progress toward competency in physiology as well as their knowledge and skill of ultrasound.

1.2.4 Integration Across Life Sciences and Medical Curricula

Because of its numerous educational and clinical applications, ultrasound has been successfully used to integrate many foundational basic science topics and clinical experiences across life science and medical curricula. Integration has been broadly

defined operationally as deliberately unifying separate areas of knowledge. This is an approach to education that has been encouraged and even required in educational programs by accrediting bodies in recent years. Ultrasound is being used by a number of medical schools to integrate subject content and skills across courses and clinical clerkships both horizontally and vertically in time. For example, ultrasound can be used to enhance teaching of cardiac anatomy and physiology to first year medical students and cardiac pathology, pathophysiology, and physical examination skills to second year students. Students can then apply this knowledge and skill sets in their clinical clerkships from the primary care clinic to the intensive care unit. Ultrasound clinical experiences in the first 2 years also present opportunities for early clinical exposure in the curriculum. Thus, ultrasound can serve as an early and practical bridge between the basic and clinical sciences.

1.2.5 A Learning Tool That Becomes a Clinical Practice Tool

As a clinical practice tool, ultrasound has been shown to improve patient care, increase patient safety, enhance access to quality care, and reduce healthcare costs. Thus, ultrasound can be considered a learning tool that becomes an excellent clinical practice tool. Students recognize this relationship of a learning tool to a practice tool early in their introduction to ultrasound that results in great interest and motivation to learn ultrasound. This outcome is consistent with adult learning theory that states that learners are more engaged and motivated to learn knowledge and skill they feel will be needed later in their education and/or careers.

Much has happened in recent years to make ultrasound an effective and accessible teaching tool for physiology. Principal among these have been advances in technology, reduced cost of equipment, availability of peer-reviewed literature on ultrasound education, and the growing acceptance of ultrasound as a broadly applicable educational and medical practice tool. As hand-held ultrasound is adopted across almost every level of patient care it can in many ways be thought of as the smart stethoscope of the twenty-first century.

The chapters to follow cover the basics of ultrasound and the application of ultrasound in understanding physiology and pathophysiology in the major organ systems. The final chapter addresses important issues to consider when introducing ultrasound into physiology courses and medical education. Also included are handouts and video scanning instructions for use in ultrasound physiology laboratory exercises.

Further Reading

Barloon TJ, Brown BP, Abu-Yousef MM, Ferguson KJ, Schweiger GD, Erkonen WE, Schuldt SS (1998) Teaching physical examination of the adult liver with use of real-time sonography. Acad Radiol 5(2):101–103

Bell F, Wilson B, Hoppmann R (2015) Using ultrasound to teach medical students cardiac physiology. Adv Physiol Educ 39:392–396

Brauer DG, Ferguson KJ (2015) The integrated curriculum in medical education: AMEE guide no. 96. Med Teach 37:312–322

Brunner M, Moeslinger T, Spieckermann PG (1995) Echocardiography for teaching cardiac physiology in practical student courses. Am J Phys 268(6 Pt 3):S2–S9

Frank JR, Snell LS, Cate OT et al (2010) Competency-based medical education: theory to practice. Med Teach 32:638–645

Hoppmann R, Rao V, Bell F et al (2015) The evolution of an integrated ultrasound curriculum (iUSC) for medical students: 9-year experience. Crit Ultrasound J 7(1):18–33

Liaison Committee on Medical Education (LCME) (2019) Functions and structure of a medical school: standards for accreditation of medical education programs leading to the MD Degree. Washington, DC. http://lcme.org/publications/. Accessed 20 Sep 2020

Lotter C, Hoppmann R, Bailey S et al (2019) A project-based biology unit: star athlete collapses on the football field. Am Biol Teach 81(6):442–448. https://doi.org/10.1525/abt.2019.81.6.442

Moore CL, Copel JA (2011) Point-of-care ultrasonography. N Engl J Med 364:749–757

Teichgräber UK, Meyer JM, Poulsen Nautrup C, von Rautenfeld DB (1996) Ultrasound anatomy: a practical teaching system in human gross anatomy. Med Educ 30(4):296–298

Chapter 2
The Basics of Ultrasound Physics

Floyd E. Bell III and Robert Haddad

2.1 What Is Ultrasound?

Ultrasound is an imaging modality that uses high frequency sound waves to produce images. The frequency of a wave refers to the number of cycles within a period of time. Specifically, 1 hertz (Hz) is 1 cycle/s. Frequency is inversely related to wavelength such that higher frequency waves have shorter wavelengths. The amplitude of a wave refers to the displacement from baseline to peak or baseline to trough. Figure 2.1 illustrates waves with different frequencies.

Ultrasound waves have frequencies greater than 20,000 Hz, which is above the range of human hearing. Figure 2.2 illustrates the range of sound waves. Diagnostic ultrasound typically uses sound waves in the range of 2–15 megahertz (MHz). One MHz is a million Hz.

2.2 How Does Ultrasound Work?

The probe or transducer produces ultrasound waves that typically travel through the skin into the body. These waves then interact with structures in the body. Some of the original waves return back to the probe as echoes. The probe converts the echoes into electrical signals that are processed by the ultrasound machine and displayed as an image on the monitor. The probe alternates between sending out pulses of ultrasound waves and detecting the returning echoes. Transmit time is the length of time during which pulses are sent into the body. Receive time is the length of time

F. E. Bell III (✉) · R. Haddad
University of South Carolina School of Medicine, Columbia, SC, United States
e-mail: Floyd.bell@uscmed.sc.edu; Robert.Haddad@uscmed.sc.edu

L. B. Wilson et al. (eds.), *Understanding Physiology with Ultrasound*, Physiology in Health and Disease, https://doi.org/10.1007/978-1-0716-1863-9_2

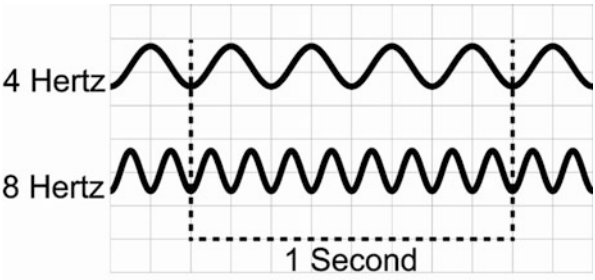

Fig. 2.1 Concept of wave frequency. The 4 Hz wave has 4 cycles within the 1 s time period while the 8 Hz wave has 8 cycles in that time period

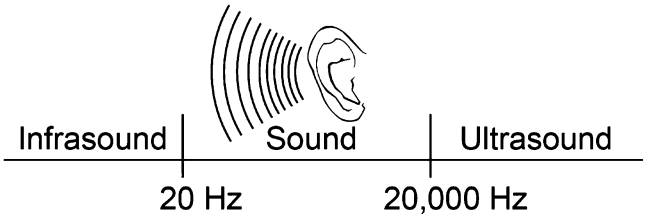

Fig. 2.2 Range of sound. Note that ultrasound frequencies are above the range of human hearing

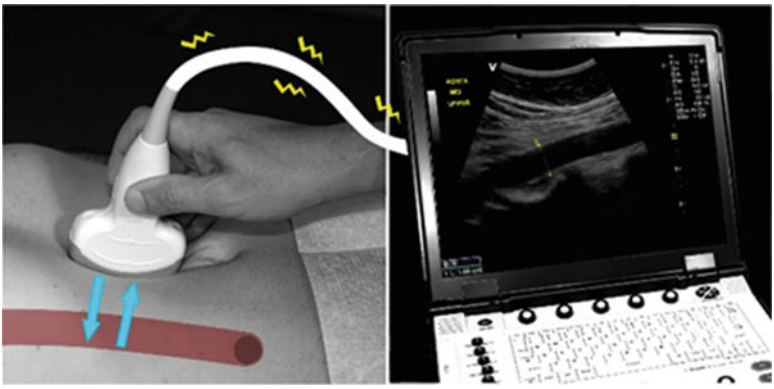

Fig. 2.3 Overview of how ultrasound works. This image shows an ultrasound probe sending waves into the body as well as receiving the returning echoes to be processed and displayed on the monitor

during which the unit "listens" for returning echoes. Figure 2.3 illustrates the concept of ultrasound image production.

This process of sending out ultrasound waves and detecting the returning echoes is analogous to echolocation used by some members of the animal kingdom like bats and dolphins (Fig. 2.4).

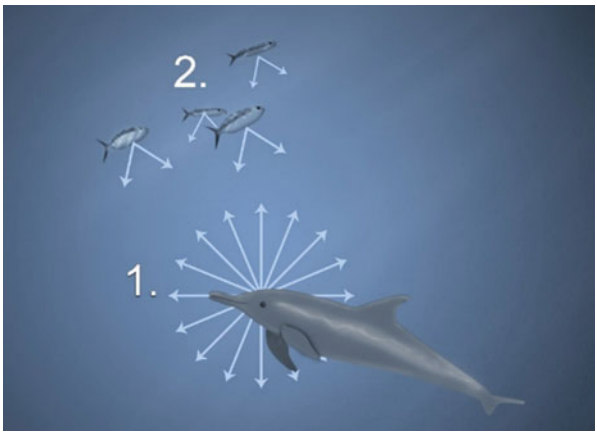

Fig. 2.4 Echolocation. Note the dolphin using echolocation to find fish

2.3 Interactions of Sound Waves in the Body

When ultrasound waves enter the body they can interact with structures in various ways. These all have an effect on the image produced.

2.3.1 Reflection

Reflection is the process whereby the ultrasound waves bounce off a structure and return back toward the probe as echoes. The waves that reach the probe are used to create an image. Among those, the ones that return on a course perpendicular to the probe create the most accurate image of the structure of interest. Factors that influence reflection are angle of incidence of the ultrasound beam as well as the intrinsic acoustic impedance of the tissues being imaged (see below).

Ultrasound waves coursing from the probe toward a target are called incident waves. Those returning from the target to the probe are called reflected waves. The angle that a reflected wave leaves a target (angle of reflection) equals the angle that an incident wave strikes a target (angle of incidence). These angles are illustrated in Fig. 2.5a.

Reflection back to an ultrasound probe is greatest when incident sound waves strike a structure in a perpendicular fashion as illustrated in Fig. 2.5b. If incident waves strike a structure obliquely, they are reflected in an oblique manner. Depending upon the angle, some of the reflected waves may not return to the probe. Therefore they will not contribute to image production.

Acoustic impedance is an intrinsic property of a tissue that can be thought of as the resistance a tissue offers to an ultrasound beam attempting to pass through it. Specifically, it is a product of tissue density and propagation speed through the tissue. In order for echoes to be produced, the ultrasound waves have to encounter

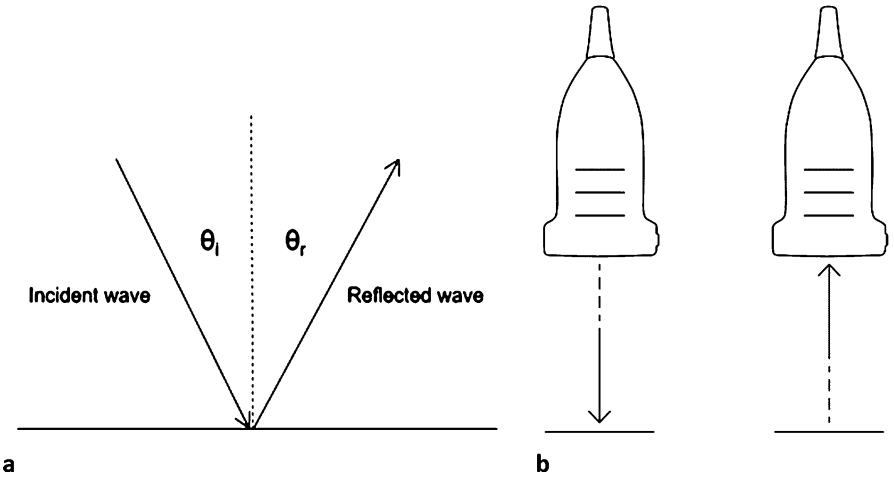

Fig. 2.5 Reflection. (**a**) Angle of incidence (θ_i) equals the angle of reflection (θ_r). (**b**) This figure demonstrates an incident wave traveling in a perpendicular course to the target and the reflected wave traveling in a perpendicular course back to the probe

tissues with different acoustic impedances. Reflection increases as the difference in acoustic impedance increases. When the difference is minimal, most of the ultrasound beam is transmitted through to deeper structures. When the difference is very large, most of the ultrasound beam is reflected.

2.3.2 Scatter

When the ultrasound waves encounter an irregular surface, they are diffusely reflected in multiple directions. This process called scatter is shown in Fig. 2.6. A scattered wave either does not reach the probe or contacts it at a location other than where the original wave left the probe. This process of scatter weakens the returning echo signal and degrades detail of images.

2.3.3 Refraction

In addition to reflection, ultrasound waves encountering an interface at an oblique angle can undergo further transmission through the tissues. When they are transmitted they change direction in a process called refraction. The angle of refraction is related to the difference in the speed of the waves through the two different tissues at that interface. The process of refraction in shown in Fig. 2.7.

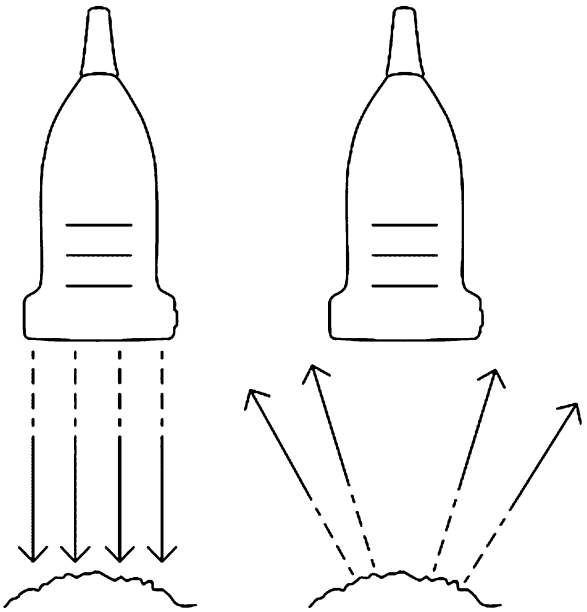

Fig. 2.6 Scatter. This figure demonstrates the process of scatter where incident ultrasound waves are deflected by the irregular surface. Some of these waves do not return back to the probe

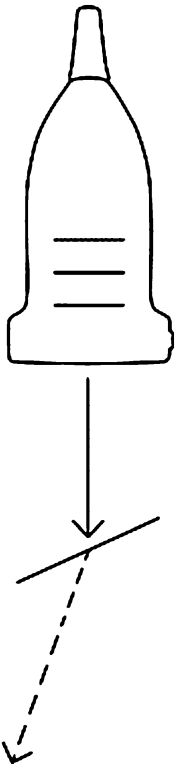

Fig. 2.7 Refraction. This figure demonstrates the process of refraction where an incoming ultrasound wave (*solid arrow*) with an oblique angle of incidence changes direction (*dashed arrow*) as it is transmitted through an interface of tissues with different acoustic properties

2.3.4 Absorption

Some of the original incident waves are absorbed by tissues and converted to heat energy. This process called absorption weakens the collective beam of ultrasound waves. The degree of absorption is greater with high frequency probes than with low frequency probes. Increasing scan depths also increase the amount of absorption. Absorption is illustrated in Fig. 2.8.

2.3.5 Attenuation

Attenuation is a term that refers to weakening of the beam of ultrasound waves as it passes through tissues. Reflection, scatter, refraction, and absorption all contribute to the decrease in strength of the ultrasound beam as it passes deeper into the body. Absorption is the greatest contributor to attenuation. Longer path lengths and higher frequencies lead to greater attenuation through absorption. Due to the issue of attenuation, low frequency probes are needed to image deep structures since they

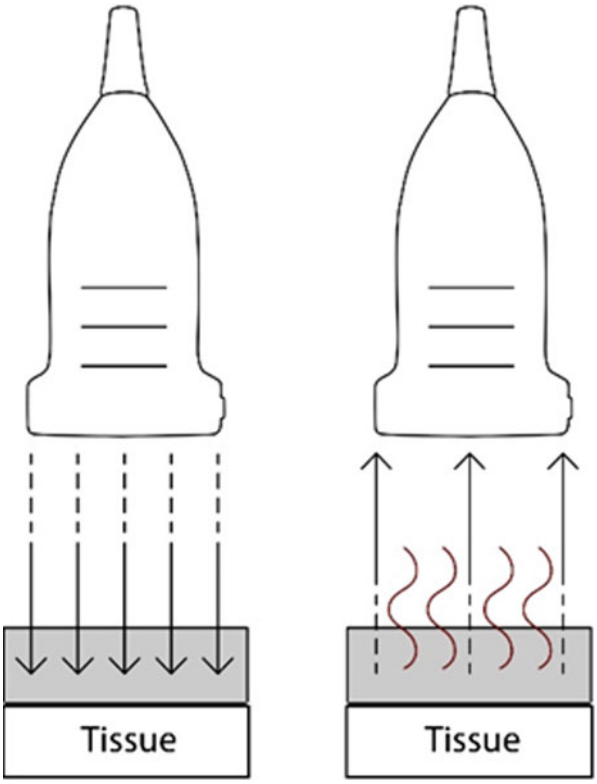

Fig. 2.8 Absorption. This figure illustrates absorption of some of the incoming ultrasound waves (*arrows*) and conversion to heat (*red waves*)

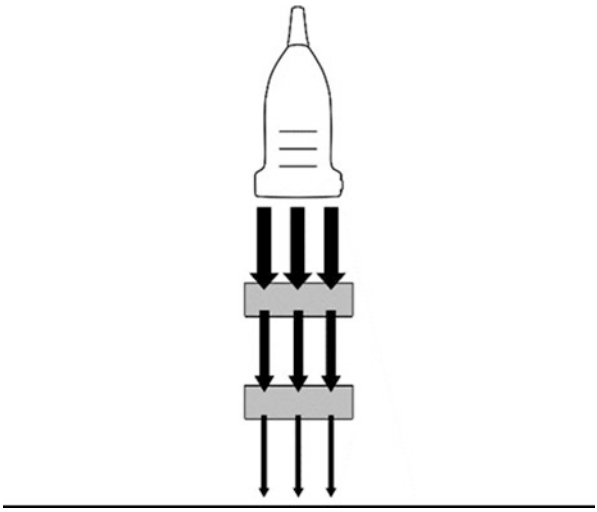

Fig. 2.9 Attenuation. This figure demonstrates weakening of an ultrasound beam as it passes into deeper structures

undergo less absorption. The resulting compromise is that the lower frequency probe has less resolution. Attenuation is shown in Fig. 2.9.

2.3.6 Interactions Summary

In summary, the process of reflection is the key interaction for producing images. The ultrasound waves that reflect at 90 degrees and return directly to the probe produce the most accurate representation of the structure being imaged. The other interactions cause weakening of the intensity of the returning ultrasound beam or lead to inaccurate depictions of the true location of a structure.

2.4 Propagation Speed of Ultrasound Waves

Ultrasound waves travel at different velocities within different media. They travel fastest through solids and slowest through gases. This relates to the compressibility of a medium. The waves travel faster through less compressible structures. The average velocity through soft tissues is 1540 m/s. Ultrasound waves travel faster through bone and slower through lung. The relationship of velocity to compressibility is illustrated in Fig. 2.10.

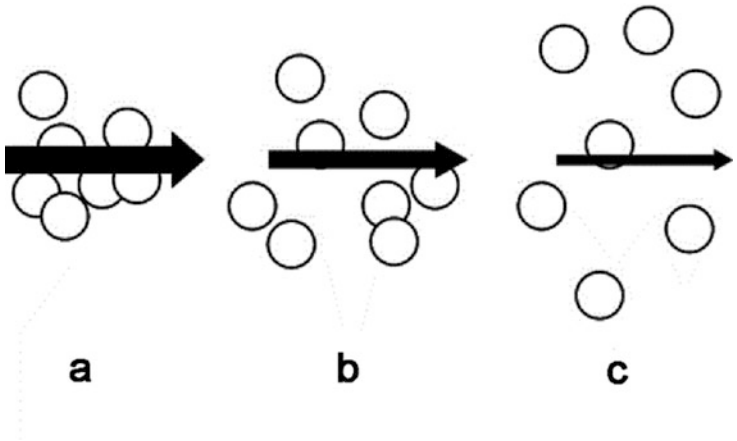

Fig. 2.10 Velocity of ultrasound in media. (**a**) Medium with the least compressibility has the fastest propagation speed (*large arrow*). (**b**): Medium with intermediate compressibility has intermediate propagation speed (*intermediate arrow*). (**c**) Medium with the most compressibility has the slowest propagation speed (*small arrow*)

2.5 What Determines Returning Echo Signal Strength?

Several factors affect the degree of reflection and thus the amplitude or strength of the returning echo signal. A stronger echo signal is produced when there is a larger difference in acoustic impedance between two adjacent structures. There is also a greater degree of reflection back to the probe when the ultrasound waves encounter a smooth interface. These types of structures are called specular reflectors. Rough interfaces create scattering and reduce the amount of reflection back to the probe. The orientation of an interface with respect to the probe also influences reflection. There is a greater amount of reflection when an interface is perpendicular to the incident ultrasound beam. If the interface is obliquely oriented, some of the echoes do not make it back to the probe since they reflect at angle equal the angle of incidence. Higher output power also increases the strength of the returning echo signal. Figure 2.11 illustrates various factors that determine echo signal strength.

2.6 What Characteristics of Echoes Contribute to Image Display?

2.6.1 Echo Signal Amplitude

Conventional gray scale ultrasound images are displayed in B-mode, which stands for brightness mode. In this mode, the echo signal amplitude determines the brightness of a structure on the image. This echo amplitude is encoded and displayed in

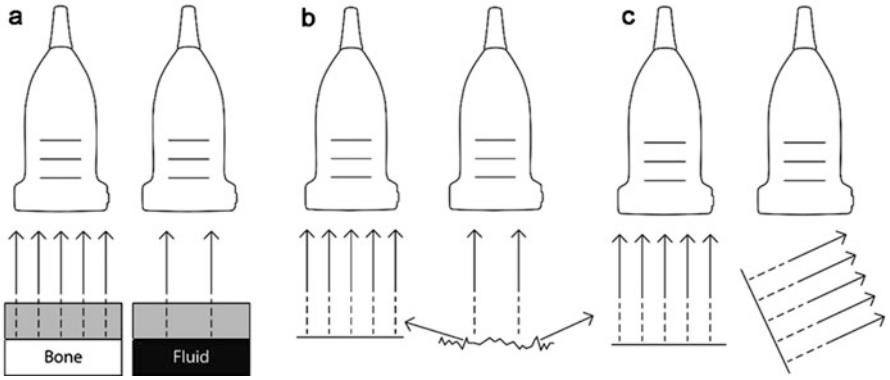

Fig. 2.11 Factors affecting echo signal strength. (**a**) Greater refection from a soft tissue/bone interface than a soft tissue/fluid interface. (**b**) Greater reflection from a smooth surface than a rough surface. (**c**) Greater reflection from a perpendicular surface than an oblique surface

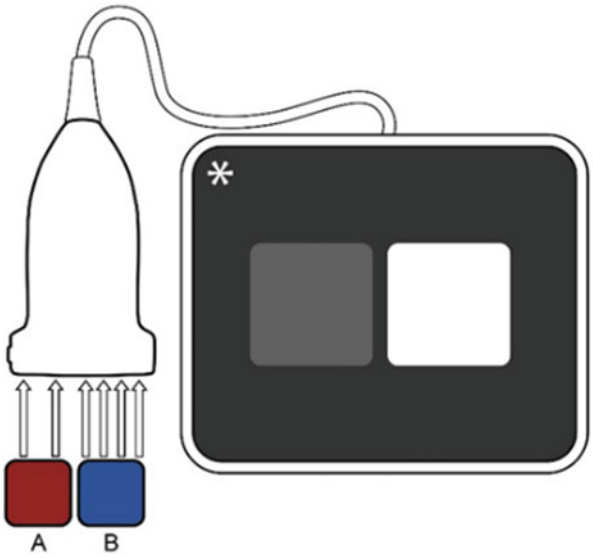

Fig. 2.12 Echo signal amplitude as a determinant of brightness on image display. More reflection occurs from structure *B* than from structure *A*. As a result, structure *B* is displayed brighter on the screen

various shades of gray. Structures that reflect more ultrasound waves back to the probe are displayed as brighter than those that reflect less waves. If no echoes are returned from a structure, it is displayed as black and called anechoic. The relationship between echo signal amplitude and brightness is shown in Fig. 2.12.

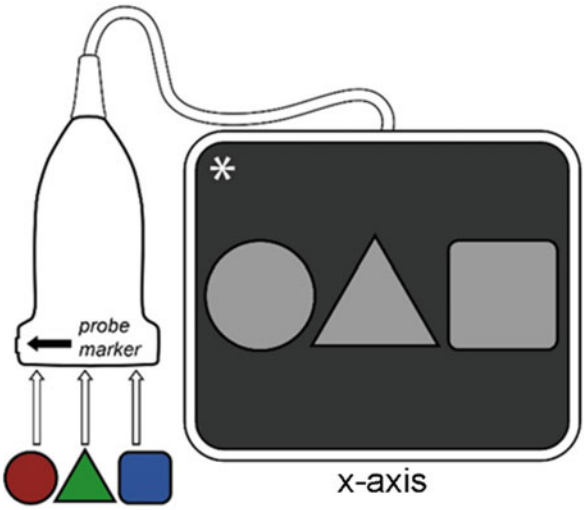

Fig. 2.13 Position of returning echo as a determinant of location. The location of each of the three structures on the x-axis of the image display is determined by its position relative to the ends of the probe footprint. * is a symbol or logo on the display monitor that corresponds to the probe marker end of the transducer

2.6.2 Position of Returning Echo on Probe Footprint

The position of a structure along the x-axis of the image display is determined by where the returning echoes strike the probe footprint. Those striking the footprint closer to the probe marker are displayed closer to the corresponding orientation marker on the image display. The relationship of the position of returning echoes to x-axis image display is shown in Fig. 2.13.

2.6.3 Time for Echo Return

The time it takes for an ultrasound wave to return to the probe determines the depth of a structure on the y-axis of an image display. The longer it takes for an echo to return, the deeper the structure is displayed. The total time it takes for an ultrasound wave to leave the probe and return as an echo is also referred to as time of flight. If the echo from "structure A" takes twice as long to return as an echo from "structure B," then "structure A" is displayed twice as deep on the image display. The relationship between time and depth on the image display is shown in Fig. 2.14.

2.6.4 Frequency Shifts

Frequency shifts of returning echoes are used in Doppler imaging. When an incoming ultrasound wave encounters a moving target, the echo produced returns to the probe with a different frequency. Specifically, the returning echo shifts to a higher

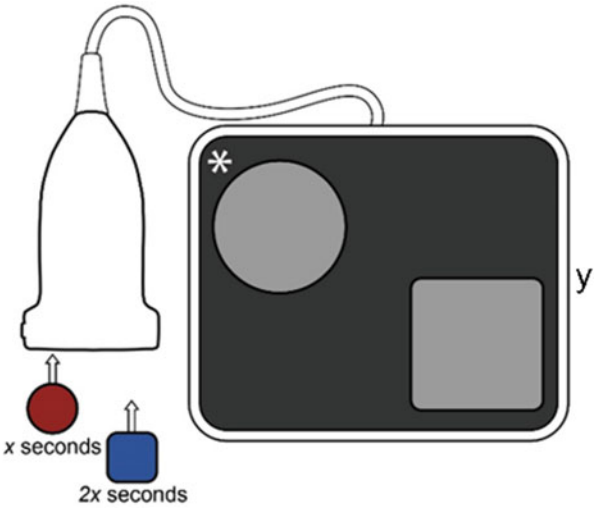

Fig. 2.14 Time for echo to return as a determinant of depth on the y-axis. The time of flight of the ultrasound wave returning from the *square* is twice as long (2*x*) as that of the *circle* (*x*). The *square* is therefore depicted to be twice as deep as the *circle* on the y-axis (*y*) of the image display

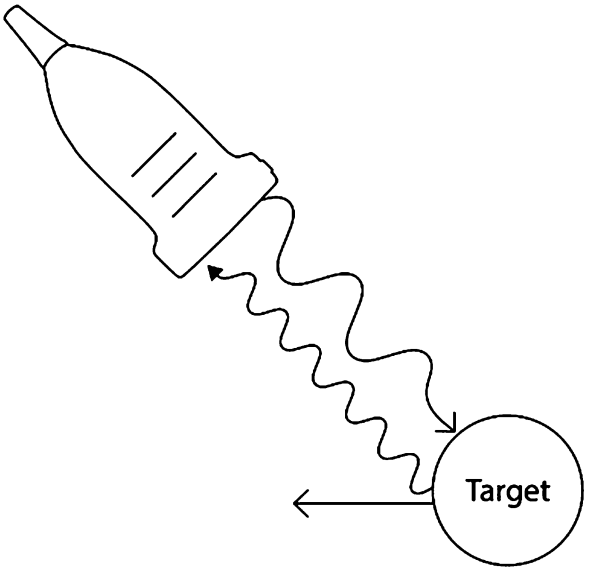

Fig. 2.15 Frequency shift. Note that the target is moving toward the probe. In this situation, the returning echo has a higher frequency than the original incident ultrasound wave

frequency when the target moves toward the incident wave and to a lower frequency when the target moves away from the incident wave. Thus the ultrasound machine uses the change to a higher or lower frequency to determine the direction of the moving target. The magnitude of the frequency shift is used by the ultrasound machine to determine the velocity of the moving target. Given the same angle of incidence of the incoming beam, a greater frequency shift will be produced by a faster moving target than by a slower moving target. The concept of frequency shift is illustrated in Fig. 2.15.

2.7 Modes of Ultrasound

2.7.1 Brightness Mode (B-Mode)

This is the mode that generates the conventional two dimensional gray scale images. Structures are displayed as black, white, or shades of gray depending on the amplitude of the returning echo signal. Structures that reflect more ultrasound waves back to probe are displayed as brighter than those that reflect less waves back to the probe.

2.7.2 Motion Mode (M-Mode)

This is the mode used to assess movement of a structure. M-mode graphically displays a portion of a B-mode image as it changes over time. Specifically, the user moves a cursor to select a thin slice through the structure of interest. A graphical display is then generated that detects movement of the structures in that slice during the sample period. Figure 2.16 demonstrates application of M-mode during imaging of an inferior vena cava.

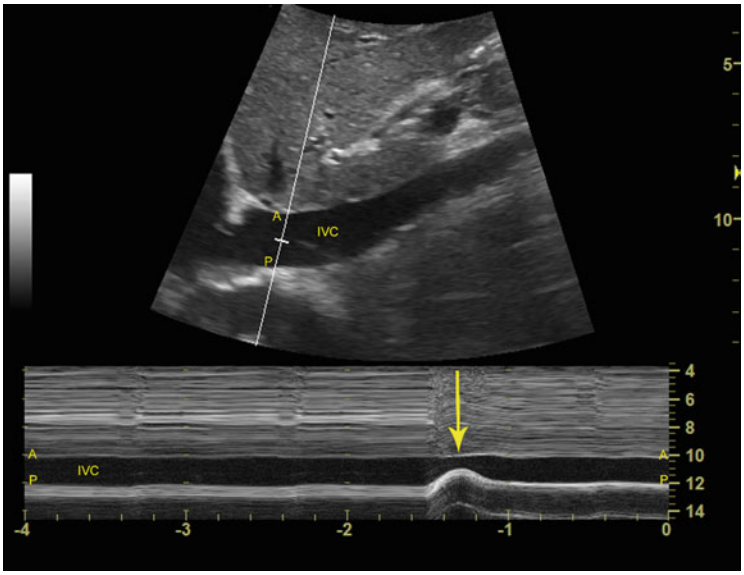

Fig. 2.16 M-mode of an inferior vena cava (*IVC*). The M-mode sampling line intersects the anterior and posterior walls of the IVC at the points marked *A* and *P* respectively. These points are represented by the same letters on the graph below. The graph displays the anteroposterior diameter of the *IVC* between those two points over time. Note the sudden decrease in lumen size at the *arrow* corresponding to a rapid inspiratory sniff performed by the patient

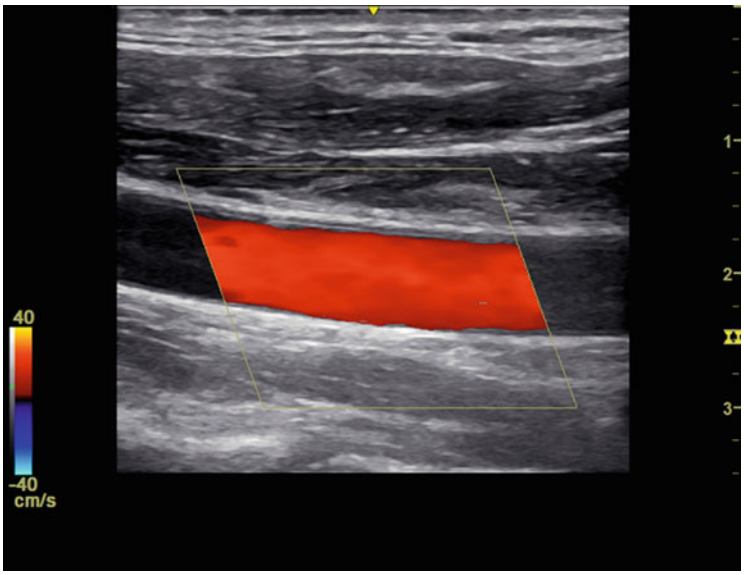

Fig. 2.17 Color Doppler of a common carotid artery. Note that the portion of the lumen within the sample area (*yellow box*) is displayed as red. This indicates that blood is flowing toward the incident ultrasound beam

2.7.3 Color Doppler

This is the mode that uses color to depict moving structures. A typical use is for assessing flow within a blood vessel. The frequency shifts that occur when the ultrasound waves encounter a moving target are encoded with a color scale. By convention, movement of a target toward the incident ultrasound beam is displayed as red, and movement away from the incident beam is displayed as blue. In addition to direction, the color scale gives an estimate of velocity of the target. The different shades of blue and red are used to display varying velocities. Figure 2.17 demonstrates an image of a common carotid artery with color Doppler.

2.7.4 Spectral Doppler

This mode is also referred to as pulsed Doppler. It is used to determine specific velocities of blood flow within vessels using frequency shifts. It demonstrates changing velocities over time in a graphical display. The display includes information on both direction and velocity of blood flow. The velocities are displayed on the y-axis of the graph while the x-axis represents time. Velocities extending into the negative range of the graph indicate flow away from the incident ultrasound beam. Figure 2.18 demonstrates spectral Doppler of a common carotid artery.

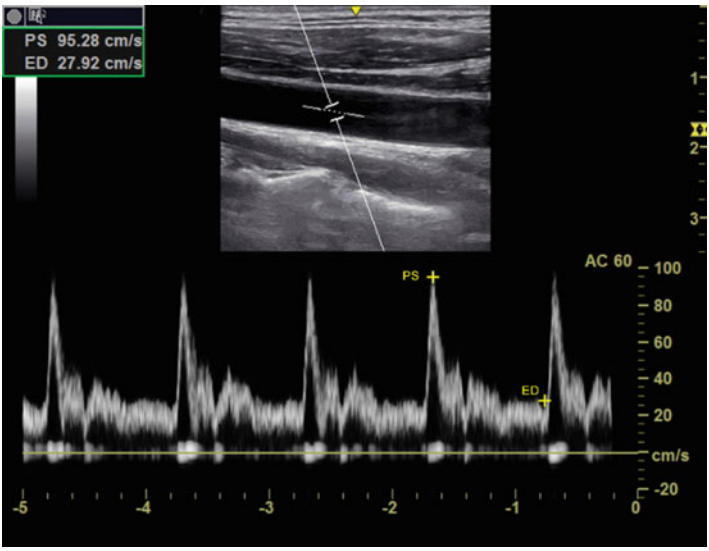

Fig. 2.18 Spectral Doppler of a common carotid artery. Note the sample area in the central aspect of the vessel lumen. The graph depicts change in velocity of blood over time at that location. Peak systolic (*PS*) velocity and end diastolic (*ED*) velocity are measured

2.7.5 Power Doppler

This mode is used to show the magnitude of blood flow within a structure. It utilizes the power or amplitude or Doppler signals rather than frequency shifts. It is more sensitive to detecting flow than color Doppler or spectral Doppler. A typical use is to demonstrate the presence or absence of blood flow within an organ. It does not provide information about direction or velocity of the blood flow. Figure 2.19 shows power Doppler applied to a right kidney.

2.8 Ultrasound Machine Considerations

2.8.1 Probe Frequency

2.8.1.1 High Frequency

High frequency probes are designed for shallow imaging. They have excellent resolution but have limited penetration capabilities of around 10–12 cm. They are ideal for imaging structures that are closer to the skin surface, such as carotid arteries, jugular veins, extremity vessels, musculoskeletal structures, and the thyroid gland. There is often a number on the side of the probe designating its frequency in MHz or millions of cycles per second. For example, 12 L is a probe with 12 MHz or

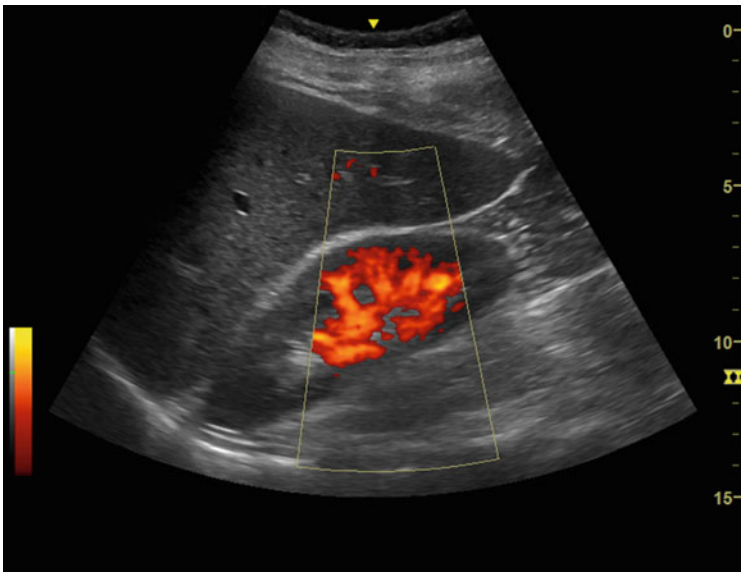

Fig. 2.19 Power Doppler of a right kidney. The red, orange, and yellow areas represent the presence of blood flow with the sampled portion of the kidney

12 million cycles/s, making it a high frequency probe. Figure 2.20 shows a high frequency probe.

2.8.1.2 Low Frequency

Low frequency probes are designed for maximum penetration. They can image as far as 30 cm, but they produce lower resolution images that degrade as the ultrasound beam progresses deeper into the body. They are typically used for abdominal and cardiac applications that require deep penetration of the ultrasound beam. There is often a number on the side of the probe designating its frequency in MHz or millions of cycles per second. For example, 3S and 4C are probes with 3 and 4 MHz respectively, making them low frequency probes. Figure 2.21 shows two different types of low frequency probes.

2.8.2 Shape/Design of Probe

The three main types of ultrasound transducers are: Sector, Linear, and Curvilinear. These are traditional transducers that use piezoelectric crystals to produce the ultrasound waves. Some newer technology transducers use semiconductors instead to produce ultrasound waves. This allows one transducer to have a wide range of

Fig. 2.20 High frequency linear probe

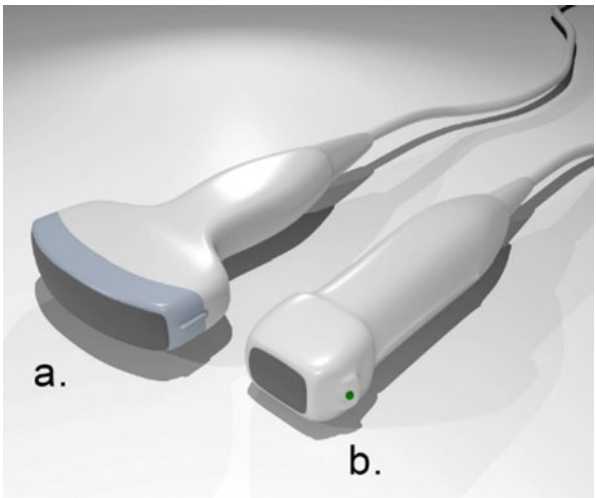

Fig. 2.21 Low frequency probes. (**a**) Curvilinear low frequency. (**b**) Sector low frequency

frequencies from 2 to 12 MHz thereby eliminating the need to change between three different types of probes.

2.8.2.1 Sector

Sector probes are low frequency probes that have a small footprint (the part of the probe that makes contact with the skin surface). Since the ultrasound beam is

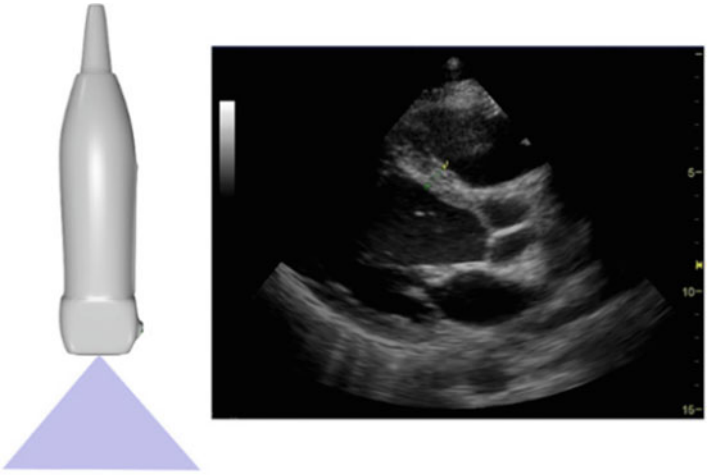

Fig. 2.22 Sector probe. Note the small footprint of this probe and the sector display. The image is a parasternal long axis view of the heart

generated from a small spot on the surface of the transducer, it makes it ideal for cardiac imaging since the beam can fit between the intercostal spaces on the chest. Since this transducer is low frequency, it can also be used for abdominal imaging in the absence of a curvilinear transducer. However, the field of view is narrower for the part of the display closest to the footprint. Figure 2.22 shows a typical sector transducer.

2.8.2.2 Curvilinear

Curvilinear probes are low frequency probes that have a large footprint where the ultrasound-producing crystals are arranged in a curved orientation. This probe is designed for deep imaging and produces a large field of view ideal for abdominal scanning and obstetrics. Figure 2.23 shows a typical curvilinear transducer.

2.8.2.3 Linear

Linear probes are mainly high frequency probes designed for shallow imaging. The ultrasound-producing crystals are arranged in a straight line that produce a rectangular shaped image on the screen. This transducer is ideal for structures closer to the skin surface. Figure 2.24 shows a typical linear transducer.

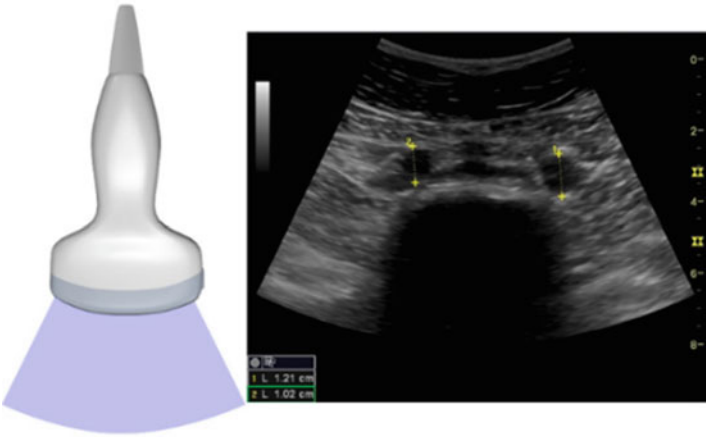

Fig. 2.23 Curvilinear probe. Note the large curved footprint of this probe with a wide field of view. The image shows a short axis view of the common iliac arteries

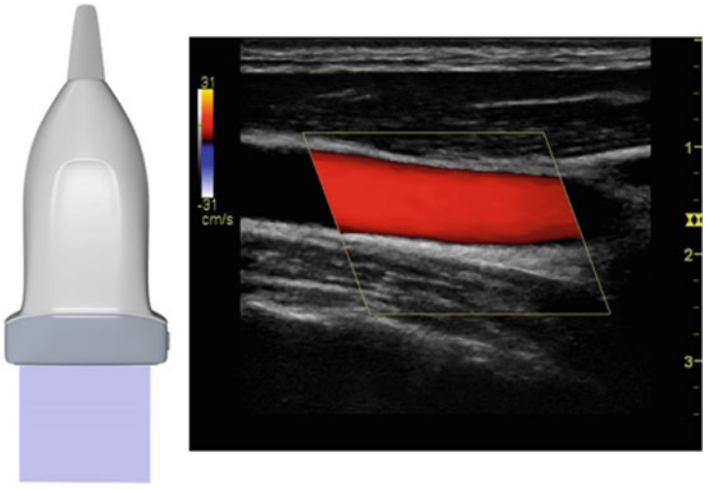

Fig. 2.24 Linear probe. Note the straight surface of the footprint of this probe is larger than the sector probe. The image shows a common carotid artery

2.8.3 Display Parameters for Optimizing Images

2.8.3.1 Depth

Depth is important in ensuring that the structure of interest is visualized on the screen without cutting-off or excluding adjacent structures that may be relevant to interpreting the image. It is helpful to continuously be aware of the depth in order

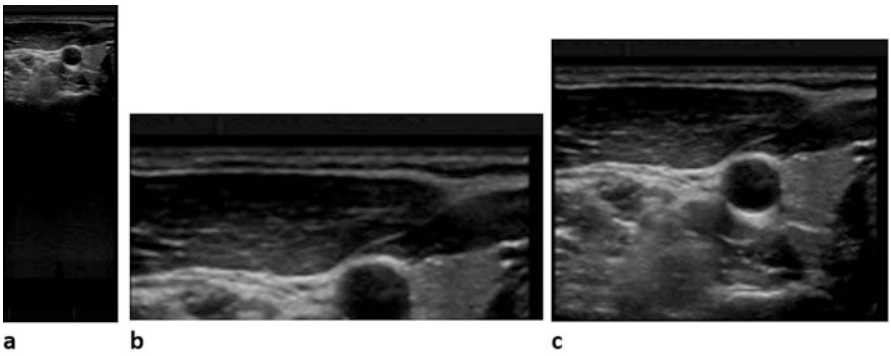

Fig. 2.25 Depth. (**a**) Image of the right lobe of the thyroid gland with depth set too deep. There is too much "wasted" space on the deep edge of the field of view deep to the thyroid gland. (**b**) Same image with the depth set too shallow. The deep edge of the thyroid gland is excluded. (**c**) Same image with the depth set appropriately

to maximize screen usage and avoid "wasted" screen real-estate. Figure 2.25 shows the difference between proper and improper depth settings on images of the right common carotid artery and right lobe of the thyroid.

2.8.3.2 Gain

Gain has to do with image brightness. Increasing the overall gain makes the entire image brighter by electronically amplifying the signals from returning echoes. Decreasing gain produces the opposite effect, rendering structures on the image darker. Adjusting the gain does not affect the strength of the beam of incident ultrasound waves entering the body. Increasing output power can also increase image brightness but it does so by increasing the strength of the ultrasound beam. Therefore, for safety reasons, adjusting gain settings is the preferred initial way to optimize image brightness. Figure 2.26 shows the difference between improper and proper gain settings on images of the right kidney.

2.8.3.3 TGC

TGC stands for time gain compensation. As an ultrasound beam travels into the body it is attenuated by processes such as reflection, refraction, scatter, and absorption. As the beam travels deeper into the body it becomes more and more attenuated. Thus, the amplitude of echoes returning from deep structures is less than the amplitude of echoes returning from shallow structures due to the weakening of the ultrasound beam. Without correction, a deeper structure would be displayed darker than an

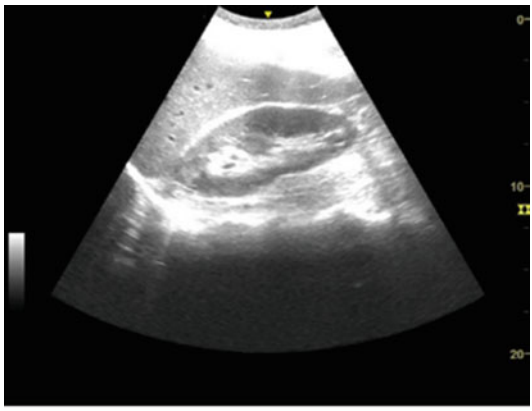

a

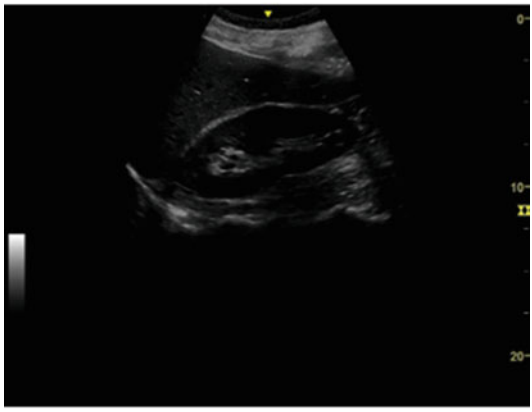

b

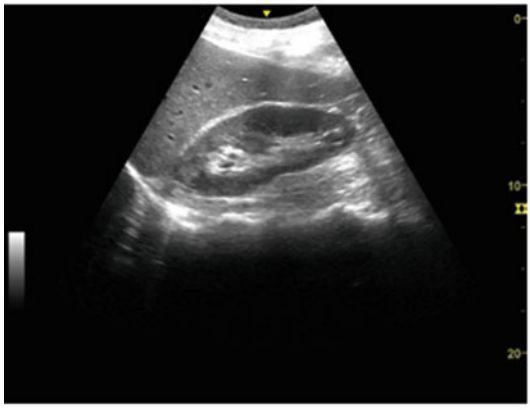

c

Fig. 2.26 Gain. (**a**) Image of the right kidney with the gain set too high. The image is too bright. (**b**) Image of the right kidney with the gain set too low. The image is too dark. (**c**) Image of the right kidney with appropriate gain setting

identical structure located in a more superficial position. TGC helps correct for the normal attenuation that occurs with increasing depth. The TGC controls are slide bars allowing the operator to adjust the gain settings at different depth layers on the image display. Using slide bars corresponding to different depths, the user can increase the brightness (gain) of the deeper structures. Increasing the "gain" at the deeper levels compensates for the attenuation of the echoes arising from those structures. The element of "time" in the name of this control comes from the fact that the return time of an echo is an indicator of the distance it travels. In effect, structures that have longer echo return times are deeper, and the TGC allows the user to optimize the image display by increasing the amplitude of those late returning echoes. Figures 2.27 shows the difference between suboptimal and optimal TGC settings respectively.

2.8.3.4 Focus

The ultrasound beam is narrowest at the level of the focal zone. The ability to resolve two structures located at the same depth as separate entities is greatest at the site of the focal zone. This type of resolution is referred to as lateral resolution. The user can adjust the focus to the depth of the structure of interest to improve detail by maximizing lateral resolution. Figure 2.28 illustrates the difference between improper and proper focal zone settings.

2.8.3.5 Frequency

Frequency is a measure of the number of cycles per second of the waves in the ultrasound beam. It affects the penetration of the beam as well as the axial resolution. Higher frequency waves are attenuated to a greater degree than lower frequency waves. This attenuation results in decreased penetration. Thus, low frequency probes are needed for scans of deep structures where more penetration is needed. Higher frequency ultrasound waves generate images with greater axial resolution. This refers to the ability to resolve two separate structures sharing the same x-axis position on the screen but having different depths along the y-axis. Greater axial resolution means that structures separated by a minute distance can be identified as two separate entities. This improves detail of the image. Figure 2.29 illustrates the difference between using the correct and incorrect probe.

2.8.3.6 Presets

Presets are manufacturer established settings that serve to optimize imaging of particular structures or regions. When a preset is selected, the various parameters are adjusted in a manner to produce high quality images in most patients. Due to

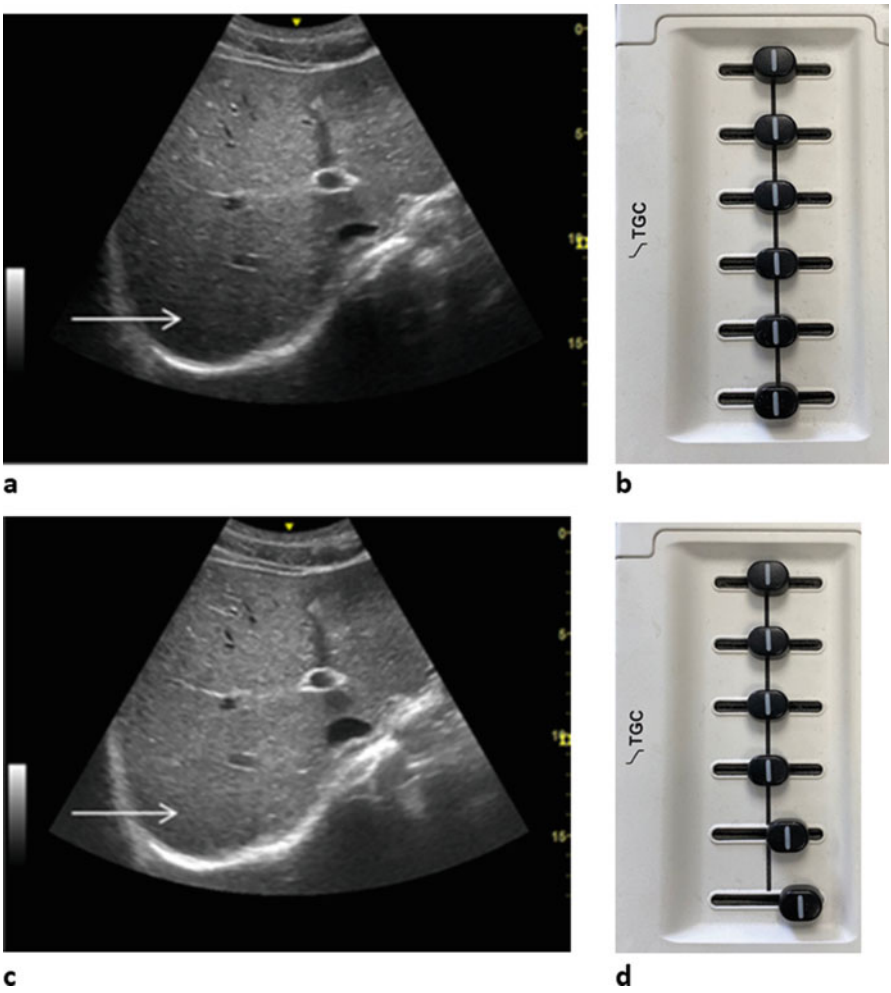

Fig. 2.27 TGC. (**a**) Image of a liver obtained with all the TGC slide bar controls centered. Note that the deeper structures such as the posterior aspect of the right lobe of the liver (arrow) appear somewhat darker than the shallower structures. (**b**) Position of the slide bar controls for image (**a**). (**c**) Same view obtained with adjustment of the TGC controls. The slide bars for the deeper levels were adjusted to the right to increase gain at those depths. The result is increased echogenicity of the deeper structures when compared to image a leading to a more uniform echogenicity of the liver. (**d**) Position of the slide bar controls for image (**c**)

normal variations and pathology, the default parameter settings are unlikely to be ideal for all patients. In that circumstance, the scanner manually adjusts particular parameters to obtain the best image possible. Examples of presets include “thyroid,” “cardiac,” “abdomen,” and “knee” among many others.

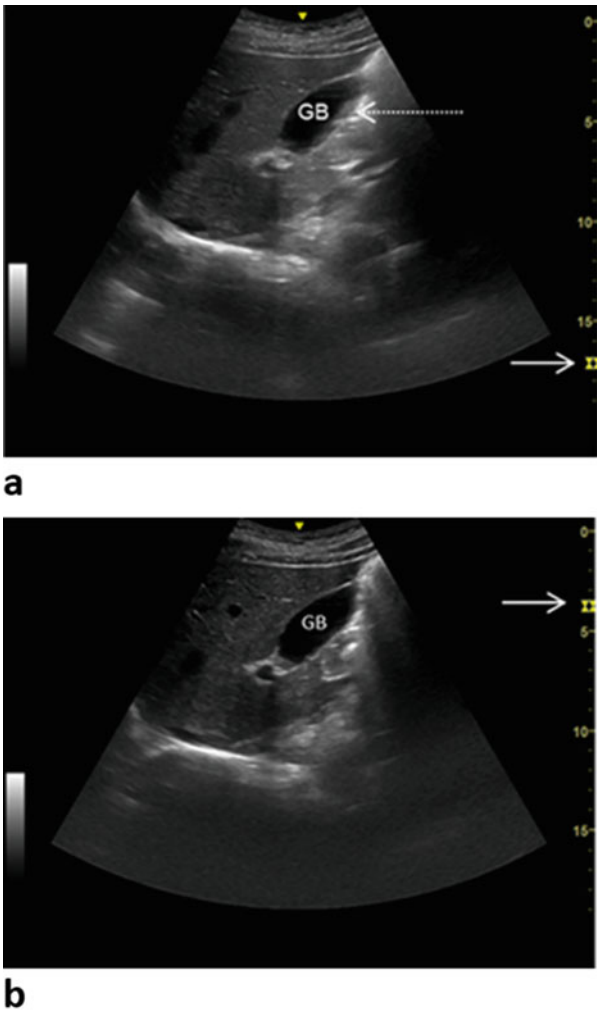

Fig. 2.28 Focal zone. (**a**) Longitudinal view of a gallbladder (*GB*) with the focal zone (*solid arrow*) set too deep. The detail of the gallbladder is suboptimal with artifactual echoes (*dashed arrow*) along the interface of the lumen and posterior wall. (**b**) Same view with the focal zone set at the level of the gallbladder. Note that the borders of the gallbladder are better defined with a targeted focal zone

2.8.4 Other Machine Features

2.8.4.1 Freeze

This is a button that stops image acquisition. Upon pressing this button, the last image obtained during real-time scanning is displayed on the screen. This freeze feature is required to save a still image from the scan. The frozen image can be annotated with comments or measurements before it is saved.

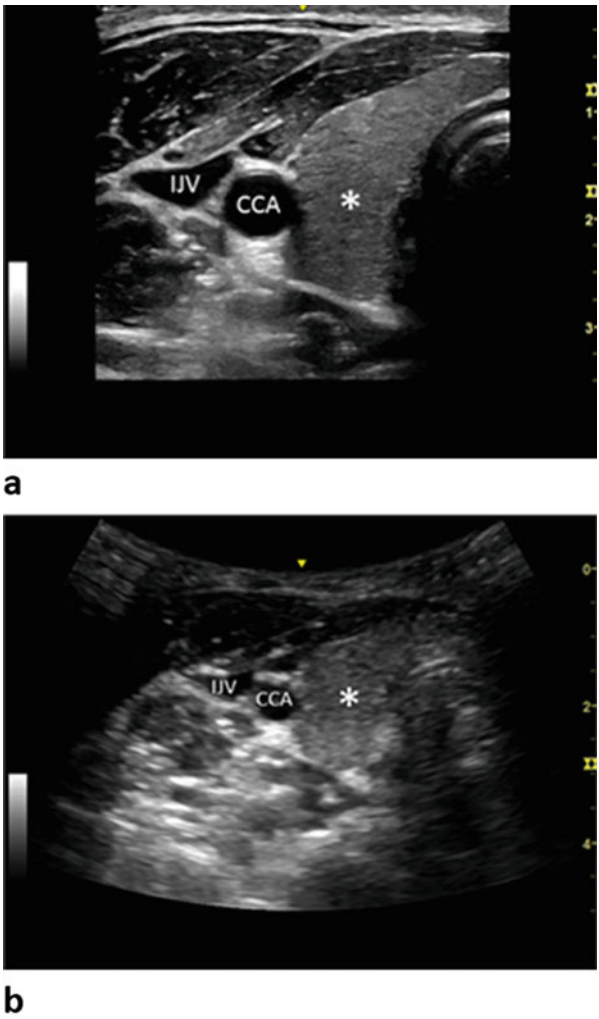

Fig. 2.29 Relationship of frequency and resolution. (**a**) Image of the right lobe of a thyroid gland obtained with a high frequency linear transducer. The thyroid gland (*asterisk*) and surrounding structures are well seen because of the high resolution. (**b**) Same view obtained with a low frequency curvilinear transducer. Note that the resolution of this image is diminished making it difficult to discern the structures. *IJV* = internal jugular vein, *CCA* = common carotid artery

2.8.4.2 Measure

This button permits the scanner to perform various measurements on a frozen image. Measuring typically involves setting two calipers in place to obtain a linear distance. Short and long axis views of a structure are required when trying to obtain the length, width, and height.

2.8.4.3 Save

This button is used for storing still images or video clips. To save a still image, the freeze button must be pressed first. At that point, the still image can be saved to the hard drive of the ultrasound machine, an external drive, or a server.

Video clips are a continuous collection of images obtained during real-time scanning. They are typically a few seconds in length. A video clip can be obtained by simply pressing the save button during scanning. Alternatively, the scanner can first freeze the image and then press a cine loop playback button. This will display a loop of the images obtained prior to pressing the freeze button. When the loop in playing, pressing the save button will save a video clip.

2.9 Patient Considerations

2.9.1 Patient Preparation

Bowel gas can greatly reduce the image quality of an ultrasound scan and can create artifacts that cover or mask essential structures on the screen. It is important to advise the patient, in certain situations or prior to certain scans to refrain from eating, drinking, smoking, or chewing gum in order to reduce the introduction of air into the bowel. Some ultrasound exams, like heart, neck, and peripheral vessels in the upper and lower extremities are not affected by eating or drinking prior to performing an ultrasound exam.

2.9.2 Position

Most scans can be done with the patient in a supine position, but some scans can be greatly enhanced with some positional manipulation that renders structures closer to the chest wall, or the transducer, leading to much improved images on the screen. For example, in cardiac imaging, tilting the patient onto their left side (left lateral decubitus position) and having them lift their left arm up, can greatly improve the images and allows the ultrasound beam to fit nicely between the rib spaces. The left lateral decubitus position is shown in Fig. 2.30.

2.9.3 Maneuvers and Manipulations

Sometimes body positioning or breathing can prevent a structure of interest from being optimally visualized on an ultrasound image. Some maneuvers may be necessary to help improve image quality such as inhaling, exhaling, or flexing an arm, leg, or hip. These types of maneuvers can move structures higher or lower in the abdomen, shift adjacent structures out of the way, or bring structures closer to the skin for better visualization.

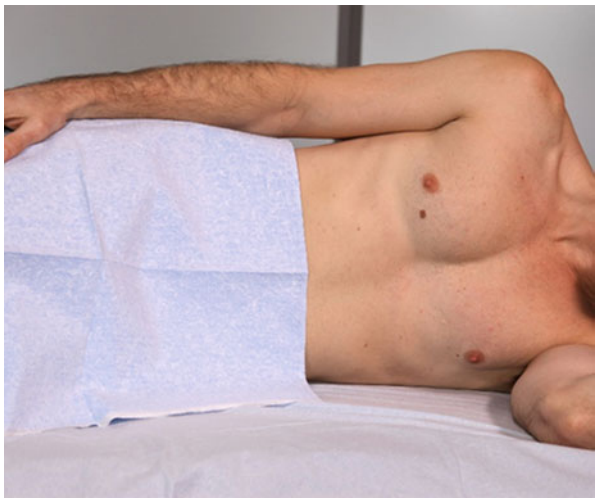

Fig. 2.30 Left lateral decubitus position. Patient is lying with his left side down on the bed

2.10 Scanner Considerations

2.10.1 Probe Placement

Plenty of ultrasound gel should be placed on the probe footprint or skin surface of the patient before attempting to acquire images. This coupling gel is necessary to allow penetration of ultrasound waves into the body. Without gel, the sound waves immediately reflect back to the probe once they encounter an air gap between the skin and probe.

The scanner should grip the probe near the footprint with his or her dominant hand. This allows for better control of fine movements of the probe during scanning. Resting part of the scanning hand on the patient's skin surface also helps with stability. Without an anchor point, the probe may have a tendency to slide away from the target area during scanning (Fig. 2.31).

It is important to keep in mind that not all anatomy appears similar or is found from the same skin surface location from one patient to another. Once the probe is placed on the skin, it is often helpful to make large initial movements to get a good sense of the best window to visualize the structure of interest. In ultrasound imaging, the word window refers to a general location where views of a structure can be obtained. For example, in cardiac imaging, the heart can be interrogated from many windows. Representative windows for obtaining cardiac views are illustrated in Fig. 2.32.

Once the structure is found, then smaller more calculated movements can be made to optimize the image and visualize the structure more clearly.

The word view refers to different images of a structure of interest that can be obtained from each window depending on the probe marker alignment on the body. Each probe has a marker on it, and depending on where the marker is pointing, a

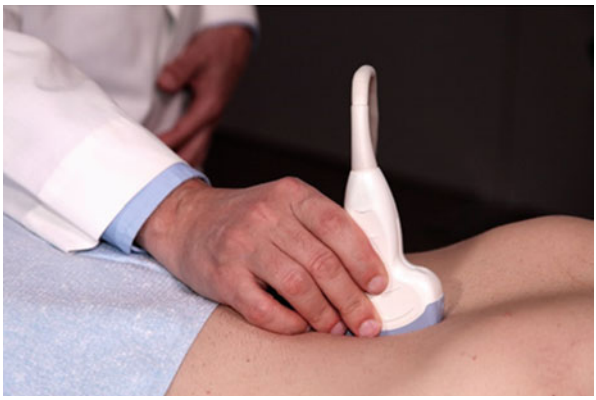

Fig. 2.31 Probe grip. This image demonstrates a scanner using an appropriate grip close to the footprint of the probe. Note that part of the hand is resting on the patient for stabilization

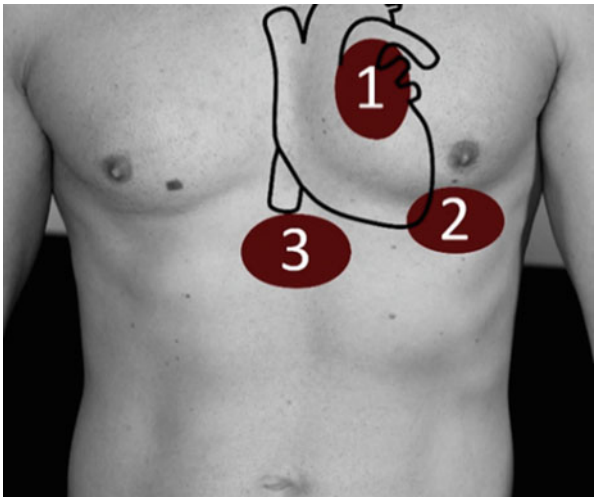

Fig. 2.32 Cardiac windows. Image shows location of (1) Parasternal windows, (2) Apical windows, and (3) Subcostal windows

different image can be produced on the screen. This is due to how the ultrasound beam slices through a structure (i.e. longitudinally, transversely, obliquely, etc.), which is illustrated for parasternal long axis and parasternal short axis views of the heart in Fig. 2.33.

2.10.2 Probe Manipulation

When teaching someone how to scan or when discussing ultrasound exams, it is important to use the same terminology to keep concepts clear and avoid misunderstandings. Some basic terms have been designated to describe probe movements on the skin in a uniform fashion.

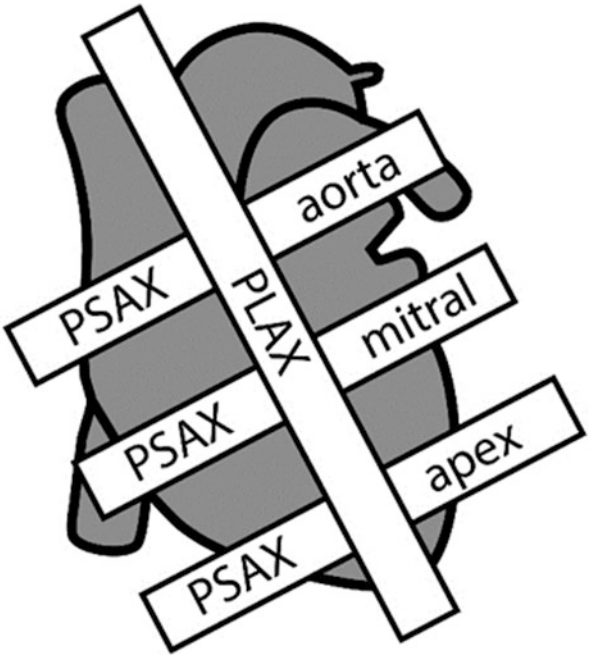

Fig. 2.33 Cardiac views. Illustrations of slice planes for *PLAX* (parasternal long axis) and *PSAX* (parasternal short axis) views of the heart

2.10.2.1 Rocking

Rocking the probe involves an angling motion along its long axis. This motion angles the ultrasound beam toward and away from the direction of the probe marker end of the probe. This angling is done while keeping the probe footprint at the same location on the skin surface. Understanding this concept can greatly help in keeping the structure of interest centered on the x-axis of the screen and easily visualized. Rocking motion is illustrated in Fig. 2.34.

2.10.2.2 Fanning

Fanning the probe involves angling the ultrasound beam along its short axis toward one side of the probe or the other. This motion is done while keeping the footprint of the probe at the same location on the skin surface. Fanning is particularly helpful when trying to visualize the entirety of a large structure like the liver. In many cases, the entire structure of interest can be scanned by fanning through it from one margin to the other. In others, sliding or sweeping the probe on the skin surface may be needed as well. Seeing the entire organ is important to avoid missing pathology. Fanning is shown in Fig. 2.35.

Fig. 2.34 Rocking. The ultrasound beam is angled toward and away from the direction of the probe marker end of the probe

Fig. 2.35 Fanning. The ultrasound beam is angled from one side of the probe to the other side of the probe

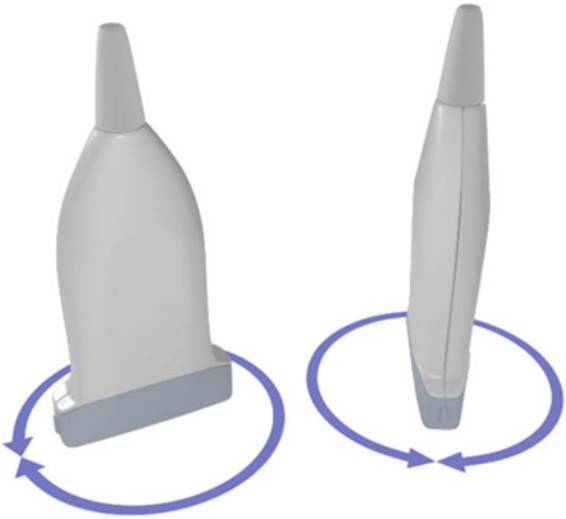

Fig. 2.36 Rotation. The probe is rotated in a clockwise or counterclockwise direction while maintaining contact with the skin

2.10.2.3 Rotation

Rotating the probe clockwise or counter clockwise allows for the rotation of the beam and contributes to different cuts or slices of a structure to be seen from different angles. Rotation is illustrated in Fig. 2.36.

2.10.2.4 Compression

When imaging certain deeper abdominal structures, it is often helpful to press down firmly in order to dissipate some bowel gas, or move closer to a structure for better visualization. It is recommended to let the patient know prior to pushing as to prepare him or her for the possibility of experiencing some discomfort, especially if the area is tender. Pressing down is illustrated in Fig. 2.37.

2.10.2.5 Sliding or Sweeping

These motions involve moving the probe from one location to another across the body. This can be done along the probe's long axis (slide) or short axis (sweep). These motions are shown in Fig. 2.38.

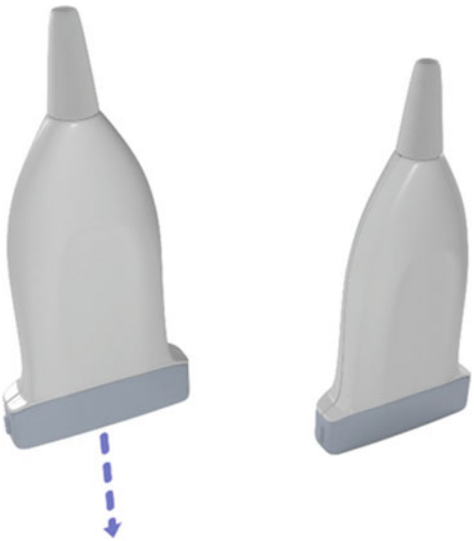

Fig. 2.37 Compression. More pressure is applied to the probe to press the footprint more firmly against the skin

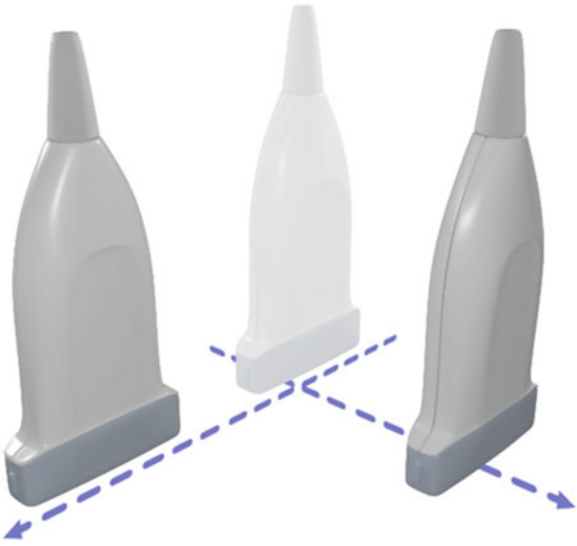

Fig. 2.38 Sliding and Sweeping. The probe stays in contact with the skin while it is moved to a different surface anatomy position

2.11 Scan Planes

2.11.1 Long Axis

Cutting a structure along its long axis or longitudinally. Figure 2.39 shows probe position for a long axis view of the abdominal aorta.

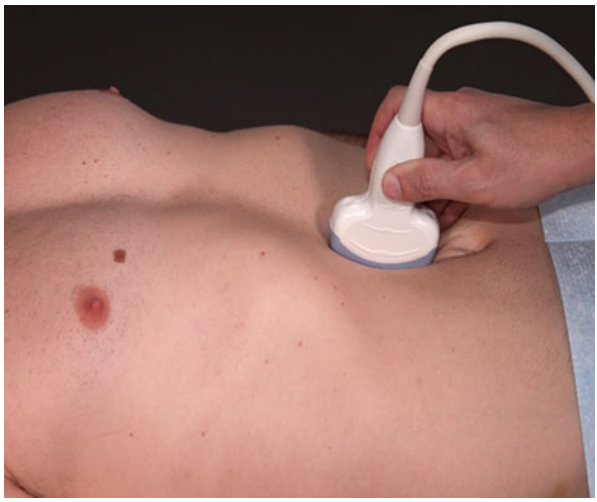

Fig. 2.39 Long axis. Typical orientation of the probe for a long axis view of the aorta with the probe marker facing cephalad

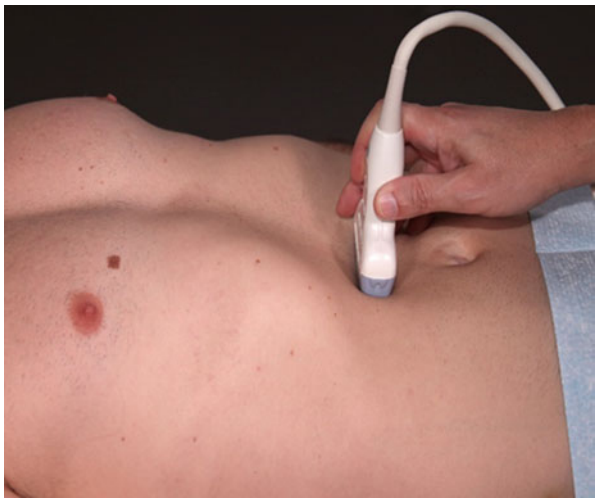

Fig. 2.40 Short axis. Typical orientation of the probe for a long axis view of the aorta with the probe marker facing toward the patient's right side

2.11.2 Short Axis

Cutting a structure along its short axis or transversely. Figure 2.40 shows probe position for a short axis view of the abdominal aorta.

2.11.3 Scan Plane vs Body Plane

One concept to keep in mind is that a structure can lie in the body in an oblique orientation that differs from the conventional body planes such as axial, coronal, or

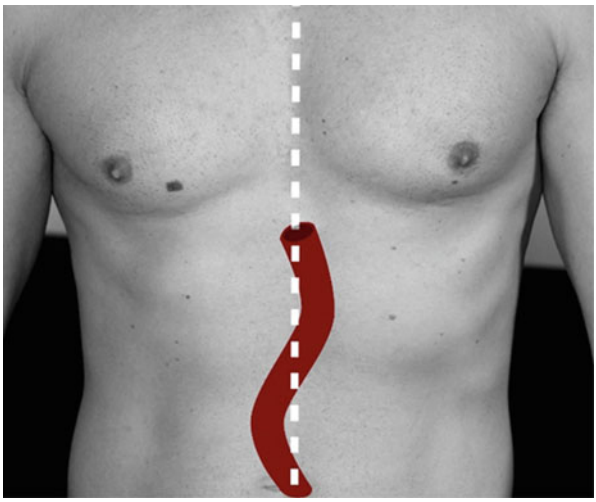

Fig. 2.41 Longitudinal plane of organ. An oblique orientation of the probe would be needed to obtain a long axis views of this tortuous aorta (*red tube*)

sagittal. Adjustment maneuvers may be necessary in order to line up with the longitudinal orientation of the structure rather than the longitudinal orientation of the body. For example, the abdominal aorta can sometimes be tortuous and not align with the sagittal plane of the body as illustrated in Fig. 2.41.

2.12 Image Display Orientation

It is widely accepted for most non-cardiac scanning that the probe marker points to the patient's right side when imaging in a transverse fashion, and to the patient's head (cephalad) when imaging in a longitudinal fashion. This method helps ensure that when scanning in a transverse fashion, the structures on the left side of the screen correspond to the patient's right side, and the structures on the right side of the screen correspond to the patient's left side. Conversely, when scanning in a longitudinal fashion, the structures on the left side of the screen correspond to the patient's head, and structures on the right side of the screen correspond to the patient's feet. Figure 2.42 shows the position of a marker on the image display corresponding to the probe marker.

2.13 Image Description Terminology

Anechoic: Free of echoes. This refers to a property of an ultrasound image where structures appear black or devoid of echoes. For example, a cyst filled with clear fluid, or a full urinary bladder appear anechoic or black on the screen.

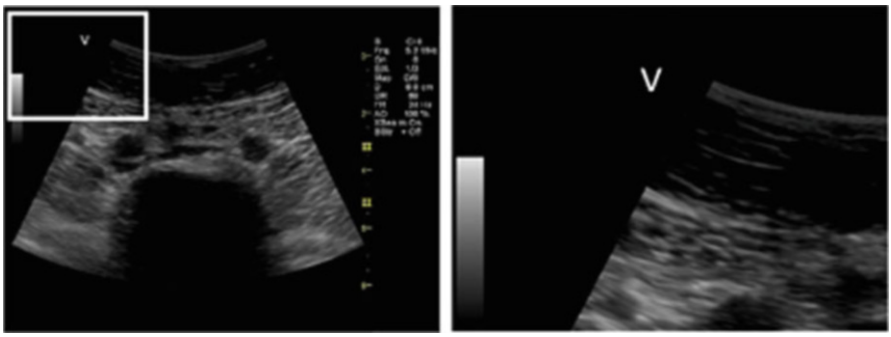

Fig. 2.42 Image display. Image orientation marker (*V*) corresponds to the probe marker on the transducer

Hyperechoic: This refers to a property of an ultrasound image where the structures produce echoes of higher amplitude than surrounding tissue and appear brighter on the screen. For example, the diaphragm is typically seen as hyperechoic compared to adjacent normal liver.

Hypoechoic: This refers to a property of an ultrasound image where the structures produce echoes of lower amplitude than surrounding tissue and appear darker on the screen. For example, neck muscles adjacent to the thyroid gland are typically hypoechoic compared to the gland.

Isoechoic: This refers to structures that have similar echogenic properties or producing echoes equal to those of neighboring tissues and appear similar in brightness to one another.

2.14 Artifacts

2.14.1 Shadowing

Some structures markedly limit transmission of incident ultrasound waves through absorption and/or reflection. The result is a vertical band of decreased echogenicity deep to that structure known as a shadow. Shadowing can be seen with normal structures as well as pathology.

Commonly encountered sources of normal shadowing include bones and bowel gas. When imaging bones, only the cortex closest to the probe is visualized and appears as a thin bright linear/curvilinear area. The remainder of the bone is obscured by a dark shadow due to significant attenuation of the sound waves when they reach the cortex.

Shadows from the sternum and ribs can be encountered when trying to find adequate acoustic windows for scanning the heart. Rib shadows can be helpful as a point of reference when scanning the lungs/pleura. Rib shadows, however, can limit at times visibility of upper abdominal structures like the spleen and kidneys.

The spine is routinely seen during abdominal imaging as a large shadow posterior to the aorta and inferior vena cava.

Bowel gas also produces shadowing. The highly reflective nature of the gas markedly limits transmission of sound waves, which leads to a shadow. Bowel gas can typically be recognized as bright arcs with shadows posterior to them. Some of the sound waves travelling back to the probe are reflected off the probe and re-enter the body. The echoes created from those re-entrant waves are interpreted by the ultrasound machine as arising from deeper in the body due to the time delay. Thus, they create some echoes within the vertical band of shadowing. This brighter type of shadowing has been referred to as "dirty" shadowing in contrast to the very dark "clean" shadowing seen with structures like bones. Figure 2.43 shows examples of "clean" and "dirty" shadows. Bowel gas shadows can interfere with visibility of normal structures deep to them. Thus, patients are asked to fast before abdominal scans in attempt to reduce the amount of bowel gas. Figures 2.44 shows the difference in visibility of deep structures when bowel gas shadowing is present and when it is absent.

A classic example of pathologic shadowing is gallstones. Ultrasound is the test of choice for diagnosing gallstones. They are seen as echogenic foci in the dependent portion of the gallbladder lumen. Many gallstones exhibit shadowing which helps distinguish them from polyps. Figure 2.45 shows shadowing stones in a gallbladder.

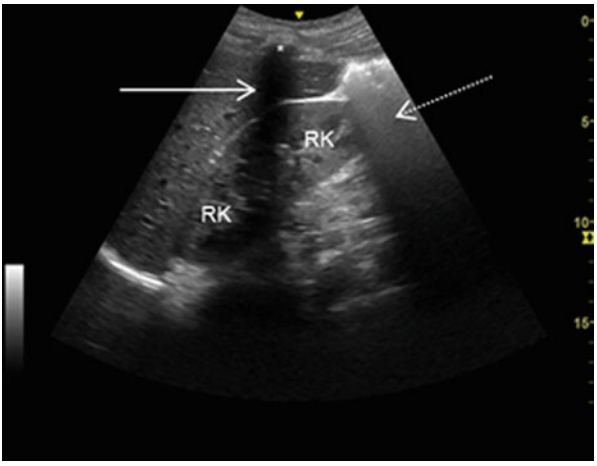

Fig. 2.43 Clean vs dirty shadowing. This longitudinal image of the right kidney (*RK*) demonstrates a shadow (*solid arrow*) traversing the mid aspect of the kidney. This shadow arising from a rib (*asterisk*) has the typical appearance for a "clean" shadow since it is dark. Note also the brighter shadows (*dashed arrow*) arise from bowel gas and obscure the lower pole of the right kidney. They are "dirty" shadows since they are more echogenic

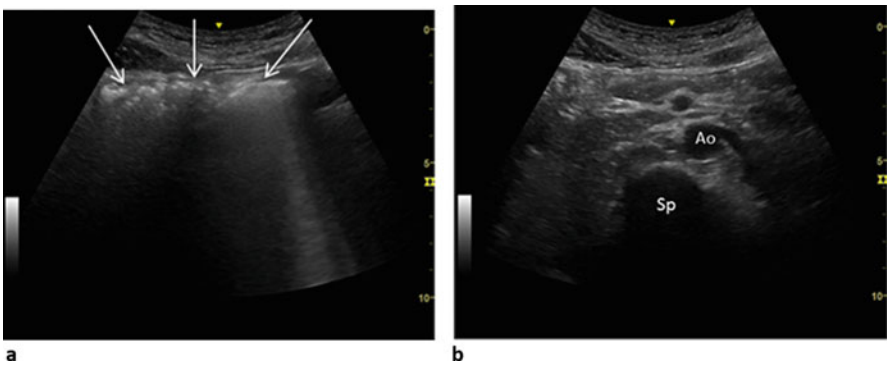

Fig. 2.44 Effect of bowel gas shadowing. (**a**) This transverse image through the mid abdomen shows multiple bright arcs (*arrows*) with "dirty" shadows deep to them. This is a classic appearance of shadowing caused by bowel gas. The intra-abdominal structures are obscured by the shadowing. (**b**) The same view was obtained while applying more pressure to the transducer which displaced the gas filled bowel loops. Deeper structures such as the abdominal aorta (*Ao*) and spine (*Sp*) are visible on this image without the obscuration by bowel gas

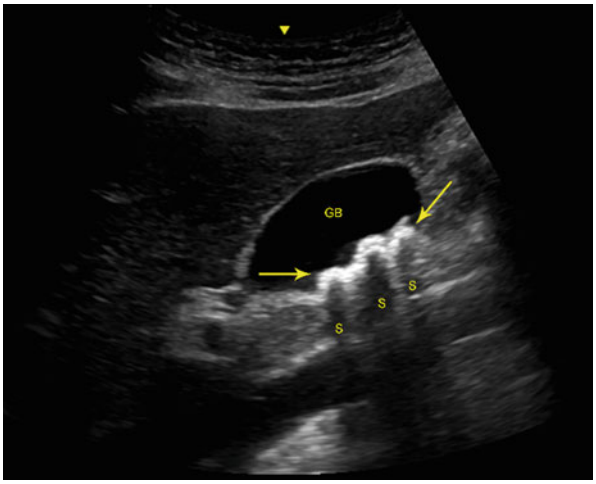

Fig. 2.45 Gallstones. Multiple echogenic stones (*arrows*) are seen in the gallbladder (*GB*). Note the shadowing (*S*) deep to the stones

2.14.2 Enhancement

Acoustic enhancement, also called increased through transmission, is seen as a vertical band of increased echogenicity deep to a structure. This is in contrast to the decreased echogenicity seen with shadowing. Structures that exhibit posterior enhancement allow greater transmission of sound waves than adjacent structures at the same depth. Since there is less attenuation of the sound waves, relatively more

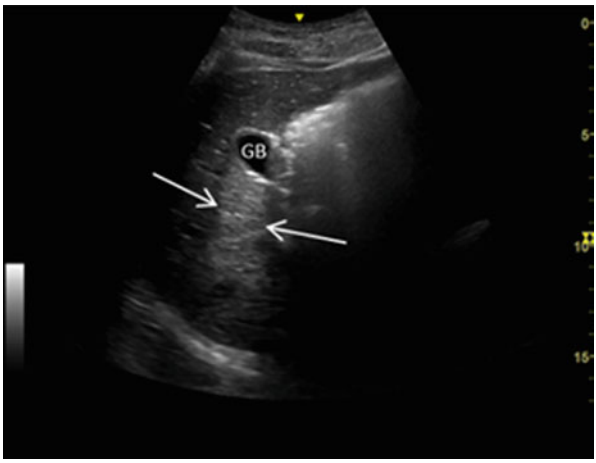

Fig. 2.46 Acoustic enhancement. This transverse view of the liver shows acoustic enhancement as a band of relatively increased echogenicity (*arrows*) extending deep to the gallbladder (*GB*)

echoes are generated from the tissues deep to that structure. This accounts for the increased brightness deep to the involved structure. Fluid filled structures allow good transmission of sound waves. For this reason, posterior enhancement can be seen deep to normal structures such as the gallbladder (Fig. 2.46) and the urinary bladder. Cysts in various organs also produce posterior enhancement.

2.14.3 Mirror Image

This artifact occurs when incident ultrasound waves encounter a highly reflective interface such as the one between aerated lung and the diaphragm. The sound waves reflecting off such an interface interact with more superficial structures on their way back to the probe. Specifically some are redirected back to the highly reflective interface before ultimately returning to the probe as secondary echoes. The result is a mirroring effect. This display deep to the interface looks like a mirror image of the structures superficial to the interface. It is commonly seen at the interface between tracheal rings and the air in the lumen of the trachea when imaging the thyroid gland (Fig. 2.47). Figure 2.48 illustrates mirror images of the cricoid and tracheal cartilages when imaging over the airway. Mirror image artifact is also commonly seen at the interface between the right hemidiaphragm and the lung when imaging the right upper quadrant (Fig. 2.49).

2.14.4 Reverberation

Reverberation artifact occurs when sound waves bounce back and forth between two highly reflective surfaces. A common source of this artifact is reverberation between

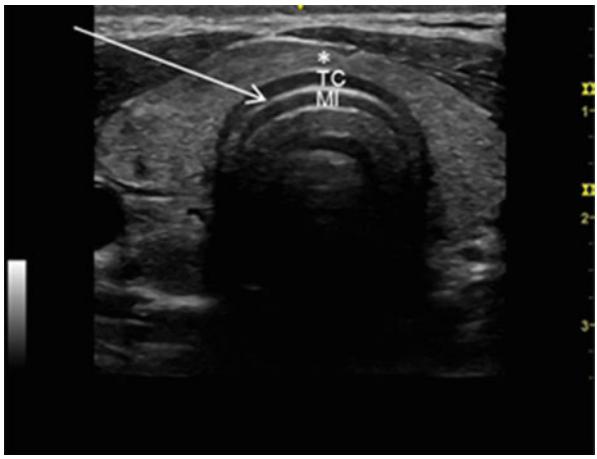

Fig. 2.47 Mirror image of tracheal cartilage. This transverse view through the thyroid gland shows a tracheal cartilage ring (*TC*) as a hypoechoic arc deep to the isthmus (*asterisk*) of the thyroid gland. The bright echogenic arc (*arrow*) deep to the tracheal ring is caused by air in the tracheal lumen. The hypoechoic arc deep to the air is a mirror image (*MI*) of the tracheal ring

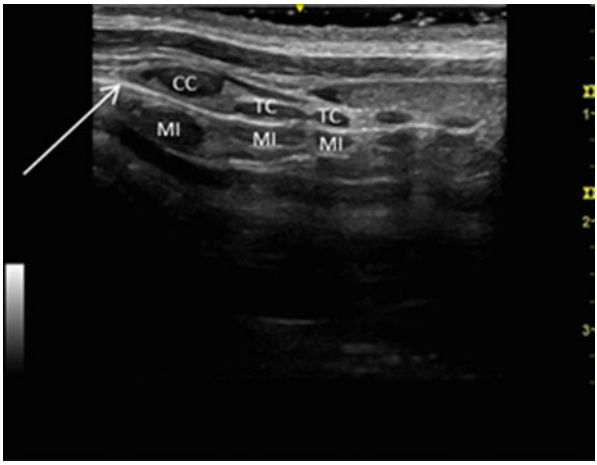

Fig. 2.48 Mirror image of cricoid and tracheal cartilages. This longitudinal view of the airway below the level of the thyroid cartilage shows the cricoid cartilage (*CC*) and tracheal cartilage rings (*TC*) as oval hypoechoic structures. The thin echogenic line (*arrow*) immediately deep to those cartilages represents air in the lumen of the airway. Note the mirror images (*MI*) of the cartilages just deep to the air interface

a reflective surface in the body and the ultrasound probe itself. In this circumstance, some of the echoes returning from a highly reflective interface reflect off the probe and re-enter the body. Those re-entrant sound waves then reflect off the same interface again and return to the probe to be processed by the ultrasound machine. Since the second set of returning echoes takes twice as long to reach the probe, a copy of the interface is displayed twice as deep as the original. Multiple copies of the interface can be displayed if the reverberation process occurs multiple times. Each copy is displayed at regular intervals equal to the depth from the skin to the interface. This reverberation artifact is regularly seen when imaging the lungs/pleura. The interface between the aerated lungs and the pleura is highly reflective and is displayed as a thin bright line. Reverberations occur between that interface and the probe leading to copies of that pleural line deeper on the image. These copies are referred to as "A-lines" and occur at intervals equal to the distance from the skin surface to the lung/pleura interface. Examples of "A-lines" are shown in Fig. 2.50.

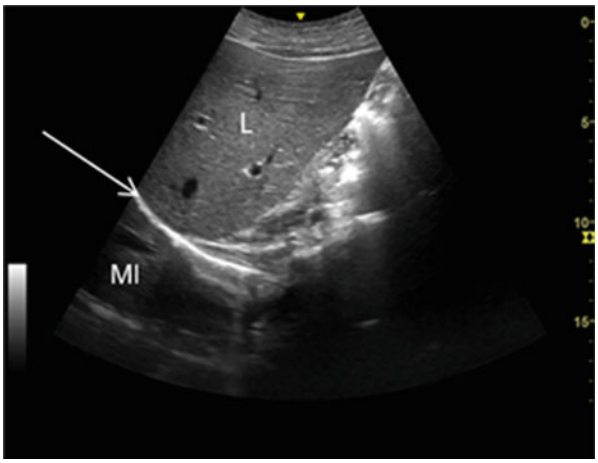

Fig. 2.49 Mirror image of liver. This is a longitudinal view of the right lobe of the liver (*L*). The diaphragm is the curvilinear echogenic structure (*arrow*). Note the mirror image of the liver (*MI*) that is displayed cephalad to the diaphragm

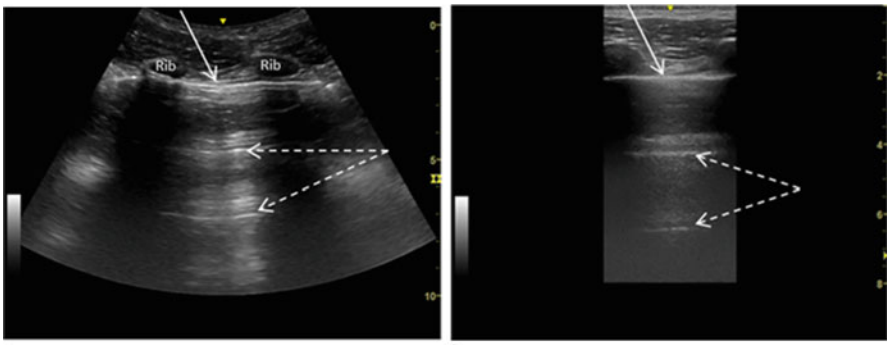

Fig. 2.50 Reverberation artifact. (**a**) This image which was obtained through an intercostal space with a curvilinear transducer shows two ribs casting anechoic shadows. The pleural line (*solid arrow*) is seen as a thin echogenic line just deep to the posterior borders of the ribs. Two repetitions of that pleural line are displayed deeper on the screen (*dashed arrows*). These reverberation artifacts are called A-lines. (**b**) This image was obtained through an intercostal space with a linear transducer. Note the A-lines (dashed arrows) caused by reverberations from the pleural line (*solid arrow*)

2.14.5 Ring Down

This type of artifact occurs when incident sound waves interact with tissues in a manner that results in continuous sound emanation. The ultrasound machine displays this continuous sound as a vertical band of increased echogenicity deep to the

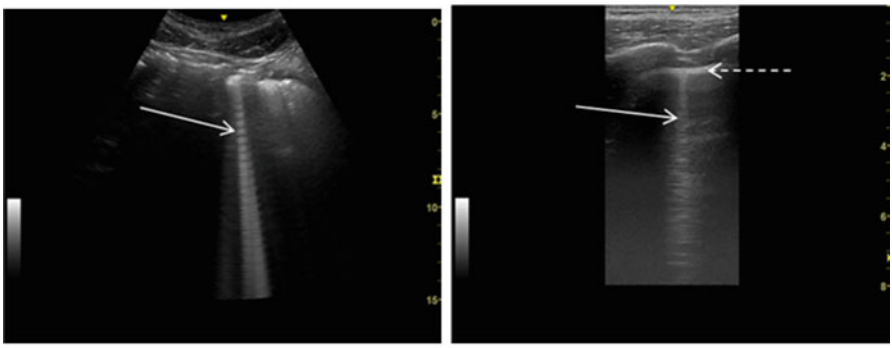

Fig. 2.51 Ring down artifact. (**a**) Transverse image through the mid abdomen shows ring down artifact from air within bowel. It is seen as an echogenic beam (arrow) extending from the bowel to the deep edge of the field of view. Intra-abdominal structures are obscured by the bowel gas. (**b**) Longitudinal view through an anterior intercostal space shows a B-line as an echogenic beam (*solid arrow)* arising from the pleural line (*dashed arrow*) and extending to the deep edge of the field of view

site of origin. The mechanism for this type of artifact is thought to be resonant vibrations arising from air bubbles. Ring down artifacts can be encountered intermittently when the ultrasound beam interacts with segments of bowel which contain air bubbles (Fig. 2.51a). Ring down artifacts seen during lung scanning are referred to as B-lines. An increase in B-lines can be seen in the setting of pulmonary edema. Figure 2.51b shows an example of a "B-line."

2.14.6 Comet Tail

This is a subtype of reverberation artifact. It occurs due to multiple short distance reverberations of sound waves between highly reflective surfaces. Comet tail artifacts are recognized as vertical streaks of increased echogenicity extending deep to a structure. The deeper parts of these streaks taper and become progressively less echogenic due to eventual attenuation of the energy from the original incoming waves. Comet tail artifacts may be normally encountered at the interface between the diaphragm and the air filled lung as seen in Fig. 2.52.

2.14.7 Anisotropy

This is a specific type of artifact that can occur when imaging linearly organized structures such as tendons or ligaments. If the ultrasound beam does not strike the tendon/ligament in a perpendicular fashion, dark hypoechoic areas appear within

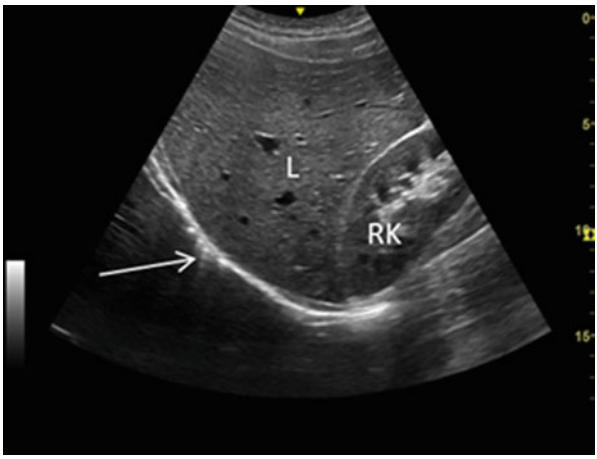

Fig. 2.52 Comet tail artifacts. This longitudinal view of the liver (*L*) and right kidney (*RK*) shows comet tail artifacts as short echogenic streaks arising from the diaphragm/lung interface (*arrow*)

the structure. This type of artifact can be corrected by changing the orientation of the probe such that the incident sound waves are perpendicular to the structure of interest. Determining whether the hypoechoic areas resolve is important when trying to distinguish pathology from this anisotropy artifact. Figure 2.53 shows the difference in the appearance of the quadriceps tendon with and without anisotropy artifact.

2.14.8 Loss of Contact

This artifact occurs when a portion of the probe loses contact with the skin. The sound waves emitted from that portion of the probe do not enter the body. Instead they immediately reflect back to the probe once they encounter air. The result is a dark vertical band on the image display corresponding to the segment of the probe that is not touching the skin surface. Figure 2.54 shows the difference between an image with loss of contact artifact and one without it.

2.14.9 Edge Artifact

This is shadowing that occurs at the edges of a curved structure. The mechanism is refraction of the incident ultrasound waves that leads to decreased echo signal returning from the tissues deep to the edges of that structure. On the image, this artifact is recognized as thin vertical hypoechoic streaks deep to the margins of the curved structure. This type of artifact is commonly seen associated with the edges of vessels coursing through the liver (Fig. 2.55) as well as the edges of the gallbladder (Fig. 2.56). Figure 2.57 shows multiple artifacts including edge artifact from the gallbladder and “dirty” shadowing from bowel.

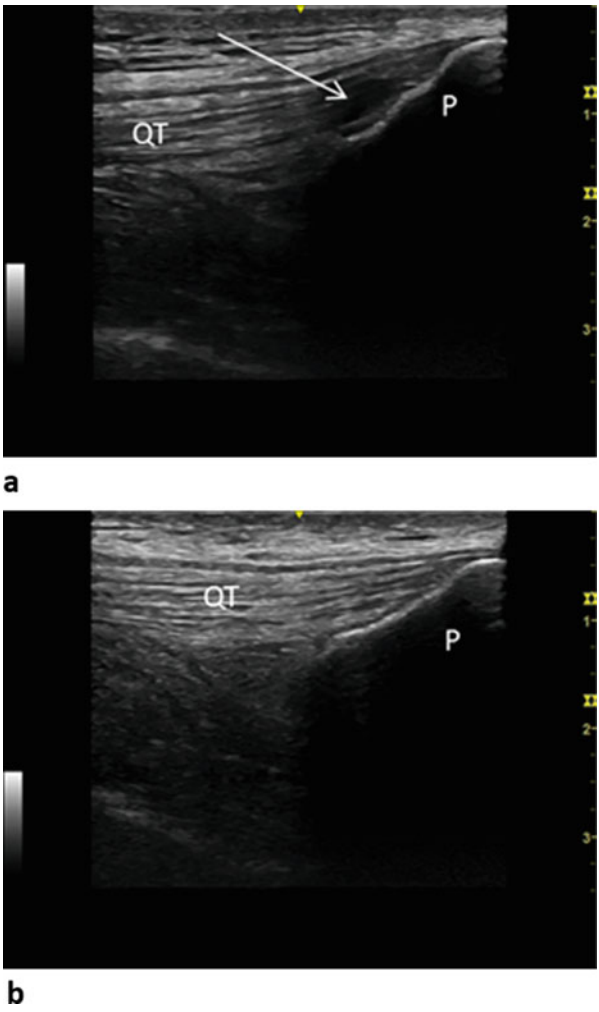

Fig. 2.53 Anisotropy artifact. (**a**) Longitudinal suprapatellar view of the knee shows anisotropy artifact (*arrow*) as an area of decreased echogenicity in a portion of the quadriceps tendon (*QT*) near the patella (*P*). (**b**) Same view obtained with the ultrasound beam oriented perpendicular to the course of the quadriceps tendon. The parallel fibers within the tendon can be readily seen without the hypoechoic anisotropy artifact

2.14.10 Aliasing

Aliasing is an artifact that occurs during Doppler imaging. It manifests as a "wrap-around" effect on the spectral or color Doppler display when the velocity scale range is too low. With spectral Doppler, a portion of a waveform on the positive side of the graph can "wrap-around" to the negative side of the graph and vice versa. If positive direction flow is faster than the upper limit setting for a color Doppler velocity scale, there is a "wrap around" effect such that the flow is displayed as a color on the negative side of the scale. Figure 2.58 shows aliasing artifact on spectral and color Doppler images.

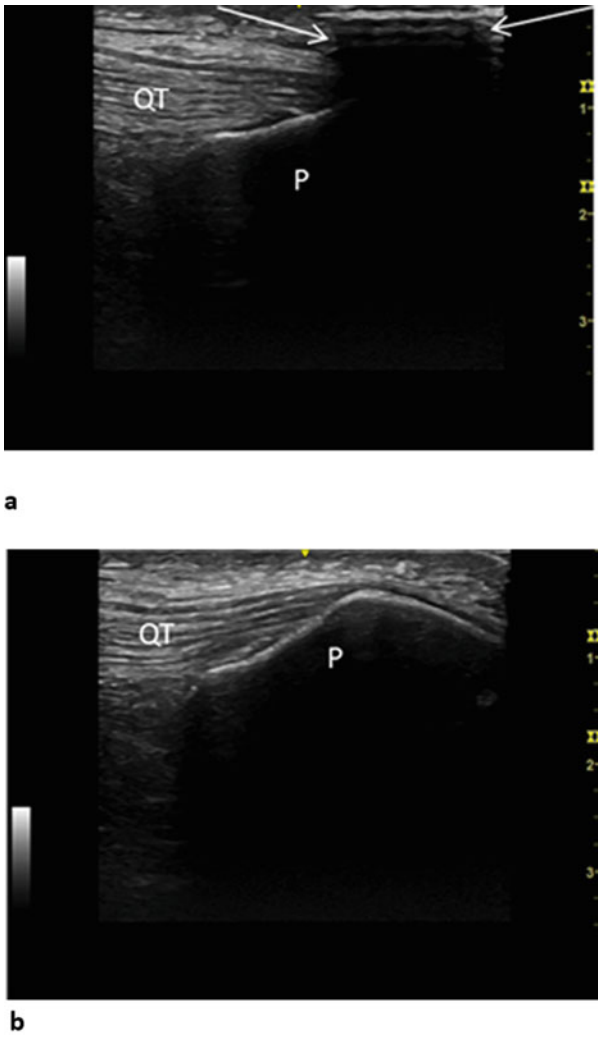

Fig. 2.54 Loss of contact artifact. (**a**) Longitudinal suprapatellar view of the knee shows a vertical dark band (*arrows*) on the right side of the image. This is due to loss of contact between the inferior aspect of the probe and the skin overlying the patella (*P*). (**b**) The same view was obtained with the transducer completely applied to the skin surface overlying the patella. Note the lack of the vertical dark band and better visualization of the patella. *QT* = quadriceps tendon

2.15 Safety Considerations

2.15.1 Output Power

Output power refers to the total energy of the ultrasound pulse passing through a surface per unit of time. The unit of power is Watts. Increasing the power of the ultrasound beam leads to stronger returning echoes. A stronger returning echo signal in turn leads to brighter images on a B-mode scan. The output level is typically displayed as a percentage of the maximum. The tradeoff is that higher power output has a greater likelihood of causing biologic effects. The output should be kept at the

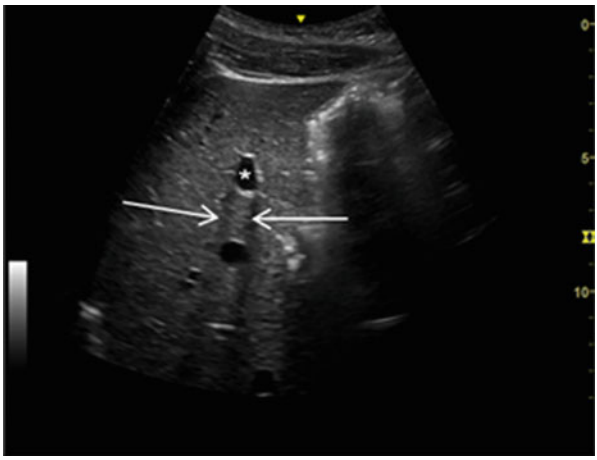

Fig. 2.55 Edge artifact from liver vasculature. This view of the liver demonstrates edge shadowing as two vertical hypoechoic streaks (*arrows*) arising from the margins of a branch of the left portal vein (*)

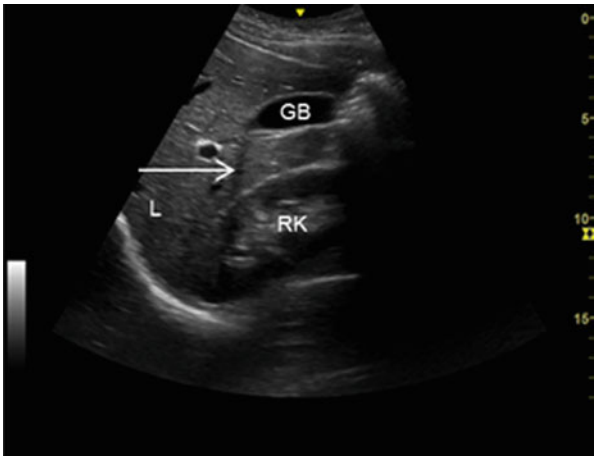

Fig. 2.56 Edge artifact from the gallbladder. This long axis view of the gallbladder (*GB*) demonstrates an edge shadow (*arrow*) as a dark streak arising from the neck of the gallbladder. It courses through the deep aspect of the liver (*L*) and upper pole of the right kidney (*RK*)

level set by the manufacturer unless high quality images cannot be obtained by altering other parameters like gain and frequency.

Intensity refers to the level of concentration of the energy in an ultrasound beam. It accounts for the area of the ultrasound beam. Specifically, intensity is the total energy per unit area per unit time. It is expressed as Watts per square centimeter. Intensity changes with the width of the ultrasound beam such that a narrower beam has a higher intensity. Power and intensity are both measures of the strength of an ultrasound beam.

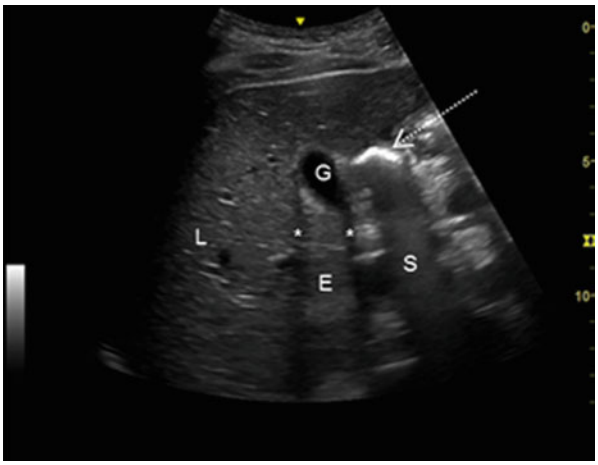

Fig. 2.57 Multiple artifacts. This transverse view through the liver (*L*) and gallbladder (*G*) shows edge artifacts as two vertical hypoechoic streaks (*asterisks*) arising from the margins of the gallbladder. The liver deep to the gallbladder appears slightly more echogenic than the remainder of the liver due to acoustic enhancement (*E*) from the fluid filled gallbladder. The hyperechoic arc (*dashed arrow*) on the right side of the screen with a bright band extending deep to it is caused by a gas filled loop of bowel with dirty shadowing (*S*)

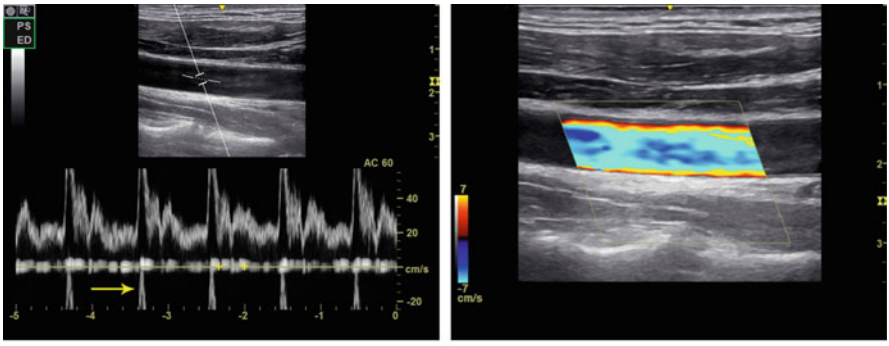

Fig. 2.58 Aliasing. (**a**) Spectral Doppler image of a common carotid artery with the velocity range set too low. Notice that the peaks of the positive direction velocities during systole extend beyond the top end of the graph. They "wrap-around" to the bottom of the graph below the "zero" velocity line in the negative direction side. The *arrow* indicates one of these peaks that has "wrapped-around." **(b)** Color Doppler of the same common carotid artery with the velocity range set too low. With an appropriate range, the lumen would fill in with shades of red and yellow. Since the range is too low, velocities that are greater than 7 cm/s "wrap-around" to be displayed in shades of blue. The darker blue areas correspond to the highest velocities

2.15.2 Mechanical Index

Mechanical index (MI) gives an estimate of the risk of inducing non-thermal biologic effects such as cavitation. Cavitation can occur due to the interaction of ultrasound waves with gas bubbles. Specifically, alternating contraction and expansion of the gas bubbles caused by cyclic pressure changes related to the ultrasound waves can lead to cavitation. Sites containing sufficient gas bodies for cavitation include the lung and intestine. In laboratory mammals, 0.4 is the threshold MI for pulmonary capillary hemorrhage, and the threshold for intestinal capillary hemorrhage is 1.4. The implications for human exposure is uncertain according to the AIUM.

2.15.3 Thermal Index

Ultrasound output can induce heating of the tissues that are scanned. Thermal index (TI) provides an estimate of the risk of these heating effects. TI is defined as a ratio of the output power of the ultrasound beam to the output power known to raise the temperature of specific tissue by 1 °C. A TI value is only an estimate of the actual temperature increase in tissues and can underestimate or overestimate the maximum temperature change by a factor of 2. Thus, a scan with a TI of 1.0 could potentially have a rise in temperature of 2 °C. Actual temperature increases are dependent on ultrasound output characteristics, tissue properties, and length of scan time. All other factors being equal, color Doppler leads to greater temperature elevations than B-mode and spectral Doppler leads to greater elevations than color Doppler. The AIUM has published recommended maximum scan times for specific ranges for TI.

2.15.4 ALARA

ALARA stands for “as low as reasonably achievable.” This an important patient safety principle that is intended to reduce risks associated with various imaging modalities. Regarding ultrasound, risks can be minimized by keeping output parameters and scan time as low as possible for the scan or procedure. Generally ultrasound is considered a safe modality since it does not utilize ionizing radiation. The potential thermal and mechanical effects must be kept in mind. As with other forms of imaging, the risks and benefits of an ultrasound scan should be considered.

Further Reading

Aldrich JE (2007) Basic physics of ultrasound imaging. Crit Care Med 35(5):S131–S137
American Institute of Ultrasound in Medicine (2014) As Low As Reasonably Achievable (ALARA) Principle. American Institute of Ultrasound in Medicine website. https://www.aium.org/officialStatements/39. Accessed 18 December 2019
American Institute of Ultrasound in Medicine (2015) Statement on mammalian biological effects in tissues with naturally occurring gas bodies. American Institute of Ultrasound in Medicine website. http://www.aium.org/officialStatements/6. Accessed 18 December 2019
American Institute of Ultrasound in Medicine (2016a) Recommended maximum scanning times for displayed thermal index (TI) values. American Institute of Ultrasound in Medicine website. http://www.aium.org/officialStatements/65. Accessed 18 December 2019
American Institute of Ultrasound in Medicine (2016b) Statement on mammalian biological effects of heat. American Institute of Ultrasound in Medicine website. http://www.aium.org/officialStatements/17 Accessed 18 December 2019
American Institute of Ultrasound in Medicine (2019) Prudent use and clinical safety. American Institute of Ultrasound in Medicine website. http://www.aium.org/officialStatements/34. Accessed 18 December 2019
Baad M, Lu ZF, Reiser I, Paushter D (2017) Clinical significance of US artifacts. Radiographics 37:1408–1423
Bahner DP, Blickendorf JM, Bockbrader M, Adkins E, Vira A, Boulger C, Panchal AR (2016) Language of transducer manipulation: codifying terms for effective teaching. J Ultrasound Med 34:183–188
Church CC, Carstensen EL, Nyborg WL, Carson PL, Frizzell LA, Bailey MR (2008) The risk of exposure to diagnostic ultrasound in postnatal subjects: nonthermal mechanisms. J Ultrasound Med 27:565–592
Enriquez JL, Wu TS (2014) An introduction to ultrasound equipment and knobology. Crit Care Clin 30:25–45
Feldman MK, Katyal S, Blackwood MS (2009) US artifacts. Radiographics 29:1179–1189
Goldstein A (1993) Overview of the physics of US. Radiographics 13:701–704
Hangiandreou NJ (2003) B-mode US: basic concepts and new technology. Radiographics 23 (4):1019–1033
Harris GR, Church CC, Dalecki D, Ziskin MC, Bagley JE (2016) Comparison of thermal safety practice guidelines for diagnostic ultrasound exposures. Ultrasound Med Biol 42:345–357
Hertzberg BS, Middleton WD (2016) Ultrasound: the requisites, 3rd edn. Elsevier, Philadelphia, PA
Jamadar DA, Robertson BL, Jacobson JA, Girish G, Sabb BJ, Jiang Y, Morag Y (2010) Musculoskeletal sonography: important imaging pitfalls. AJR 194:216–225
Kremkau FW, Taylor KJW (1986) Artifacts in ultrasound imaging. J Ultrasound Med 5:227–237
Prabhu SJ, Kanal K, Bhargava P, Vaidya S, Dighe MK (2014) Ultrasound artifacts classification, applied physics with illustrations, and imaging appearances. Ultrasound Q 30:145–157
Robinson P (2009) Sonography of common tendon injuries. AJR 193:607–618
Scanlan KA (1991) Sonographic artifacts and their origins. AJR 156:1267–1272
Shriki J (2014) Ultrasound physics. Crit Care Clin 30:1–24
Sommer FJ, Filly RI, Minton MJ (1979) Acoustic shadowing due to refractive and reflective effects. AJR 132:973–977
Thickman DI, Ziskin MC, Goldenberg NJ, Linder BE (1983) Clinical manifestations of the comet tail artifact. J Ultrasound Med 2:225–230
Wongwaisayawan S, Suwannanon R, Sawatmongkorngul S, Kaewlai R (2016) Emergency thoracic ultrasound; the essentials. Radiographics 36:640–659
Ziskin MC (1993) Fundamental physics of ultrasound and its propagation in tissue. Radiographics 13:705–709

Chapter 3
Ultrasound of the Vascular System

L. Britt Wilson, Victor Rao, and Floyd E. Bell III

3.1 Anatomy and Physiology of the Vascular System

The cardiovascular system is composed of the heart and blood vessels and a basic diagram showing this is illustrated in Fig. 3.1. In the next chapter, we discuss the heart in more detail. As a prelude, the heart consists of two pumps (right and left ventricles) and two "receiving" chambers, the right and left atria. Within the cardiovascular system there are two circulations, the systemic (outer portion of the figure) and pulmonary circulations (inner portion showing flow to the lungs). The vasculature for these circulations contains arteries, arterioles (small, muscular arteries) capillaries, venules (small veins), and veins. The fundamental function of the systemic circulation is to deliver nutrients to the various tissues of the body, one very important nutrient is oxygen (O_2). Arterial blood is high in O_2, low in carbon dioxide (CO_2) and is indicated by the red in Fig. 3.1. This blood is delivered to the tissues, thus providing the nutrient O_2. It also removes waste products generated by tissue metabolism, one very important one being CO_2. Venous blood refers to blood that is low in O_2 and high in CO_2. Venous blood is depicted as blue in Fig. 3.1. The

Supplementary Information The online version contains supplementary material available at https://doi.org/10.1007/978-1-0716-1863-9_3. The videos can be accessed by scanning the related images with the SN More Media App.

L. B. Wilson (✉)
Department of Pharmacology, Physiology, and Neuroscience, University of South Carolina School of Medicine, Columbia, SC, USA
e-mail: Britt.Wilson@uscmed.sc.edu

V. Rao
Point-of-Care Ultrasound Certification Academy™ (PCA), Rockville, MD, USA

F. E. Bell III
University of South Carolina School of Medicine, Columbia, SC, United States
e-mail: Floyd.bell@uscmed.sc.edu

L. B. Wilson et al. (eds.), *Understanding Physiology with Ultrasound*, Physiology in Health and Disease, https://doi.org/10.1007/978-1-0716-1863-9_3

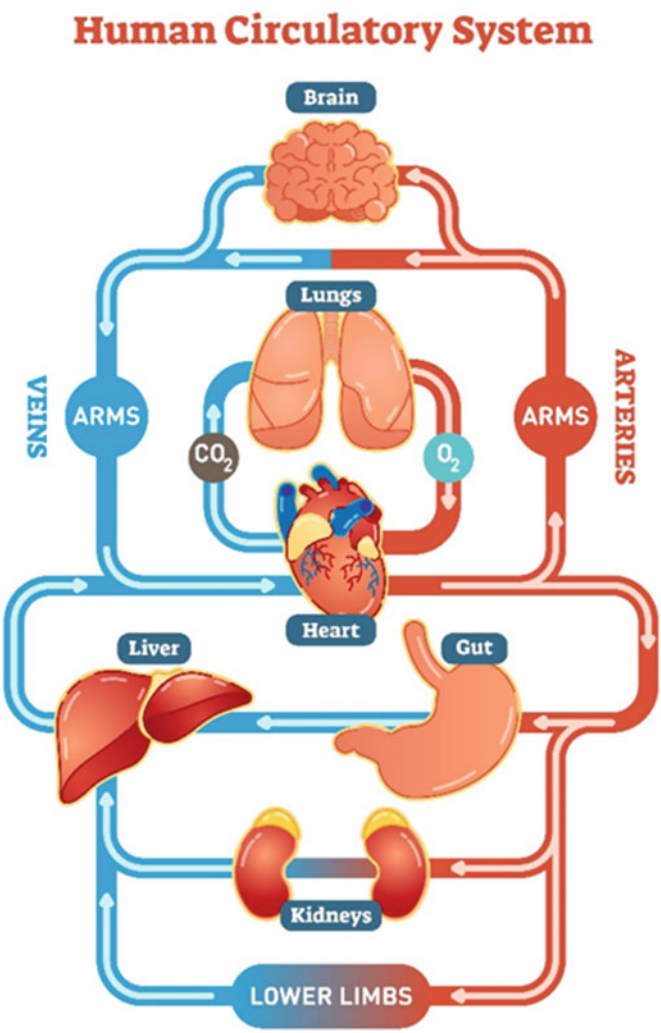

Fig. 3.1 Basic anatomy of the cardiovascular system illustrating the major arteries of the systemic circulation supplying oxygen (red indicates arterial blood) to the various organs of the body. The blue indicates venous blood

capillaries serve as the site of exchange between the tissues and the blood. Arteries carry blood to the capillaries, while veins drain blood from the capillaries. The systemic circulation begins with the left ventricle pumping blood into the aorta (largest systemic artery), which then travels through many branches of arteries and arterioles until it reaches the capillaries. From the capillaries, blood travels through numerous venules that ultimately come together to form the great veins (inferior and superior vena cava), which carry the blood to the right atrium.

Arteries have thick, muscular walls and thus don't stretch (expand) easily. This property of not being able to expand easily is termed elasticity. The inverse of elasticity is compliance, thus if a blood vessel is very compliant it means it easily expands (see also Respiratory chapter for a discussion on compliance and elasticity). Arteries and arterioles of the systemic circulation are not very compliant. The pressure inside the blood vessels of the arterial system is much higher than on the venous side. As a result, these vessels need to have thick muscular walls, which in turn reduces their compliance (increases their elasticity). Arterioles serve as the major site of resistance in the systemic circulation, and this is discussed in more detail in the hemodynamics section. Veins on the other hand have very thin walls and not a lot of smooth muscle. As a result, veins and venules are very compliant and thus are easily stretched. Because of this, most of the blood volume resides in these very compliant veins and venules.

The right ventricle pumps blood into the pulmonary artery, the start of the pulmonary circulation. Similar to the systemic circulation, hundreds of branches of blood vessels ultimately come off of the pulmonary artery carrying the blood to the pulmonary capillaries. Just like the systemic circulation, capillaries serve as the site of exchange, except here, O_2 and CO_2 move in opposite directions compared to the systemic circulation. Specifically, O_2 moves into the blood and CO_2 leaves the blood. This oxygenated blood then returns to the left atrium and then left ventricle, and in turn, is pumped to the tissues of the systemic circulation.

Ultrasound (US) can be very useful in determining if blood coursing the circulations is normal or abnormal. Cardiovascular disease is still the number one killer worldwide (see American Heart Association website) and one of the primary problems involves blocking or clogging of arteries. Basically, buildup (commonly referred to as plaque) occurs along the inside of a blood vessel, in turn causing the lumen diameter to become smaller. In some cases, debris from these plaques can break off, lodging in a blood vessel and stopping blood flow. Lack of O_2 delivery results in tissue death. When it occurs in the heart, it produces a myocardial infarction (MI or heart attack) and if in the brain, it produces a stroke (ischemic stroke). Some larger vessels may develop a narrowing because of plague buildup resulting in stenosis, e.g., carotid artery stenosis. US is one tool that can detect stenosis of blood vessels. To understand why, let's first discuss the normal physiology of blood flow, often referred to as hemodynamics.

3.2 Hemodynamics

3.2.1 Pressure/Flow/Resistance

Hemodynamics defines the physical properties that govern blood flow (Q) in the vascular system. More specifically, Q is directly proportional to the pressure gradient (ΔP) and inversely related to the resistance (R). There must be a pressure gradient to drive Q and blood always flows from higher pressure (P_1) to lower pressure (P_2). The mathematical relation is shown below. The factors influencing R are also defined

below, but given that radius (r) is to the 4th power one can easily see this is the most important factor for R. The other factor important for human physiology, is viscosity of the blood. Very simply, viscosity (honey is a good example of a very viscous liquid) refers to the relative "thickness" of the blood and the most important factor influencing viscosity is the hematocrit. Hematocrit refers the ratio of the volume of red blood cells to the total volume of blood. Normally, about 40% of the blood volume is occupied by red cells. Anemia is a condition in which the hematocrit is below normal, while polycythemia refers to an above normal hematocrit. Thus, anemia reduces the resistance to flow, while polycythemia increases the resistance to flow.

$$Q = (P_1 - P_2)/R,$$

where Q = flow; P = pressure; R = resistance

$$R = (8^{*}L^{*}\text{viscosity})/\left(\pi r^4\right),$$

where R = resistance; r = radius.

3.2.2 Velocity

A second factor involved in hemodynamics relates to the velocity (v) of blood coursing through the systemic and pulmonary circulations. Flow is a volume per unit time, while velocity is the speed, e.g., cm/s by which blood courses through a blood vessel. Although related (see below), these two concepts must be differentiated because US determines velocity, not flow.

$$\text{Velocity} = Q/\text{CSA},$$

where Q = flow; CSA = cross-sectional area.

3.2.3 Turbulence

Another key physiologic concept related to US of the vasculature is turbulence. As indicated in Fig. 3.2 (left panel), blood flow in the vasculature is normally laminar. When Q is laminar, then the aforementioned relationship ($Q = \Delta P/R$) is applicable. However, if Q becomes turbulent (Fig. 3.2, right panel), then the normal P, Q, R

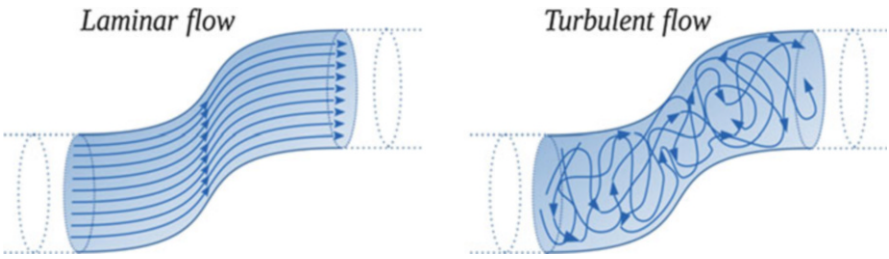

Fig. 3.2 Two flow patterns that can occur in the vascular system. The left shows laminar flow. This is the typical flow pattern in the cardiovascular system. The right shows turbulent flow, which occurs when Reynold's number exceeds 2000. See text for conditions and consequences that occur when flow becomes turbulent

relation is altered, the most important being that R is greatly elevated. Whether or not Q is turbulent is defined by Reynold's number (defined below). If Reynold's number exceeds 2000, then flow transitions from the normal laminar flow to turbulent flow. Note that velocity is in the numerator and a high velocity state is the most common reason for turbulence in a systemic blood vessel. Because US determines velocity, it is this variable that is measured when one suspects a pathologic alteration in a given patient, e.g., stenosis (see above). A stenotic peripheral artery has a markedly reduced cross-sectional area, thus a very high velocity (see equation above), which in turn can be detected by US. As a side note, this is a good opportunity to remind the student that turbulent, but not laminar flow, can be heard and an abnormal sound in a peripheral blood vessel is called a bruit. In addition, note that viscosity is in the denominator. Thus, a patient with anemia might have turbulent flow, particularly in a large diameter blood vessel with high velocity (note: both are in the numerator), e.g., the aorta.

$$\text{Reynold's number} = \frac{\text{Velocity X diameter X density}}{\text{Viscosity}}$$

3.2.4 Extravascular Pressure

If the pressure surrounding a blood vessel (extravascular pressure) changes, then it can alter blood flow within a vessel. Specifically, if extravascular pressure increases, the blood vessel can be compressed or collapse. Alternatively, if extravascular pressure decreases, the vessel remains open and blood flow is not compromised. The blood vessels that are primarily affected by this extravascular force are veins, venules, and capillaries. As indicated earlier in this chapter, veins are very compliant and thus greatly expand when intravascular pressure goes up. On the other hand, if the pressure outside of the veins goes up, then they can be compressed, reducing their size. This can easily be seen in the jugular vein when a subject performs a Valsalva maneuver. Here we cover the physiology of the Valsalva and it can be applied to the internal jugular vein procedure described below.

In between the lungs and chest wall is a fluid-filled space referred to as the intrapleural space (see also Respiratory chapter). In short, it is a membrane that is folded back on itself (imagine pushing your fist into a large balloon and the balloon wrapping itself around your fist). Since it contains fluid, it has a pressure. This intrapleural pressure (IPP) plays a pivotal role in the physiology of ventilation and the cardiovascular system because it is the pressure surrounding every structure inside the chest, including the blood vessels. Although the details are beyond the scope of this book, the lungs have an inward force and the chest wall has an outward force at rest. Thus, the intrapleural space is being "pulled" in opposite directions. In short, it is being "stretched" from the sides. This causes the pressure inside (IPP) to be less than atmospheric pressure. For convenience, atmospheric pressure is considered to be zero mmHg (this is because it is relatively constant at any given location). Because IPP is less than atmosphere and atmospheric pressure is zero, IPP is negative. This means that in the resting state, the pressure outside the veins in the chest is negative. In short, this negative pressure acts like a vacuum, pulling open the very compliant veins, thereby helping to keep them open.

The Valsalva maneuver is a forced expiration (breathe out) against a closed glottis (meaning air does not come out even though one is "trying" to push it out). The bearing down during defecation is an example of a Valsalva maneuver. The forced expiratory effort pushes the chest wall down and inward, thereby "squeezing" the intrapleural space, in turn causing IPP to become positive. This positive IPP compresses the great veins, causing their diameter to decrease and thus blood flow to fall. This compression of the great veins causes pressure inside the veins leading into the chest, e.g., internal jugular vein, to rise and because they are compliant, they expand. As indicated, this is one of the procedures described below and it can be a very dramatic visualization illustrating compliance of veins.

3.3 Vascular Ultrasound: Settings

3.3.1 Preset

The vascular application preset is recommended for the assessment of the vascular hemodynamics. You can also choose the preset for a specific blood vessel for best results. It is important to select the correct preset for a particular exam for best results.

3.3.2 Color Doppler

Color Doppler mode helps to identify flow in a blood vessel (Fig. 3.3). It superimposes a color Doppler box on the B-mode image and if there is any movement seen within that box, then the system overlays a color code in that region. The color Doppler gives us directional information about the flow, and a gross estimate of the velocity. For more quantitative information you must perform spectral Doppler (Fig. 3.4).

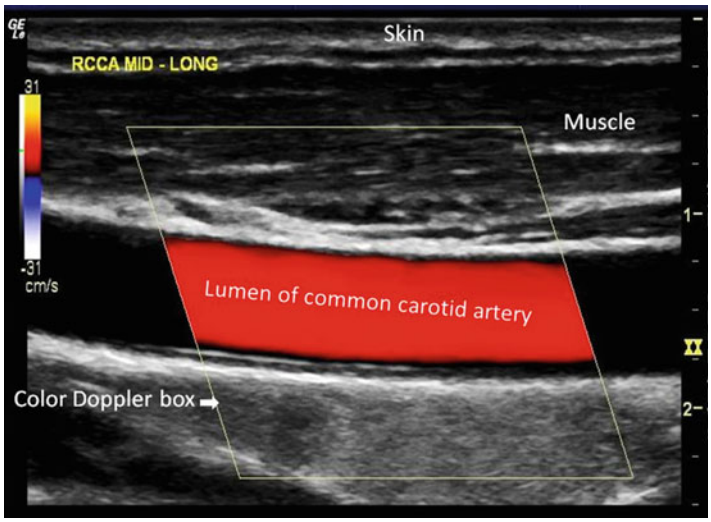

Fig. 3.3 This shows a typical color Doppler display on a B-mode image with a color Doppler legend displayed on the left side of the monitor

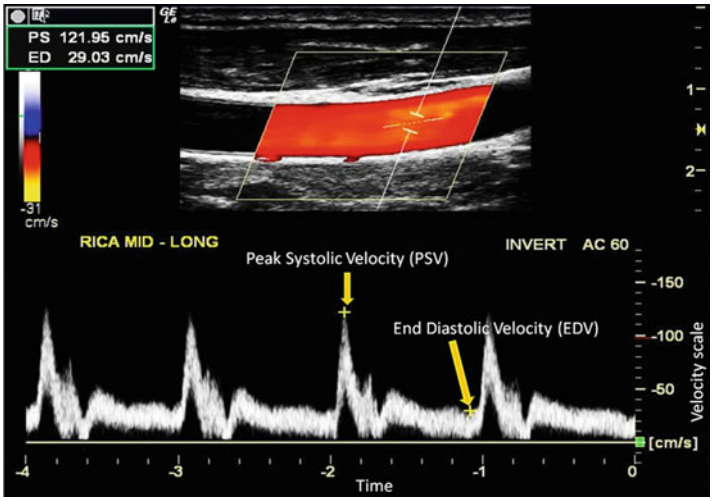

Fig. 3.4 This shows a typical spectral Doppler display. The spectral Doppler display is shown below the B-mode + color Doppler image

Always observe the color Doppler legend on the monitor (left-hand side in Figs. 3.3 and 3.4). By default, the red and yellow colors represent flow towards the transducer and the blue and light blue represent flow away from the transducer. In these figures, yellow represents faster velocity than red and lighter blue represents faster velocity than darker blue.

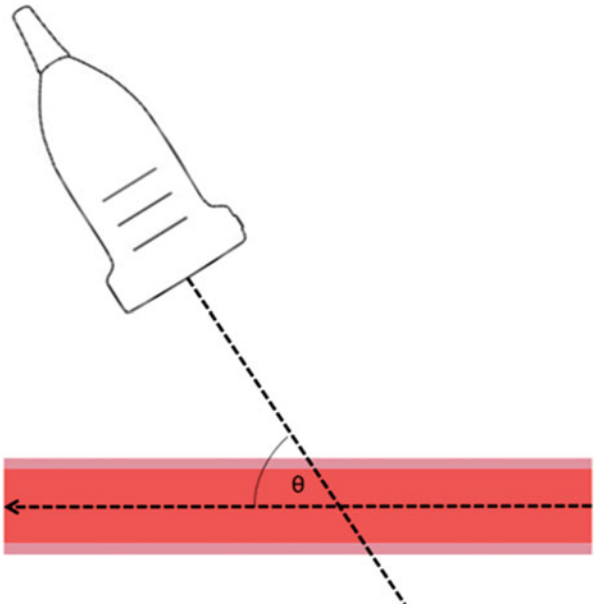

Fig. 3.5 Doppler angle Θ. The ultrasound transducer is transmitting a Doppler ultrasound beam. Observe the angle Θ that is the angle of insonation (Doppler angle) of the ultrasound beam to the blood flow in the blood vessel lumen

3.3.3 Spectral Doppler

Figure 3.5 below shows the formation of the Doppler angle Θ. This is also known as the angle of insonation of the ultrasound beam to the direction of blood flow. In the figure below, the blood flow is seen from the right to the left of the image inside the blood vessel. The dotted line is representing the Doppler ultrasound beam. This angle should ideally be close to zero which may be difficult to achieve. So, a Doppler angle of up to 45–60 degrees is acceptable when performing Carotid Doppler studies in the neck. As we understand the Doppler equation, it will become clear why this angle must be close to zero.

3.3.4 Doppler Equation

Figure 3.6 shows the Doppler equation and the formation of the Doppler angle Θ. Note, that in this example, the blood flow is seen moving from the left of the screen to the right. This scenario can be seen in the lower extremity (example—femoral or popliteal artery). The velocity of the blood (V) is calculated from the Doppler frequency shift Fd. So, the velocity of blood in the target blood vessel in the sample volume region is determined by the equation $V = (Fd \times c)/(2 \times Ft \times \cos\theta)$.

Fd is calculated automatically by the ultrasound system. The ultrasound system knows what frequency Doppler ultrasound beam pulse it transmits into the body

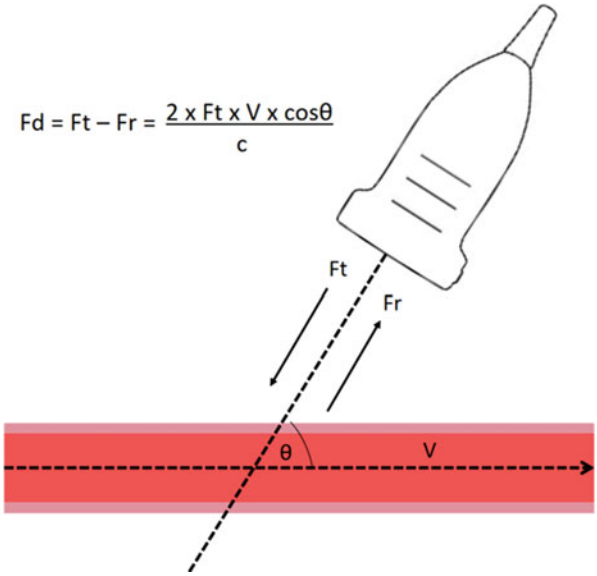

Fig. 3.6 Doppler equation. Note the angle between the Doppler beam and the flowing blood θ. The Doppler shift frequency is the difference in frequency between the transmitted beam frequency (Ft) and the received beam frequency (Fr). This is influenced by the velocity of the blood in the vessel (V), the insonation angle (θ), the Ft, and the speed of sound in soft tissue (c)

(Ft) and is also able to calculate the received frequency (Fr) of the Doppler beam returning to the probe. "C" is the velocity of ultrasound beam in human tissue. Even though the velocity of the ultrasound beam is slightly different in blood, the ultrasound device manufacturers plug in a fixed value of 1540 m/s for "c" in the algorithm.

While performing spectral Doppler, most ultrasound devices are dependent on the user to align the Doppler cursor correctly with the direction of blood flow. So, it is critical to align the Doppler cursor correctly using the heel-toe maneuver on the ultrasound probe and also ensure at the same time that the Doppler angle Θ is up to a maximum of 60 degrees. Doppler angle more than 60 degrees is not acceptable as the accuracy of the velocity calculation drops dramatically.

For Doppler studies of the carotid arteries and the extremities, some institutions use a fixed value of 60 degrees. Keep in mind that if the Doppler angle is 90 degrees then the calculated velocity will be zero because the value of cosine 90 is zero. During echocardiography, while evaluating flow across the mitral and aortic valves, a Doppler angle close to zero is possible and that results in the most accurate velocity readings. So, a Doppler insonation angle of zero to 15 degrees is recommended for those studies.

3.4 US Laboratory Exercises

In this section, we indicate laboratory exercises for students. The first involves visualizing the common carotid artery and internal jugular vein. These can be seen on ultrasound, but adding in color Doppler and determining pulse wave velocities really adds to the laboratory teaching physiologic concepts. While other vessels can

be visualized and we discuss them below, the carotid artery and jugular vein are the most convenient.

3.4.1 Exercise 1: Common Carotid Artery (CCA) and Internal Jugular Vein (IJV)

3.4.1.1 Learning Objectives

Using B-mode ultrasound, visualize the structure of the CCA and the IJV in the transverse and longitudinal planes.

Using color Doppler, see color flow in these two structures in the transverse and longitudinal planes.

3.4.1.2 Transducer/Probe

High frequency linear probe.

3.4.1.3 Additional Equipment and Supplies

None, other than those related to performing ultrasound.

3.4.1.4 Patient Position and Image Orientation

The patient should be resting comfortably in the supine position with the neck region fully exposed as shown in shown in Fig. 3.7.

An orientation marker, usually the company logo, will be on the top left side of the screen. The logo matches up with the probe marker, often a palpable ridge on one side of the probe. Whichever side of the vessel the probe marker is on, that side of the vessel will match up with the orientation marker on the screen. The top of the screen is always superficial or where the probe makes contact with the body surface.

3.4.1.5 Performing the Scan

1. Use the carotid preset
2. Apply acoustic coupling gel to the footprint of the high frequency linear transducer. Place the transducer footprint on the right side of the neck in the region overlying the common carotid artery with the probe marker pointing towards the patient's right side (See Fig. 3.7).

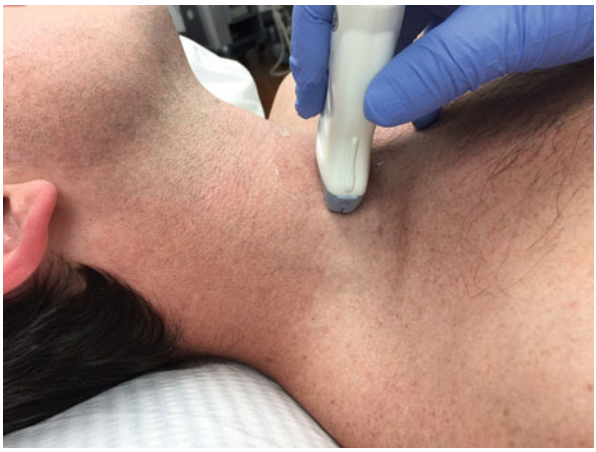

Fig. 3.7 This picture shows the correct placement of the probe to get a transverse image in which the right common carotid artery and internal jugular vein can be visualized. Note that the probe is placed on the right side of the patient's neck over the right proximal common carotid artery region

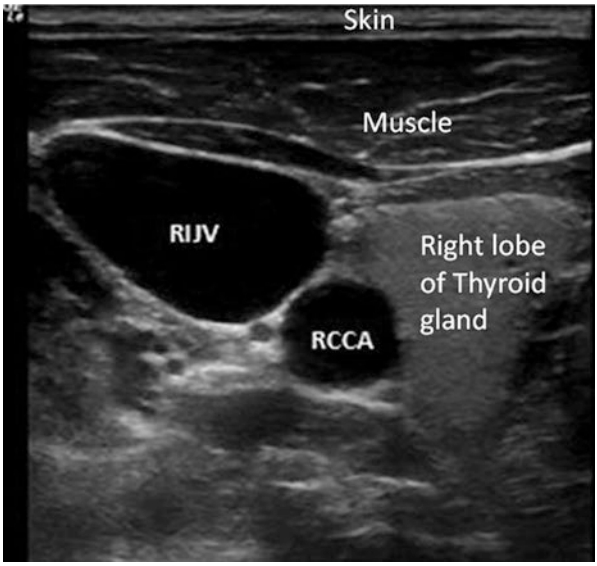

Fig. 3.8 Transverse view showing the right common carotid artery (RCCA) and the right internal jugular vein (RIJV)

3. Start scanning at the base of the neck and sweep the probe towards the head. Position the probe to orient the right common carotid artery (RCCA) in the middle of the image (See Fig. 3.8). Identify the right internal jugular vein (RIJV: Fig. 3.8). The right lobe of the thyroid may be visible just medial to the RCCA. The RCCA will be circular in cross section and will show pulsatility corresponding to the peripheral arterial pulse. The RIJV will generally appear elliptical in most patients. The RIJV will collapse easily when direct pressure is applied on it with the transducer.
4. Rotate the transducer in a clockwise direction (Fig. 3.9) to obtain a long-axis view of the RCCA. Figure 3.10 illustrates a representative image. Note the lumen of

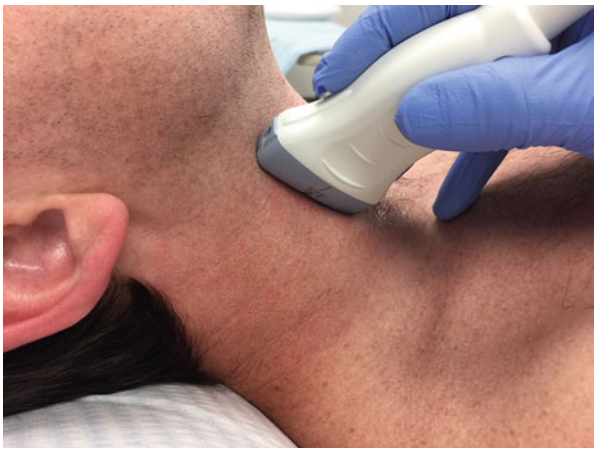

Fig. 3.9 Picture illustrating probe placement on the right side of the patient's neck over the right common carotid artery region to obtain a long axis image of the common carotid and internal jugular vein

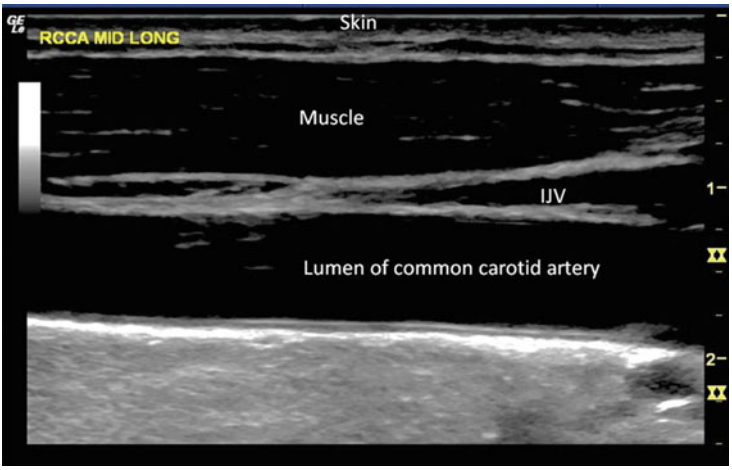

Fig. 3.10 This figure shows the B-mode long axis view of the right common carotid artery. The RIJV is barely visible just above the common carotid artery (see color Doppler image below)

the carotid artery. Depending on the patient's anatomy and position of the probe, a portion of the RIJV may be visualized on the same image. Note that the RIJV is partially visualized on Fig. 3.10 just above the RCCA. To better see the RIJV, move the probe slightly laterally.

5. Re-obtain a transverse view of the RCCA and the RIJV and activate color Doppler by pressing the CF button on the console.
6. Reposition the color box with the mouse or trackball over the two vessels mentioned above. The color box will display the red or blue color overlying the blood vessel as shown below (Fig. 3.11). Note that the red color indicates flow towards the transducer and the blue color represents flow away from the transducer.

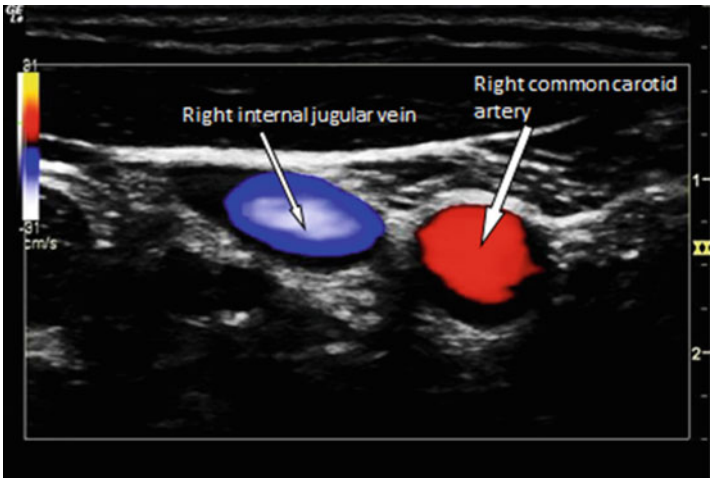

Fig. 3.11 Transverse view showing the right common carotid artery (RCCA) and the right internal jugular vein (RIJV) with color Doppler box superimposed over the vessels

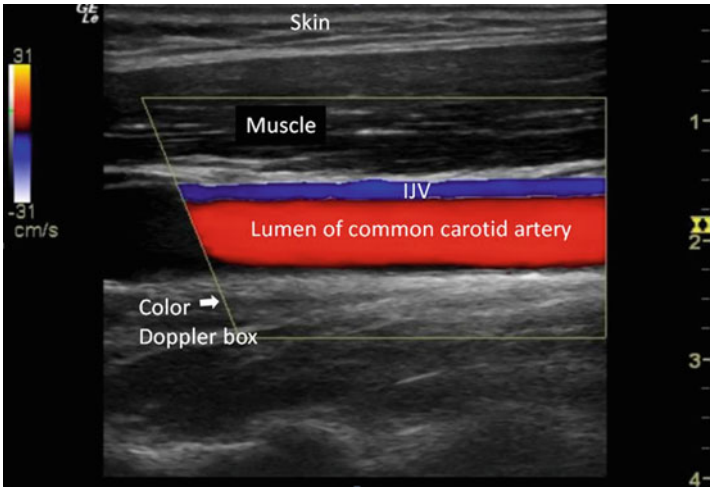

Fig. 3.12 Longitudinal view of the right common carotid artery (RCCA). The color box overlying the common carotid artery shows the red color and the RIJV is seen blue

7. As described previously, rotate the probe clockwise to reacquire a long axis image of the common carotid artery and internal jugular vein as seen in Fig. 3.12. Figure 3.13 is a video loop demonstrating opposite directions of flow in a common carotid artery and an internal jugular vein.
8. While scanning, press the B button or the 2D button to return to the B-mode imaging mode. Position the probe over the RCCA and RIJV as in Fig. 3.7 to acquire a transverse view. Ask the patient to perform a Valsalva maneuver (see

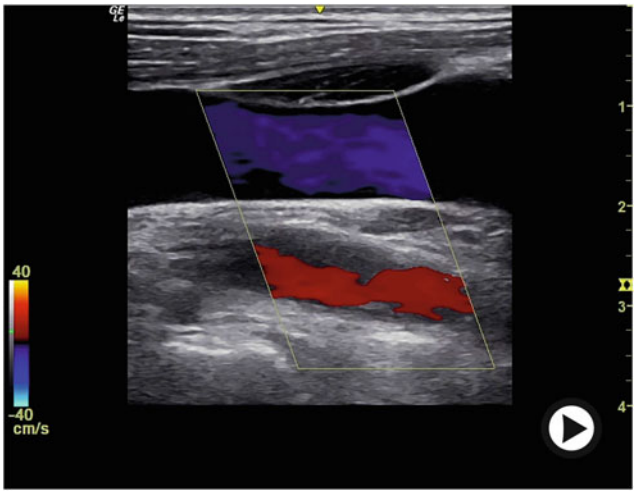

Fig. 3.13 (Video 3.1) A video loop showing a scan obtained with the transducer positioned laterally on the neck with the probe marker pointed cephalad (toward the head). This approximate coronal plane allowed visualization of both the RCCA and RIJV. The RCCA is the deeper of the two vessels on this loop. Note that the Doppler sample box is angled in such a manner that the transmitted ultrasound beam travels left to right on the screen as it moves deeper. The red color within the RCCA indicate flow is moving from right to left on the screen toward the transmitted ultrasound beam. The blue color within the RIJV indicates flow is moving left to right on the screen away from the transmitted beam (▶ https://doi.org/10.1007/000-7pk)

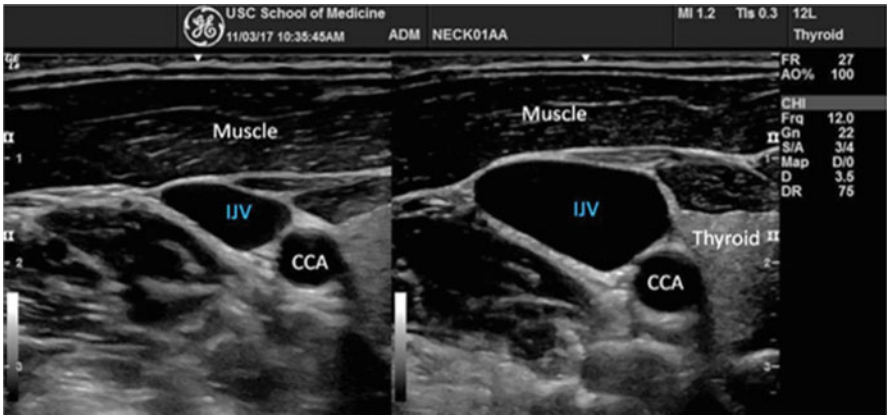

Fig. 3.14 Picture illustrating the "blowing up" of the internal jugular vein with Valsalva. Left image shows the IJV as not distended and the image on the right shows the IJV as dilated during the Valsalva maneuver

above for the physiology of the Valsalva) and observe the RIJV balloon out as shown in the figure below (Fig. 3.14). Figure 3.15 is a video loop showing the change in a RIJV with this maneuver.

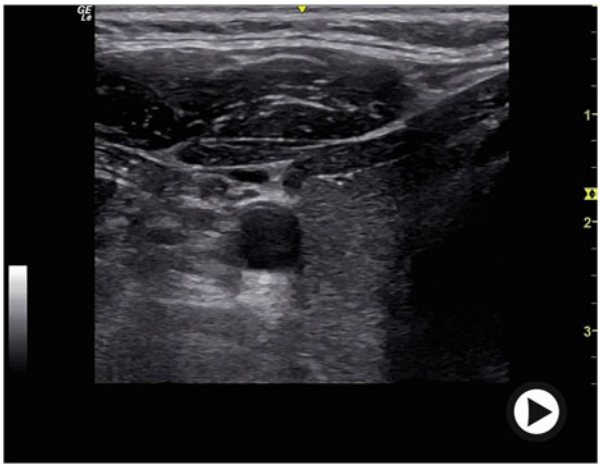

Fig. 3.15 (Video 3.2) A video illustrating distension of the RIJV during a Valsalva maneuver. Initially, the vein is small in size as the patient is upright for this loop. When the patient does the Valsalva maneuver, the vein distends and becomes more visible (▶ https://doi.org/10.1007/000-7pj)

3.4.2 Exercise 2: Quantitating Velocity in the Common Carotid Artery

3.4.2.1 Learning Objectives

The purpose of this exercise is to determine the actual velocity of blood in the common carotid artery.

3.4.2.2 Transducer/Probe

High frequency linear probe.

3.4.2.3 Additional Equipment and Supplies

None, other than those related to performing ultrasound.

3.4.2.4 Patient Position and Image Orientation

The patient should be resting comfortably in the supine patient position with the neck region fully exposed as shown in shown in Fig. 3.7.

An orientation marker, usually the company logo, will be on the top left side of the screen. The logo matches up with the probe marker, often a palpable ridge on one side of the probe. Whichever side of the vessel the probe marker is on, that side of the

vessel will match up with the orientation marker on the screen. The top of the screen is always superficial or where the probe makes contact with the body surface.

3.4.2.5 Performing the Scan

1. Use the carotid preset
2. Apply acoustic coupling gel to the footprint of the high frequency linear transducer. Place the transducer footprint on the right side of the neck in the region overlying the common carotid artery with the probe marker pointing towards the patient's head (See Fig. 3.9).
3. Obtain a mid-longitudinal view of the common carotid artery and hold the probe steady in place (Figs. 3.10).
4. Press the Pulse Wave (PW) Doppler button to activate spectral Doppler. Use the trackball to position the sample volume in the middle of the blood vessel.
5. The sample volume (SV) size should be approximately 1/3 the diameter of the vessel (See Fig. 3.16). Also make sure that the Doppler angle cursor is parallel to the wall of the vessel and the Doppler angle (AC value on the screen) is 60 Degrees or less as discussed above.
6. Press the freeze button to see the automatically calculated peak systolic velocity (PSV) and end diastolic velocity (EDV). As part of the laboratory exercise, have

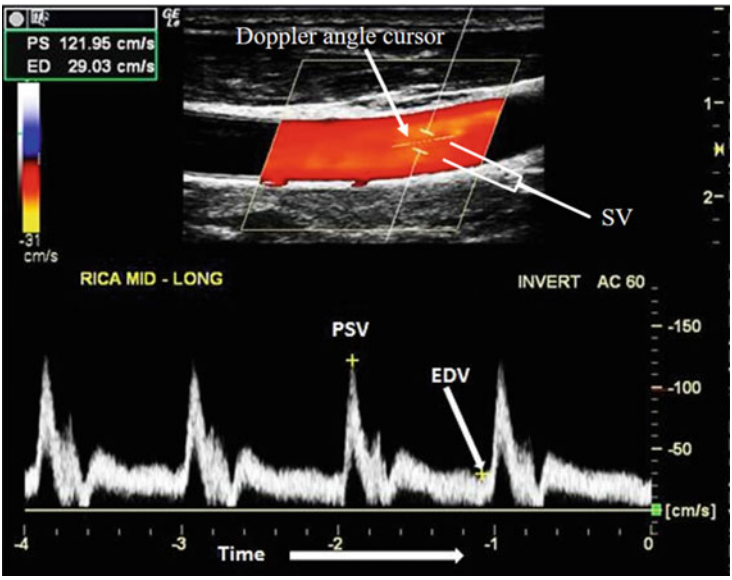

Fig. 3.16 Spectral Doppler tracing showing the placement of measurement calipers to determine the peak systolic velocity (PSV) and the end diastolic velocity (EDV). The X-axis represents time and the Y-axis represents velocity. Note that the Doppler angle cursor is parallel to the long axis of the vessel and that the sample volume (SV) is positioned in the center of the lumen

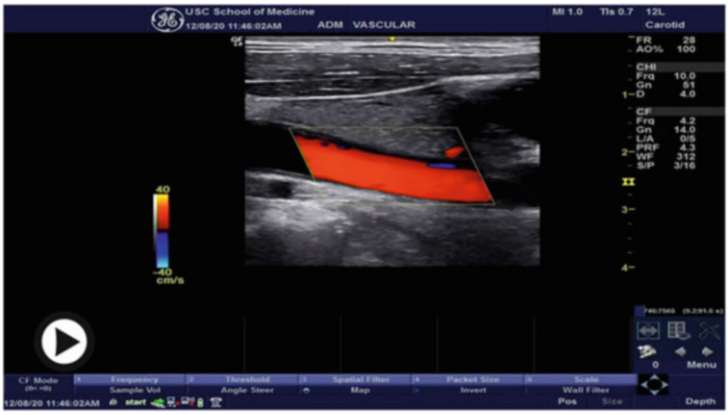

Fig. 3.17 (Video 3.3) A video showing blood flow through the carotid artery using spectral Doppler. Note the sound of the flowing blood in the CCA. The sounds correspond to the velocity tracing on the spectral Doppler display (▶ https://doi.org/10.1007/000-7pm)

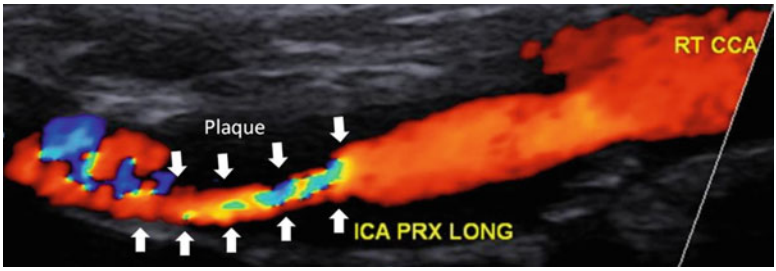

Fig. 3.18 Image showing a hypoechoic (dark) plaque in the distal segment of the internal carotid artery. The color Doppler signal is not seen in the region of the plaque. The stenotic (narrowed) segment is indicated by the white arrows. Note that the color Doppler signal displays other colors (yellow, blue) in addition to the red color in the region of the stenosis and in the post stenotic segment. The appearance of other colors suggests higher velocity and turbulent flow

the students manually determine PSV and EDV using the measurement button and trackball to place the calipers in the correct locations (see Fig. 3.16).

7. Figure 3.17 is a video allowing one to appreciate the sound of the flowing blood in a common carotid artery during spectral Doppler acquisition.

As indicated earlier in this chapter, one of the things Doppler US can evaluate clinically is stenosis of a blood vessel resulting from the buildup of plaque along the inner diameter. Figure 3.18 shows color Doppler US changes in a common carotid artery as a result of plaque accumulation. Figure 3.19 shows spectral Doppler from a stenotic internal carotid artery. Note the very high velocity seen in this figure compared to Fig. 3.16.

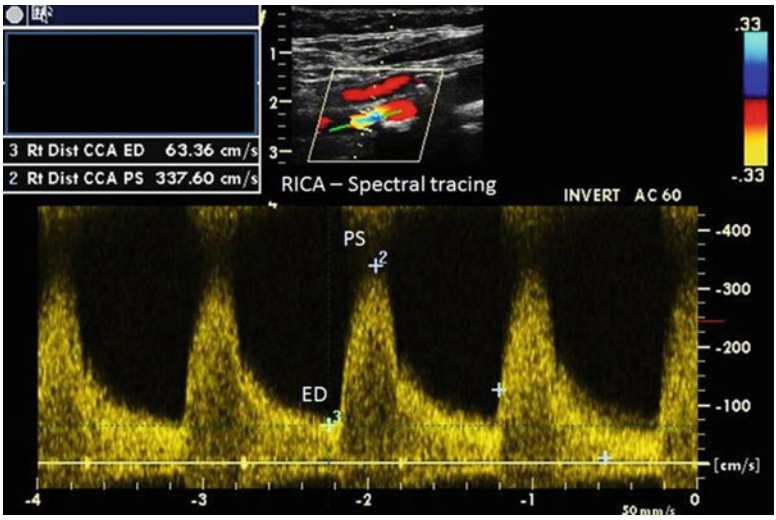

Fig. 3.19 Doppler imaging showing increased velocity just beyond the stenosis in the right internal carotid artery (RICA) The peak systolic velocity is 337.60 cm/s (compare to the less than 150 cm/s from the normal depicted in Fig. 3.16)

Further Reading

Mohrman DE, Heller LJ (2010) Cardiovascular physiology, 7th edn. McGraw-Hill, New York
Raff H, Levitzky MG (2011) Medical physiology: a systems approach. McGraw-Hill, New York

Chapter 4
Ultrasound of the Heart

Richard Hoppmann, Robert Haddad, L. Britt Wilson, and David Schrift

4.1 Anatomy and Physiology of the Heart

As discussed in the previous chapter, the primary role of the cardiovascular system is to pump blood throughout the body to provide oxygen and essential life sustaining nutrients to all organ systems while also removing waste products and toxins from the body. At the center of this system is the heart, which contains two pumps: the right and left ventricles. These two pumps and their corresponding circulatory systems (pulmonary and systemic circulations) are in series and are complementary, but each has a slightly different physiological role and physical characteristics specific to those roles.

With respect to the heart itself, the right heart pumps blood into the pulmonary circulation and the left heart pumps blood into the systemic circulation. Both are composed of three layers of specialized cardiac tissue. The outermost layer is the pericardium. The pericardium forms a sac around the heart. It has a tough outer fibrous layer that protects the heart externally. An inner layer of the pericardium attaches to the muscle cells of the heart and in between the inner and outer layers of the pericardium is a fluid layer that allows the heart to beat with little to no friction. The middle layer of the heart is the muscular layer or myocardium. The myocardium

Supplementary Information The online version contains supplementary material available at https://doi.org/10.1007/978-1-0716-1863-9_4. The videos can be accessed by scanning the related images with the SN More Media App.

R. Hoppmann (✉) · R. Haddad · D. Schrift
University of South Carolina School of Medicine, Columbia, SC, United States
e-mail: Richard.Hoppmann@uscmed.sc.edu; Robert.Haddad@uscmed.sc.edu; David.Schrift@uscmed.sc.edu

L. B. Wilson
Department of Pharmacology, Physiology, and Neuroscience, University of South Carolina School of Medicine, Columbia, SC, USA
e-mail: Britt.Wilson@uscmed.sc.edu

L. B. Wilson et al. (eds.), *Understanding Physiology with Ultrasound*, Physiology in Health and Disease, https://doi.org/10.1007/978-1-0716-1863-9_4

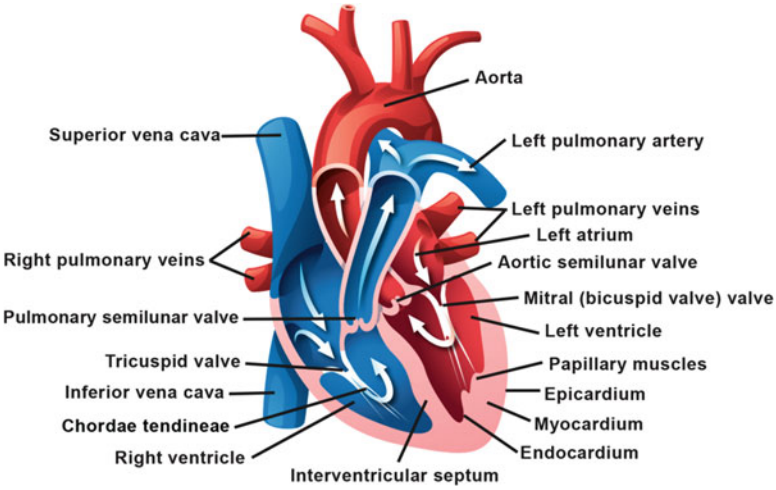

Fig. 4.1 Cross section of the heart exposing the right and left heart and major vessels. Direction of blood flow is indicated by the arrows through the chambers

contains both the cardiac muscle pumping component as well as modified cardiac cells that serve as the electrical conduction system of the heart. The inner most layer of the heart wall is the endocardium which is made of endothelium and subendothelial connective tissue that forms the inner lining of the heart.

As can be seen from Fig. 4.1, the walls of the left ventricle are thicker than those of the right ventricle and this is necessary because it must generate higher pressures to pump blood throughout the higher resistant systemic circulation. One-way valves are used to insure the correct direction of blood flow throughout the heart. The atrioventricular valves allow blood to flow from the atria into the ventricles and block back flow into the atria during ventricular contraction. The mitral valve (MV) or bicuspid valve separates the left atrium and the left ventricle and the tricuspid valve (TV) separates the right atrium and the right ventricle. The aortic valve (AV) controls one-way blood flow from the left ventricle into the aorta and the systemic circulation and the pulmonary valve (PV) ensures one-way blood flow from the right ventricle into the pulmonary artery and pulmonary circulation. The cardiac valves plus the principle of flow dynamics that liquids always flow along the pressure gradient from higher to lower pressure dictate the correct sequential filling and ejection of blood in the cardiac chambers throughout the cardiac cycle in the normal heart.

The right side of the heart receives deoxygenated blood into the right atrium from the systemic circulation via the superior vena cava and the inferior vena cava and from the heart itself via the coronary sinus. Blood passes first passively then actively by contraction of the right atrium into the right ventricle, which then pumps the blood into the pulmonary circulatory system via the pulmonary artery for uptake of oxygen and removal of carbon dioxide in the lungs. The oxygenated blood returns to the left atrium of the heart via four pulmonary veins before passing into the left ventricle passively, then actively by left atrial contraction. The left ventricle then pumps the blood to the rest of the body through the aorta into the systemic circulation.

4.2 Cardiac Muscle Contraction

Like skeletal muscle, the basic contractile unit of cardiac muscle is the sarcomere that contains thick and thin filaments. The thick filaments are composed of myosin which form cross-bridges with the protein actin on the thin filaments. A process of cycling of cross-bridges results in sliding of the thick and thin filaments producing muscle contraction (see also Musculoskeletal Chap. 8). This muscle contraction creates the cardiac chamber pressure that propels blood throughout the heart and into the pulmonary and systemic circulatory systems.

The strength of contractility of cardiac muscle is dependent on the degree of overlap of the thick and thin filaments in the resting myocardial cell. Up to a point, increasing the length of the resting cardiac muscle, such as with increased blood volume in the ventricle before contraction, increases the force of contraction and the volume of blood ejected with each beat of the heart. This relationship of volume of blood ejected and muscle cell length is termed the Frank-Starling mechanism.

4.3 Ultrasound Anatomy

Ultrasound of the heart or echocardiography (ECHO), is a safe non-invasive imaging technique to assess the anatomical structures and physiological function of the heart. It is also an excellent clinical tool to identify cardiac pathology and help learners understand pathophysiologic processes of the cardiovascular system. Two standard ECHO views will be covered in this chapter and used in the laboratory sessions to follow. They are the parasternal long axis (PLAX) view and the apical 4/5 chamber view.

Figures 4.2 and 4.3 are ultrasound image of the PLAX view in B-mode or brightness mode. The degree of brightness of various structures in an ultrasound image is a function of the number of ultrasound waves that reflect ("echo") off the body tissue and return to the ultrasound probe to be converted into electrical activity and an image on the ultrasound screen. The more waves that return, the brighter the tissue appears in the ultrasound image. As can be seen in the PLAX image, the

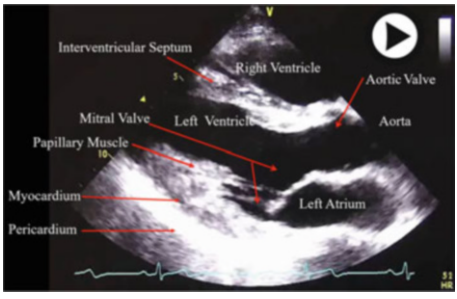

Fig. 4.2 (Video 4.1) Left panel: parasternal long axis video of the heart in B-mode with electrocardiogram (▶ https://doi.org/10.1007/000-7ps)

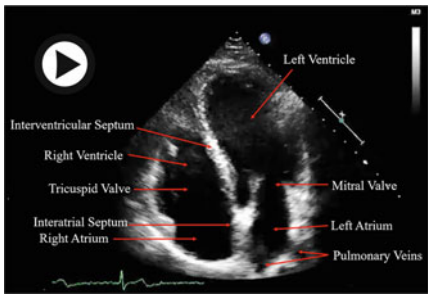

Fig. 4.3 (Video 4.2) Right panel: apical 4 chamber video B-mode with electrocardiogram (▶ https://doi.org/10.1007/000-7pp)

pericardial tissue, which is very reflective of ultrasound waves, is brighter than the myocardium which is brighter than blood in the cardiac chambers. Blood reflects very few ultrasound waves and should appear almost black on an ultrasound image. As can be seen in Figs. 4.2 and 4.3 of the apical 4 chamber view, the relative size of the right and left ventricles can be appreciated. The right ventricle should be approximately two thirds that of the left ventricle. The left ventricle should appear bullet shaped. This view allows all four chambers of the heart and the interventricular and interatrial septa to be visualized.

As can be seen in Fig. 4.4 of the apical 5 chamber view in B-mode with color Doppler (Duplex imaging), direction of flow, relative velocity of flow, and quality of blood flow can be determined by the color and homogeneity of the color of the blood. By convention, blood flow toward the ultrasound probe is red and flow away from the probe is blue. Relative velocity of flow can be appreciated using the color flow bar with darker colors/shades indicating lower velocities of flow and lighter colors/shades indicating higher velocities of flow. Turbulent flow, as opposed to smooth laminar flow, produces a mixture of colors that can detect significant stenosis or narrowing of a vessel or flow through an abnormal cardiac valve.

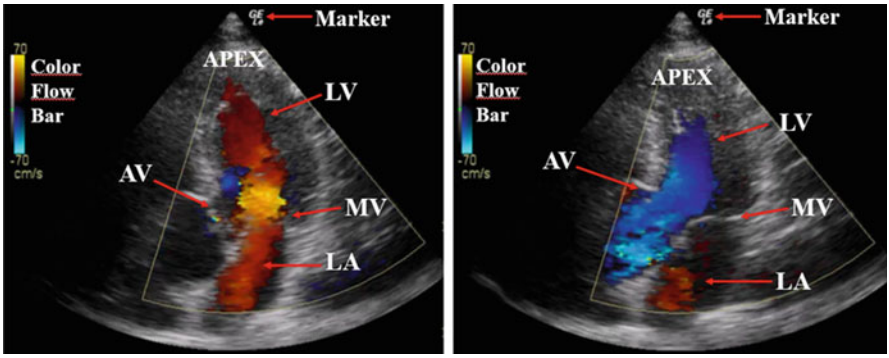

Fig. 4.4 Apical 5 chamber view of the heart with color Doppler showing image orientation marker, apex of the heart, left ventricle (LV), mitral valve (MV), left atrium (LA), and aortic valve (AV). Left panel: image during diastole. Right panel: image during systole

In diastole (left panel of Fig. 4.4), blood is flowing from the left atrium through the mitral valve into the left ventricle. This is in the direction of the ultrasound probe located on the chest at the apex of the heart approximately in the mid-clavicular line in the fifth intercostal space and pointing toward the right shoulder (positioning of probe described in more detail below). There is a slight increase in the velocity of blood flow coming through the mitral valve with atrial contraction in this image which creates the short segment of yellow color. The aortic valve is closed. During systole the blood is moving from the left ventricle through the outflow tract and the aortic valve into the aorta which is away from the apex of the heart and the ultrasound probe (blue color in right panel of Fig. 4.4). There is some filling of the left atrium from the pulmonary veins (note the red) as would be expected during ventricular systole. The mitral valve is closed.

When observing cardiac images in the cardiac preset, the image orientation is different from that of other ultrasound imaging. The image orientation marker (usually a company logo or initial at the top of the screen) is on the right side of the screen instead of the left side. This orientation makes the left side of the screen correspond to the left side of the patient's body and the right side of the screen correspond to the right side of the patient's body, with the probe marker pointing to the right side of the patient as is done with the PLAX view. When the probe marker is pointing toward the left side of the patient as is standard for the apical 4/5 chamber view, the right side of the screen is the left side of the patient.

Orientation from the top to the bottom of the screen remains the same as with other ultrasound imaging with the top of the screen being where the ultrasound probe rests on the body surface and moving down the screen from top to bottom reveals progressively deeper anatomical structures in the body. Most ultrasound machines allow the depth of the image to be adjusted. For more on viewing images and ultrasound instrumentation see *The Basics of Ultrasound Physics*—Chap. 2.

4.4 Common Applications of Cardiac Ultrasound

There are many cardiac ultrasound applications being used in clinical practice today. A wide variety of healthcare providers including nurses, medics, physician assistants, sonographers, and physicians are using portable laptop ultrasound systems and hand-held ultrasound devices to assess cardiac function much like the stethoscope has been used in healthcare for over 200 years.

The following five examples of ultrasound applications provide a sense of the utility of bedside or point of care ultrasound in assessing cardiac anatomy and function.

1. Left Ventricular Hypertrophy (LVH) is thickening of the ventricular muscle wall and is common in chronic hypertension, aortic stenosis, and other clinical situations of increased afterload or pressure that the ventricle pumps against. If not adequately addressed, these clinical conditions can lead to heart failure. ECHO

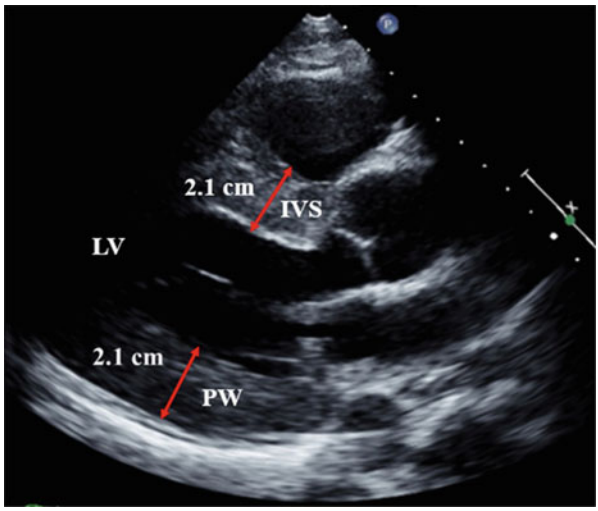

Fig. 4.5 PLAX view of the heart. Left ventricle (LV), interventricular septum (IVS), posterior wall (PW). Note that both the posterior wall and the septal wall are symmetrically hypertrophied (concentric hypertrophy)

allows the identification and measurement of ventricular wall thickening. Greater than 1.0 cm is considered hypertrophy (Fig. 4.5).

2. Heart failure is the inability of the heart to provide adequate blood to meet the metabolic needs of the tissue throughout the body. Ultrasound can assess cardiac pump function as the percentage of blood ejected from the ventricle with each contraction (ejection fraction) and can be used to follow progression or regression of heart failure with treatment. Enlarged chambers and poor contractility of the heart are defining features of heart failure seen on ECHO (Fig. 4.6).

3. Hypertrophic cardiomyopathy (HOCM) is a genetic heart disease that can cause heart failure and sudden death in otherwise healthy individuals, including athletes. HOCM can be diagnosed with ECHO and assist in the medical management of these patients. The ECHO shows marked thickening of the ventricular walls of the heart which may be symmetric or asymmetric. Ventricular chamber size is often decreased and there may also be ventricular outflow obstruction during systole. Family members can be screened for evidence of the disease with ECHO (Fig. 4.7).

4. Pericardial effusion is the abnormal accumulation of fluid in the pericardial sac. Cardiac tamponade can develop with rapid accumulation of fluid in the pericardial sac that can compress the heart chambers and severely limit the filling and pumping action of the heart creating a life-threatening situation. Pericardial effusion and cardiac tamponade can be identified with ECHO. Ultrasound can also be used to guide a needle to the area of the pericardial fluid to remove the fluid and restore cardiac function (i.e. pericardiocentesis). With large pericardial

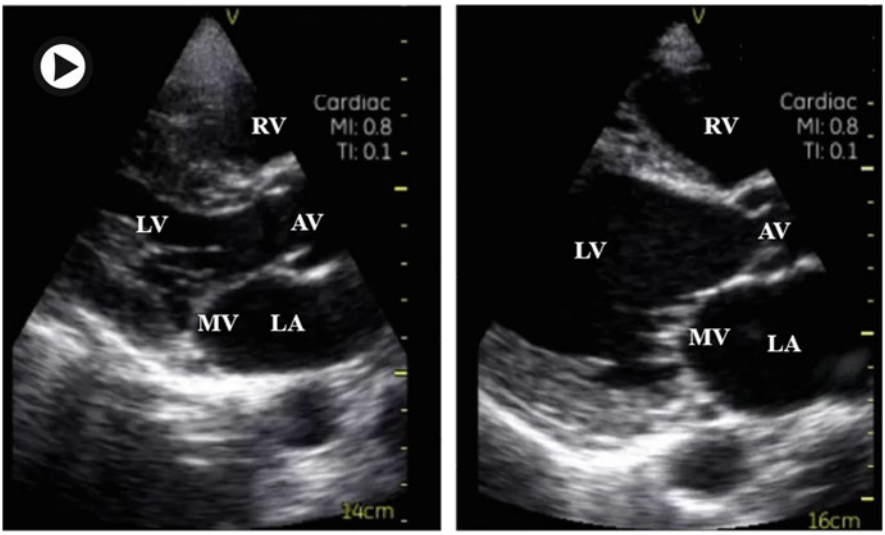

Fig. 4.6 (Video 4.3) PLAX view videos. Left panel: a healthy heart. Right panel: a heart in failure. Right ventricle (RV), left ventricle (LV), left atrium (LA), mitral valve (MV), and aortic valve (AV). Note loss of contractility and enlarged LV and LA in the heart failure video (▶ https://doi.org/10.1007/000-7pq)

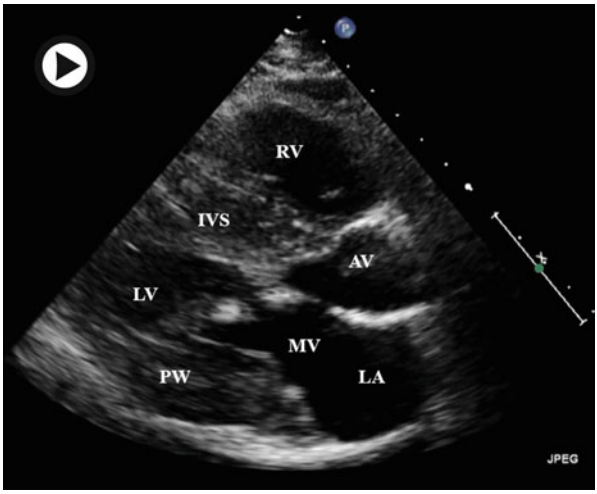

Fig. 4.7 (Video 4.4) PLAX view video of a patient with hypertrophic cardiomyopathy. Right ventricle (RV), interventricular septum (IVS), left ventricle (LV), mitral valve (MV), aortic valve (AV), posterior wall (PW), left atrium (LA). Note marked thickening of the posterior and septal walls and decreased size of the ventricular chamber (▶ https://doi.org/10.1007/000-7pr)

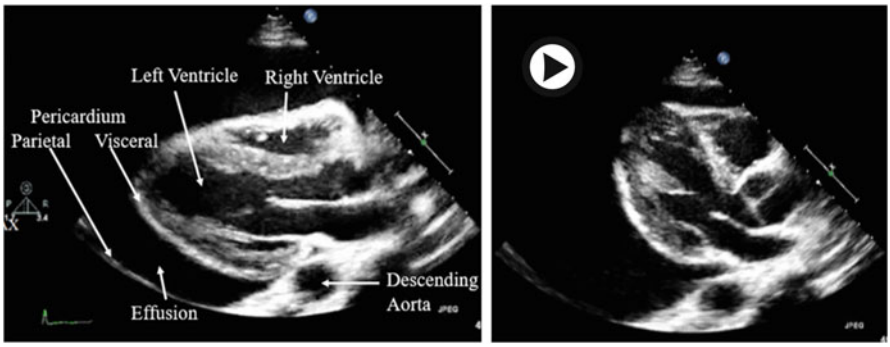

Fig. 4.8 (Video 4.5) Left panel: PLAX view of the heart with a large pericardial effusion. Right panel: PLAX view video of a "swinging" heart within very large pericardial effusion (▶ https://doi.org/10.1007/000-7pn)

effusions, the heart can appear to be "swinging" in the fluid with each heartbeat (Fig. 4.8).

5. Pulmonary embolism most commonly develops when a blood clot breaks free from a vessel in the systemic circulation and becomes lodged in the pulmonary circulation. Large clots can severely compromise both the respiratory and cardiovascular systems. The diagnosis of pulmonary embolism is supported by ECHO findings of increased right ventricular pressure (strain), right ventricular enlargement, and poor ventricular contractility, especially at the mid free-wall level. The enlarged right ventricle pushes the septum into the left ventricle. The source of the embolism can often be detected in the deep veins of the pelvis and legs by vascular ultrasound. Early identification of pulmonary embolism can direct appropriate therapy such as thrombolytics and can be life-saving (Fig. 4.9).

4.5 The Electrical Activity of the Heart

The electrocardiogram (EKG or ECG) is a measurement of the electrical activity of the heart as it beats. As seen in Fig. 4.10, the electrical activity begins with an automatic action potential and depolarization in the sinoatrial node (SA node), which is the normal pacemaker of the heart and is located in the right atrium. From there it spreads via three tracts across the right and left atria down to the atrioventricular node (AV node) located at the juncture of the atria and the ventricles. Electrical conduction slows within the AV node to allow time for the ventricles to fill with blood before they are depolarized and contract. From the AV node, the conduction and depolarization travels rapidly down the Bundle of His to the Right and Left Bundle Branches then to the Purkinje fibers in the endocardial surface to spread

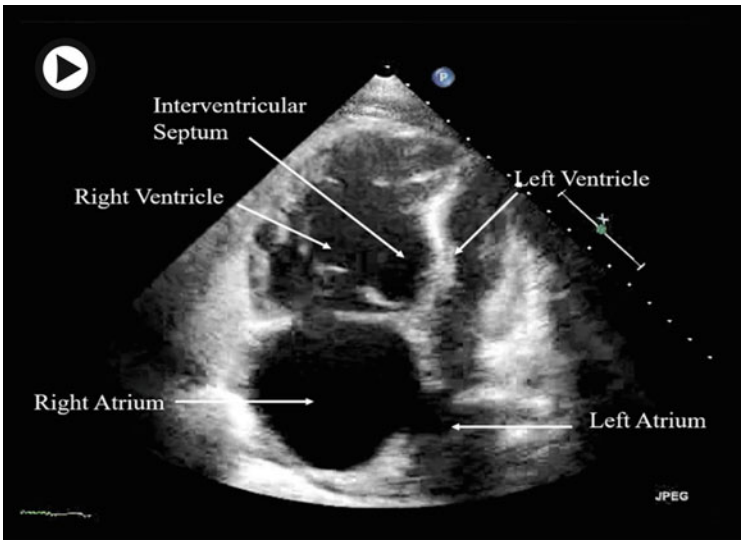

Fig. 4.9 (Video 4.6) Apical 4 chamber video of the heart in a patient with a large pulmonary embolism. Note the enlarged right ventricle relative to the left ventricle causing the interventricular septum to be pushed into the left ventricle. The right atrium is also enlarged (▶ https://doi.org/10.1007/000-7pt)

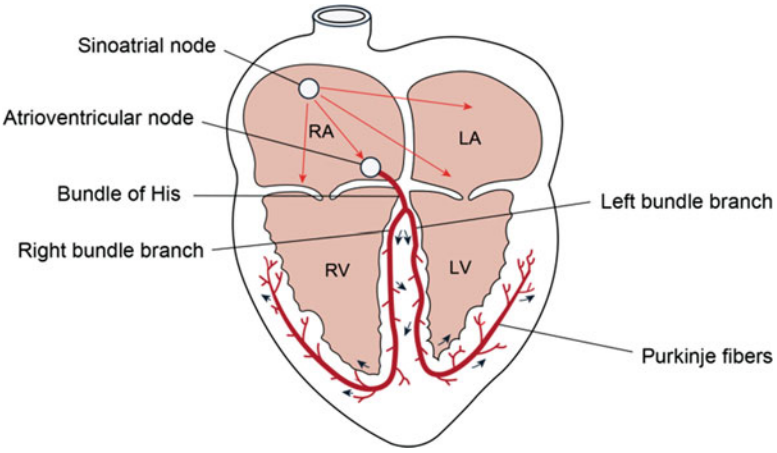

Fig. 4.10 The conduction system of the heart

throughout the ventricles. The rapid well-organized conduction and depolarization of the heart ensures a coordinated, effective ventricular muscle contraction to eject blood from the right and left ventricles into the pulmonary and systemic circulations respectively. It should be noted that if the automaticity of the SA node, which is approximately 100–120 beats/min fails, the AV node with an automaticity of 40–60 beats/min will take over and, if it fails, there is a third level of automaticity of 20–40 beats/min that originates in ventricular foci. Repolarization within the heart tissue is also a well-coordinated, sequential process.

Much of the depolarization and repolarization of the heart can be analyzed by body surface electrodes of the ECG that can detect small potential differences (voltage) corresponding to depolarization and repolarization of specific areas of the heart throughout the cardiac cycle. Thus, the ECG can record and measure the timing, sequence, and voltage changes associated with depolarization (initiates contraction) and repolarization (initiates relaxation) of cardiac muscle in specific locations of the heart. Multiple electrodes placed on the chest and limbs can be used to capture an individual's electrical activity profile of the heart. This can be used in diagnosing and treating a wide variety of heart conditions from arrhythmias (irregular heart rhythms) to myocardial ischemia and myocardial infarction (heart attack and cell death).

Figure 4.11 shows a single lead ECG with conventional labeling of waves of atrial and ventricular depolarization and repolarization. Segments by definition are between waves and intervals include the segment and the wave or waves.

From left to right in Fig. 4.11, the P wave represents depolarization of the atria. The PR Segment is the isoelectric flat segment from the end of the P wave until the

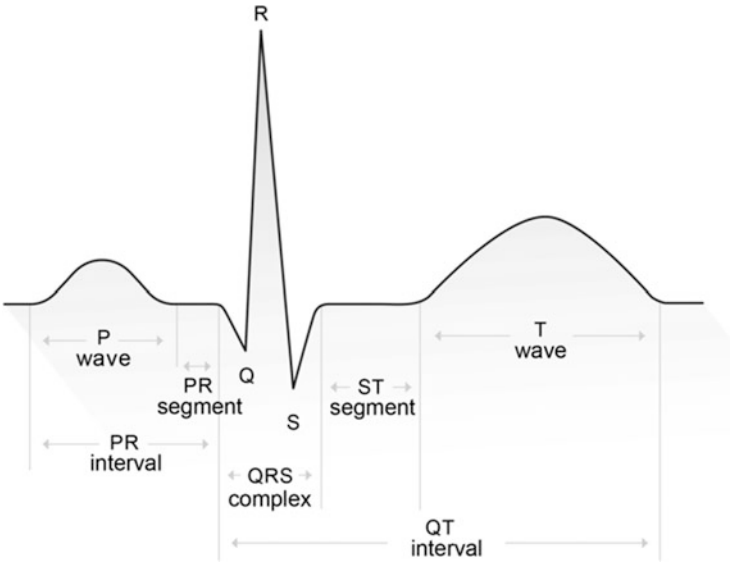

Fig. 4.11 Single lead electrocardiogram of the heart

initial depolarization of the ventricle. The PR interval covers the time from the initial depolarization of the atria to the initial depolarization of the ventricles. The QRS complex represents depolarization of the ventricles. The ST Segment is the isoelectric flat segment from the end of the QRS complex to the start of the T wave. The QT interval covers the time from the start of the QRS complex to the end of the T wave and the T wave represents the repolarization of the ventricles. The presence, shape, size, and duration of the waves and the time between waves provide critical information about the structure, function, conduction, and overall health of the heart.

4.6 Heart Sounds

The first heart sound is S1 and is high pitched. S1 is primarily due to the closure of the mitral and tricuspid valves. The second heart sound is S2 and is higher pitched than S1 and of shorter duration. S2 is due to closure of the aortic and pulmonic valves. The time from S1 to S2 defines cardiac systole and the time from S2 to S1 defines cardiac diastole.

The diastolic sounds of S3 and S4 are not typically heard in healthy older adults but can occasionally be heard in healthy young adults and children. S3 is a low-pitched sound classically heard early in diastole during rapid passive filling of an enlarged, very compliant, thin walled, left ventricle as is seen in patients with advanced heart failure. S4 is also a low-pitched sound but occurs late in diastole just before S1 and coincides with atrial contraction. S4 is the result of blood being forced by contraction of the left atrium into a relatively noncompliant, stiff left ventricle. A noncompliant left ventricle can be the result of left ventricular hypertrophy that develops in chronic hypertension or aortic stenosis. S4 can also be heard in the setting of myocardial ischemia as the ventricle has impaired relaxation and is less compliant.

Other sounds, such as heart murmurs, that can be heard with a stethoscope and provide clinical information regarding heart valve pathology can be further assessed with ultrasound. The degree of valve narrowing or stenosis and incompetency or leaking of heart valves can be measured with ultrasound and assist in clinical decision making such as medication choices and timing of cardiac valve repair or replacement. Heart sounds S1–S4 will be covered in this chapter but additional sounds such as murmurs will not be covered.

4.7 The Cardiac Cycle

The cardiac cycle is typically divided into the ventricular contractile and ejection phase of systole and the ventricular relaxation and filling phase of diastole. The cardiac cycle can be further divided into seven sequential phases as outlined in the Wiggers Diagram (Fig. 4.12). These were first described by Carl John Wiggers and

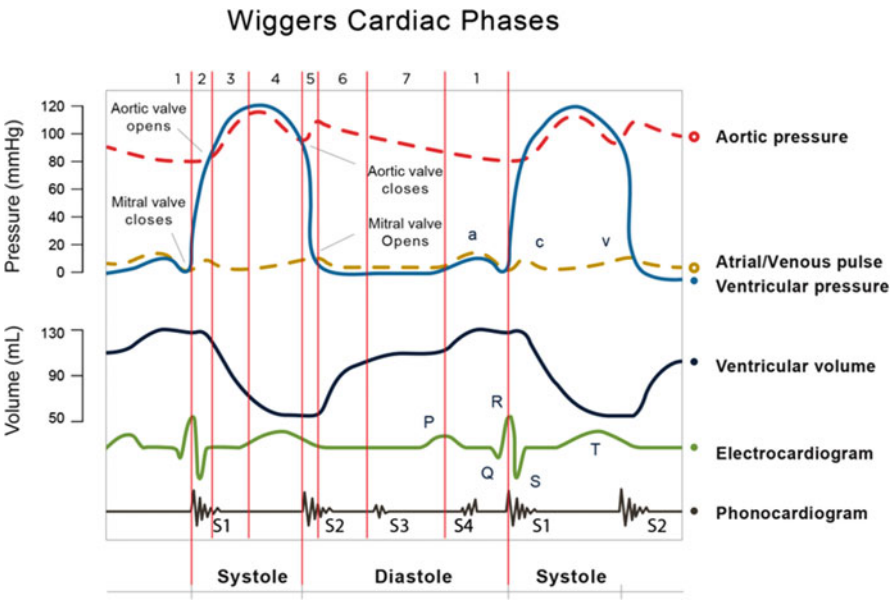

Fig. 4.12 Wiggers diagram. Seven phases of the cardiac cycle. See text for explanation. 1. Atrial Systole; 2. Ventricular Isovolumetric Contraction; 3. Ventricular Rapid Ejection; 4. Ventricular Reduced Ejection; 5. Ventricular Isovolumetric Relaxation; 6. Ventricular Rapid Filling; 7. Ventricular Reduced Filling (Diastasis)

came out of his many contributions to cardiac physiology in the first half of the twentieth century. The Wiggers Diagram has become a standard teaching tool for understanding cardiac physiology.

These seven phases describe the sequence of important changes in cardiac chamber volume and pressure, aortic pressure, opening and closing of heart valves, heart sounds, and ECG activity throughout the cardiac cycle. Figure 4.12 is a Wiggers diagram for the left side of the heart but a similar corresponding process takes place in the right heart as well.

Ultrasound can serve as a visual aid in understanding the various components of the cardiac cycle in the Wiggers Diagram. It has been shown that adding ultrasound to the study of cardiac hemodynamics increases learners' understanding of this important physiological process.

A three-signal hand-held ultrasound device has been used to capture an ultrasound image of the heart and the corresponding ECG and heart sounds as shown in Fig. 4.13. Each of the seven phases of the normal cardiac cycle will be presented along with a description of the role each phase plays in cardiac physiology and pathophysiology. Characteristic features of the ultrasound image, ECG, and heart sounds for each phase are highlighted in the "Look and Listen" box next to the ultrasound image and can be used as a guide to identify the important aspects of each image.

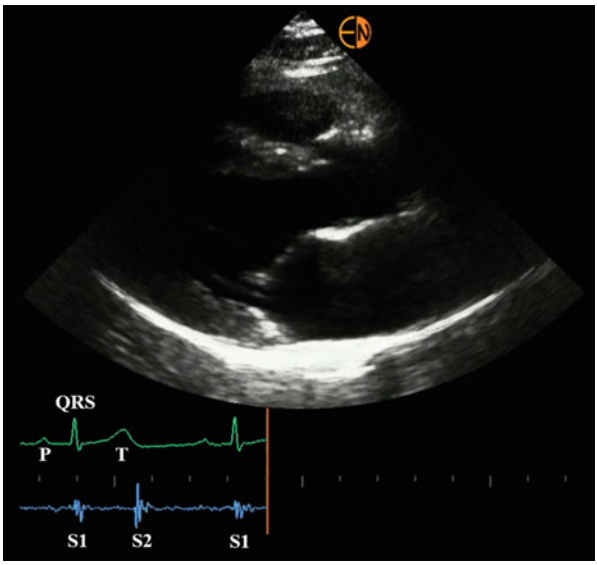

Fig. 4.13 PLAX view with EKG and heart sounds labeled. It may be necessary to increase the volume on viewing device to better hear the heart sounds

Note that it may be hard to identify all features of a Wiggers' cardiac phase in a single ultrasound image due to the continuum of heart motion within a phase and the relatively thin slice of each ultrasound image. Identifying structures and cardiac motion are generally easier while observing a cardiac video loop as shown in Figs. 4.14 and 4.15. This loop also provides the normal S1 and S2 heart sounds so their locations in the normal cardiac cycle can be appreciated. Refer back to this loop as needed when assessing each of the seven Wiggers phases of the cardiac cycle. Observing the loop in half-time also shown in Figs. 4.14 and 4.15 can also be utilized to help identify important hemodynamic features.

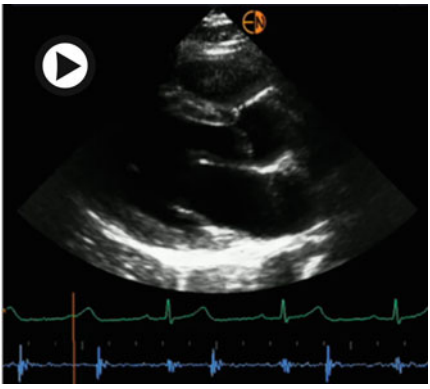

Fig. 4.14 (Video 4.7) Left panel: PLAX view video of the heart with EKG and heart sounds (▶ https://doi.org/10.1007/000-7pv)

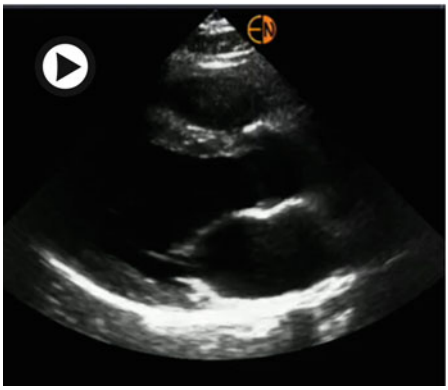

Fig. 4.15 (Video 4.8) Right panel: same video at half speed (▶ https://doi.org/10.1007/000-7pw)

4.7.1 Phase 1: Atrial Systole (Fig. 4.16)

Electrical activity in the heart slightly precedes mechanical activity. Thus, the P wave on the ECG indicates depolarization of the atrium and slightly precedes atrial contraction. Until the atrium contracts, blood from the atrium is passively flowing from the left atrium into the left ventricle through the open mitral valve during diastole. With atrial contraction, blood is actively propelled into the ventricles, and accounts for approximately 10–40% of the total volume of blood in the ventricle at the end of diastole, which is known as the end-diastolic volume (EDV). The atrial contribution to EDV is heart rate dependent. As the heart rate increases there is less diastolic time for passive filling and the relative contribution of atrial contraction to the EDV is greater. The ECG cannot detect atrial repolarization. An "A" wave appears on the atrial/venous pulse relating to the rise in pressure from atrial contraction. When present, an S4 is heard during atrial systole. Note that if there is no

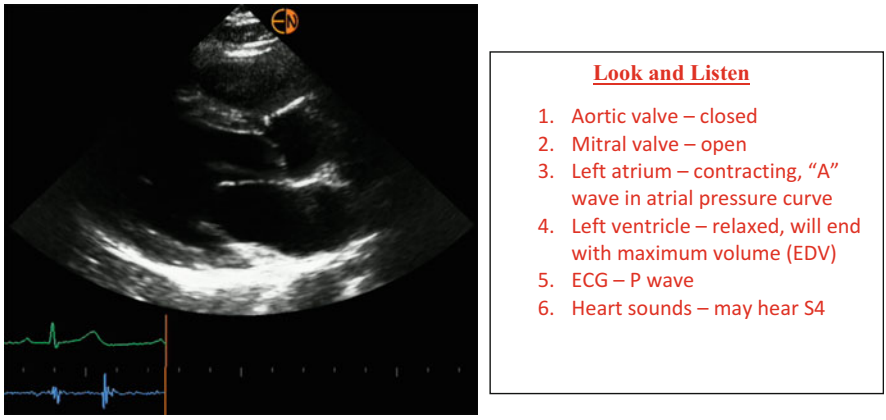

Fig. 4.16 Wiggers phase atrial systole

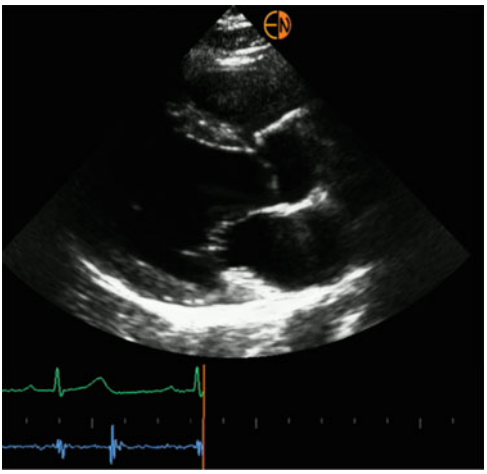

Look and Listen

1. Aortic valve – closed
2. Mitral valve – closed
3. Left atrium – filling with blood, "C" wave in atrial pressure
4. Left ventricle – contracting and good volume (EDV)
5. ECG – QRS complex
6. Heart sounds – S1

Fig. 4.17 Wiggers phase isovolumetric contraction

distinct atrial contraction, as in atrial fibrillation, there can be no S4 heart sound even if the predisposing ventricular conditions such as left ventricular stiffness are present.

4.7.2 Phase 2: Ventricular Isovolumetric Contraction (Fig. 4.17)

At the start of ventricular contraction, the mitral and tricuspid valves close producing the S1 heart sound. During this phase, all four valves are now closed and no blood is coming into or leaving the ventricles. Thus, this period is referred to as isovolumetric contraction. On the ECG, the three-wave QRS complex, indicating ventricular depolarization, begins just prior to the start of ventricular contraction. As the ventricle continues to contract, pressure rises in the ventricular chamber. A "C" wave appears on the atrial pressure curve and is due to isovolumetric contraction and bulging of the mitral valve into the left atria, thereby increasing its pressure.

4.7.3 Phase 3: Ventricular Rapid Ejection of Blood (Fig. 4.18)

Once the pressure in the left ventricle exceeds that of the aorta, the aortic valve opens and there is rapid ejection of blood into the aorta with a corresponding rise in aortic pressure.

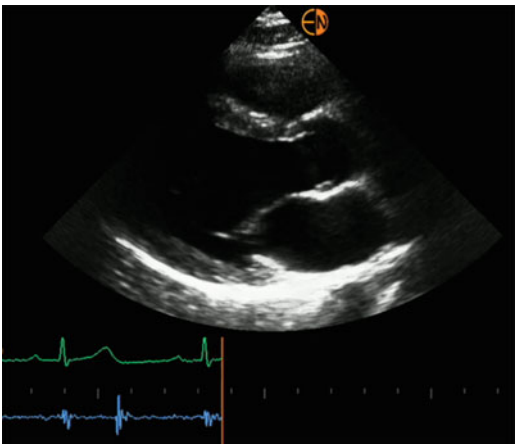

Look and Listen

1. Aortic valve – open
2. Mitral valve – closed
3. Left atrium – filling
4. Left ventricle – contracting and decreasing in volume
5. ECG – mostly isoelectric

Fig. 4.18 Wiggers phase rapid ejection

4.7.4 Phase 4:Ventricular Reduced Ejection (Fig. 4.19)

After the initial rapid ejection of blood into the aorta, the rate of ejection of blood lessens. At the end of systole, the volume of blood within the ventricle reaches a minimal value known as the end-systolic volume (ESV). During this cardiac phase, the ECG displays a T wave, indicating repolarization of the ventricle.

During the initial ejection phase of the ventricle, atrial pressure falls as it relaxes. Once the left atrium is fully relaxed, its pressure slowly rises throughout the

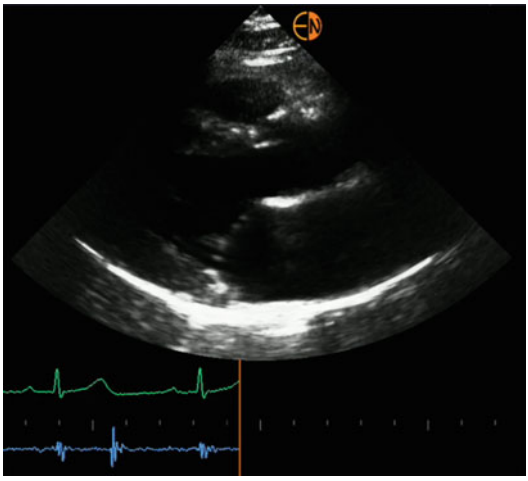

Look and Listen

1. Aortic valve – open
2. Mitral valve – closed
3. Left atrium – V wave
4. Left ventricle – contracting and close to minimal volume (ESV)
5. ECG – T wave

Fig. 4.19 Wiggers phase reduced ejection

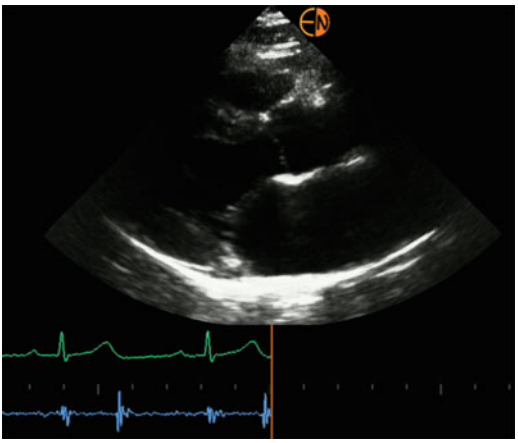

Fig. 4.20 Wiggers phase isovolumetric relaxation

ventricular ejection because it is filling with blood (venous return). This is the V wave of the atrial/venous pulse.

4.7.5 Phase 5: Ventricular Relaxation Isovolumetric (Fig. 4.20)

As the ventricle begins to relax, ventricular pressure drops. The aortic valve closes as the pressure in the aorta exceeds that of the ventricle and all four valves are again closed with no flow of blood in or out of the ventricle (isovolumetric relaxation). The second heart sound (S2) is heard with closure of the aortic and pulmonic valves.

This phase begins after the T wave of repolarization of the ventricles and continues until the mitral valve opens. Because flow into the aorta from the ventricle ceases, the elastic properties of the aorta cause it to recoil. This recoil transiently pushes blood against the closed aortic valve resulting in a transient upward blip in aortic pressure referred to as the dicrotic notch.

4.7.6 Phase 6: Ventricular Rapid Filling (Fig. 4.21)

Once pressure in the left ventricle drops below that in the left atrium, the mitral valve opens and blood passively, but rapidly, fills the ventricle. In patients with heart failure, this rapid filling into a left ventricle that is dilated with blood that was not ejected can produce a third heard sound (S3). This transfer of blood from the atrium into the ventricle causes atrial pressure to fall.

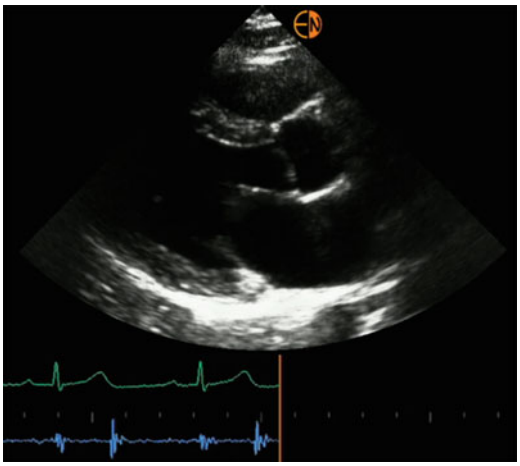

Look and Listen

1. Aortic valve – closed
2. Mitral valve – open
3. Left atrium – passive emptying
4. Left ventricle – passive filling
5. ECG – isoelectric
6. Heart sounds – may hear S3

Fig. 4.21 Wiggers phase ventricular rapid filling

4.7.7 Phase 7: Ventricular Reduced Filling (Diastasis) (Fig. 4.22)

As the ventricle fills with blood, passive filling from the atria slows. This is the longest component of the cardiac cycle and is identified as diastasis. Diastasis ends with atrial systole. The ventricle is still relaxed and pressure has only increased slightly. This concludes the final phase of the cardiac cycle and the atria will soon contract to "top off" the blood volume in the ventricle, resulting in the end-diastolic volume (EDV) and a new cardiac cycle begins.

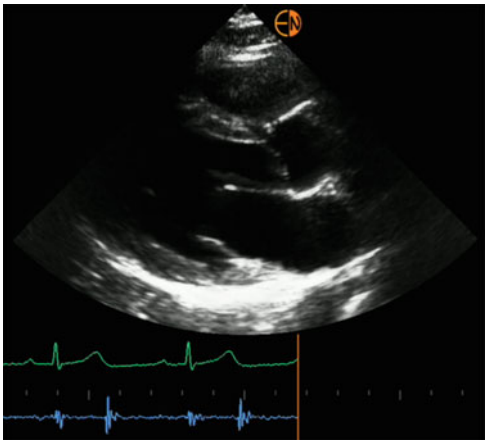

Look and Listen

1. Aortic valve – closed
2. Mitral valve – open
3. Left atrium – passive emptying
4. Left ventricle – passive filling
5. ECG – isoelectric then start of P wave

Fig. 4.22 Wiggers phase ventricular reduced filling

4.8 The Ventricular Pressure-Volume Relationships and the Cardiac Loop

To better understand the mechanical pumping activity of the heart it is helpful to visualize the pressure-volume relationships of the ventricles during systole and diastole and then apply these relationships to a cardiac pressure-volume loop based on the Wiggers' seven phases.

The systolic active contraction component of the cardiac cycle is defined by the end-systolic pressure-volume curve (ESPVC; also known as the isovolumetric line) and the passive filling diastolic component is defined by the end-diastolic pressure-volume curve (EDPVC) as shown in Fig. 4.23.

These basic relationships and principles of cardiac hemodynamics come from the ground breaking work of Otto Frank, Ernest Starling, Carl John Wiggers, and others in the late 19th and early 20th centuries. They form the foundation of our modern day understanding of human cardiac physiology and pathophysiology.

Figure 4.23 is a graph of the pressure developed in the ventricle with left ventricular pressure (an index of myocardial contraction) on the "y" axis and volume of blood filling the ventricle during diastole on the "x" axis. Time as a variable is not considered in these relationships.

As described by the Frank-Starling relationship, the volume of blood ejected with ventricular contraction is directly related to the volume of blood in the resting ventricle just prior to systolic contraction. This volume of blood, known as the end diastolic volume (EDV), determines ventricular stretch and the cardiac muscle length. Thus, muscle length could be substituted for ventricular volume along the X axis.

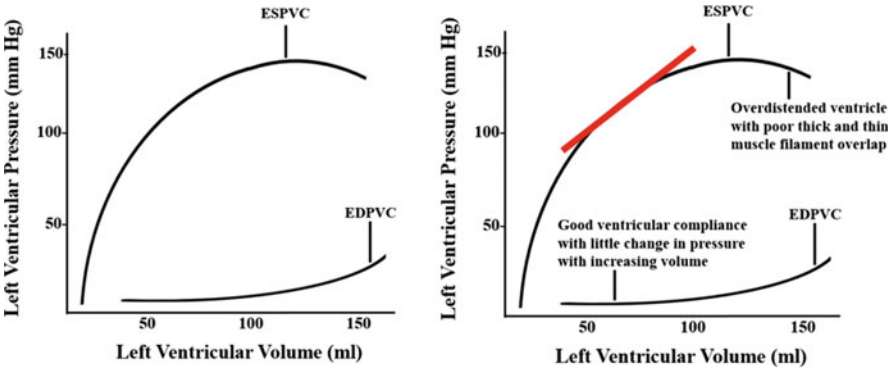

Fig. 4.23 Left panel: graph of the end-systolic pressure-volume curve (ESPVC) and the end-diastolic pressure-volume curve (EDPVC). Right panel: note the slow rise in pressure in the EDPVC reflecting good compliance of the ventricle and an almost linear relationship of pressure to volume in the ESPVC in the normal physiological volume range (red line) with a plateau effect then a drop in pressure when volume expands beyond this range

Note that the relationship of the pressure generated in the ventricle to the ventricular volume is approximately linear in the range of normal cardiac physiology (red line). This ventricular volume corresponds to a cardiac muscle length of approximately 1.8–2.2 μm. As the ventricular volume approaches optimal volume, the ventricular pressure curve begins to show a plateau effect and then with increasing volume, ventricular pressure decreases. Clinically, this loss of force with large ventricular volumes helps explain the worsening of heart failure as the ventricle dilates further away from the most effective muscle length, which determines thin and thick filament overlap.

The slowly rising passive filling pressure in the ventricle with increasing blood volume during diastole labeled as the end diastolic pressure-volume curve (EDPVC) reflects good compliance of the normal ventricle. A significant rise in pressure only begins to develop late in the filling phase at larger volumes. By definition, compliance of a container is determined by change in volume over the change in pressure as follows: $\mathbf{C = \Delta V/\Delta P}$. Thus, in a healthy heart chamber (the container), there is good physiological compliance and little change in pressure with change in volume over a fairly extended range of volumes.

Figure 4.24 is the pressure volume loop of a complete cardiac cycle as originally defined by the seven Wiggers phases. Point A to B represents the early Rapid Filling of diastole with the aortic valve closed and the mitral valve open. Filling then slows down at point B. Then Diastasis or Reduced Filling starts and ends with initiation of Atrial Contraction at C which ends at point D and closure of the mitral valve.

The ventricular blood volume increases during diastole from the end systolic volume (ESV) at point A of about 50 ml to the beginning of isovolumetric contraction at point D with about 120 ml of blood. These are average volumes observed in the healthy resting heart that will vary somewhat with age, physique, gender and

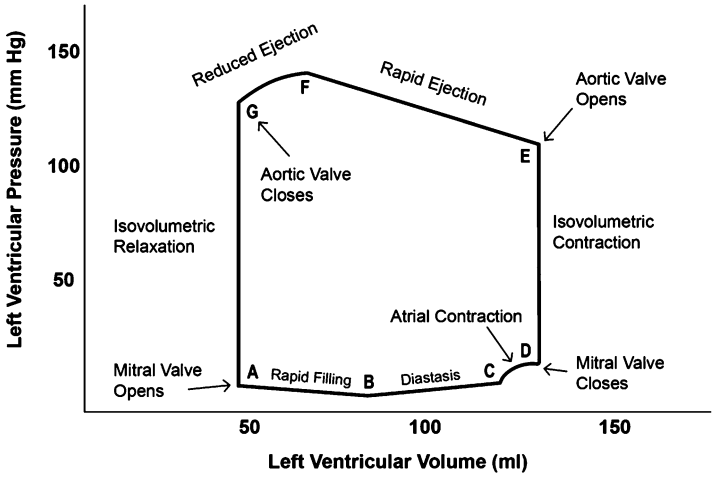

Fig. 4.24 A pressure-volume loop of the cardiac cycle using the seven Wiggers' phases. See text for explanation

overall physical conditioning of the individual. During diastole there is little increase in ventricular pressure due to the good compliance of the left ventricle. However, as the heart contracts, a rapid rise in pressure is seen from point D to the end of isovolumetric contraction and opening of the aortic valve at point E. The volume then decreases steadily with Rapid Ejection of blood from the left ventricle while pressure continues to increase until reaching a plateau at F. The ejection of blood slows (Reduced Ejection) and a drop in ventricular pressure proceeds the closure of the aortic valve at point G with an ESV back to 50 ml. Point G signifies the start of Ventricular Isovolumic Relaxation and a return to point A where the pressure has dropped to below that of the left atrium and the mitral valve opens and a new cardiac loop begins.

The volume difference between the end diastolic volume (line D-E) and the end systolic volume (line G-A) is the volume the heart ejects with each contraction and is known as the stroke volume (volume of blood ejected per beat). Thus, for this contraction, the stroke volume would be 120 ml minus 50 ml or 70 ml of blood ejected.

The end-systolic and end-diastolic pressure-volume curves can be used to set the limits between which a ventricular pressure-volume loop for a cardiac cycle can be constructed.

Figure 4.25 is the application of the systolic and diastolic pressure-volume relationships to a simplified version of the Wiggers' cardiac loop. The approximately linear relationship of ventricular pressure generated to ventricular volume is used to further simplify this physiological model which can then be used to explain changes in cardiac hemodynamics when conditions deviate from the normal physiological resting state.

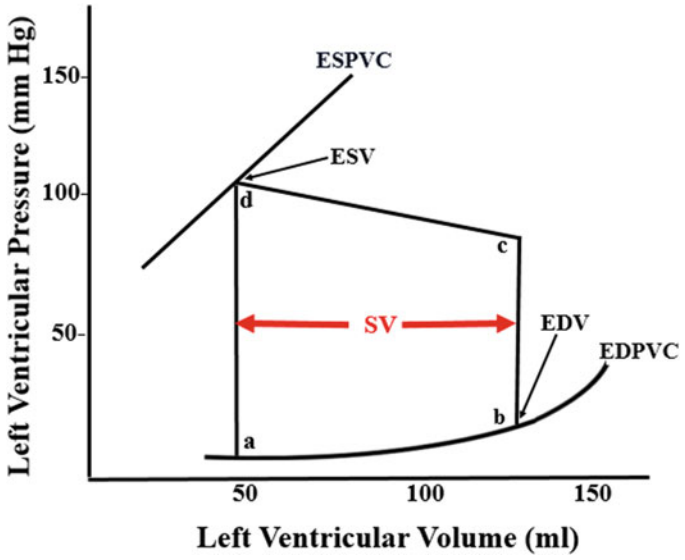

Fig. 4.25 Pressure-volume graph in normal resting state

4.9 Cardiac Output

For the heart to provide adequate blood to tissues of the body, it must be an effective pump and also be able to adjust to the dynamic demands of a wide variety of metabolic states. Cardiac output (CO) is the volume of blood pumped by the heart in a unit of time and is calculated as the product of stroke volume (SV) and heart rate (HR): CO = SV (ml) × HR (beats/min).

The cardiac output of a resting healthy adult is approximately 5000 ml/min based on a heart rate of 72 contractions per minute and a stroke volume of approximately 70 ml. A healthy heart can respond to increased metabolic needs by increasing cardiac output several fold.

4.10 Determinants of Stroke Volume

There are three major determinants of SV: preload of the ventricle, contractility or strength of muscle contraction of the ventricle, and afterload on the ventricle.

4.10.1 Preload

Preload is the ventricular end-diastolic volume (EDV). As predicted by the Frank-Starling Mechanism, stroke volume should increase with increasing EDV. This relationship is depicted by the graph in Fig. 4.26. With increased preload, the EDV increases as noted by the change from b to b'. The shift in the EDV to the right creates a greater difference between EDV and ESV thus resulting in an increase in stroke volume.

4.10.2 Afterload

Afterload is the load or impedance the ventricle has to work against to eject blood or the load opposing ventricular muscle fiber shortening. Clinically, it is typically considered to be the systolic aortic pressure, which is the highest pressure in the systemic circulation. Two common examples of increased afterload are hypertension and aortic stenosis. As can be seen in Fig. 4.27, the increased afterload requires a greater pressure to be reached before opening of the aortic valve for ejection of blood from the LV (c to c'). With increase of afterload, less volume is ejected leaving more blood in the ventricle at the end of systole (increased ESV) (d to d'). Thus, increased afterload shifts the cardiac loop upward and to the right and decreases stroke volume. Conversely, a decrease in afterload will increase stroke volume.

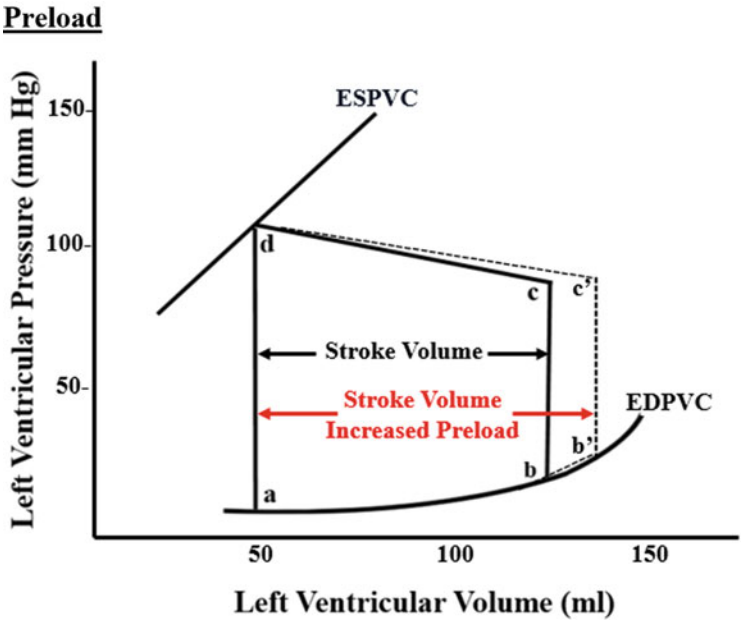

Fig. 4.26 Pressure-volume graph of change in stroke volume with increased preload. Changes related to increased preload are identified by the dotted lines

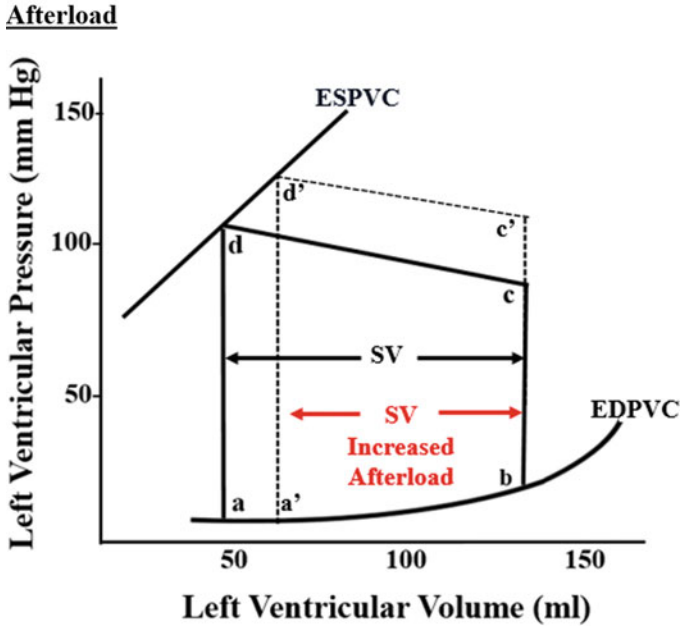

Fig. 4.27 Pressure-volume graph of change in stroke volume with increased afterload. Changes noted by dotted lines

4.10.3 Contractility

Contractility or inotropism is the intrinsic ability of myocardial cells to develop force at a given muscle cell length. Positive inotropism results in an increase in force of contraction and thus an increase in stroke volume. Negative inotropism results in a decreased force and stroke volume. There are several physiological mechanisms to increase contractility, including sympathetic nervous system stimulation of the heart, circulating catecholamine effects, and an increase in heart rate. There are also external mediators that can affect contractility such as the cardiac glycosides like digoxin and β-adrenoreceptor agonists like dobutamine that have positive inotropic effects and are frequently used to treat heart failure.

As can be seen in Fig. 4.28 of the Ventricular Pressure-Volume Loop, an increase in contractility moves the end-systolic pressure-volume curve (ESPVC) upward and to the left resulting in an increase in SV.

4.11 Ejection Fraction

Although SV is a reasonable measure of cardiac function, there are situations when measuring just the volume of blood ejected with each heartbeat can be misleading. For example, if the ventricle is enlarged, the volume of blood ejected may be

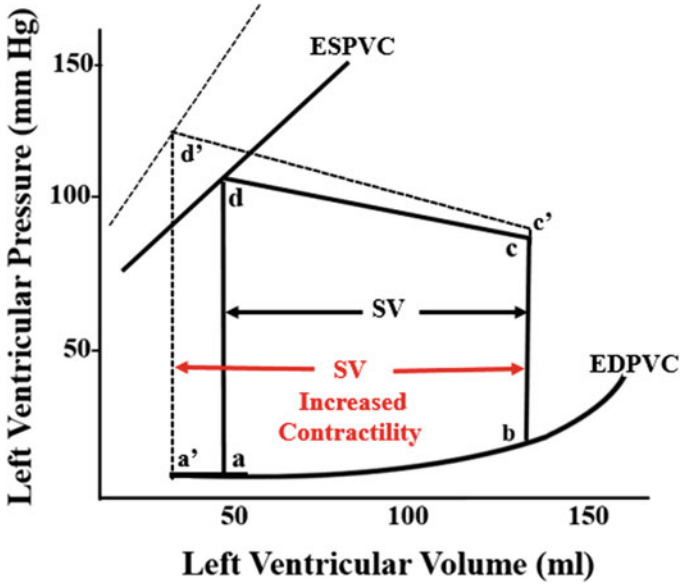

Fig. 4.28 Pressure-volume graph of change in stroke volume with increased contractility. Changes noted by dotted lines

relatively normal but the overall pumping action and effectiveness of the heart may be seriously compromised. A more meaningful measurement of cardiac function that is commonly used in clinical medicine is the ejection fraction (EF). The EF is calculated by dividing the stroke volume by the end-diastolic volume to give a percentage of blood ejected with each heartbeat: EF = SV/EDV. Normal EF is greater than 55%.

Ejection fraction can be determined on large ultrasound systems by methods that graphically outline the volume of the ventricle at end diastole and end systole to compute the percentage of blood ejected.

A rough approximation of EF can be readily obtained with portable ultrasound by noting how close the anterior mitral valve leaflet comes to the septal wall during diastole. With a normal ejection fraction the leaflet should come within 0.8–1.0 centimeters of the septal wall. As a failing heart enlarges, the papillary muscle tethering of the mitral valve leaflet progressively limits excursion toward the septal wall and serves as an approximation of the ejection fraction and heart failure.

Figure 4.29 are images from the normal and heart failure loops we saw earlier: note how the anterior mitral valve leaflet (the one closest to the probe or top of the screen) comes within 0.2 cm of the septal wall in the healthy heart loop. In the heart failure loop, there is minimal movement of the mitral valve leaflet toward the septal wall and the valve leaflet-septal wall gap is 3.2 cm. This would suggest severe heart failure. The enlarged left ventricle and left atrium along with very little ventricular contraction or "squeeze" during systole further suggest severe heart failure. This quick visual inspection of the heart with ultrasound provides valuable diagnostic and patient management information at the bedside when it is needed for clinical

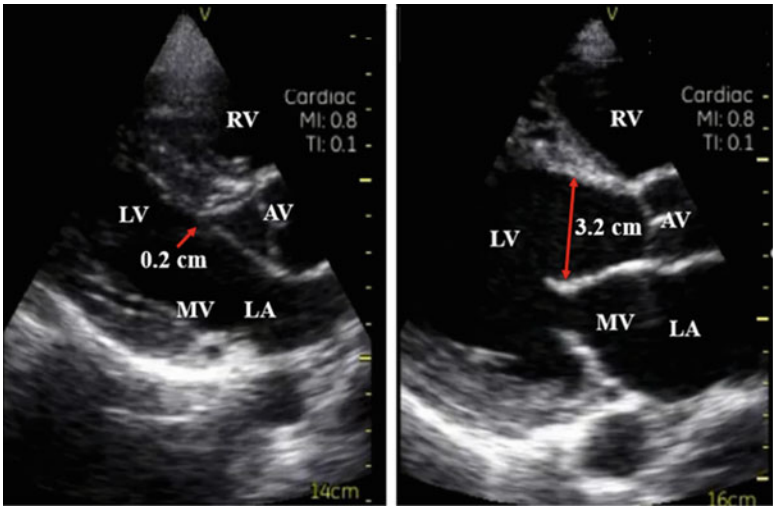

Fig. 4.29 PLAX views. Left panel: a healthy heart. Right panel: a heart in failure. Right ventricle (RV), left ventricle (LV), left atrium (LA), mitral valve (MV), and aortic valve (AV). Note distance from the mitral valve leaflets to the septal wall. Normal function 0.2 cm and heart failure 3.2 cm

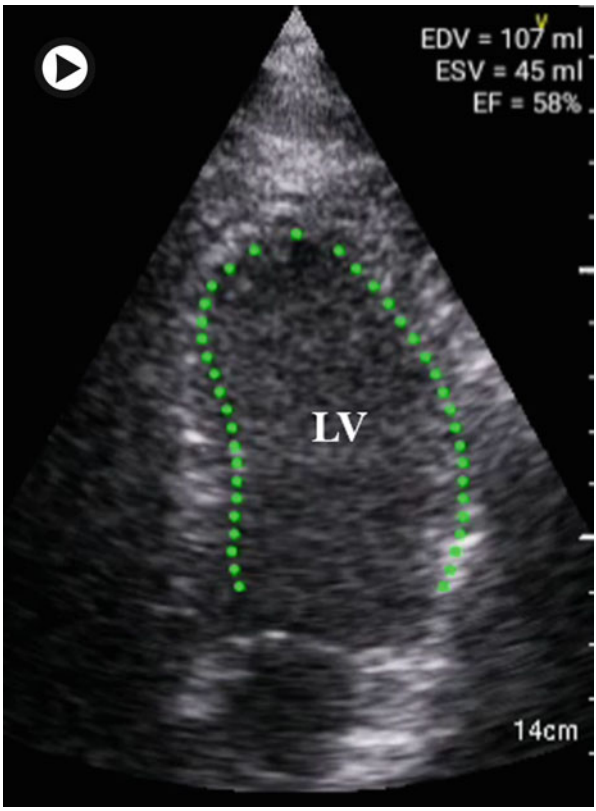

Fig. 4.30 (Video 4.9) A hand-held ultrasound device video using graphic mapping of the left ventricle (LV) of an apical cardiac view and artificial intelligence to calculate the ejection fraction as 58% based on an end-diastolic volume of 107 ml and end-systolic volume of 45 ml (▶ https://doi.org/10.1007/000-7px)

decision making and medical management. Note that there are some clinical situations when this method is not an accurate estimate of heart failure such as in patients with mitral stenosis or aortic insufficiency.

There are now portable ultrasound systems, including hand-held devices, that with the assistance of artificial intelligence automatically compute the EF once an adequate cardiac ultrasound image is obtained (Fig. 4.30). These systems use graphic software to determine left ventricular volume at end-diastole and end-systole to measure EF with very good accuracy.

4.12 Hypertension, Cardiac Remodeling, and Heart Failure

To compensate for the increased pressure afterload seen in chronic hypertension, a major cause of heart failure world-wide, the heart has the ability to structurally remodel the ventricle to increase contractility and overcome the additional afterload. Remodeling begins with activation of genes in ventricular muscle and genes involved in growth during fetal stages of development.

The result of remodeling in patients with hypertension is development of cardiac myocyte hypertrophy resulting in concentric thickening of the left ventricular wall. The thickened wall allows for increased contractility to maintain stroke volume, ejection fraction, and cardiac output in the face of increased afterload. This myocyte hypertrophy results in left ventricular hypertrophy (LVH). The thickness of the left ventricular muscle wall can be directly measured with ultrasound and is characterized as mild (1.1–1.3 cm), moderate (1.4–1.6 cm), or severe hypertrophy (>1.7 cm).

This compensatory mechanism of LVH can be explained by the Law of Laplace, which states that the pressure a sphere, which is roughly the shape of the ventricle, can generate is directly related to the tension and wall thickness or height of the container and is inversely related to the radius as follows: $P = 2HT/r$ where P is pressure, T is tension, H is wall thickness of height, and r is radius. Thus, with thickening of the muscular wall, the ventricle is able to generate greater ventricular pressure to overcome the resistance of the systemic hypertension. The Law of Laplace also explains the natural difference in wall thickness of the left and right ventricles as a function of the greater pressure needed for the systemic circulation compared to the pulmonary circulation.

For chronic pathological afterload conditions such as hypertension and aortic stenosis, the compensatory mechanism of hypertrophy, although effective in preserving relatively normal ejection fraction and cardiac output in the short term can fail over time. Persistently elevated blood pressure can lead to myocyte cell death (apoptosis), collagen deposition, and a stiff ventricle with progression to a dilated thin-walled ventricle with poor ejection fraction and heart failure. Thus, there is a critical need for blood pressure control and management of aortic stenosis in these patients.

4.13 Diastolic Dysfunction

Although this chapter has focused on systolic function and cardiac output, it is now well known that diastolic dysfunction can result in reduced cardiac output and heart failure as well. In fact, most cases of heart failure are a combination of systolic and diastolic dysfunction. Without adequate filling of the ventricle during diastole, stroke volume and cardiac output will fall even if systolic function is normal.

Ventricular filling can be adversely affected during diastole by decreased relaxation of the ventricle or increased stiffness of the ventricle (reduced compliance). The ventricular wall thickness associated with chronic hypertension can alter both of these parameters. This can lead to inadequate ventricular filling, increased diastolic pressure, and heart failure. It has also been shown that myocardial ischemia can decrease ventricular relaxation and compliance causing diastolic dysfunction.

As can be seen in Fig. 4.31, the end systolic pressure-volume curve does not change in diastolic dysfunction but the end diastolic pressure-volume curve (EDPVC) is moved upward and to the left resulting in a decrease in stroke volume.

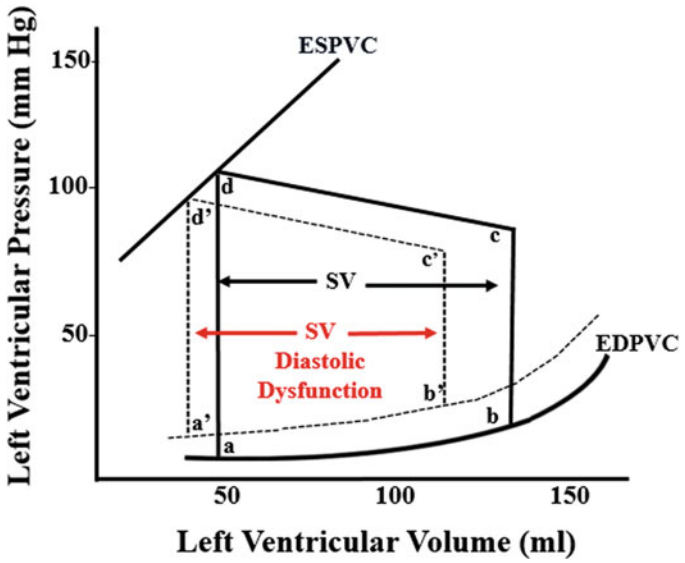

Fig. 4.31 Pressure-volume graph of change in stroke volume with diastolic dysfunction. Changes noted by dotted lines

This upward shift of the EDPVC indicates reduced ventricular compliance, which is the hallmark trait of diastolic dysfunction.

Although advanced Doppler techniques are needed to adequately assess diastolic dysfunction, standard B-mode ultrasound can identify conditions associated with diastolic dysfunction such as left ventricular hypertrophy and atrial enlargement that would suggest a component of diastolic dysfunction and the need for further diastolic dysfunction assessment. In addition, since diastolic dysfunction and systolic dysfunction commonly occur together, the identification of one should prompt evaluation for the other.

4.14 Ultrasound Laboratory Exercises

Understanding cardiac physiology is essential to understanding human health and disease. Ultrasound provides a powerful tool to look inside the body to study living anatomy and physiology of the heart. Several ultrasound laboratory exercises follow to further enhance your understanding of cardiac physiology and provide first-hand experience of ultrasound scanning and its potential as a learning tool as well as a clinical practice tool.

4.14.1 *Exercise 1: The Parasternal Long Axis (PLAX) View of the Heart*

4.14.1.1 Learning Objectives

Learn to obtain a parasternal long axis (PLAX) view of the heart and recognize relevant anatomical structures and normal physiological function.

4.14.1.2 Transducer/Probe

Cardiac imaging is best performed with a low frequency sector probe with a small footprint to fit between the ribs.

4.14.1.3 Additional Equipment and Supplies

None, other than those related to performing ultrasound.

4.14.1.4 Patient Position and Image Orientation

A supine patient position may be tried first but if an acceptable PLAX view of the heart is not obtained then a left lateral position should be used as shown in Fig. 4.32.

Cardiac imaging uses a different screen orientation than other ultrasound imaging. An orientation marker, usually the company logo, will be on the top right side of the screen for cardiac imaging. For other imaging applications, it is on the left side of the screen. The logo still matches up with the probe marker which is most often a palpable ridge on one side of the probe. Whichever side of the target organ (i.e. heart) the probe marker is on, that side of the target organ will match up with

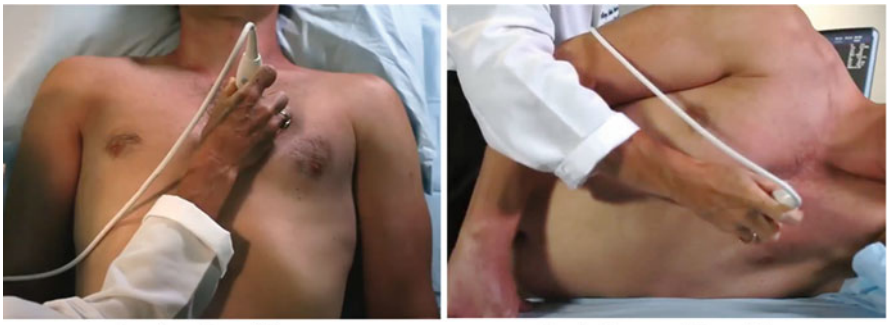

Fig. 4.32 Left panel: patient in the supine position. Right panel: patient in the left lateral position

the orientation marker on the screen. The top of the screen is always superficial or where the probe makes contact with the body surface.

4.14.1.5 Performing the Parasternal Long Axis View

1. Use the cardiac preset.
2. Apply adequate gel to the probe then place the probe in the second intercostal space immediately left of the sternum with the probe marker pointing toward the right shoulder (Fig. 4.33). The long axis of the heart runs roughly parallel to a line from the right shoulder to the left hip.
3. Slide the probe inferiorly down the chest staying just lateral to the sternum until the PLAX view is obtained (Fig. 4.33).
4. If adjustable, place the ultrasound beam focus position close to the level of the posterior wall of the left ventricle. The depth setting should be approximately 2.0 cm deep to the posterior wall of the left ventricle to help identify the descending aorta and any pericardial effusion.
5. The gain can be adjusted to obtain optimal brightness of the image. Avoid unnecessary brightness.
6. Once a PLAX view is obtained, it can usually be improved with very small movements of the probe such as fanning/tilting, sliding, rocking, rotating, and applying more pressure.
7. Capture (freeze) a good image and identify the anatomical structures in Fig. 4.33. Note that the distal part of the left ventricle including the apex cannot usually be visualized in the PLAX view. The posterior wall of the left ventricle should be between 0.7 and 1.1 centimeters in thickness which is greater than the right ventricular wall due to the need to generate greater circulatory pressures.

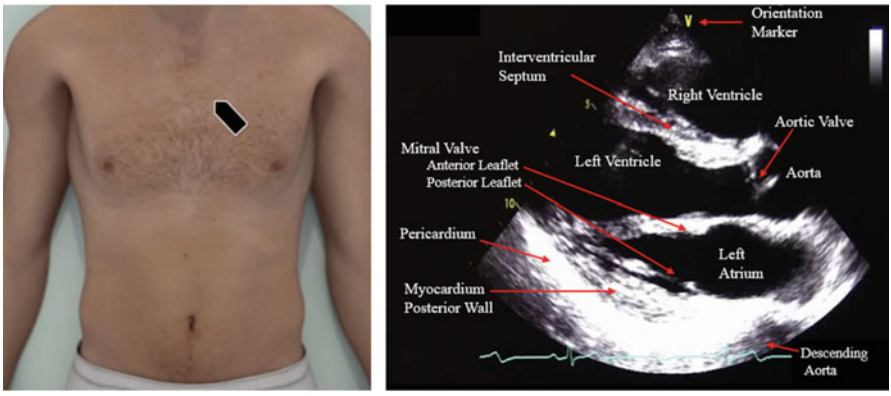

Fig. 4.33 Left panel: placement of ultrasound probe. Right panel: PLAX view with aortic valve closed and mitral valve open

8. Capture a short video loop of the PLAX view including several cardiac cycles to view the hemodynamics of the cardiac structures. Left ventricular contractions should be coordinated and symmetrical. There should be full opening and complete closure of the aortic and mitral valves with each heartbeat. The anterior mitral valve leaflet should come within 1.0 cm of the septal wall during a complete cardiac cycle which, in general, indicates a normal ejection fraction.

4.14.2 Exercise 2: Combining Ultrasound with Auscultation of the Heart

4.14.2.1 Learning Objectives

Learn to auscultate the heart with a stethoscope while viewing a real-time ultrasound PLAX view of the heart. Understand the hemodynamic causes of the first (S1) and the second (S2) heart sounds from pressure changes across cardiac valves as illustrated in the Wiggers Diagram.

4.14.2.2 Transducer/Probe

A low frequency cardiac sector probe should be used.

4.14.2.3 Additional Equipment and Supplies

A stethoscope with no special specifications can be used as normal heart sounds can be heard with any standard stethoscope.

Students will work in pairs with one student performing the ultrasound while the other student listens to the heart with the stethoscope. Students should take turns scanning and listening to the heart.

4.14.2.4 Auscultation of the Heart

Figure 4.34 shows the classic locations where the heart sounds are generally best heard for each of the four valves: aortic valve (AV), pulmonary valve (PV), tricuspid valve (TV), and mitral valve (MV). There is, however, location variability of optimal heart sounds and a less localized approach to auscultation can be used as described below. Also shown in Fig. 4.34 is a PLAX view with simultaneous recordings of the electrocardiogram (ECG) and stethoscope sounds matching the mechanical, electrical, and auditory cardiac events. If such a device is available, it can be used but each student should still listen to the heart sounds with a standard stethoscope at various locations across the chest as well.

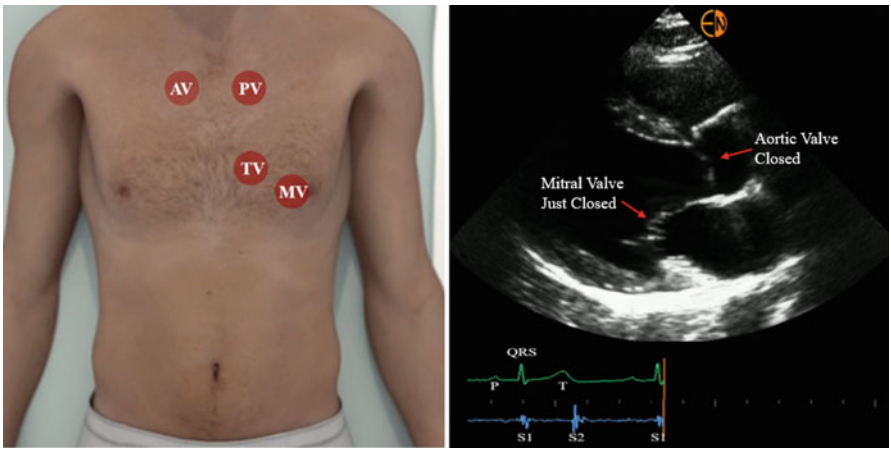

Fig. 4.34 Left panel: classic auscultation locations. Right panel: PLAX view with ECG and heart sound recordings

4.14.2.5 Ultrasound and Auscultation of the Heart

1. One student should obtain a good parasternal long axis (PLAX) view of the heart and then hold the probe steady.
2. The eartips of the stethoscope should be placed in the ears pointing forward and the flat diaphragm should be used for listening.
3. Both students should observe the real-time beating of the heart on the ultrasound screen and focus on closure of the aortic and mitral valves. The first heart sound (S1) is primarily due to closure of the mitral and tricuspid valves and the second heart sound (S2) is primarily due to the closer of the aortic and pulmonic valves. Both sounds are high pitched and best heard with the diaphragm of the stethoscope. Note the intensity of S1 and S2 as the mitral and aortic valves close respectively.
4. Begin auscultation in the second intercostal space at the right sternal border then move to the second intercostal space at the left sternal border. The stethoscope should then be inched downward along the left sternal border until the fifth intercostal space is reached and then moved laterally across the chest to just beyond the mid clavicular line. Note the intensity of each valve closure at each spot while also listening for any extra heart sounds such as S3, S4, or heart murmurs.
5. Timing of the cardiac cycle is important to note as additional sounds or murmurs will need to be classified as occurring in systole or diastole. Systole is the time interval from S1 to S2 and diastole is the time interval from S2 to S1. Diastole is longer than systole and distinguishing the two is relatively easy when the heart rate is slow or normal, but can be relatively difficult when the heart rate is fast. It can be helpful when auscultating the heart to feel for the carotid artery to time systole and diastole. The upbeat of the carotid pulse should be felt early in systole. It can also be helpful to close your eyes to better focus on the timing of the two

heart sounds and listen for sounds other than S1 and S2. The S3 sound is typically heard early in diastole in patients with heart failure. The S4 sound is typically heard late in diastole just before the S1 and can indicate a non-compliant left ventricle as is seen with left ventricular hypertrophy from chronic hypertension. S4 can occasionally be heard in healthy young adults and children. Both S3 and S4 are low pitched sounds and are heard best with the bell of the stethoscope.

6. Note in the Wiggers Diagram in Fig. 4.35, the location of S1 and S2 and the pressure differential causing the valves to close. S1 is heard when the pressure in the left ventricle rises above that in the left atrium and the mitral valve closes. The aortic valve closes when the pressure in the left ventricle falls below that of the aorta producing S2.
7. Capture a short cardiac loop and note the timing of closure of the aortic and mitral valves in relation to the Wiggers cardiac phases. Many ultrasound devices will allow the user to slow down captured video loops to more readily appreciate changes in chamber size, chamber contractility and relaxation, and valve motion. If available, use this feature or frame-by-frame analysis of the PLAX view and identify characteristics associated with the Wiggers phases.

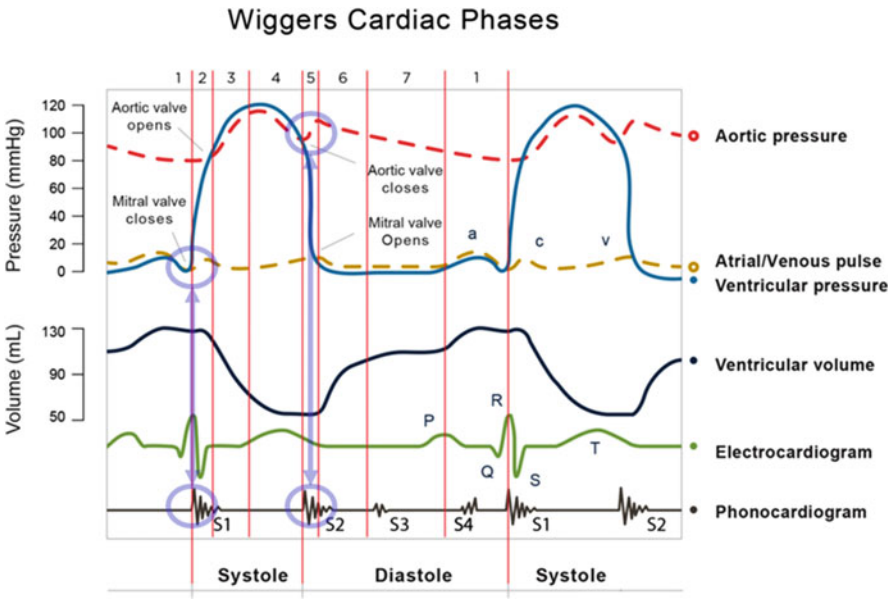

Fig. 4.35 Wiggers diagram. Pressure changes and corresponding S1 and S2 heart sounds (light blue circles)

4.14.3 Exercise 3: The Apical Four and Five Chamber Views of the Heart

4.14.3.1 Learning Objectives

Learn to obtain the apical four and five chamber views of heart and recognize the relevant anatomical structures and normal physiological function.

4.14.3.2 Transducer/Probe

A cardiac low frequency sector probe should be used.

4.14.3.3 Additional Equipment and Supplies

None, other than those related to performing ultrasound.

4.14.3.4 Patient Position and Image Orientation

A supine position can be tried first but the left lateral position with the left arm elevated is considered ideal for capturing apical four and five chamber views (Fig. 4.36). In this position, the heart comes closer to the chest wall allowing a better quality image of the heart. Raising the left arm over the head may widen the rib spaces creating a larger apical window between the ribs.

Remember cardiac imaging uses a different screen orientation from other ultrasound imaging.

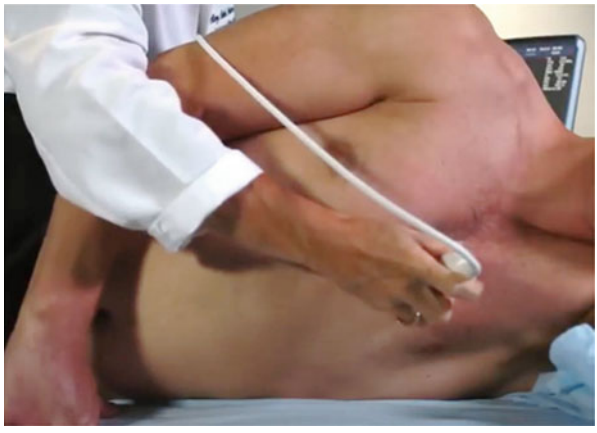

Fig. 4.36 Patient in the left lateral position for apical cardiac views

Whichever side of the target organ (heart) the probe marker is on, that side of the target organ will match up with the orientation marker on the screen. The top of the screen is always superficial.

4.14.3.5 Performing the Apical Four Chamber View

1. Use the cardiac preset.
2. With the patient in the left lateral position, apply adequate gel to the probe and place the probe on the anterior chest in the left mid-clavicular line in the fifth rib interspace with the probe marker pointing toward the patient's left side or down toward the exam table in this position.
3. The ultrasound beam should be pointed toward the right shoulder thus sectioning the heart through the long axis starting at the apex which is now closest to the probe and will be located at the top of the ultrasound screen.
4. The apical window, as shown in Fig. 4.37, shows considerable variability from patient to patient. If unable to find a good apical window initially, try large sweeps of the probe in the apical area until the beating heart comes into view. Another approach is to start with a PLAX view and slide down the septum until you come to an apical 4-chamber view.
5. To acquire a good view of all four chambers you may need to move down a rib space or slide the probe laterally, angle the probe more anteriorly or posteriorly, or rotate the probe counter-clockwise with the marker pointing more toward the left shoulder. The depth may also need to be adjusted to capture all four chambers. Adjustments of the focus and gain, as well as fine manipulations of the probe will help ensure a high quality apical four image.
6. Capture (freeze) a good Apical-4 chamber image and identify the anatomical structures in Fig. 4.37. Note the left ventricle is on the right side of the ultrasound screen with the orientation marker. The normal right ventricle is

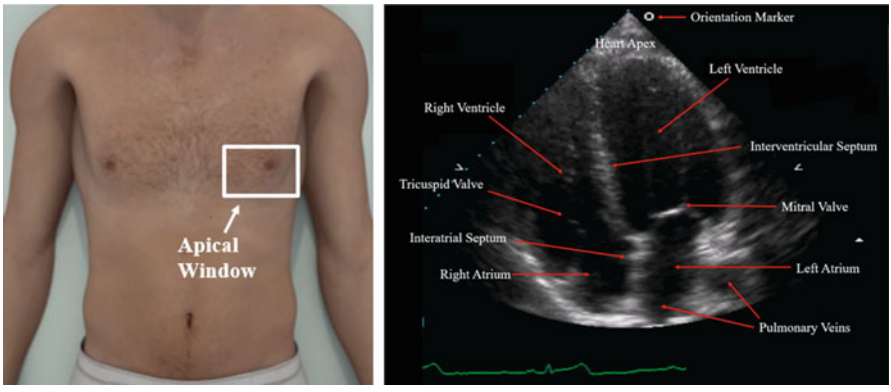

Fig. 4.37 Left panel: ultrasound cardiac window for apical views. Right panel: apical four chamber view

approximately two-thirds the size of the left ventricle. The left ventricle should appear bullet shaped. The left atrium accounts for approximately one-third of the total length of the distance of the left atrium plus the left ventricle. The septum should be relatively straight and parallel to the long axis of the heart. The free walls of the left ventricle are thicker than those of the right ventricle.

7. Capture a short video loop of the Apical 4-chamber view of the heart to include several cardiac cycles to view the hemodynamics of the cardiac structures. All areas of the ventricular walls should move inward together to decrease the size of the ventricular chamber in systolic contraction. There should be full opening and complete closure of the mitral and tricuspid valves with each heartbeat.
8. The noted orientations, dimensions, and wall movements viewed in the Apical 4-chamber view are important to appreciate as they may change with disease states such as myocardial infarction (localized poor wall motion), left heart failure (enlarged left atrium, enlarged left ventricle, and poor contractility), and pulmonary embolism (enlarged right atrium and right ventricle and displacement of the septal wall into the left ventricle).
9. To obtain an apical 5 chamber view from the 4-chamber view, slowly angle the ultrasound beam anteriorly toward the chest wall. The aortic valve and the proximal aorta will come into view creating the "fifth chamber", allowing good assessment of the anatomy and function of these structures. See Fig. 4.38.

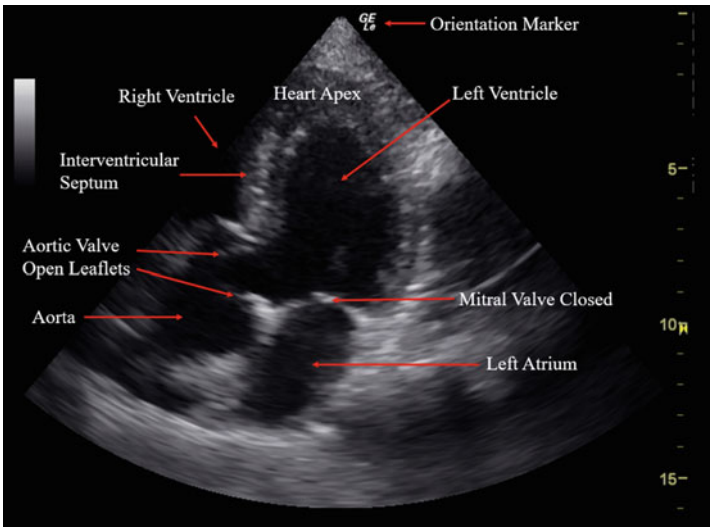

Fig. 4.38 Apical 5 chamber view in systole with mitral valve closed and aortic valve open

4.14.4 *Exercise 4: Color Doppler Ultrasound to Assess Cardiac Blood Flow and Heart Valves*

4.14.4.1 Learning Objectives

Learn to use color Doppler to assess cardiac blood flow and heart valve function.

4.14.4.2 Transducer/Probe

A cardiac low frequency sector probe should be used.

4.14.4.3 Additional Equipment and Supplies

None, other than those related to performing ultrasound.

4.14.4.4 Applying Color Doppler to Apical Cardiac Views

1. Obtain an apical 4 chamber view with the patient in the left lateral position.
2. Once a good apical 4 chamber view of the heart is obtained, turn on the color Doppler function. The color flow bar legend will appear on the left side of the screen. By convention, the red color represents blood flow towards the probe and the blue color represents flow away from the probe. The darker colors/shades indicate lower velocities of flow and the lighter colors/shades indicate higher velocities of flow (Fig. 4.39).
3. Use the trackball or touch screen to drag the color box to include the mitral valve, and part of the left ventricle, the left atrium, the right ventricle, and the right atrium as seen in Fig. 4.39. You may need to expand the size of the color box.

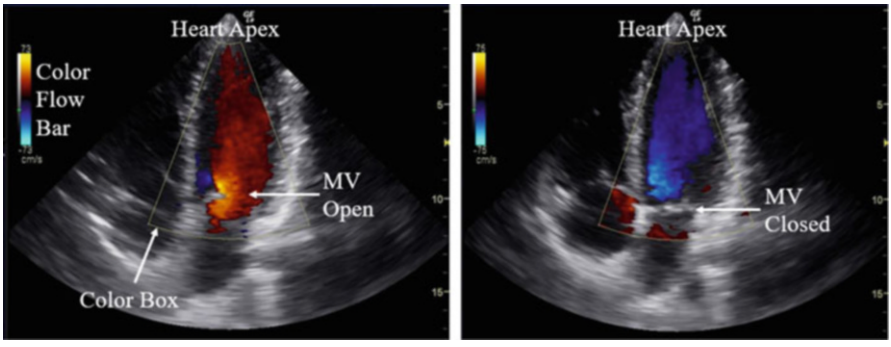

Fig. 4.39 Apical four chamber view with color Doppler in diastole (left panel) and systole (right panel)

4. Note in Fig. 4.39 that during diastole, the mitral valve is open and the red color flow shows the blood flowing from the left atrium toward the probe at the distal end or apex of the left ventricle. During systole the mitral valve is closed and there is blue color flow away from the ventricular apex and the probe during ventricular contraction toward the ventricular outflow tract and the aorta.
5. To obtain an apical 5 chamber view which includes the aortic valve and the proximal aorta, slowly angle the ultrasound beam anteriorly toward the chest wall (Fig. 4.40). With color Doppler, the blue color flow shows the ejection of blood from the left ventricle into the aorta. The relatively homogeneous blue color of the blood flowing across the aortic valve into the aorta is consistent with a normal aortic valve and not the mixed colored flow of turbulence that would suggest valvular pathology like aortic stenosis. Note also no blue or mixed color back flow across the closed mitral valve into the left atrium during systole that would be seen with an incompetent mitral valve and mitral regurgitation. Some blood is entering the left atrium from the pulmonary veins as the mitral valve remains closed.
6. A similar assessment can be made during diastole in that there is no red or turbulent back flow from the aorta into the left ventricle across the closed aortic valve that would be seen with aortic valve insufficiency. There is also no turbulent flow from the left atrium into the left ventricle across the open mitral valve in diastole that would be seen with mitral stenosis.
7. Capture short video loops of the apical four and five chamber views with color Doppler to better view the hemodynamics of these views. Slow down the loop speeds, if possible, for more detailed hemodynamic analysis.

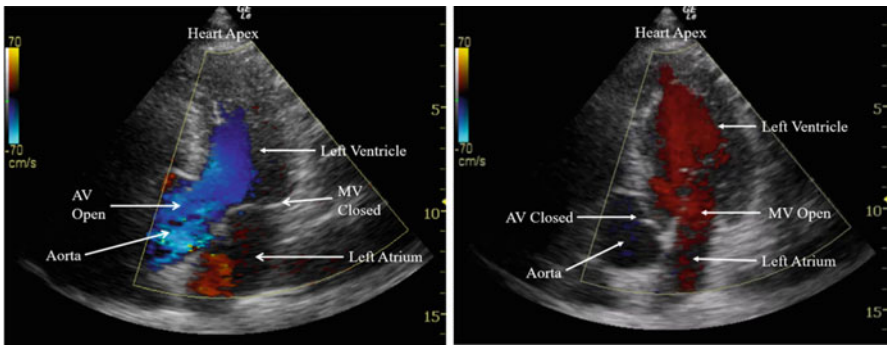

Fig. 4.40 Apical 5 chamber view with color Doppler in systole (left panel) and diastole (right panel)

Further Reading

Bell F, Wilson B, Hoppmann R (2015) Using ultrasound to teach medical students cardiac physiology. Adv Physiol Educ 39:392–396

Hoppmann R, Rao V, Bell F et al (2015) The evolution of an integrated ultrasound curriculum (iUSC) for medical students: 9-year experience. Crit Ultrasound J 7(1):18–33

Johnson C, Montgomery L, Quinn J et al (2016) Ultrasound imaging in teaching cardiac physiology. Adv Physiol Educ 40:354–358

Via G, Hussain A, Wells M et al (2014) International evidence-based recommendations for focused cardiac ultrasound. J Am Soc Echocardiogr 27(7):683.e1–683.e33. https://doi.org/10.1016/j.echo.2014.05.001

Chapter 5
Ultrasound of the Respiratory System

Keith R. Barron, Duncan Norton, and Michael Blaivas

5.1 Anatomy and Physiology of the Respiratory System

The important physiological role the respiratory system plays is to take blood that is low in oxygen (O_2) and high in carbon dioxide (CO_2), often called venous blood, and turn it into arterial blood, which is high in O_2 and low in CO_2. Oxygen is an important "nutrient" for tissues, cells require it to make sufficient energy to maintain cellular function. Carbon dioxide is constantly produced as part of metabolism. It represents a waste product and the lungs must remove it from the body. This crucial role of bringing in O_2 and eliminating CO_2 is pivotal for normal physiology and one that is required for survival.

Inspiration is the term used for breathing in, which brings O_2 into the lungs. This O_2 then diffuses into the blood in small air sacs called alveoli (alveolus is singular). Your lungs have millions of alveoli. CO_2, made by the tissues, diffuses into the

Supplementary Information The online version contains supplementary material available at https://doi.org/10.1007/978-1-0716-1863-9_5. The videos can be accessed by scanning the related images with the SN More Media App.

K. R. Barron (✉)
Prisma Health Midlands/University of South Carolina School of Medicine, Columbia, SC, USA
e-mail: Keith.Barron@uscmed.sc.edu

D. Norton
Prisma Health Midlands/University of South Carolina School of Medicine, Columbia, SC, USA

Prisma Health Children's Hospital–Midlands, Columbia, SC, USA
e-mail: Duncan.Norton@prismahealth.org

M. Blaivas
Prisma Health Midlands/University of South Carolina School of Medicine, Columbia, SC, USA

Saint Francis Hospital, Columbus, GA, USA
e-mail: mike@blaivas.org

L. B. Wilson et al. (eds.), *Understanding Physiology with Ultrasound*, Physiology in Health and Disease, https://doi.org/10.1007/978-1-0716-1863-9_5

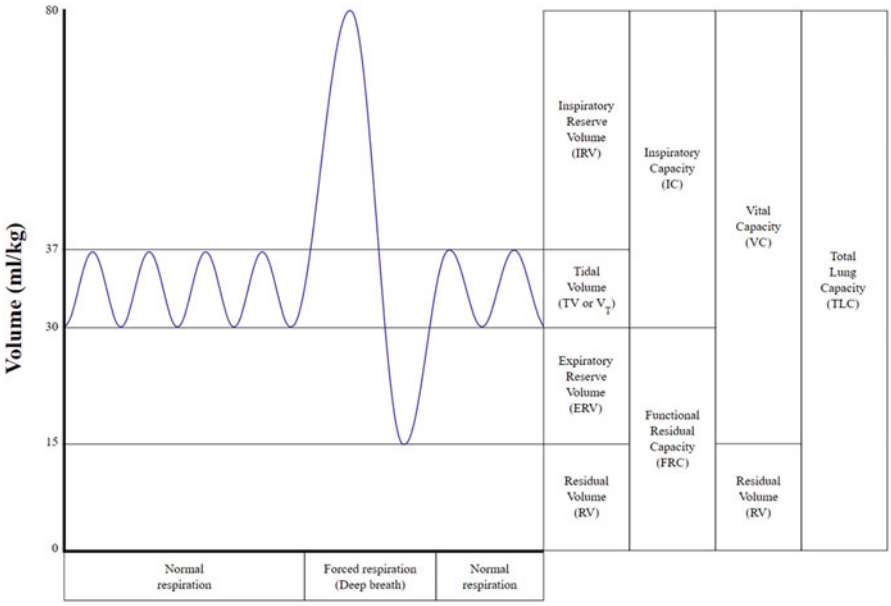

Fig. 5.1 Graphical depiction of lung volumes and capacities. Unedited reproduction from https://commons.wikimedia.org/wiki/File:Lungvolumes.svg. License for use https://creativecommons.org/licenses/by-sa/3.0/deed.en (Cooper and William 2018)

alveoli from the blood and expiration is the term used for blowing air out. Thus, expiration removes CO_2 from the body. More details regarding inspiration and expiration as it relates to ultrasound (US) are provided later in this chapter.

The volume of gas that the lung can hold is dependent on the compliance (discussed below) of the lung tissue and the surrounding musculoskeletal system. Lung volume is measured with a spirometer. There are 4 lung volumes and 4 lung capacities (a capacity is 2 or more volumes added together: Fig. 5.1). A complete discourse on these is beyond the scope of this book. However, some things are noted here. When breathing quietly, the volume of air entering or leaving the lungs is called tidal volume. This is approximately 500 ml in the typical adult. If you take a deep breath in with all the effort you can muster, this is total lung capacity. If you try to blow out all the air you can, called a maximal forced expiration, air remains in your lungs. This air is called residual volume. Regardless of how hard you blow out, this air remains. This residual volume is important, because it keeps your alveoli inflated.

To help understand the physiology of the respiratory system, one needs to have a basic understanding of the anatomy that makes up this system. The lung is the major anatomic organ that makes up the respiratory system (Fig. 5.2). The respiratory system can be thought of as having two zones: a gas transmission zone known as the conducting zone and a gas exchange zone known as the respiratory zone. The conducting zone is made up of the nose, mouth, trachea, bronchi, and large bronchioles. In this zone, gas is conducted from outside of the body into the lungs down

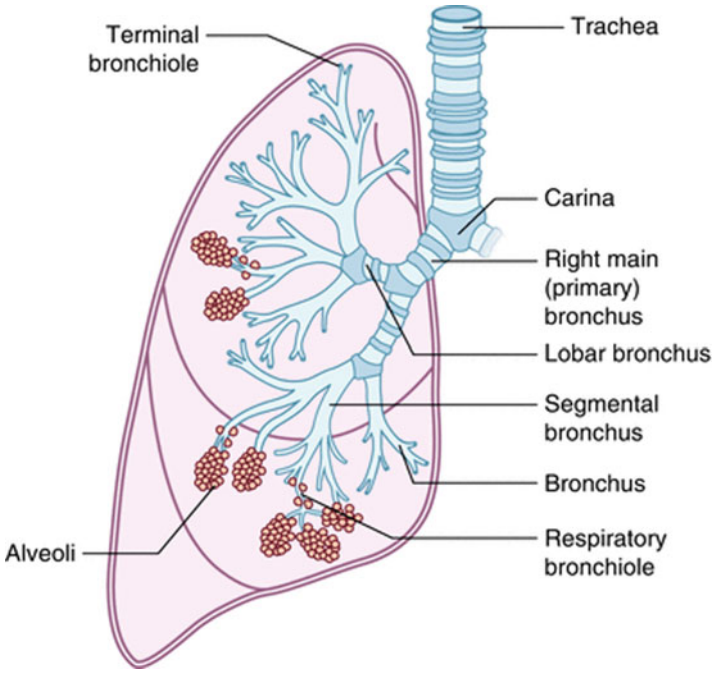

Fig. 5.2 Basic anatomy of the respiratory system (Rehfeld et al. 2017)

to the respiratory zone. The respiratory zone is composed of the respiratory bronchioles, alveolar ducts and alveoli where gas exchange can occur across cellular membranes. Gas exchange only occurs in these alveoli via diffusion. Because the conducting zone does not have alveoli, no gas exchange occurs here. This conducting zone constitutes anatomic dead space. Since gas exchange can only occur by diffusion, it requires a large surface area and small distance between air and blood flow. The process of gas exchange takes place in the alveoli, which are composed of a specialized cells known as pneumocytes. Type I pneumocytes are flat with a large surface area to facilitate gas exchange. Type II pneumocytes produce an important phospholipid known as surfactant. Surfactant, which will be discussed in more detail later, causes a reduction in surface tension and thus assists in preventing alveolar collapse.

The circulatory system associated with the respiratory system can be divided into the pulmonary vasculature and bronchial vasculature. The pulmonary vasculature is composed of the main pulmonary arteries that carry venous blood from the right ventricle of the heart until they divide down to capillaries. Gas exchange of O_2 and CO_2 occurs at the capillary system of the alveoli and is then carried back to the left atrium via the pulmonary veins.

Overall, the amount of blood flow in the bronchial vasculature is small, but it is an important component of the respiratory vasculature. The bronchial vasculature is not involved in gas exchange. Instead, the bronchial vasculature is responsible for delivering oxygenated blood to the large airways in the transmission zone.

5.2 How We Breathe

The respiratory system functions primarily to extract and provide oxygen to tissues, and to remove carbon dioxide. This is accomplished by the act of breathing, which is an active, although often subconscious act, that humans perform approximately 15 times a minute. Within limits, breathing may be a conscious exercise when needed for various activities. Although seemingly simple, breathing is a complex act of mechanical manipulations and regulatory checks and balances. Breathing can be grossly broken down into two different aspects: Mechanical and Regulation.

Air is a fluid, in that it moves from regions of high pressure to low pressure. For air to move into the respiratory tract from the outside, pressure inside the lungs needs to be less than that of the atmospheric pressure. At rest, the pressure in all parts of the respiratory tree equals atmospheric pressure. Thus, to inspire air into the lungs, a pressure lower than that of the atmosphere needs to be generated. This pressure differential is accomplished by contractions of muscles, resulting in what is known as negative-pressure breathing. Positive pressure breathing occurs when the atmospheric pressure is increased at the level of the mouth and nose; this is what ventilators do for individuals who cannot generate a negative pressure gradient.

The first stage of breathing begins at rest. This is the point in time when pressure throughout the respiratory tree, including down to the alveolar level, equals atmospheric pressure. By convention, atmospheric pressure is given the value of zero. This is not "technically" correct, but since it does not change from room to room, it is simpler to consider it zero (also discussed elsewhere in this book). The lungs are physically connected to the chest by the pleura and the pressure inside this fluid-filled pleural space (intrapleural pressure) is less than the atmosphere, thus it is negative. Thus, in short, the lungs are surrounded by a negative pressure (negative intrapleural pressure). This negative intrapleural pressure is generated by the tension of two opposing forces: an inward and outward force referred to as elastic recoil. The first force is the inward elastic recoil of the lung, which acts as a force attempting to collapse or pull the lung away from the chest wall. This is balanced by the outward elastic recoil of the chest wall. These opposing forces generate the negative pressure surrounding the lungs, thus keeping the lung expanded while at rest. The magnitude of this negative intrapleural pressure is approximately -5 cm H_2O. The difference between alveolar and pleural pressures is referred to as the transpulmonary or transmural pressure.

In healthy people, the lungs and chest wall move together, with a parietal (portion of the pleura connected to the chest wall) and visceral pleura (portion of the pleura connected to the lungs) freely sliding against each other during respiration. With ultrasound, the junction of the static parietal and dynamic visceral pleura appear as an echogenic pleural line below the ribs within an intercostal space. This pleural line is very echogenic and generates a repeating, horizontal reverberation artifact of the visceral-parietal pleura interface (VPPI) below and parallel to the pleural line; this is referred to as an A-line pattern (Fig. 5.3). The sliding of the pleura can be easily visualized with ultrasound. During breathing, the pleura freely slide against each other, causing a subtle shimmering or "lung sliding" appearance on ultrasound (Fig. 5.4).

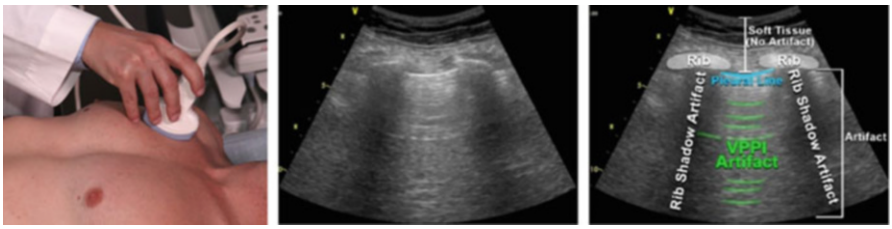

Fig. 5.3 The left-hand figure shows probe placement for US of the lung. Using a curvilinear, low-frequency probe, a longitudinal view of an intercostal space is shown between two ribs that appear as curved, echogenic structures with posterior acoustic shadowing (figure to the right). The pleural line is an echogenic line deep to the ribs that generates a repeating reverberation artifact of the visceral and parietal pleural interface, referred to as A-lines

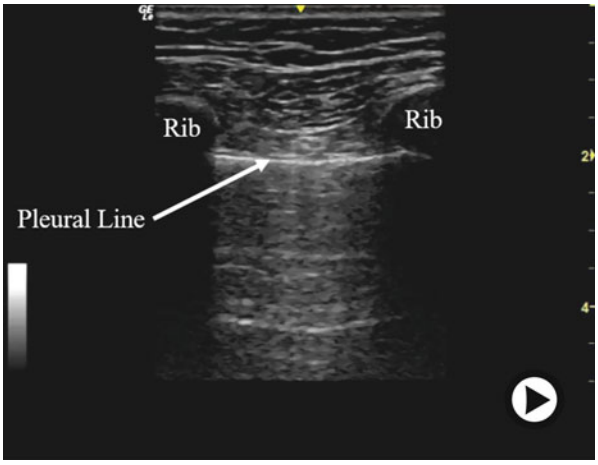

Fig. 5.4 (Video 5.1) Video of Lung Sliding. Lung sliding appears as a subtle "shimmering" or "sliding" appearance of the pleural line, which indicates that the parietal and visceral pleura are freely sliding against each other during respiration (▶ https://doi.org/10.1007/000-7q0)

M-mode may also be used at the pleural line to assess for lung sliding, where it creates a distinct pattern similar to a "sandy beach." The absence of lung sliding produces a more-linear appearance above and below the pleural line. See this chapter's lab exercise, Figs. 5.14 and 5.15, and Chap. 2 for more details.

5.2.1 Alterations in Intrapleural Pressure due to Pathologic States: Appearance on Ultrasound

The intrapleural space may fill with exogenous liquids (blood for example) or air in different pathologic states. If exogenous fluid or air is present, there is a resultant loss

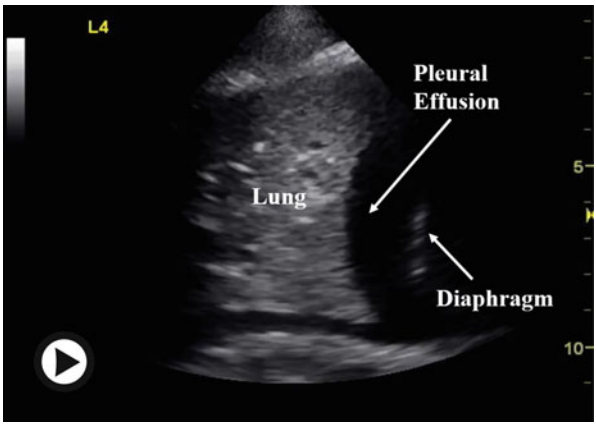

Fig. 5.5 (Video 5.2) Video of Atelectasis. Using a low-frequency, phased-array transducer to obtain a coronal cut of the right lung base, no A-lines are seen, but rather a gray, mostly homogeneous area of atelectasis is present superior to (above) the diaphragm. A pleural effusion is imaged as well, appearing as an anechoic area between the lung parenchyma and diaphragm (▶ https://doi.org/10.1007/000-7pz)

of contact between the visceral and parietal pleura. In both conditions, the inherently elastic lung pulls away from the chest wall due to loss of contact between the parietal and visceral pleura. In larger pleural effusions (excess liquid in the intrapleural space) and high-pressure pneumothoraces (air in the intrapleural space), portions of the lung, or the entire lung can collapse with the consequent decrease in lung volume below its usual resting state. The resultant alveolar collapse is referred to as atelectasis and when present, atelectasis causes an increased surface tension that then leads to a reduction in compliance. In an atelectatic area of the lung that abuts the chest wall or diaphragm, ultrasound waves are now able to image the lung parenchyma itself, which appears as a grey, more-homogeneous area of lung tissue cephalad to the diaphragm or deep to the pleural line (Fig. 5.5).

Free intrapleural air, termed a pneumothorax, is readily and accurately assessed by ultrasound. When free intrapleural air is introduced into the space between the visceral and parietal pleura, as occurs when the chest wall is punctured, the chest suddenly pulls away from the lung, and the intrapleural pressure equalizes with atmospheric pressure, typically resulting in collapse of the lung. Examining the chest wall with ultrasound in this condition, an intercostal space appears very similar to a normally aerated lung. The free intrapleural air still generates an A-line pattern due to the persistence of a tissue-air interface that is highly reflective of ultrasound, but since the parietal and visceral pleura are separated by air, no sliding is seen Fig. 5.6. If present, atelectasis is not generally seen in this condition given that free intrapleural air obscures deeper structures.

While the finding of A-lines without sliding indicates a pneumothorax, this condition can be definitively diagnosed if the transition zone between normal lung and free intrapleural air is seen. This dynamic point, with sliding on one side of the

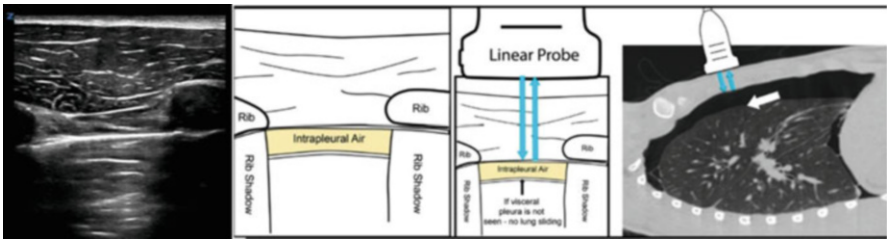

Fig. 5.6 From left to right, free intrapleural air (seen in a pneumothorax) separates the parietal and visceral pleura with resultant loss of the lung sliding artifact. Reverberation artifacts, or A-lines, are still generated by the presence of a tissue-air interface, however. A sagittal computed tomography (CT) scan is also included to demonstrate how free air separates the lung from the chest wall: the arrow indicates the visceral pleura, now separated from the parietal pleura by free air (the radiolucent, darker area above the arrow)

screen and no sliding on the other, is referred to as a lung point. Free intrapleural air rises to the least dependent portion of the chest (dependent referring to the directional influence of gravity: toward the feet when upright, toward the back when supine). Thus, in a supine patient the examination begins lateral to the sternum in the least-dependent intercostal space, tracking toward the back to find the transition zone, or lung point (Figs. 5.7 and 5.8).

Clinically, because a pneumothorax can be a life-threatening situation, a rapid diagnosis may be lifesaving; ultrasound is portable and accurate for identifying this condition, whether at the bedside or at the site of traumatic injury. Historically, thoracic chest x-ray has been a common initial diagnostic imaging study for identification of pneumothorax, but some studies suggest that ultrasound may be a more sensitive test for this diagnosis.

Free intrapleural liquid, or pleural effusion, also generates a distinct appearance on ultrasound. Placing the transducer to obtain a coronal plane of cut at the level of the diaphragm, and fanning posteriorly (Fig. 5.9), free liquid pleural effusions generally appear as anechoic fluid superior to the diaphragm while the patient is supine. The atelectatic, or collapsed portion of the lower part of the lung can often be seen "flapping" in the fluid (Fig. 5.5 Video)**,** appearing like a swimming jellyfish on ultrasound.

5.2.2 Inspiration

During inspiration, the muscular diaphragm contracts, causing the volume of the thorax to increase. The volume increase results in a decrease in intrapleural pressure. This decrease in pressure occurs due to the effects of Boyle's law, which states that the pressure of a gas multiplied by volume remains constant when temperature remains unchanged. Thus, an increase in volume causes a decrease in pressure.

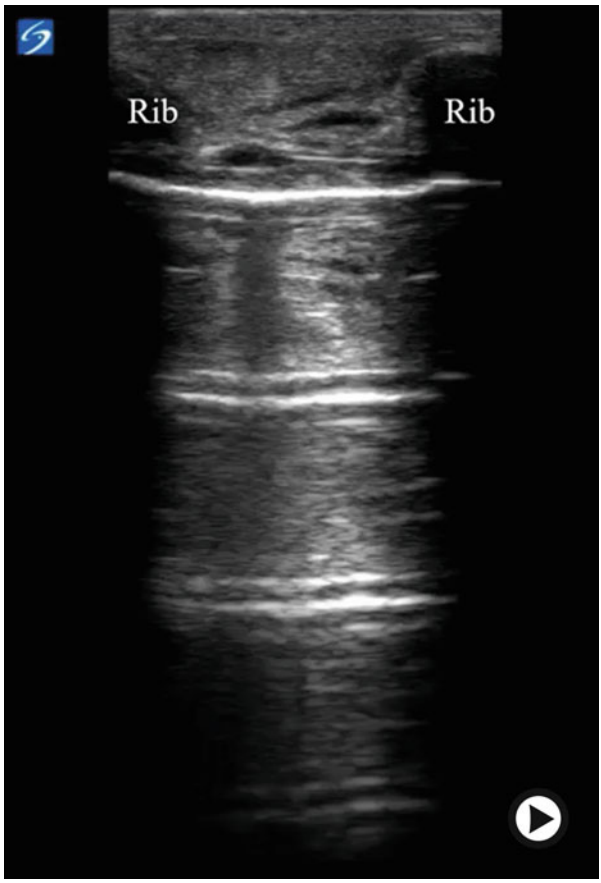

Fig. 5.7 (Video 5.3) Video of Lung Point: A lung point is generated by visualizing the transition point between lung sliding and no sliding, indicating where free intrapleural air separates the pleura. This point is dynamic and varies with respiration. In the video the lung point slides in and out of the left portion of the intercostal space (▶ https://doi.org/10.1007/000-7py)

The resultant change in intrapleural pressure results in a negative alveolar pressure. Once alveolar pressure becomes negative (subatmospheric) air flows into the lung until alveolar pressure again equals atmospheric pressure. At this point inspiration ceases. Air inside the body is highly reflective of ultrasound waves, therefore ultrasound imaging is not well-suited to capture air flow. Contraction of the diaphragm and other muscles of breathing can help infer information about this phase. The diaphragm can also be visualized well (Fig. 5.10).

During inspiration, the air travels through the conducting zone (see above), into the respiratory zone. As indicated above, this respiratory zone contains the alveoli, which is the site of gas exchange with the blood. These structures are not well-imaged by transthoracic ultrasound.

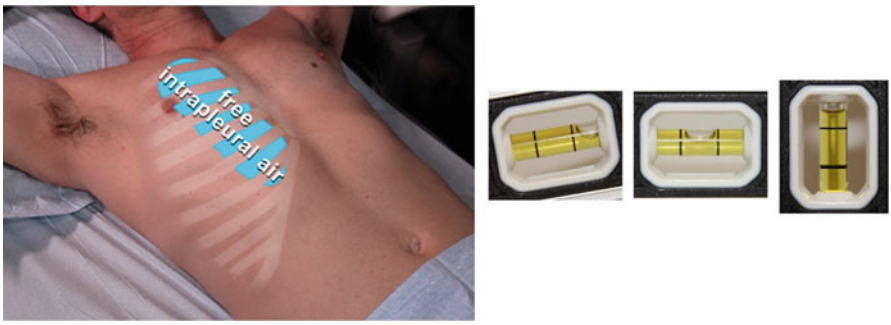

Fig. 5.8 The picture on the left shows a subject in a supine position with an outline illustrating the location of the right ribs. Like free air within a level (picture to the right), free intrapleural air will generally rise to the least-dependent portion of the chest. This is where the examination for pneumothorax should begin

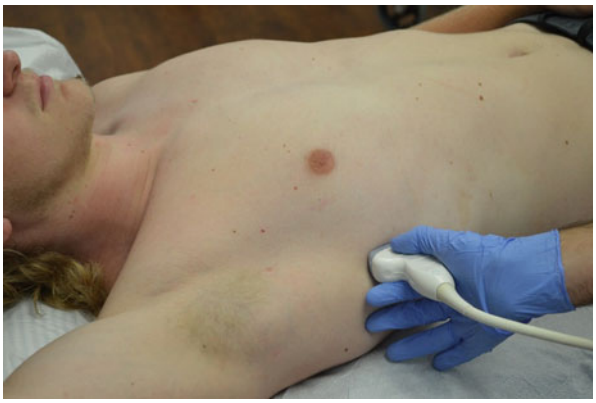

Fig. 5.9 The transducer should be fanned or angled posteriorly to visualize the costophrenic angle superior (towards head) to the diaphragm where free intrapleural fluid, or pleural effusion may be visualized

5.2.3 Expiration

Expiration during normal quiet breathing is passive in nature. During quiet breathing, the diaphragm relaxes and the elastic recoil of the lung pulls the chest wall back to its original position, decreasing lung volume. This in turn increases alveolar pressure compared to atmospheric pressure and air flow out of the lungs, until the pressures equalize.

5.3 Diaphragmatic Excursion: Appearance on Ultrasound

The diaphragm serves as the main driver of inspiration, both in quiet and forceful breathing. It is a dome-shaped structure separating the abdominal and thoracic cavities and consists of a fibrous tendon and two muscular parts. When contracting,

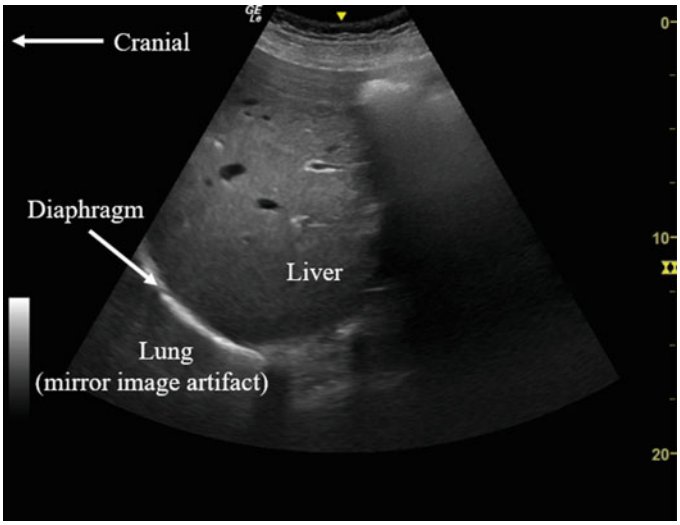

Fig. 5.10 This image, obtained with a low-frequency curvilinear probe is a sagittal view of the liver, with the diaphragm appearing as a curved, echogenic structure cephalad and posterior to the liver (arrow). Anatomically, the lung lies above the diaphragm, towards the head and the left in the scanning window shown, but is not seen in this image due to the diaphragmatic reflection of ultrasound waves, resulting in a mirror image artifact

the muscular diaphragm expands the volume of the thoracic cavity, resulting in a negative pressure in alveoli that in turn drives air flow into the lungs. This contraction results in muscle thickening that can readily be assessed by ultrasound at the zone of apposition, or where the muscle attaches to the inner aspect of the rib cage.

5.4 Other Respiratory Muscles

Active or forceful expiration occurs typically during periods of activity such as exercise, singing, or speech. This is a forceful expiration that is generated by contracting the abdominal and internal intercostal muscles. The contraction of the abdominal musculature increases intra-abdominal pressure forcing abdominal contents superiorly (toward the thorax) while simultaneously pulling the lower ribs downward. The contraction of the internal intercostal muscles further presses down on the chest wall. These coordinated contractions result in a large increase in intrapleural pressure that then correlates to a corresponding increase in alveolar pressure. The increased pressure triggers a rapid, forceful expiration until the alveolar pressure again equals that of atmospheric pressure. By sliding the transducer cranially from the diaphragm, a midsagittal cut can be obtained of an intercostal muscle as well. Ultrasound can assess how the intercostal muscles contract and thicken during respiration (Fig. 5.11).

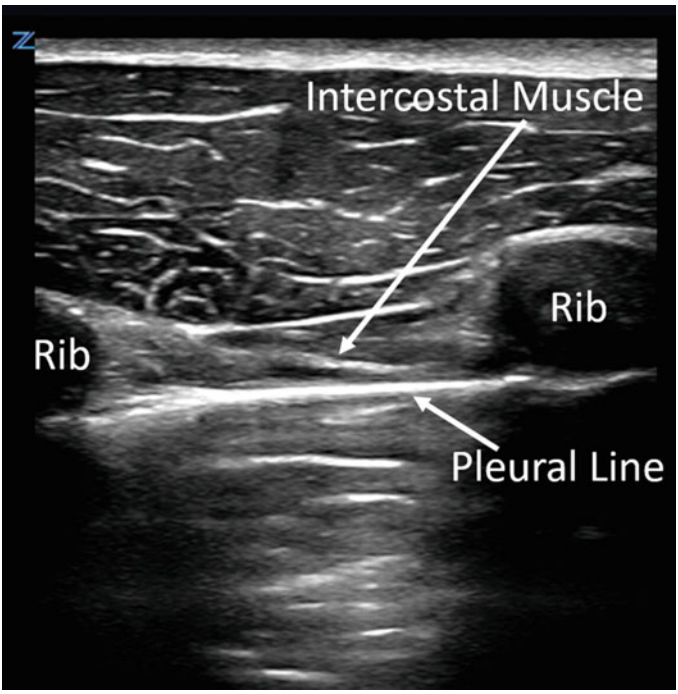

Fig. 5.11 A mid-sagittal view of an intercostal muscle between two ribs, just above the echogenic pleural line

5.5 Compliance and Elasticity

Breathing relies on the changes in pressure generated by inspiration with the resultant change in lung volume. The measure of how volume changes in response to pressure change is referred to as compliance. Compliance can be thought of as how easily the lung can expand. Imagine a balloon or rubber band. If it is very compliant, then it means it stretches or expands easily. If it takes very little effort to stretch it, then it is very compliant. Mathematically, compliance is directly correlated with the pressure-volume relationship in that $\Delta V/\Delta P$ = compliance. Although beyond the scope of this book, pressure-volume curves can be drawn not only for the lungs, but also for the chest-wall/lung structure, and for the combination of the two.

Elasticity is the inverse of compliance. Elasticity is the property that resists change. Thinking of a balloon or rubber band, elasticity is the force that returns the balloon or rubber band back to its original shape. A very thick rubber band that is hard to stretch has high elasticity and since it is the inverse, low compliance. The greater the elasticity of the lung, the greater the force tending to collapse the lung. Lung compliance/elasticity can change with different disease states. In emphysema, for example, individuals may experience small airway collapse due to the loss of elastic fibers, resulting in increased compliance of the lung. This loss of elasticity

decreases the ability to trigger a rapid, forceful expiration. Conversely, in fibrosis, a type of restrictive lung disease, lung tissues become stiff, resulting in decreased compliance and high collapsing force.

Reduced lung volumes occur in restrictive lung disease. An example is pulmonary fibrosis, an intrinsic restrictive lung disease. An overproliferation of cellular structures, production of collagen, and subpleural cystic changes causes a complex fibrotic pattern that results in a rise in elasticity. These subpleural fibrotic changes can be inferred with ultrasound by the presence of B-lines. B-lines are hyperechoic vertical artifacts that arise from the pleural line, extend to the edge of the screen, and vary with respiration (Fig. 5.12 and Video). B-lines also may be seen, however, with pulmonary edema, increasing in number as the air content in the lung decreases.

Compliance is further affected by the small size of the alveoli. Surface tension is created as a result of a thin layer of fluid that line the alveoli. Molecules between liquid forces are stronger than the attractive forces between gas and liquid molecules. This attractive force (surface tension) attempts to become as small as possible and thus is a force tending to collapse alveoli. This force is a major component of the elastic forces trying to collapse alveoli. In other words, surface tension increases the elasticity and reduces the compliance of the lungs. This is demonstrated by the law of Laplace in which $P = 2\ T/r$ where P equals the alveolar pressure, T equals surface tension, and r equals the radius of the alveolus. In order to combat surface tension, the lung produces an oily substance known as surfactant. This is made by type II pneumocytes and it is a mixture of phospholipids. This substance disrupts the attractive forces between adjacent molecules. In other words, it reduces the elastic force. As a result, this increases lung compliance and thus leads to a reduction of work for expanding the lung during inspiration. However, in premature infants,

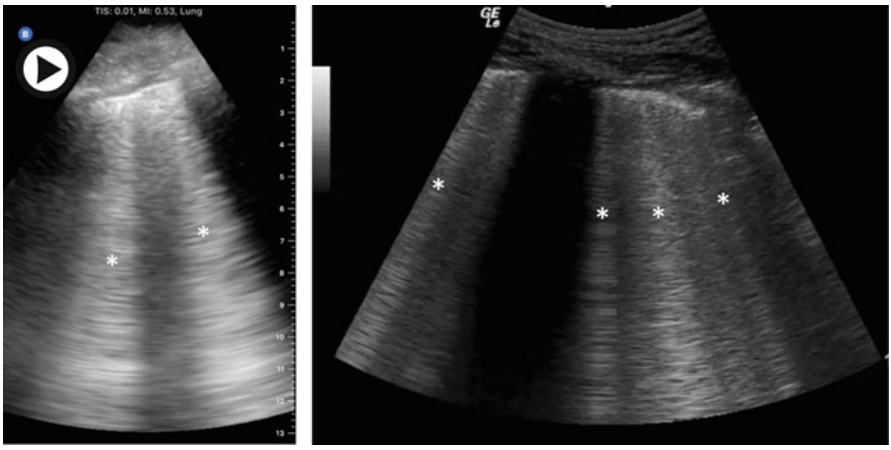

Fig. 5.12 (Video 5.4) Video of B-lines: B-lines are hyperechoic vertical artifacts that arise from the pleural line, extend to the edge of the screen, and vary with respiration (labeled with asterisks in figure). They may be a sign of pulmonary edema or fibrosis, among other conditions that affect the pleura (▶ https://doi.org/10.1007/000-7q1)

surfactant has not begun to be made or has been disrupted such as in an infant of a diabetic mother, the surface tension is high, particularly in small alveoli, and this may cause them to collapse. This is known as neonatal respiratory distress syndrome.

5.6 Gas Exchange and Hypoxemia

As indicated above, the goal of ventilation is to deliver oxygen to the blood vessels. Inspired oxygen passively diffuses from the alveoli to the pulmonary capillary and then either binds to hemoglobin or dissolves in the plasma. The greater the ventilation, the more oxygen there is because breathing brings oxygen into the alveoli.

Gravity influences blood flow throughout the body, including the lungs. As a result, pulmonary blood flow is gravity dependent with flow being greatest in the bases of the lung (more gravity) and least in the apexes (less gravity) when a person is standing. Upon lying down, blood flow is distributed evenly throughout the lung. The amount of oxygen in alveoli is an important factor influencing the distribution of blood flow throughout the lungs. In poorly ventilated regions of the lung, oxygen is low (hypoxia). In these hypoxic regions, vasoconstriction occurs, thereby diverting blood to better ventilated areas, which have more oxygen because there is more ventilation.

When oxygenation is impaired, resulting in a low level of oxygen in the blood, it is referred to as hypoxemia. There are multiple causes that will be explored here, with a focus on how ultrasound can aid identification of the different causes of impaired gas exchange.

Alterations in the mechanics of breathing, as described above, may impair delivery of oxygen to the lungs. An example of which would be hypoventilation. This may occur in states that impair regulation of the ventilatory drive, or with diaphragmatic weakness.

Ultrasound can aid in identification of other causes of hypoxemia, particularly when there is an imbalance between ventilation and perfusion.

In a patient whose heart is failing, e.g., congestive heart failure, elevated ventricular filling pressure results in increased pressure in the pulmonary capillary bed. This causes fluid to shift into the pulmonary interstitium and alveolar space, resulting in cardiogenic pulmonary edema (edema is an accumulation of fluid in the interstitial space). These areas of the lung may be perfused, but oxygen cannot adequately diffuse from the alveolus to the blood. This means blood returning to left heart is not adequately oxygenated. On ultrasound, this extravascular lung water is characterized by a diffuse, symmetrical B-line pattern bilaterally, with predominance to the most dependent regions of the lungs. B-lines are vertical, hyperechoic artifacts that arise from the pleural line, extend to the edge of the screen, and vary with respiration (Fig. 5.12 and Video).

Another example of decreased oxygen delivery due to alveolar filling is pneumonia, which is a process resulting in interlobular edema. When this process abuts

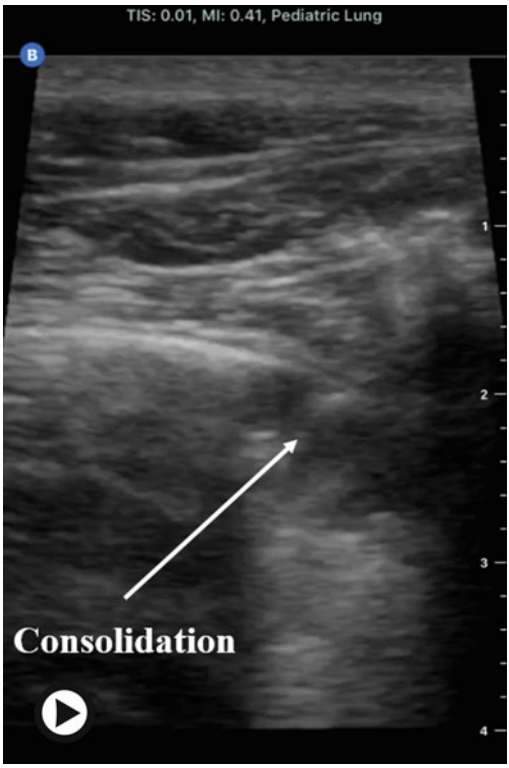

Fig. 5.13 (Video 5.5) Video of consolidation. Ultrasound waves are able to pass through the pleural line without creating a strong reverberation artifact that would be seen in normally aerated lungs (i.e. A-line pattern). Rather, the waves penetrate the lung tissue similar to atelectasis, but long, linear air bronchogram artifacts are seen with occasional B-lines surrounding the area of consolidation. This pattern is consistent with pneumonia (▶ https://doi.org/10.1007/000-7q2)

the pleura, it may be imaged with ultrasound, appearing as a hypoechoic, heterogeneous region deep to the pleural line, often with B-lines around the margins (Fig. 5.13 and Video of Consolidation).

5.6.1 Lab Excercise: Assessment of Lung Sliding and Pneumothorax Simulation

5.6.1.1 Learning Objectives

Learn to obtain a view of the pulmonary plurae and lung sliding to assess for pneumothorax.

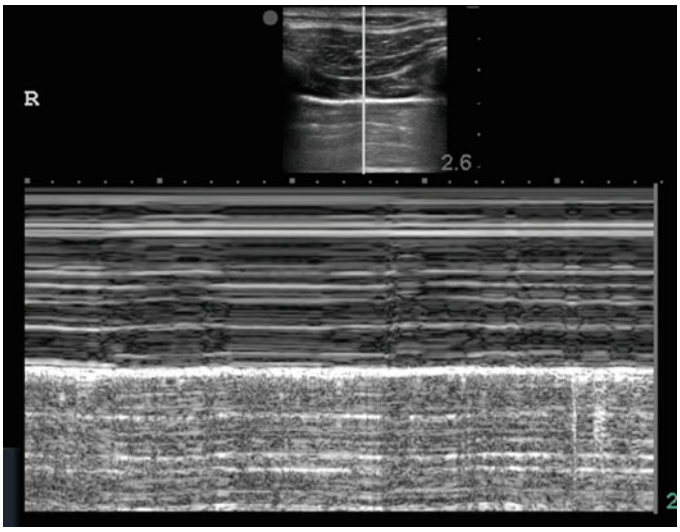

Fig. 5.14 In M-mode, the presence of lung sliding, indicating that the visceral and parietal pleura are sliding against each other normally, results in a clearly demarcated zone deep to (below) the pleural line that is less-defined, less-linear appearance. Contrast this with the lack of lung sliding that produces a linear image without a clear transition zone deep to the pleural line

5.6.1.2 Transducer/Probe

High-frequency, or linear probe.

5.6.1.3 Patient Position and Image Orientation

Position the patient supine on a flat surface. This will allow optimal visualization of the anterior lung bilaterally.

5.6.1.4 Evaluating the Pleural Surface and Lung Sliding

1. Choose “lung” or “pleural” preset if available.
2. While the standardized patient is supine, place the transducer just lateral to the sternum on the right side, at the least-dependent portion of the chest (Fig. 5.8, left panel). Identify an intercostal space, framed by ribs on either side: a high- or low-frequency probe may be used, ideally in a pleural or lung preset.
3. Find the pleural line, which is a linear, hyperechoic structure that slides or shimmers deep to (below) the ribs (Fig. 5.4 and video). Have the patient hold their breath and observe how the sliding decreases, although a faint, subtle pulsation of the pleural line may be observed, which is termed lung pulse, caused by a transmission of cardiac movement.

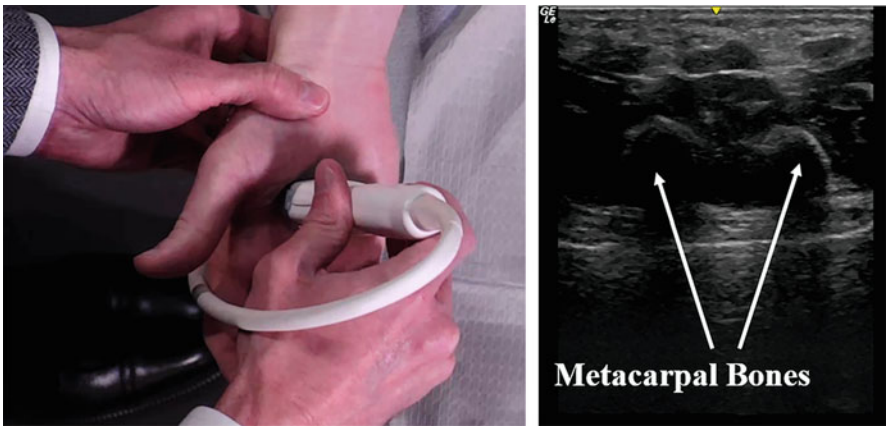

Fig. 5.15 Using a linear probe, obtaining a mid-transverse view of the hand (left image) may simulate an intercostal space. The metacarpal bones appear similar to ribs (right image), with a deeper echogenic line representing a tissue-air interface. In this case, however, the echogenic line is the back of the hand. Placing m-mode over this line shows there is no sliding, generating a bar-code-like appearance, which can be seen in pneumothorax as well

4. If M-mode is available, during normal respiration, place the marker in the center of the intercostal space and observe how the top portion of the tracing has a different appearance from the bottom portion that corresponds to the area deep to the pleural line (Fig. 5.14). This lower portion often has a less-defined, less-linear appearance due to the presence of lung sliding motion. Now have the patient hold his or her breath and note the difference in appearance.
5. Place a linear transducer on the anterior palm of a hand and note that the metacarpal bones appear similar in appearance on ultrasound to the ribs, with echogenic curves and posterior acoustic shadowing (Fig. 5.15). Deep to this is a bright white line, corresponding to a tissue-air interface at the dorsum of the hand (below the hand). This is similar in appearance to the pleural line. If M-mode is used in this area, the pattern is linear above and below the echogenic line, almost barcode-like (Fig. 5.16). This is because there is no sliding of parietal and visceral pleura in this area. This simulates a pneumothorax, whereas if sliding had been present it would appear like a seashore (normal).

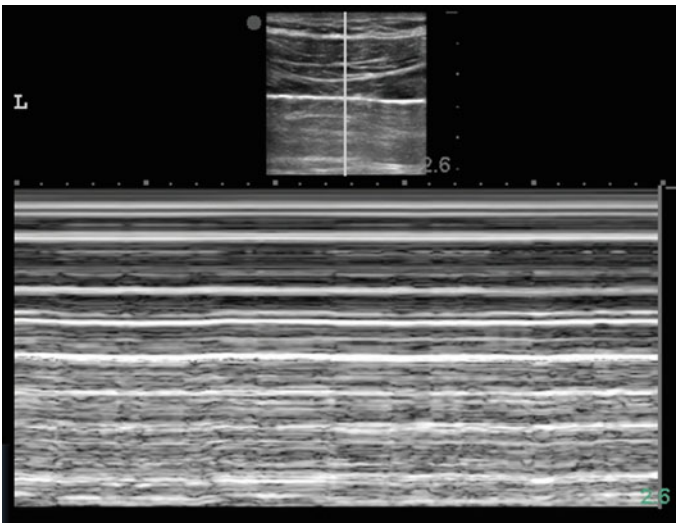

Fig. 5.16 In M-mode, the absence of lung sliding, produces a linear image without a clear transition zone deep to the pleural line. This creates a barcode-like appearance

References

Cooper B, William T (2018) Applied lung physiology. In: Hart S, Greenstone M (eds) Foundations of respiratory medicine. Springer, New York

Rehfeld A, Nylander M, Karnov K (2017) The respiratory system. In: Rehfeld A, Nylander M, Karnov K (eds) Compendium of histology: a theoretical and practical guide. Springer, Cham, pp 351–377

Further Reading

Blaivas M (2012 June) Lung ultrasound in evaluation of pneumonia. J Ultrasound Med 31(6): 823–826

Dietrich CF, Mathis G, Blaivas M, Volpicelli G, Seibel A, Atkinson NS et al (2016 Dec 5) Lung artefacts and their use. Med Ultrason 18(4):488–499

Fein D, Abbasi M (2020) Chapter 8: Lung and pleural ultrasound technique. In: Soni NJ (ed) Point of care ultrasound, 2nd edn. Elsevier, New York, pp 53–62

Volpicelli G, Elbarbary M, Blaivas M, Lichtenstein DA, Mathis G, Kirkpatrick AW et al (2012) International evidence-based recommendations for point-of-care lung ultrasound. Intensive Care Med 38(4):577–591

Wagner M, Barron K (2021) Chapter 12: Does the patient have a pleural effusion? In: Ultrasound for primary care, 1st edn. Wolters Kluwer, Philadelphia

Chapter 6
Ultrasound of the Gastrointestinal Tract

Michelle LaBrunda, Dina Brown, Floyd E. Bell III, and Andrew D. Vaughan

6.1 Anatomy and Physiology of the Gastrointestinal Tract

The use of ultrasound is valuable in learning both the physiological and structural layout of the GI system. The gastrointestinal tract is essentially a 30-foot tube that lies in neatly folded yet still mobile layers stretching from the mouth to the rectum. Its purpose is to take in food, extract the useable components and eliminate what is not needed in the form of feces. While simple to summarize, digestion is an incredible complex process involving at least 9 organs and no fewer than 26 hormonal and peptide regulators. The epiglottis must move to cover the tracheal opening every time we swallow, approximately 600 times per day without fail, or food and secretions go into the lungs resulting in a condition called aspiration. It takes 50 pairs of muscles working in perfect synchrony to take a bite of food and pass it to the stomach and uncountable others to process the food from stomach through the intestines and out the anal canal.

The gastrointestinal (GI) system is comprised of multiple organs including the oral cavity, esophagus, stomach, small intestine, large intestine, pancreases, liver, and gallbladder. The primary purpose of this system is the digestion of food,

Supplementary Information The online version contains supplementary material available at https://doi.org/10.1007/978-1-0716-1863-9_6. The videos can be accessed by scanning the related images with the SN More Media App.

M. LaBrunda · D. Brown · F. E. Bell III (✉)
University of South Carolina School of Medicine, Columbia, SC, USA
e-mail: michelle.labrunda@uscmed.sc.edu; Dina.brown@uscmed.sc.edu; Floyd.bell@uscmed.sc.edu

A. D. Vaughan
University of South Carolina School of Medicine, Columbia, SC, USA

Prisma Health Department of Family and Preventative Medicine, Columbia, SC, USA
e-mail: Andrew.vaughan@uscmed.sc.edu

L. B. Wilson et al. (eds.), *Understanding Physiology with Ultrasound*, Physiology in Health and Disease, https://doi.org/10.1007/978-1-0716-1863-9_6

absorption of nutrients, and elimination of wastes. Digestion is the process by which food is broken down into smaller components called nutrients. Nutrients are able to be absorbed in the GI tract and are then transported to the remainder of the body where they are utilized. Absorption is the process by which nutrients, electrolytes, and water are absorbed from the intestines and transported to the blood stream for distribution throughout the body. Not all food can be broken down into usable nutrients. Food that is unable to be processed into nutrients passes through the GI tract and eliminated.

The order of the structures that comprise the digestive tract are oral cavity, esophagus, stomach, small intestine, and large intestine. The liver, gallbladder, salivary glands, and pancreas are secretory organs of the gastrointestinal tract as can be seen in Fig. 6.1.

The average transit time from mouth to anus is 30–40 h but anything under 72 h is considered normal. It has been subject of scientific debate whether or not the transit time between men and women differ significantly and whether or not the menstrual cycle affects transit time. Despite numerous research articles on the topic, no consensus exists.

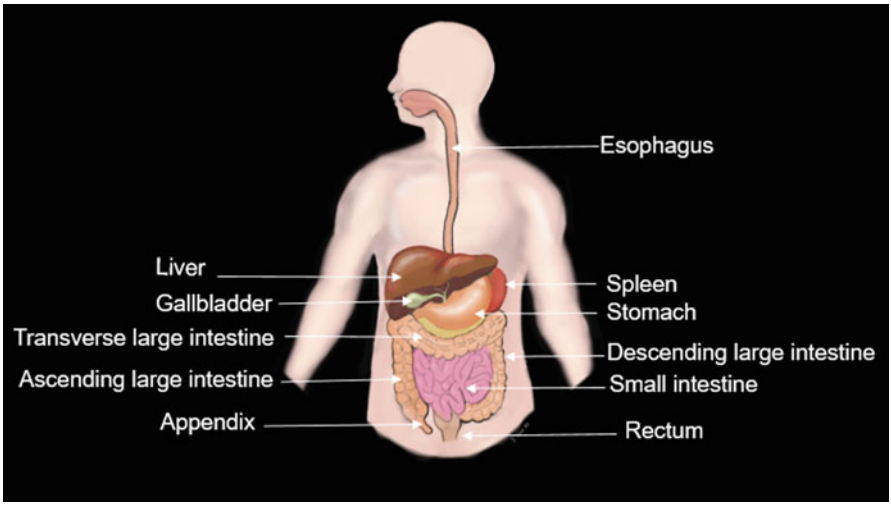

Fig. 6.1 Schematic showing the basic structure of the gastrointestinal tract. The primary organs of the gastrointestinal tract are esophagus, stomach, small intestine, large intestine, liver, gall bladder, and pancreas. Drawing by Naushad Amin

6.2 Motility

Motility is an important feature of the gastrointestinal system. Without motility, food would not be propelled forward through the gastrointestinal tract. There are two types of contraction in the gastrointestinal tract, phasic and tonic. Phasic contractions are found in the esophagus, stomach, and small intestine. Phasic contractions are periodic increments in smooth muscle tone followed by periods of relaxation. The second type of contraction is a tonic contraction. Tonic contractions are constant contractions that maintain a stable muscle tone without periods of relaxation. Tonic contractions are seen in the stomach, esophagus and in some sphincters.

Sphincters are areas of specialized circular muscle that occur at the site where organs of the gastrointestinal tract join. They are important for regulating the flow of food through the digestive tract. Sphincters include the upper esophageal sphincter, which divides the upper esophagus and pharynx, and the internal and external anal sphincters that permit control of intestinal movements.

6.3 Absorption

Absorption is the process by which the body takes nutrients from the GI tract and passes them into the body where they can be distributed and utilized. Many of the water-soluble nutrients are able to pass from the wall of the small intestine to the capillaries of the GI tract through the process of diffusion. In some instances, active transport is needed to move important substances such as glucose, amino acids, and sodium bicarbonate into the mucosa of the intestine and on to the bloodstream.

The inner wall of the small intestine is called the mucosa. It is covered in folds called plicae circulares. On these folds are finger-like projections called villi and on the surface of the villi are even smaller projections called microvilli. The purpose of these structures is to increase the surface area of the small intestine where most nutrients are absorbed.

With some exceptions, the majority of nutrients are absorbed in the second portion of the intestine called the jejunum. Iron for example, is absorbed in the first part of the small intestine called the duodenum. Vitamin B12 and bile salts are absorbed in the terminal ileum. Water, electrolytes, and vitamins are absorbed in both the small and large intestine. Micro-organisms in the large intestine are an important source of vitamins including Vitamin K and biotin. Vitamins are both produced and absorbed in the large intestine.

6.4 Excretion

Another important function of the gastrointestinal system is excretion. Excretion allows for elimination of indigestible substances and waste products. In general terms, the kidneys eliminate water soluble wastes and the intestinal tract is responsible for disposal of waste that is not water soluble such as cholesterol, steroids, and certain drug metabolites.

The average person makes approximately 400 g (14 ounces) of feces per day which is roughly 150 kg (320 pounds) per year. Stool consists of undigested fiber and other food residuals, dead and transiting microorganisms, sloughed off intestinal cells, and bile containing the breakdown products of red blood cells that give stool its distinctive color.

6.5 Immunity

The plicae circulares, villi, and microvilli mentioned in the absorption section serve a second purpose as well. They contain the greatest number of immune cells in the body. Mucosa represent unique immunological challenges. They are in contact with the outside world, therefore they have to be tolerant of beneficial and non-harmful microorganisms while providing protection against pathogens. The gastrointestinal associated lymphoid tissue (GALT) is the site where much of the immune activity of the GI tract occurs. Peyer's patches are aggregates of lymphatic tissue similar to lymph nodes that serve to sample antigens as they pass through the GI tract.

6.6 Regulation of the Gastrointestinal Tract

The digestive process requires coordination of numerous organs and an array of feedback systems. One of the most important of these systems is the autonomic nervous system. There are dozens of regulatory gastrointestinal peptides including hormones, neurocrine molecules, paracrine molecules, and other signaling molecules central to the regulatory processes of the gastrointestinal tract. These regulatory systems help to control motility, secretion, and absorption.

There are two components to the gastrointestinal nervous system. The external component consisting of the autonomic nervous system. This system connects the nervous control of the gastrointestinal tract to the central nervous system. The other component is the internal or enteric nervous system. This system can function independently of the central nervous system. Even if the autonomic nervous system is damaged, the gastrointestinal tract will continue to function because the enteric nervous system will continue to operate independently.

The gastrointestinal nervous system contains two nerve plexuses, the submucosal and the myenteric plexus. The submucosal plexus (Meissner plexus) is located between the submucosa and the circular muscle layer. It is responsible for regional control including local absorption, muscle movements, secretion, and blood flow. The myenteric plexus is located between the circular and longitudinal muscle layers. The myenteric plexus serves to regulate muscle and motility of the gastrointestinal tract. The myenteric plexus primarily serves to increase muscle tone, but also regulates relaxation of sphincter muscle permitting transit of material through the gastrointestinal tract.

Parasympathetic innervation of the gastrointestinal tract is primarily supplied by the vagus nerve and sympathetic innervation is supplied by the prevertebral ganglia. Unlike the parasympathetic nervous system, which is contained within the wall of the gastrointestinal tract, the ganglia of the sympathetic gastrointestinal innervation are found outside the wall of the gastrointestinal tract. In the gastrointestinal tract, the parasympathetic nervous system serves to stimulate digestion and the sympathetic system to inhibit digestion.

Gastrin, cholecystokinin (CCK), and secretin are three important regulatory hormones of the gastrointestinal tract. Gastrin serves to stimulate gastric acid secretion. Cholecystokinin has several actions including stimulation of gallbladder contraction, secretion of pancreatic enzymes, and inhibition of gastric emptying. Secretin stimulates a bicarbonate rich secretion from the pancreas that enters the duodenum.

6.7 Layers of the Gastrointestinal Wall

The gastrointestinal tract has four basic layers, the mucosa, submucosa, muscular, and adventitia. The mucosa is the innermost layer that comes into direct contact with digesting food. The mucosa has unique characteristics that are different from organ to organ, but some generalities exist. It is at this layer where most of the absorption and secretion occurs. It contains blood vessels, lymphatic vessels, and smooth muscle. The next layer is the submucosal layer. This layer contains connective tissue, blood vessels, lymphatics as well as autonomic nerves such as the submucous plexus and enteric nervous plexus that help regulate the digestive processes. The muscular layer is made up of circular and longitudinal smooth muscle. Contractions of these muscles are responsible for the generation of peristalsis. Peristalsis is wave-like muscular contractions responsible for propelling food through the digestive tract. The outermost layer is the adventitia or serosa. This is a connective tissue layer that serves to anchor the organs in place while providing free movement required for peristalsis and digestions. Layers of the gastrointestinal wall can be seen in Fig. 6.2.

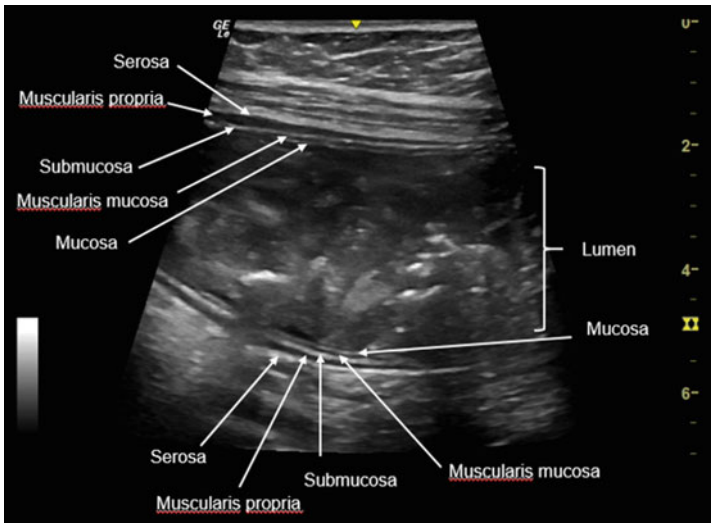

Fig. 6.2 Ultrasound image illustrating the layers of the intestinal wall. There are four basic layers of the gastrointestinal wall, the mucosa, submucosa, muscular, and adventitia. There is a hyperechoic (white) layer formed where the mucosa and the lumen of the intestine meet. The muscularis mucosa, part of the mucosa layer, is hypoechoic (black). The submucosa is peripheral to the mucosa and is echogenic (white) on ultrasound. The muscular layer is hypoechoic (black). The hyperechoic (white) adventitia or serosa is seen peripheral to the muscular layer

6.8 Unique Ultrasound Features of the GI Tract

Examining the abdomen with ultrasound (US) is unique in several ways. Ultrasound of the abdomen involves the examination of many deep, soft structures of similar echotexture that may be constantly changing due to peristalsis and when a person last ate.

6.8.1 Depth

Compared to an ultrasound examination of the heart, bladder, or thyroid, the abdominal ultrasound examination often requires sound waves to penetrate more deeply. The required penetration may be 20 cm or more (8 inches). In order to achieve deeper penetration, low frequency ultrasound probes must be used. Unfortunately, the lower the frequency, the lower the resolution, thus making identification of organs and interpretation of images more challenging. A good understanding of anatomy and a practiced pattern recognition is needed to overcome this challenge.

6.8.2 *Intestinal Air*

A normal intestine contains air, especially after eating. Structures that lie below air-filled structures, such as the intestines, are unable to be seen on ultrasound because the ultrasound waves are reflected by air instead of passing through to deeper structures. This air can make it difficult to examine structures that might otherwise be easily seen because it leads to shadows that obscure those structures. The shadows associated with intestinal air are described as "dirty" shadows when they have bright echoes within them. See Fig. 6.3 for an example of "dirty" shadowing from intestinal air. To some degree, intestinal air can be moved by applying pressure with the ultrasound probe. Given time, peristaltic movements of the intestine move intestinal air, so patience is required when examining abdominal structures.

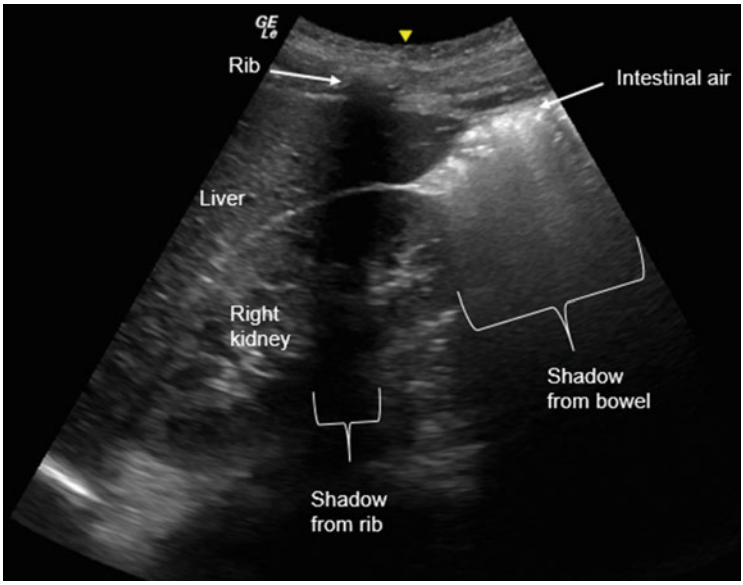

Fig. 6.3 Ultrasound image showing shadowing from intestinal air. This is a longitudinal view through the liver and right kidney. Intestinal air is seen as the hyperechoic (bright) areas near the tip of the liver on the right side of the screen. Note that "dirty" shadows extend deep to the air in the intestine and obscure detail of deeper structures including part of the lower pole of the right kidney. They are referred to as "dirty" because they are brighter than "clean" shadows that arise from structures like ribs

6.8.3 Peristalsis

Peristalsis is the wavelike muscular contractions of the gastrointestinal tract that propel the food, digestive juices, and air forward through the gastrointestinal tract. Intestines are in a constant state of motion and the air within them can obscure visualization of deeper structures only to move a minute later allowing visualization. Peristatic contractions of the intestines can be visualized with ultrasound. The constantly moving intestine is often a nuisance for ultrasonographers, but there are clinical applications of intestinal ultrasound. For example, in cases of intestinal obstruction, peristalsis will be absent at the site of obstruction.

6.8.4 Fed or Fasting

Another unique feature of gastrointestinal ultrasound is that the exam changes based on whether the person has eaten. For example, prior to eating, the gallbladder will be large and full of bile. After eating, the gallbladder will be smaller and much more difficult to locate. In normal individuals, the portal blood flow increases significantly after eating. In people who suffer from portal hypertension this normal change in flow may be blunted or absent. Gases accumulate in the gastrointestinal tract as a normal part of the digestive process. Fasting subjects have less intestinal gas than those who have recently eaten.

6.9 Gastrointestinal Tract

6.9.1 Oral Cavity

Digestion begins in the oral cavity. Chewing mechanically breaks food into smaller pieces making the food particles easier to process, and mixes food with saliva. Saliva is a lubricant but also contains salivary amylase that initiates the digestion of carbohydrates.

The average person makes about 1 liter (1 quart) of saliva per day. There are three pairs of major salivary glands responsible for saliva production, the parotid glands, the submandibular glands, and the sublingual glands. Saliva is delivered to the mouth through salivary ducts. An ultrasound image of a submandibular salivary gland can be seen in Fig. 6.4.

Most students have seen the “tongue map” at some point during their science careers, which neatly maps out the taste receptors with sweet on the tip of the tongue, salty and sour on the sides and bitter receptors in the back of the tongue. This map persists in many physiology texts despite its inaccuracy. It started in the 1940s when a Harvard psychologist misinterpreted a German research article from 1901. The

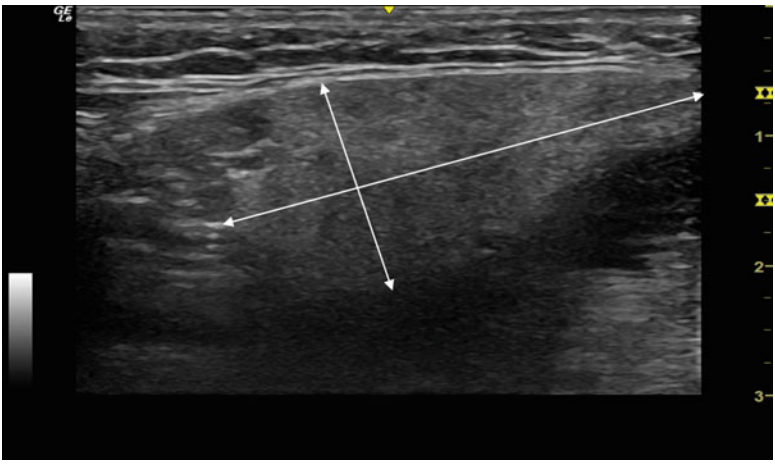

Fig. 6.4 This is a transcutaneous ultrasound of a normal submandibular salivary gland. It has a homogeneous echogenicity (all the same color). For this view, the ultrasound probe is placed just below the body of the mandible

average person has roughly 10,000 taste buds. This number decreases as a normal part of the aging process. Taste buds are groups of taste receptors, approximately 50–100 receptors per bud. Taste buds are mostly distributed around the periphery of the tongue. There are receptors for salty, sweet, bitter, umami, sour, and possibly fat but there is no one specific molecule responsible for activation of a taste receptor. Taste receptors are found outside the mouth as well. They have been discovered in the nasal epithelium, trachea, bile duct, small intestine, and stomach. Bitter receptors have even been found in the heart and vascular system. It seems that bitter compounds are involved in regulation of smooth muscle contraction, but our understanding of this mechanism is in its infancy.

Once chewing is complete, food is passed from the mouth through the esophagus and into the stomach, a process called swallowing. Swallowing consists of three phases. In the oral phase, the tongue pushes a bolus of food into the pharynx. In the pharyngeal phase, the epiglottis moves to cover the entrance of the trachea, the upper esophageal sphincter relaxes, and food is passed into the esophagus. In the esophageal phase, food passes down the esophagus and into the stomach.

6.9.2 Larynx/Pharynx

Air entering through the nose or mouth travels through portions of a structure called the pharynx before passing through another structure called the larynx on the way to the trachea. Food entering the mouth passes through the pharynx before passing into esophagus. It is the pharyngeal location where the digestive and respiratory systems diverge.

6.9.3 *Esophagus*

The esophagus is a muscular tube approximately 25 cm (10 inches) long that connects the pharynx to the stomach. The inferior pharyngeal constrictor muscle keeps the esophagus closed, except when swallowing or vomiting occurs. The esophagus has two sphincters. The upper esophageal sphincter lies at the superior portion of the esophagus and is under conscious control. It is involved in breathing, eating, belching, and vomiting. The upper esophageal sphincter also aids in directing food and secretions away from the lungs and into the gastrointestinal tract. The gastroesophageal junction sphincter (also called lower esophageal sphincter) lies at the junction between the esophagus and stomach and is under involuntary control. It prevents gastric material from passing into the esophagus. Dysfunction of the lower esophageal sphincter can allow digestive material into the esophagus, causing pain and inflammation of the esophagus, a condition call gastroesophageal reflux disease (GERD). Ultrasound image of the esophagus can be seen in Fig. 6.5.

The esophagus contains two muscle layers. The innermost layer is circular in orientation and the outer layer is oriented longitudinally. The proximal third is made up of striated muscle, middle third is both striated and smooth muscle, and the distal third is smooth muscle.

The central swallowing center of the central nervous system controls the contractile function of the striated muscle and the vagus nerve predominantly supplies the smooth muscle. Peristalsis is stimulated by distension of the esophagus. The enteric nervous system coordinates muscular contractions resulting in peristalsis, which moves the bolus through the esophagus as seen in Fig. 6.6.

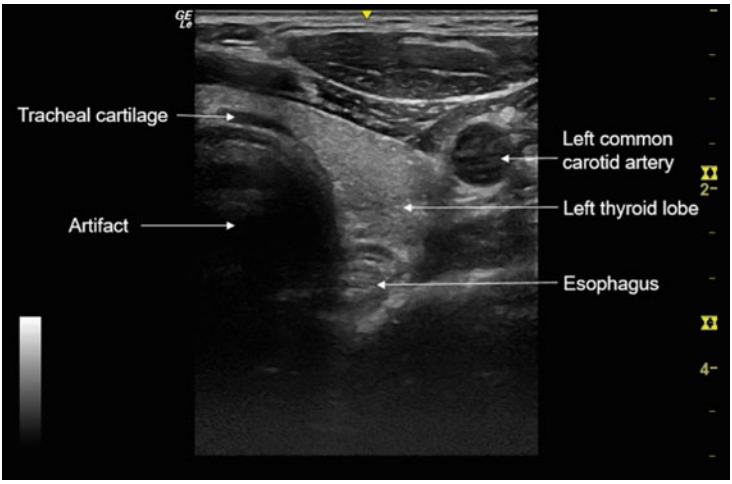

Fig. 6.5 A cross sectional ultrasound image of the neck showing a normal appearing esophagus. Note the esophagus is seen deep to the left lobe of the thyroid gland

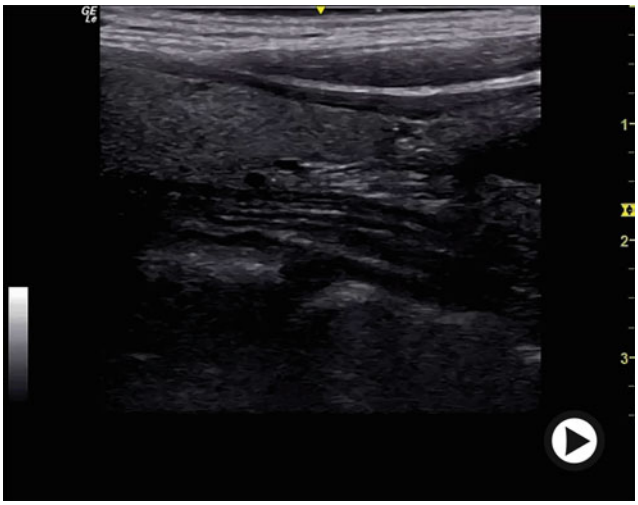

Fig. 6.6 (Video 6.1) A video of a longitudinal view of the esophagus in the neck demonstrating peristalsis. Muscular contractions propel a bolus of fluid and air within the lumen of the esophagus. Note the bolus moves from left to right on the screen as it courses toward the portion of the esophagus within the chest (not included on this view). Ultimately it will pass into the stomach within the abdomen (▶ https://doi.org/10.1007/000-7q6)

6.9.4 Stomach

The stomach is a muscular organ situated between the esophagus and small intestine. It is located on the left side of the abdominal cavity, just below the diaphragm and above the pancreas. It secretes 1.5 liters (1.5 quarts) of fluid on an average day. The stomach consists of five sections: cardia, fundus, body, antrum, and pylorus. An US image of the stomach can be seen in Fig. 6.7.

The uppermost portion where the stomach meets the esophagus is called the cardiac segment. The fundus comprises the upper curved portion of the stomach. The body forms the primary part of the stomach and the lower portion of the stomach that connects to the duodenum is called the pyloris. The pyloric sphincter separates the stomach from the duodenum as can be seen in Figs. 6.8 and 6.9.

Treatment of hypertrophic pyloric stenosis is the most common surgery done on babies in the first few months of life. In these infants, the pyloric sphincter fails to relax appropriately making it impossible for food to pass from the stomach to the intestine. Ultrasound is the favored modality for diagnosing hypertrophic pyloric stenosis as seen in Fig. 6.10.

The stomach has several functions. It serves as a storage container so that food can be held while waiting for small intestine contents to pass forward. Because of the very low pH, it also helps to decontaminate food, mix the food with digestive juices, and break food into smaller particles before passing food into the small intestine. The stomach breaks down food through mechanical and enzymatic activity.

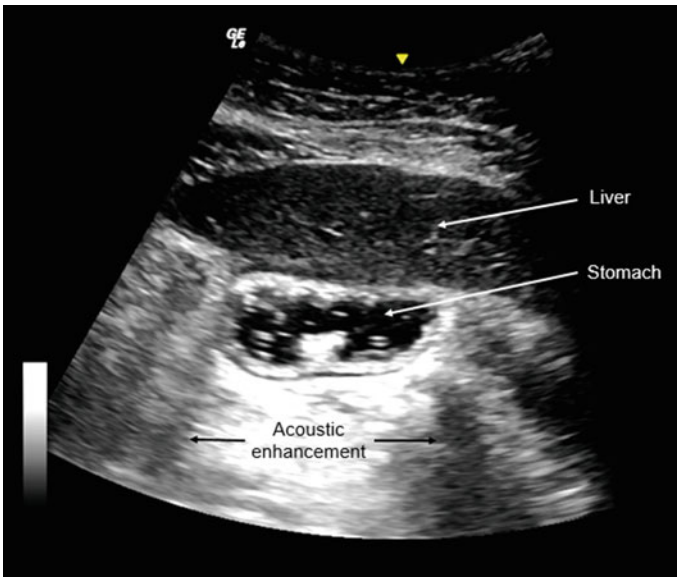

Fig. 6.7 Ultrasound image illustrating the stomach. The stomach and gastric contents are seen. The stomach is filled with anechoic (black) liquid and some hyperechoic (white) particulate matter. Note the band of acoustic enhancement (bright region) deep to the stomach

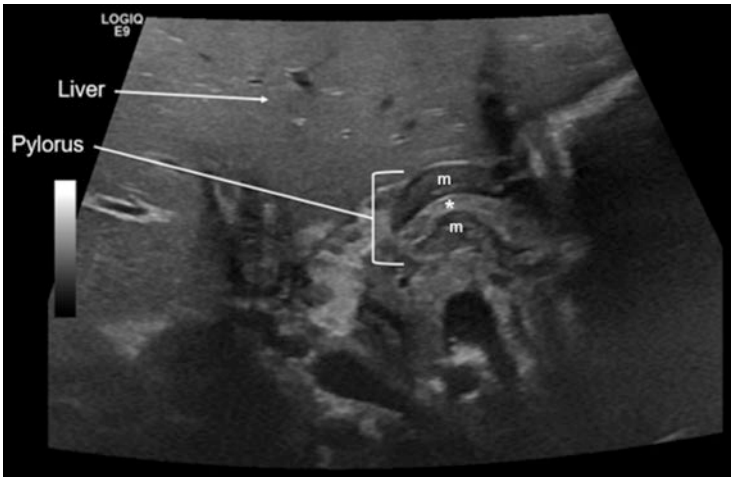

Fig. 6.8 The pylorus is the distal portion of the stomach where it empties into the duodenum. This is an ultrasound image of a normal longitudinal view through the pyloric sphincter in a newborn infant. m = pyloric muscle. * = pyloric canal

Once the food bolus reaches the stomach, it is mixed by contraction of the stomach with gastric juices transforming it into a semi-liquid substance called chyme. The stomach contains smooth muscle arranged in both a circular and

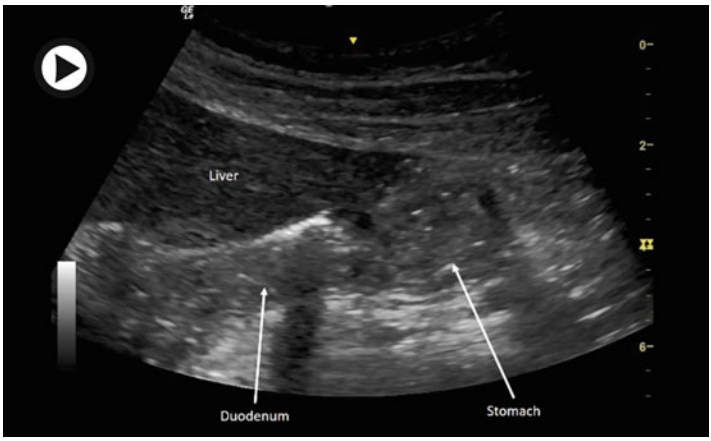

Fig. 6.9 (Video 6.2) A video of transit of food from the stomach through the pyloric sphincter into the first portion of the duodenum. Note that initially muscular contractions lead to a change in configuration of the stomach with mixing of its contents. Subsequently there is propulsion of some of this material toward the left side of the screen into the duodenum (▶ https://doi.org/10.1007/000-7q4)

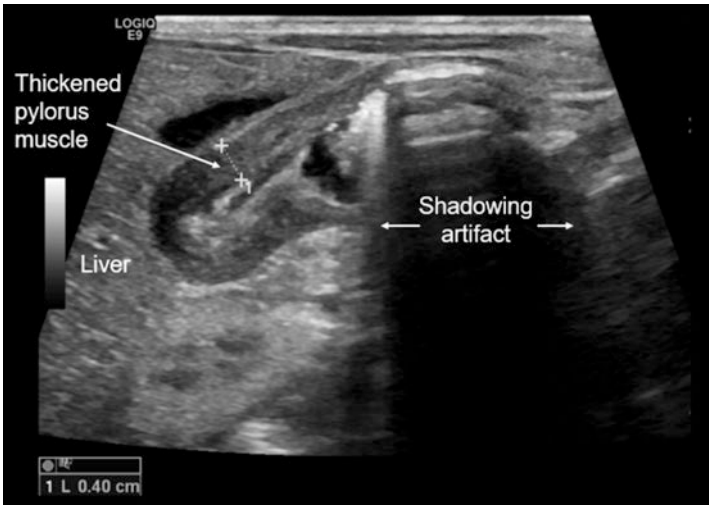

Fig. 6.10 Ultrasound image illustrating a hypertrophied pylorus. Roughly 3 in every 1000 babies develops a condition called hypertrophic pyloric stenosis. This disease prevents normal transit of food through the digestive tract. It is caused by hypertrophy (thickening) of the pyloric sphincter. In this case the muscle is thickened to 4 mm as noted by the calipers. Note the dark shadowing artifact caused by the presence of air in the lumen of the stomach

longitudinal pattern. The smooth muscle exhibits phasic and tonic contractions. Phasic contractions are short, lasting a matter of seconds, while tonic contractions typically last for minutes. Together, these contractions produce the mixing and

peristaltic movements of the stomach. Once food particles are sufficiently broken down, gastric contents are forced toward the outlet of the stomach. Larger food particles circulate back up toward the body and fundus of the stomach where they are mixed with additional gastric juices to further reduce the particle size until they are small enough to exit through the pylorus. The pyloric sphincter is a circular muscular tube at the stomach outlet that empties the stomach contents into the small intestine. The volume of liquid in the stomach normally ranges from 60 ml (2 oz) when empty to 1 liter (1 quart) when full, although it can be stretched to hold significantly more.

Gastric acid is produced by parietal cells in the cardia and fundus (portion closest to the esophagus) of the stomach and the hormone gastrin is one compound that stimulates acid secretion. Stomach acid kills most bacteria in food, stimulates hunger, and activates digestive enzymes. Parietal cells also secrete intrinsic factor. Intrinsic factor is required for absorption of vitamin B12. Pernicious anemia is an autoimmune disease where antibodies destroy the parietal cells. People with pernicious anemia develop lifelong anemia unless vitamin B12 supplements are given. Goblet cells lie in the body and fundus of the stomach. They secrete mucous that prevents the stomach from self-digesting. Helicobacter pylori is the bacteria responsible for causing the majority of diagnosed gastritis and peptic ulcers. The specific mechanism of the disease process is under study, but it appears that disruption in mucous turnover plays at least some part.

Movement of material through the stomach is controlled in part by the autonomic nervous system (working through the enteric nervous system) and in part by hormones. Gastrin is a hormone produced by G cells found in the pyloric, cardia, and fundus of the stomach. This hormone stimulates the release of stomach acid. CCK primarily serves to stimulate gallbladder contraction, but also decreases gastric emptying.

The primary function of the stomach is to breakdown food into smaller particles, but it participates in some nutrient absorption. Water, some medications, amino acids, and alcohol can all be absorbed from the stomach.

6.9.5 Small Intestine

From the stomach, food is passed into the small intestine. The small intestine is approximately 6 m (20 feet) long and is the site where most of the absorption of nutrients takes place. It has three distinct segments: duodenum, jejunum, and ileum. The small intestine is easily seen on ultrasound as shown in Fig. 6.11.

The duodenum is the first portion of the small intestine. Chemical digestion continues in this area. It is the site where the bile from the gallbladder and pancreatic juice drain into the small intestine. Brunner's glands, also known as duodenal glands, are found in the duodenum. They secrete alkaline fluid to neutralize the acid in chyme. These cells also secrete mucous to lubricate the digestive tract and permit the smooth passage of gastrointestinal contents.

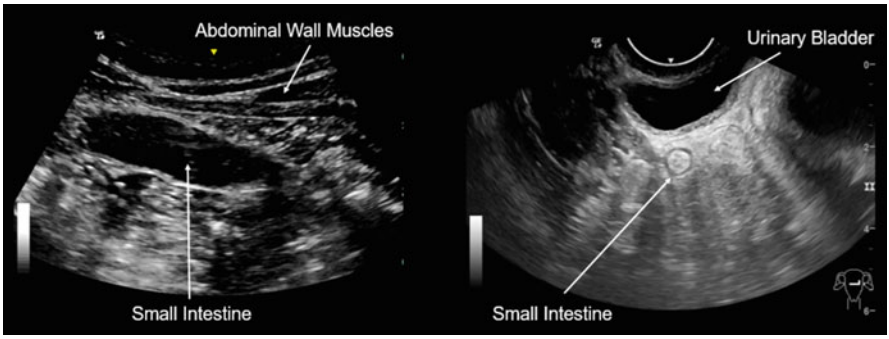

Fig. 6.11 Ultrasound images of the small intestine. Ultrasound of the intestinal tract is being used more and more often in medical practice. The left panel is a transabdominal scan that shows a tubular structure with an anechoic (black) lumen. This is a fluid filled loop of small intestine. The right panel is a transvaginal pelvic scan that shows a circular structure with a hypoechoic (dark) rim and a hyperechoic (bright) center. This is a cross section through a loop of small intestine that is not fluid filled

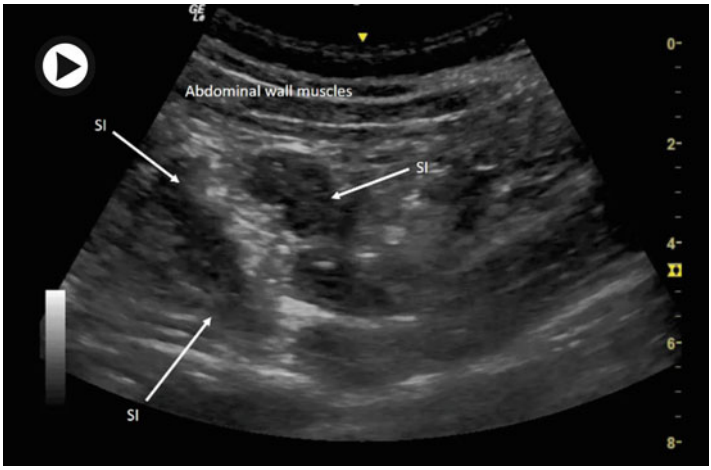

Fig. 6.12 (Video 6.3) Video of small intestine peristalsis. The small intestine (SI) loops are seen as tubular hypoechoic (dark) structures in this video. Note how they move and change in size due to muscular contractions (▶ https://doi.org/10.1007/000-7q5)

The second portion is the jejunum. Most absorption of carbohydrates and amino acids occur in this area.

The ileum is the last part of the small intestine. It serves to absorb vitamin B12, bile salts, and any nutrients not absorbed in the jejunum. The ileum contains Peyer's patches, which are islands of lymphoid tissue that help protect the intestine from infection.

Digesting food is propelled through the small intestine by peristalsis. Peristalsis of the small intestine can be seen in Fig. 6.12.

The small intestine is lined with projections called villi. Villi increase the surface area of the intestine providing a larger area from which nutrients can be absorbed. The villi in the small intestine are covered in an even finer set of structures called microvilla. Absorption occurs at the level of the microvilli. They are highly vascular and are the site of most of the transport of nutrients from the intestine to the blood stream.

The small intestine is central to the digestive process. It is the site of majority of the chemical breakdown of food and of the bulk of absorption. In general, the digestive enzymes are produced either by the liver or the pancreas, but the enzymes responsible for protein digestion do not become active until they are in the small intestine. Lipids, carbohydrates, and proteins each have a unique set of enzymes to digest each.

Proteins must be broken down into amino acids or short chains of amino acids called peptides (di- and tri-peptides to be more precise) before they can be absorbed. The digestion of proteins starts in the stomach with the gastric acid and an enzyme called pepsin. Enzymes such as trypsin are secreted by the pancreas and mix with the chyme in the duodenum. Additional breakdown occurs and amino acids are cleaved from the protein one at a time. Most of the amino acids and peptides are absorbed in the small intestine.

Like proteins, lipids must also be degraded into their base components of fatty acids and glycerol before the intestine is able to absorb them for transport to the blood stream. Lipase in conjunction with bile acids break down fats into their smaller utilizable constituents. Bile salts also serve to make the hydrophobic lipids soluble in water.

The digestion of carbohydrates starts in the mouth with salivary amylase, but most of the digestion and absorption of carbohydrates occurs in the small intestine. Pancreatic amylase helps to break down large carbohydrate molecules such as starch into smaller pieces called oligosaccharides. A variety of enzymes responsible for carbohydrate digestion are present in the absorptive surface of the microvilli called the brush border. These brush border enzymes cleave oligosaccharides into their monosaccharide bases (glucose, galactose, and fructose) that can be taken up by the intestinal epithelium and transported into the blood stream.

Some carbohydrates are unable to be broken down by our own enzymatic processes. These pass into the large intestine where they encounter a large variety of intestinal bacteria. The bacteria are able to breakdown carbohydrates that humans cannot. The enzymatic complement of each person changes with time. For example, most adults have at least partially lost the ability to produce lactase leading to lactose (sugar found in milk) intolerance.

6.9.6 Large Intestine

The large intestine (also called colon) measures roughly 1.5 m (5 feet) and is divided into three portions: ascending, transverse, and descending large intestine. The first

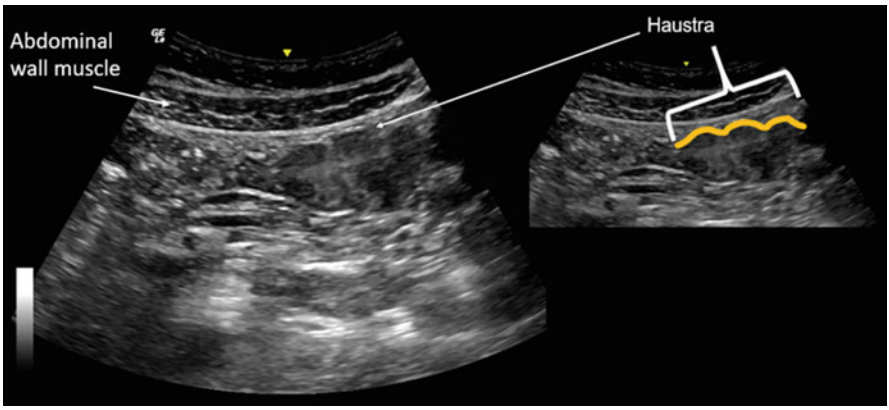

Fig. 6.13 This is an ultrasound image depicting the large intestine (colon). Pouchlike haustra are created by contraction of the teniae coli muscles of the large intestine and can be used to differentiate large intestine from small intestine. In this image haustra are seen

part of the large intestine, where it joins the end of the small intestine is called the cecum.

The large intestine differs from the small intestine in several ways. It is wider, lacks villi, has an abundance of mucous secreting cells called Goblet cells, and taeniae coli are present. Teniae coli are bands of smooth muscle that run the length of the of the large intestine. The teniae coli are shorter than the large intestine and cause a segmented shape of the large intestine. These individual segments are called haustra. Haustra are characteristic of the large intestine and differentiate it from the small intestine as seen in Fig. 6.13.

Intestinal contents are transformed from a liquid to a semisolid state in the large intestine. The motility is designed to allow optimal salvage of fluid and electrolytes. Short and long duration contractions contribute to the movement of large intestine contents from one haustra to the next.

The appendix is a small fingerlike projection attached to the cecum as can be seen using US (Fig. 6.14). It contains lymphoid tissue and is involved in the immune response of the gastrointestinal tract. Appendicitis is a common condition in which the appendix becomes blocked with infected material.

The large intestine functions to absorb water from undigested food and to compact the processing food into feces. It takes approximately 16 h for food to traverse the large intestine. In the large intestine, food is no longer broken down except by bacteria. Some bacterial byproducts are absorbed.

The large intestine is home to an enormous array of microorganisms. Many of the organisms that inhabit the intestine are unable to be cultured so no one is really sure how many species of microorganisms call the human intestinal tract home. Estimates range from 700 to 36,000 species. Microorganisms contribute approximately 10% of the total calories that a person receives by breaking down foods that we otherwise would not be able to make use of. Humans make approximately 20 enzymes to break

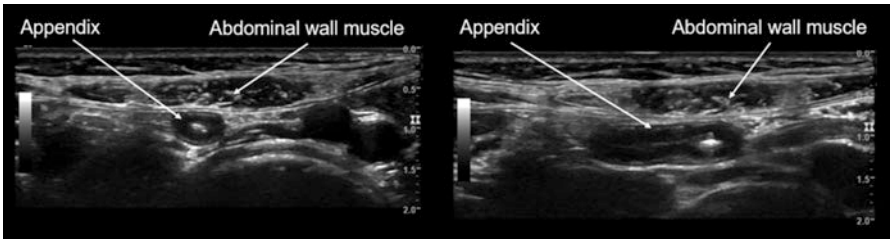

Fig. 6.14 An ultrasound image of a normal appendix. The appendix is an approximately 4 cm projection that arises from the first part of the large intestine known as the cecum. The left panel shows a circular configuration of the appendix indicating this is a short axis (transverse) view of the organ. The right panel shows the appendix as an elongated tubular structure indicating this is a long axis (longitudinal) view of the organ

down food while bacteria are able to produce tens of thousands. Microorganisms produce vitamins such as vitamin K and biotin, which we are unable to produce on our own, but we have evolved the ability to absorb these vitamins from the colon after they have been produced by our intestinal flora. Flatus is also produced by bacteria as a byproduct of polysaccharides fermentation.

Once the feces have been produced, it is stored in the rectum until it is eliminated through synchronized intestinal contractions and anal sphincter relaxation. Defecation is the process by which waste products are eliminated from the digestive tract.

6.9.7 Liver

6.9.7.1 Overview

The liver is a soft organ located in the right upper abdomen just below the diaphragm. It has four lobes: the left, right, caudate, and quadrate. It has both synthetic and detoxifying functions. It is involved in the processing of many medications, stores glycogen, synthesizes plasma proteins, and produces bile. The liver is a highly vascular organ and receives two blood supplies, the portal vein and hepatic artery.

6.9.7.2 Hepatic Circulation

The liver is a highly vascular organ. The portal vein brings nutrient rich blood from the small intestine to the liver and is responsible for roughly 75% of the blood flow to the liver. The hepatic arteries contribute 25% and is responsible for most of the oxygen delivery.

6.9.7.3 Liver Structure

At the microscopic level, the lobule is the basic building block of the liver as can be seen in Fig. 6.15. Each lobule has three components: central vein, hepatocytes, and the portal triad. The liver is made of linear stacks of lobules forming a hexagonal shape.

Branches of the portal vein and hepatic artery provide blood to the lobule. The blood then passes through specialized liver capillaries called sinusoids where exchange of nutrients, toxins, and gases can occur. Blood from the sinusoids collects into the central vein found at the center of every lobule. Central veins return blood to circulation via the hepatic vein. Hepatic veins can be seen draining into the inferior vena cava on ultrasound (Fig. 6.16).

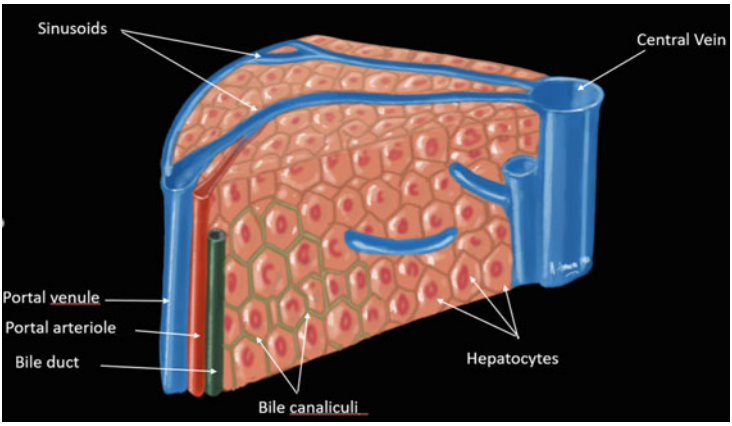

Fig. 6.15 A liver lobule is the basic building block of the liver. It consists of the portal triad and hepatocytes arranged around a central vein. The portal triad consists of a portal venule, a portal arteriole, and a bile duct. Drawing by Naushad Amin

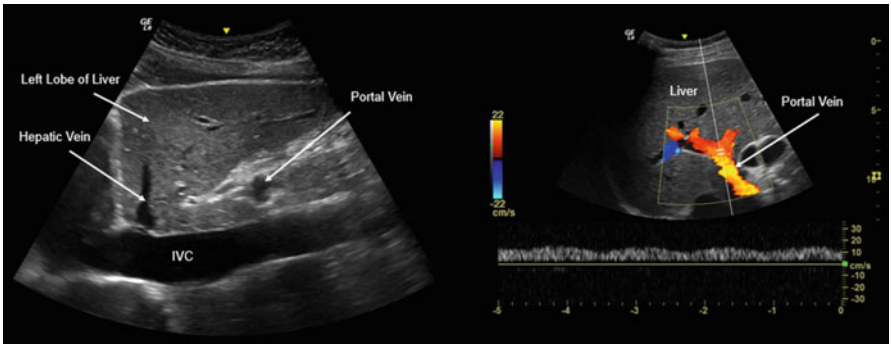

Fig. 6.16 Blood vessels of the liver can be easily visualized in ultrasound. In the image on the left, the left hepatic veins can be seen draining into the IVC. The image on the right demonstrates the portal vein with color Doppler. Note that that the portal vein brings blood into the liver

The portal triad lies on the periphery of the lobule and was first described as consisting of a hepatic artery branch, hepatic vein branch, and a bile duct. Since its initial description, two other structures, lymph vessels and branches of the Vagus nerve (cranial nerve X) have also been found to lie within the portal triad.

In ultrasound, the portal triad consists of the common bile duct, hepatic artery, and portal vein and should not be confused with the microscopic structure of the liver despite sharing the same name.

Portal blood flow is unique in many aspects. The liver receives oxygenated blood from the hepatic artery and nutrient rich unoxygenated blood from the portal vein. Blood from these two sites mix as they pass through the hepatic sinusoids, the type of liver capillary described above. The hepatic vein is unique it that blood from this vein passes through a capillary system before returning to the heart. Normal portal vein pressure is 5–10 mmHg. Portal hypertension means pressure in the portal vein is higher than normal. Portal hypertension can occur when the portal venous flow or hepatic vascular resistance increases. One of the most common causes of portal hypertension is liver cirrhosis. As indicated above, liver cirrhosis causes vascular structures to become fibrotic and tortuous, leading to increased portal pressures and portal hypertension.

The portal vein is unique in its appearance on ultrasound. It measures roughly 8 cm (3.2 in) in length and 12 mm (0.5 in) in diameter. When visualizing the liver using ultrasound, the portal vein has a hyperechoic rim seen at multiple angles. Other vessels have this rim when viewed at a directly perpendicular angle, but the portal vein is unique in maintaining its hyperechoic rim regardless of the viewing angle. The hyperechoic rim is due to nonparallel alignment of the connective tissue fibers. Only the portal vein sports non-parallel connective tissue fibers resulting in its ever-visible hyperechoic rim as seen in Fig. 6.17.

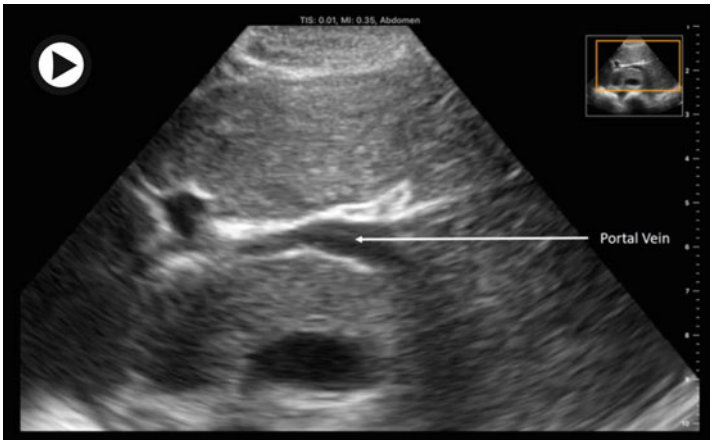

Fig. 6.17 (Video 6.4) Video of the hyperechoic rim of the portal vein. This transverse view through the liver demonstrates the portal vein as a branching anechoic (black) structure. Note the hyperechoic (white) rim surrounding it (▶ https://doi.org/10.1007/000-7q3)

6.9.7.4 Functions of the Liver

The liver is a complex organ with multiple functions. It removes nutrients and vitamins from the blood and acts as a storage depot for glycogen, vitamin D, vitamin A, vitamin B12, iron, and copper. The liver is the primary site of protein metabolism in the body. It both synthesizes and breaks down proteins. Most lipoproteins are produced in the liver. During the first 3 months of fetal life, the liver serves as the primary source of blood production. Many substances are produced in the liver including angiotensinogen, and insulin-like growth factor 1. The liver also has detoxification functions.

6.9.7.5 Liver Fibrosis and Cirrhosis

The liver is an exceptional organ in its ability to regenerate. Up to 70% of the liver can be surgically removed and it will grow back in humans. Despite this amazing capacity, liver failure is common across the globe. When part of the liver is removed the remaining liver regenerates new liver tissue. When liver cells are chronically exposed to inflammatory conditions such as alcohol or viral infections the body repairs the damaged liver tissue instead of regenerating new tissue.

Chronic repair of liver leads to tissue that is significantly different from the original liver tissue. Hepatocytes are destroyed and the excessive fibrous proteins are deposited in the extracellular matrix of the liver. The new fibrous tissue lacks the compliance of the original liver tissue. As fibrous tissue replaces normal liver tissue, the liver becomes stiff, shrunken, and scar-like. Hepatocytes die and are unable to be regenerated. When extensive fibrosis occurs, the liver ceases normal function, a condition called liver cirrhosis.

In response to hepatocyte death, growth factors such as epithelial growth factor and hepatocyte growth factor are released. The response of the liver to these growth factors is to develop nodes of hepatocellular hyperplasia and new blood vessels. Even with the addition of new blood vessels, the fibrous liver tissue prevents normal blood flow through the liver sinusoids. Blood flow falls and the pressure within the hepatic blood vessels increases, leading to a condition called portal hypertension. In response to the portal hypertension, new blood vessels that bypass the regular blood flow are developed in the liver. Blood that passes around the liver sinusoids is not detoxified. The synthetic and storage capacities of the liver are reduced in diseased states.

One of the most common complications seen in liver cirrhosis is the accumulation of intraperitoneal fluid called ascites, as can be seen in Fig. 6.18. Development of ascites is a complicated process involving multiple factors, the most important of which is portal hypertension. Decreased hepatic production of albumin also contributes to formation of ascites.

The hepatorenal recess, also called Morison's pouch, is a virtual space between the liver and right kidney in healthy individuals. The hepatorenal recess can be seen

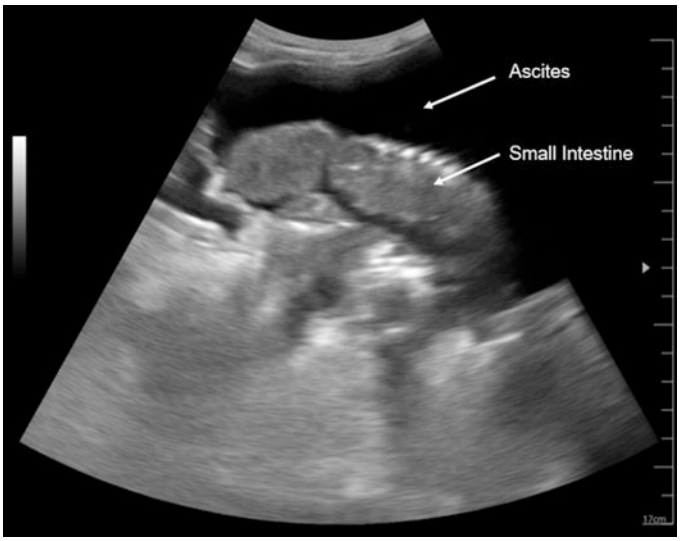

Fig. 6.18 Ascites is primarily composed of water and appears black in ultrasound. In this image a loop of intestine is seen floating in ascites

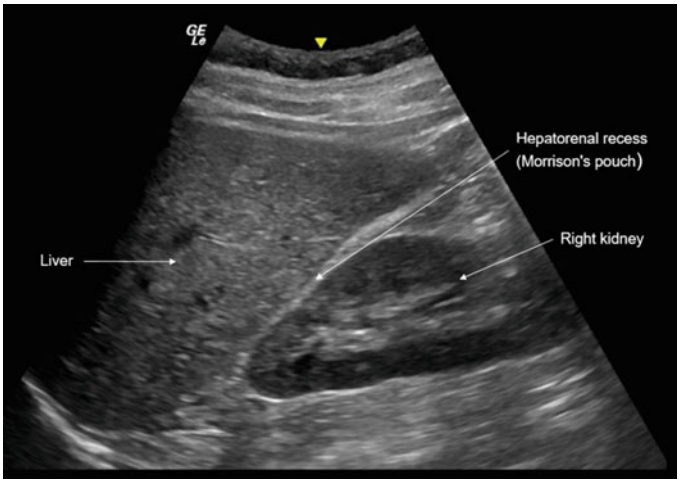

Fig. 6.19 The hepatorenal recess is a potential space between the kidney and liver. It is important to visualize this space on ultrasound because it is one of the first places where fluid, such as ascites or blood, accumulates

using US (Fig. 6.19). The hepatorenal recess is one of the first locations where intraabdominal fluid such as ascites or blood collects. It is an important radiological location for diagnosing ascites and intraabdominal blood in trauma patients. In the video below (Fig. 6.20), fluid can be seen in the Hepatorenal recess.

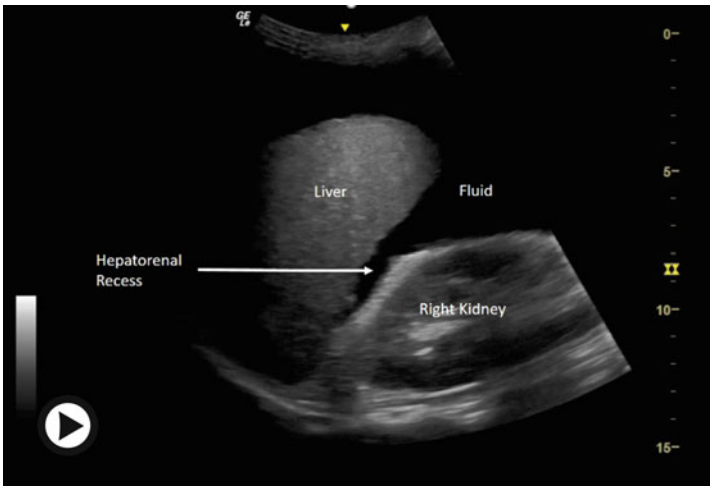

Fig. 6.20 (Video 6.5) Video of fluid in the hepatorenal recess (Morrison's pouch). This is a longitudinal view through the liver and right kidney. Note the anechoic (black) fluid in the space between those two structures called the hepatorenal recess. The fluid also extends around the liver (▶ https://doi.org/10.1007/000-7q7)

6.9.7.6 Albumin

Albumin is a protein exclusively produced by the liver and transported into the circulatory system. It is important in maintaining the oncotic (osmotic) pressure in blood and low plasma albumin levels are associated with development of edema and ascites. Albumin serves to transport numerous substances including fats, drugs, and hormones and plays a role in the elimination of toxins.

In the past, patients suffering from liver cirrhosis were recommended to consume a low protein diet to avoid stressing the remaining functional tissue, but studies have not supported this practice and it has fallen into disfavor.

6.9.8 Gallbladder and Bile

6.9.8.1 Gallbladder

The gallbladder is a water balloon shaped organ situated under the liver. Its primary purpose is to store bile that is made in the liver then dispense the bile into the duodenum when needed for digestive processes (Fig. 6.21).

The gallbladder is green in color and measures approximately 8 cm (3.2 inches) by 4 cm (1.6 inches) when fully distended. It holds roughly 50 ml (1.8 oz) of bile. The neck of the gallbladder connects to the cystic duct and is a common site where biliary stones lodge. Stones can easily be seen on ultrasound if present (Fig. 6.22).

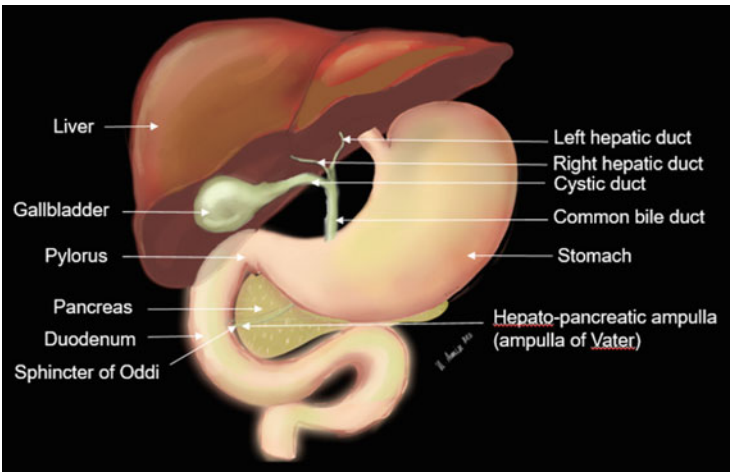

Fig. 6.21 This diagram depicts the relationship between liver, gallbladder, pancreas, ducts, ampulla of Vater and sphincter of Oddi. Bile is produced in the liver and passes into the common hepatic duct. The cystic duct connects the gallbladder to the common bile duct. The hepatic duct joins the cystic duct to form the common bile duct. The bile ducts drain bile from the liver and gall bladder through the sphincter of Oddi and ampulla of Vater into the duodenum. Secretions from the pancreas pass through the pancreatic duct and join the common bile duct just before it empties into the duodenum. Drawing by Naushad Amin

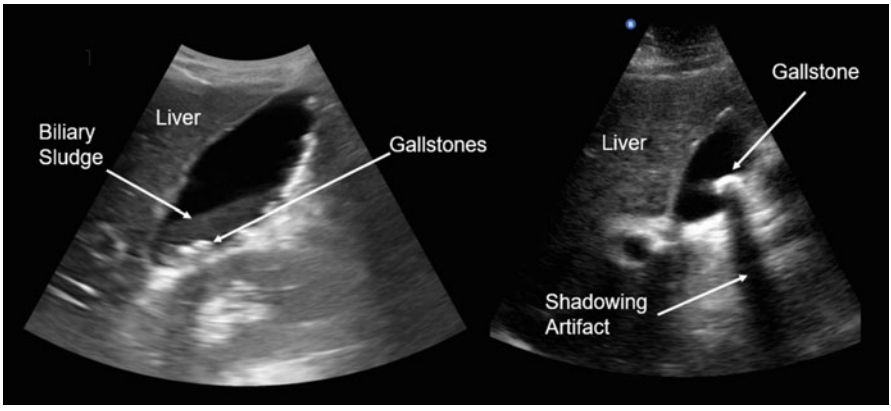

Fig. 6.22 These ultrasound images illustrate gallstones in the gallbladder. The left panel shows hypoechoic (dark) sludge in the gallbladder lumen layering along the posterior wall. It forms a straight interface with the anechoic (black) bile above it. Note the two hyperechoic (bright) gallstones also along the posterior wall. The right panel shows a different patient with a single hyperechoic stone in the gallbladder lumen. This gallstone casts a dark shadow

The gallbladder is a muscular organ that contracts when stimulated by the hormone CCK.

6.9.8.2 Common Bile Duct

The common bile duct is a tube formed by the union of the common cystic duct and the common hepatic duct. It is joined by the pancreatic duct to form the ampulla of Vater just before entering the duodenum (Fig. 6.21). The flow of bile though the common bile duct is regulated by the sphincter of Oddi. When the sphincter of Oddi is contracted, bile produced by the liver passes through the common bile duct to the gallbladder where it is stored. When the sphincter of Oddi is relaxed the bile passes from the liver and gallbladder into the duodenum. The common bile duct runs adjacent to the hepatic artery and portal vein as it travels to the duodenum. The combination of adjacent hepatic artery, portal vein, and common bile duct is referred to as the portal triad, as seen in Fig. 6.23. Despite sharing the same name, this anatomical designation should not be confused with the portal triad described at the microscopic level.

Small gallstones may develop in the common bile duct or pass from the gallbladder and become lodged in the common bile duct. This is a medical condition called choleydocolithiasis.

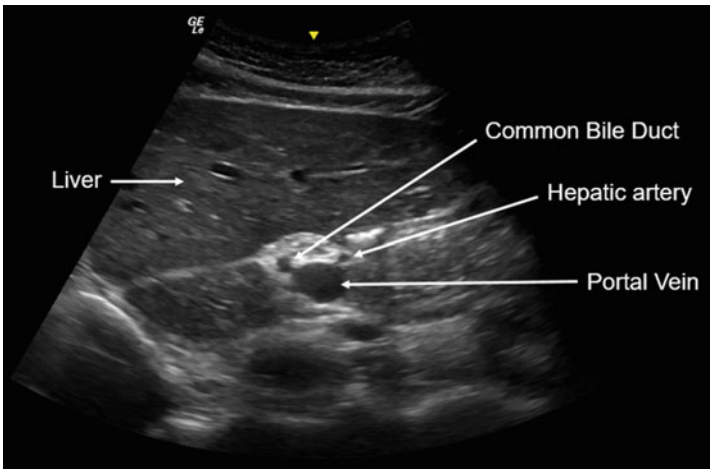

Fig. 6.23 Ultrasound is useful in visualizing vascular structures and ducts. In this image, the hepatic artery, hepatic vein, and common bile duct can be seen

6.9.8.3 Gallbladder Contraction

Nutrients in the duodenum cause the release of CCK from the cells lining the duodenum. CCK stimulates the gallbladder to contract and the sphincter of Oddi to relax, allowing bile to leave the gallbladder and move into the duodenum. When the gallbladder contracts, bile is ejected in a pulsatile fashion due to the alternating relaxation and contraction of the duodenum. Bile ejects when the duodenum is relaxed, and the duodenal pressure is low. A normal appearing gallbladder can be seen in Fig. 6.24.

6.9.8.4 Bile

Bile is synthesized in the liver then travels through the biliary ducts to the gallbladder where it is stored and concentrated until needed for digestion. When food enters the small intestine, bile is released from the gallbladder. Bile emulsifies fats and helps to neutralize acid.

Bile is a yellow-green fluid. It is 85% water 10% bile salts, 3% mucus and pigments, 1.3% lipids, and 0.7% inorganic salts. Its primary purpose is to work as a surfactant, emulsifying fats in food. The bile salts have both a hydrophobic portion and a hydrophilic portion allowing them to interact with both fats and water. When mixed with fats and water, the action of the bile salts permits pancreatic enzymes greater access to lipids by increasing the surface area of the fats. Bile salts also aid in the absorption of fat-soluble vitamins, A, D, E, and K.

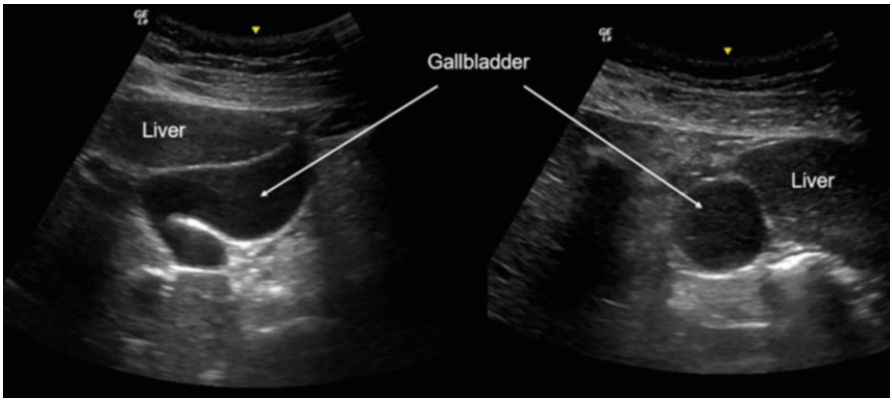

Fig. 6.24 The gallbladder serves as a reservoir for bile produced by the liver. Two normal fasting gallbladders are seen in this image. The left panel shows an elongated configuration of a gallbladder indicating this image is a longitudinal (long axis) view. The panel on the right shows a circular configuration of a gallbladder indicating a transverse (short axis) view of that organ. The anechoic areas illustrate the fluid (bile) stored in the gallbladder

Bile serves several other known functions. It is the route of excretion of the breakdown products of red blood cells called bilirubin. Bile also serves an immune function by destroying microorganisms present in food.

6.9.9 Pancreas

The pancreas participates in two organ systems, the digestive and endocrine systems. In the gastrointestinal tract, the pancreas is responsible for secreting pancreatic juice that contains enzymes that break down carbohydrates, proteins, and lipids as chyme passes through the small intestine. The endocrine function of the pancreas is to produce hormones such as insulin and glucagon.

The pancreas lies adjacent to the duodenum and posterior to the stomach in the epigastric region of the abdominal cavity (Fig. 6.21). Pancreatic juices exit the pancreas through a duct called the pancreatic duct. The pancreatic duct joins the common bile duct just before it enters the duodenum forming the hepatopancreatic ampulla, also known as the ampulla of Vater. The ampulla of Vater is surrounded by a ring of muscle called the sphincter of Oddi that regulates the flow from the gallbladder and pancreas into the duodenum.

The blood supply of the pancreas comes from the pancreatic branches of the splenic artery. The head of the pancreas is located in the duodenal curve and receives additional blood supplies from the superior and inferior pancreaticoduodenal arteries. The body and neck of the pancreas are drained by the splenic vein and the head drains into the superior mesenteric and portal veins.

The pancreas initially produces protein digesting enzymes in their inactive form called zymogens. Zymogens are activated in the duodenum. If zymogens are prematurely activated, the digestive activity occurs in the pancreas, causing destruction of the pancreatic tissue. This is a disease called pancreatitis. The pancreas also secretes bicarbonate, which neutralizes stomach acid, and this secretion is stimulated by the hormone secretin. The pancreas can be seen in Fig. 6.25.

The three main categories of enzymes produced in the pancreas are: lipases, which break down fats; proteases, which break down proteins; and amylases, which break down carbohydrates. Enzymes produced in the pancreas pass through the pancreatic duct and are released into the duodenum. In the duodenum, enzymes convert the inactive proteases (stored as zymogens, see above) to active ones. Lipases and amylases are secreted in their active form. This process is facilitated by the change in pH as the pancreatic fluid enters the duodenum.

6.10 Table of US Applications

Table 6.1 describes some of the applications of ultrasound in evaluating the gastrointestinal tract.

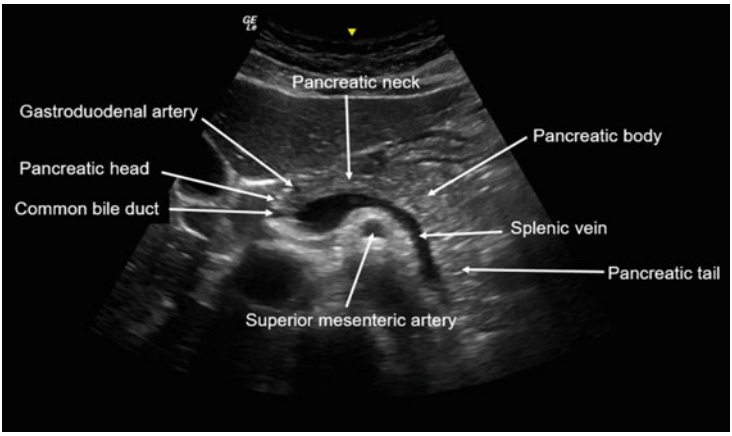

Fig. 6.25 Ultrasound image of a normal pancreas. The pancreas is located posterior to the stomach

Table 6.1 Common applications of ultrasound in the gastrointestinal tract

Organ	Ultrasound application
Salivary gland	Diagnosis of stones, abscess, mass
Esophagus	Identifying inadvertent placement of an endotracheal tube in the cervical esophagus
Stomach	Evaluation for pyloric stenosis, masses
Intestine	Evaluation of obstruction, intussusception, abscess, appendicitis, inflammatory bowel disease
Gallbladder	Evaluation for stones, sludge, polyps, wall thickening
Liver	Evaluation of masses, cysts, hematoma, abscess, fatty liver, cirrhosis
Pancreas	Evaluation for masses, abscess, pancreatitis
Vasculature	Evaluation for portal hypertension, blood clots
Other abdominal structures	Evaluation for hematoma, abscess, lymph nodes, ascites

6.11 Lab Exercises

For lab exercises we have suggested several small labs that can be used alone, or selectively combined into a single lab session depending on the length of the lab and the expertise of the instructors.

Purpose: The purpose of these lab exercises is to demonstrate the uniqueness of the abdominal physiology and allow the user to practice ultrasound skills.

6.11.1 Exercise 1: Esophagus Swallow—Examining Peristalsis

6.11.1.1 Learning Objectives

Observe the peristaltic movement of the gastrointestinal system by observing fluid passing through the esophagus.

6.11.1.2 Transducer/Probe

The high frequency linear probe is used since the cervical esophagus is fairly shallow in the neck.

6.11.1.3 Needed Supplies

A cup of water or beverage of similar viscosity.

6.11.1.4 Patient Position and Image Orientation

The patient will need to be sitting erect or semi-erect in order to comfortably swallow the beverage. Have the patient slightly lift his or her chin for better access and visibility.

You can observe movement through the esophagus in the longitudinal or transverse plane. It is easiest to locate the esophagus in the transverse plane. Therefore we will begin the scan with a transverse view.

An orientation marker, usually the company logo, will be on the top left side of the ultrasound screen. The logo matches up with the probe marker, often a palpable ridge on one side of the probe. On a transverse view, structures on the left side of the screen are closer to the patient's right side. On a longitudinal view, structures on the left side of the screen are closer to the patient's head. The top of the screen is always superficial or where the probe makes contact with the body surface.

6.11.1.5 Performing the Scan

1. Choose the thyroid preset in the ultrasound settings. Apply adequate gel to the probe.
2. It is helpful to have the patient take a mouthful of liquid in now and hold in the mouth until you have located the esophagus and steadied your hand.

3. Begin with the probe in the transverse position with the probe marker pointing toward the patient's right. Place the transducer just to the left of midline on the patient's neck (see Fig. 6.26).
4. Slowly sweep and/or fan the transducer superior and inferior to visualize the left lobe of the thyroid.
5. Locate the esophagus posterior and medial in the same image as the thyroid gland (see Fig. 6.27).

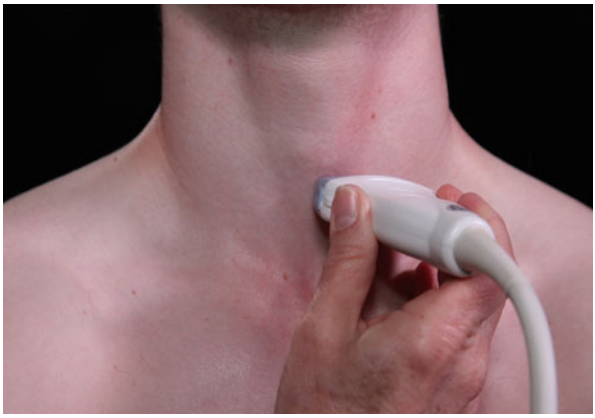

Fig. 6.26 Photo showing probe placement for a transverse view of the esophagus. The probe marker is directed toward the patient's right side

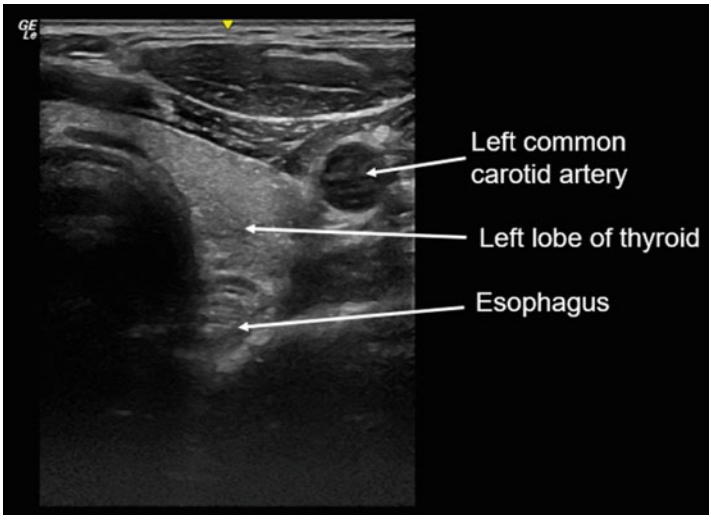

Fig. 6.27 Ultrasound image to locate the esophagus. Note the esophagus is the round target- like structure posterior to the left lobe of the thyroid gland

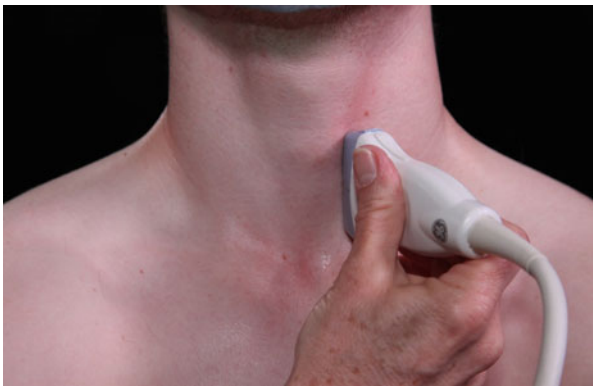

Fig. 6.28 Photo showing probe placement for a longitudinal view of the esophagus. The probe marker is directed toward the patient's head

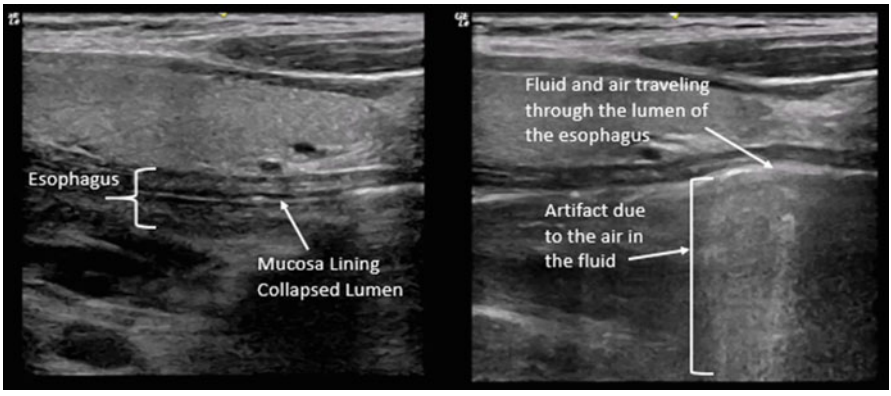

Fig. 6.29 Longitudinal views of the esophagus. The left image shows the esophagus prior to swallowing with a collapsed lumen. The right image demonstrates artifact created by air and fluid passing through the esophagus immediately after swallowing

6. Once you have located the esophagus in the transverse plane you can slowly rotate the transducer clockwise moving the probe marker to point toward the patient's head to obtain a longitudinal view (see Fig. 6.28)
7. Hold this position and ask the standardized patient to agitate the fluid in his or her mouth in order to form bubbles. *Doing this will introduce more air into the fluid and allow for better visualization of the fluid passing through the esophagus.*
8. Ask the standardized patient to swallow the fluid and watch as the fluid moves through the esophagus. Figure 6.29 demonstrates static images of the appearance of the esophagus before swallowing and while the fluid is passing through it. Figure 6.30 is a video showing the dynamic appearance.

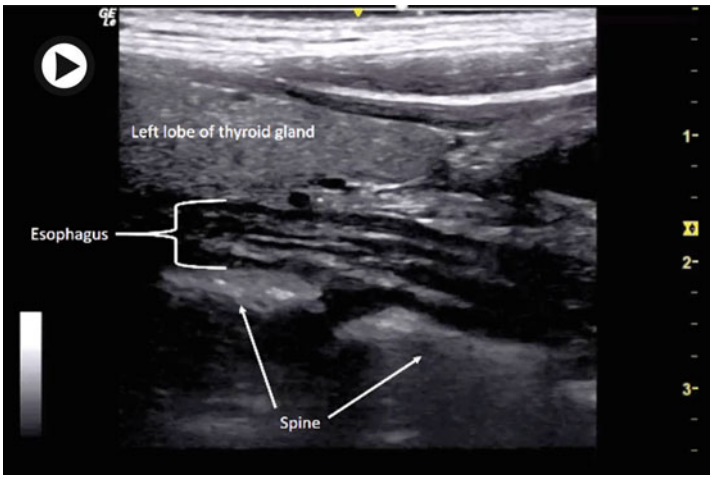

Fig. 6.30 (Video 6.6) Video of fluid passing through the esophagus. In this video water is seen rapidly coursing within the esophagus through the process of peristalsis. At the onset, the esophagus is empty with a collapsed lumen. Subsequently a bolus of fluid quickly moves from the left side of the screen toward the right side of the screen. Fluid is typically anechoic (black) on ultrasound. This bolus of water contains echogenic (bright) areas due to mixing of air within it during swallowing (▶ https://doi.org/10.1007/000-7q8)

9. Note how the fluid moves quickly through the esophagus and the esophagus quickly resumes its normal appearance.

6.11.1.6 A Step Further

Using a low frequency curvilinear probe, search the standardized patient's abdomen for other examples of peristalsis. Refer to Fig. 6.12 for an example of small intestine peristalsis.

6.11.2 Exercise 2: Observing Changes in the Fasting and Post Prandial Gallbladder

6.11.2.1 Learning Objectives

To visualize how the gastrointestinal system changes with ingestion.

6.11.2.2 Transducer/Probe

Use a low frequency curvilinear probe to best visualize the gallbladder.

6.11.2.3 Needed Supplies

A fatty snack or meal. *The bile contained within the gallbladder is used to emulsify fats for digestion, the higher the fat content the more bile will be needed!*

6.11.2.4 Patient Position and Image Orientation

Have the patient in the supine position. The patient should be fasting for at least 4 h before the initial scan.

An orientation marker, usually the company logo, will be on the top left side of the ultrasound screen. The logo matches up with the probe marker, often a palpable ridge on one side of the probe. On a transverse view, structures on the left side of the screen are closer to the patient's right side. On a longitudinal view, structures on the left side of the screen are closer to the patient's head. The top of the screen is always superficial or where the probe makes contact with the body surface.

6.11.2.5 Performing the Scan on a Fasting Gallbladder

1. Choose the general abdomen preset in the ultrasound settings. Apply adequate gel to the probe.
2. Place the transducer on the standardized patient's right anterior abdomen just below the margin of the ribs approximately in line with the mid aspect of the clavicle (collar bone) as shown in Fig. 6.31. The probe marker should point toward the patient's right side to obtain a transverse view of the gallbladder.
3. Fan the transducer superiorly and inferiorly until you locate the gallbladder. Recall that the gallbladder in located at the inferior border of the liver anteriorly. It is often helpful to ask the standardized patient to take a deep breath in and hold. This action pushes the liver and gallbladder inferiorly to make them easier to visualize. Figure 6.32 is representative image of a transverse view of the gallbladder.
4. Once you have located the gallbladder rotate the probe marker in a clockwise direction toward the patient's head to elongate the gallbladder (see Fig. 6.33). Once you have the probe marker pointing toward the patient's head, make the gallbladder appear as long as possible on this longitudinal view by making small adjustments in the degree of rotation of the transducer. You may need to fan the transducer as well. Figure 6.34 is a representative image of a longitudinal view of the gallbladder

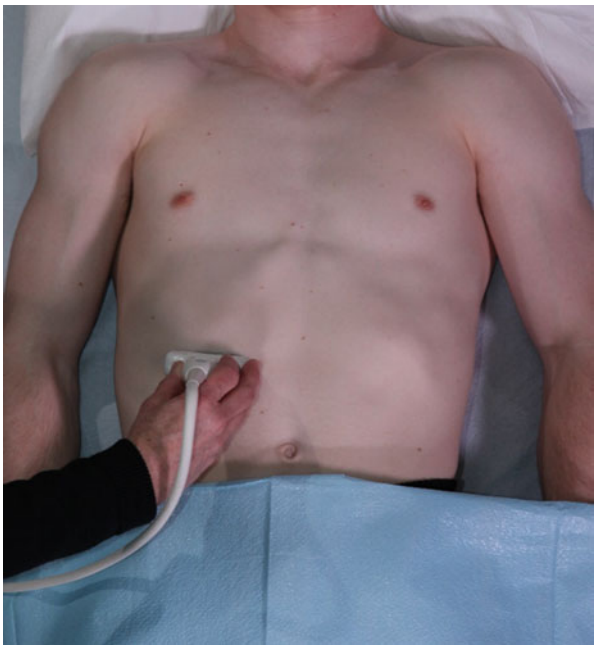

Fig. 6.31 Transverse view of gallbladder. The image on the left shows probe position for a transverse view of the gallbladder. The probe marker points toward the patient's right side

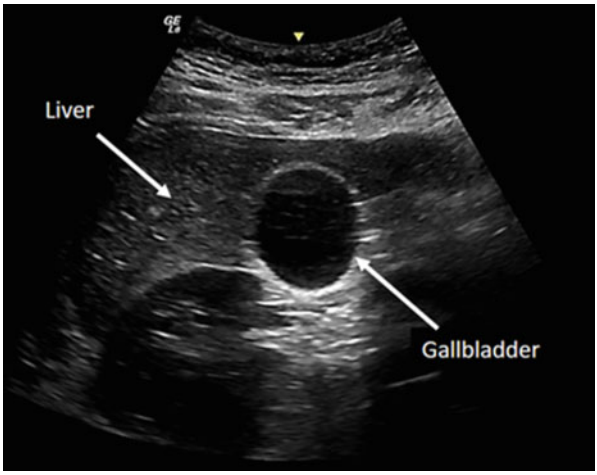

Fig. 6.32 Transverse view of the gallbladder. Note the gallbladder has a round appearance on the transverse view

5. Once you have a good longitudinal view, freeze the image. Measure the diameter and length of the gallbladder as in Fig. 6.35. Measure the thickness of the anterior wall of the gallbladder as in Fig. 6.36. During fasting the normal gallbladder will measure approximately 8–9 cm in length and 3 cm in diameter. The wall should measure <3 mm.
6. Document your measurements either as written results or with saved images

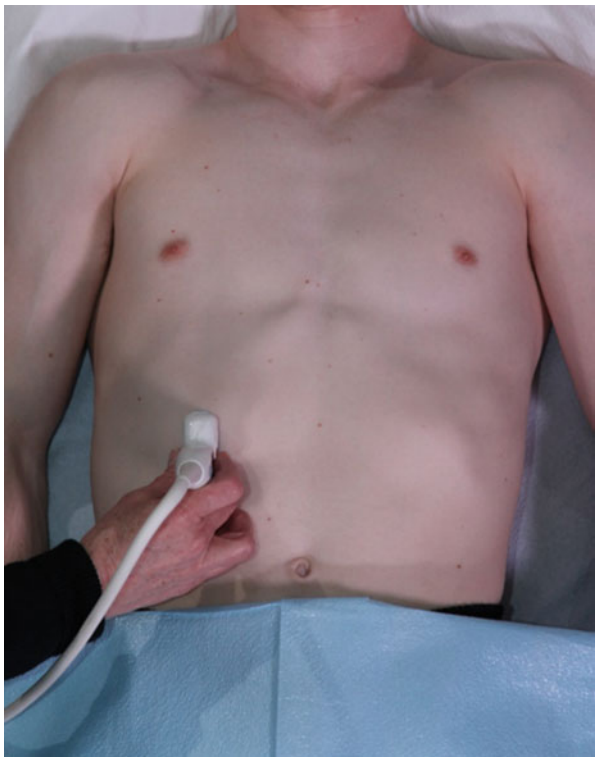

Fig. 6.33 Photo showing probe position for a longitudinal view of the gallbladder. The probe marker is initially directed toward the patient's head. It may be necessary to rotate the probe marker slightly clockwise or counterclockwise to fully elongate the gallbladder on the image

6.11.2.6 Performing the Scan on a Post-Prandial Gallbladder

1. Have the fasting standardized patient eat the snack or meal. Wait at least 30 min. The larger the snack (or meal) the better! *While waiting feel free to work on some of the other exercises!*
2. Obtain another longitudinal view of the gallbladder now in the post-prandial state.
3. Again, measure the diameter, length, and wall thickness of the gallbladder as above.
4. Compare your before and after measurements. The bile stored within the gallbladder is used to emulsify fats to aid in their digestion. When a fat containing meal is consumed, the gallbladder contracts in response to the hormone cholecystokinin (CCK). Given time after eating a fatty meal, the gallbladder should appear smaller (contracted) and have a thicker wall (see Fig. 6.37) when compared to fasting gallbladder.

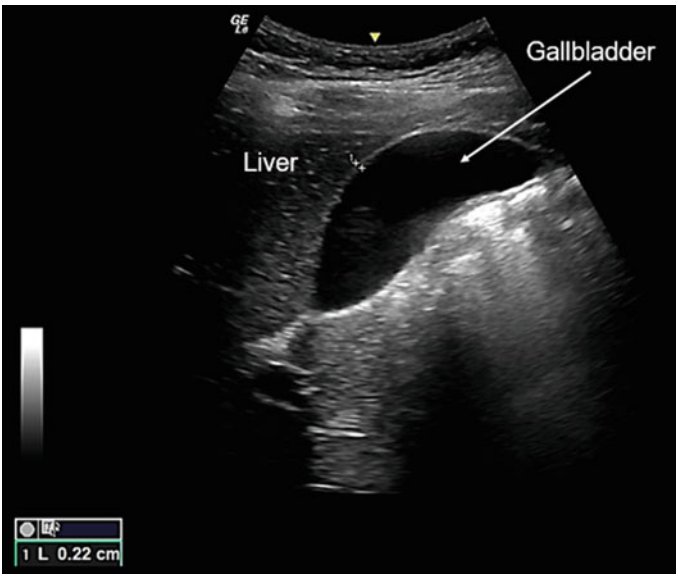

Fig. 6.34 Longitudinal view of the gallbladder. Note the elongated appearance on this view compared to the transverse view

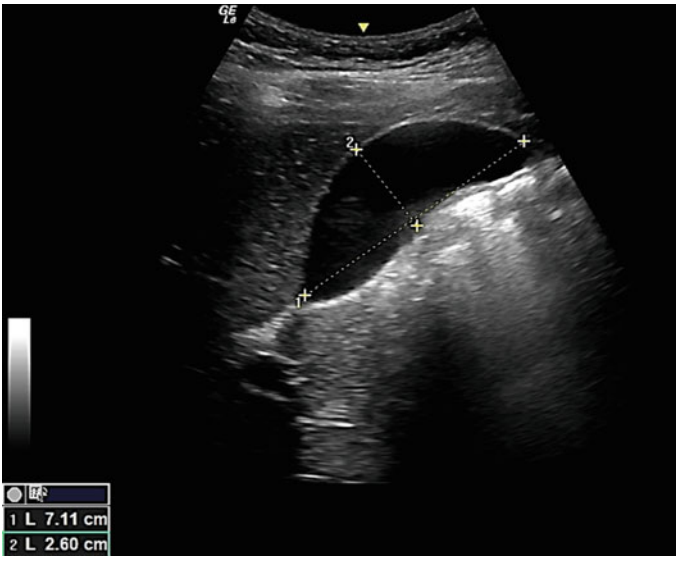

Fig. 6.35 Longitudinal view of gallbladder with diameter and length measurements. Measurement 1 is the length and measurement 2 is the diameter

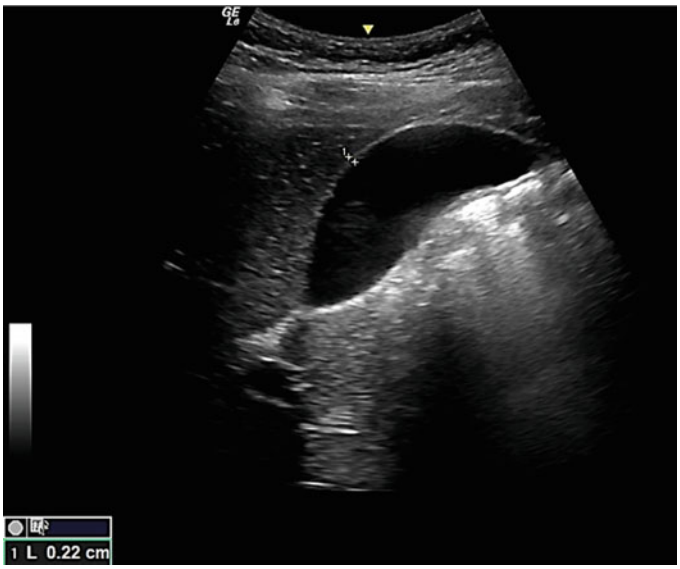

Fig. 6.36 Longitudinal view of gallbladder with wall thickness measurement. Note the anterior wall is measured

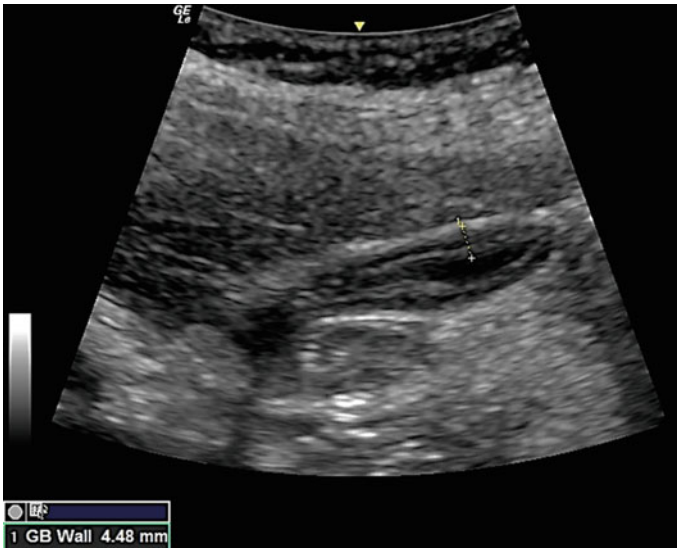

Fig. 6.37 Longitudinal view of a gallbladder in the post-prandial state. Note the gallbladder is collapsed and the wall is also thickened due to contraction stimulated by a meal. Although this is a different patient from the one scanned in Fig. 6.35, this image is representative of the typical post-prandial appearance of a gallbladder

6.11.2.7 One Step Further

Continue to periodically examine the standardized patient's gallbladder using the same low frequency transducer. After approximately 90 min, the gallbladder should appear to re-enlarge as it relaxes and refills with bile produced by the liver.

6.12 Conclusion

The gastrointestinal system is essentially a complex conduit extending from the mouth to anus. Its primary purpose is the intake of food and elimination of wastes. Despite having a straightforward purpose, its regulation and lesser known functions are still being studied. Ultrasound is a novel tool that can be used to visualize the gastrointestinal tract in action and aid in a more thorough comprehension of gastrointestinal physiology.

Further Reading

Reference Books

Connolly JA, Dean AJ, Hoffmann B, Jarman RD (eds) (2017) Emergency point-of-care ultrasound. Wiley-Blackwell, New York

Carmody K, Moore C, Feller-Kopman D (2011) Handbook of critical care and emergency ultrasound. McGraw-Hill, New York

Curry RA, Tempkin BB (2015) Sonography: introduction to normal structure and function, 4th edn. Saunders, St Louis, MO

Curry RA, Tempkin BB (2017) Workbook and lab manual for sonography: introduction to normal structure and function. Elsevier, New York

Edelman S (2012) Understanding ultrasound physics, 4th edn. ESP Ultrasound, Woodlands

Maconi G, Porro GB (2013) Ultrasound of the gastrointestinal tract. Springer, Berlin, Heidelberg.

Soni NJ, Arntfield R, Kory P (2019) *Point of care ultrasound*. Elsevier Health Sciences, London

Articles: General Ultrasound of the Gastrointestinal Ttract

Abu-Zidan FM, Cevik AA (2018) Diagnostic point-of-care ultrasound (POCUS) for gastrointestinal pathology: state of the art from basics to advanced. World J Emerg Surg 13:47. https://doi.org/10.1186/s13017-018-0209-y

Atkinson NS, Bryant RV, Dong Y, Maaser C, Kucharzik T, Maconi G et al (2016) WFUMB position paper. Learning gastrointestinal ultrasound: theory and practice. Ultrasound Med Biol *42*(12):2732–2742. https://doi.org/10.1016/j.ultrasmedbio.2016.08.026

Atkinson NSS, Bryant RV, Dong Y, Maaser C, Kucharzik T, Maconi G et al (2017) How to perform gastrointestinal ultrasound: Anatomy and normal findings. World J Gastroenterol *23*(38): 6931–6941. https://doi.org/10.3748/wjg.v23.i38.6931

Kafer I, Rennie W, Noor A, Pellerito S (2017) Hunger games: interactive ultrasound imaging for learning gastrointestinal physiology. J Ultrasound Med 36:361–365

Nylund K, Maconi G, Hollerweger A, Ripolles T, Pallotta N, Higginson A et al (2017) EFSUMB Recommendations and Guidelines for Gastrointestinal Ultrasound. Ultraschall Med *38*(3): 273–284. https://doi.org/10.1055/s-0042-115410

Chapter 7
Ultrasound of the Urinary System

Renee K. Dversdal, Kevin M. Piro, and Robert W. Rope

7.1 Anatomy and Physiology of the Urinary System

Our kidneys help preserve our homeostasis. To do so, they filter our blood at a high rate, approximately 140 liters a day. However, they expel the solutes and water we take in, along with toxins generated by our metabolism, or perhaps unfortunately ingested, in a reasonably small amount of urine. To maintain this homeostatic balance, the kidneys must excrete what we ingest, excluding what is eliminated through the bowels, lungs (in the case of carbon dioxide), or insensible losses. Along the way, the kidneys regulate our sodium, water, and potassium levels along with our acid-base status. In addition, by controlling how much sodium and water we excrete, as well as producing the enzyme renin, which directs the renin-angiotensin-aldosterone system (RAAS), our kidneys are the primary mechanism for regulating our fluid balance as well as systemic blood pressure. The kidneys also activate vitamin D, necessary for bone health, and release erythropoietin, which regulates the production of red blood cells.

With few exceptions, however, ultrasound visualization of the kidneys and bladder relies on structural assessments to infer the presence of disease. The kidneys lie in the retroperitoneal space, deep to the muscles of the back, and partially covered by the lower ribs (Fig. 7.1). In adults, a normal kidney size ranges 9–12 cm in length and 4–6 cm in width. The left and right kidneys should be reasonably symmetric and a length difference of greater than 1–2 cm may indicate reduced growth in the

Supplementary Information The online version contains supplementary material available at https://doi.org/10.1007/978-1-0716-1863-9_7. The videos can be accessed by scanning the related images with the SN More Media App.

R. K. Dversdal (✉) · K. M. Piro · R. W. Rope
Oregon Health & Science University, Portland, OR, USA
e-mail: dversdar@ohsu.edu; piro@ohsu.edu; roper@ohsu.edu

L. B. Wilson et al. (eds.), *Understanding Physiology with Ultrasound*, Physiology in Health and Disease, https://doi.org/10.1007/978-1-0716-1863-9_7

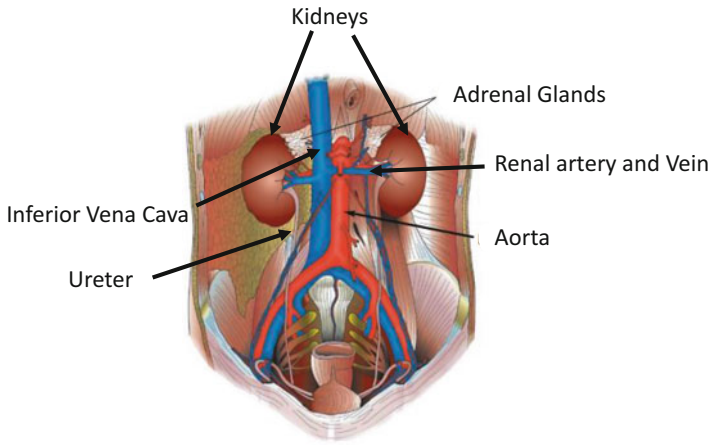

Fig. 7.1 Kidney anatomy relative to major abdominal vessels. Bladder not shown

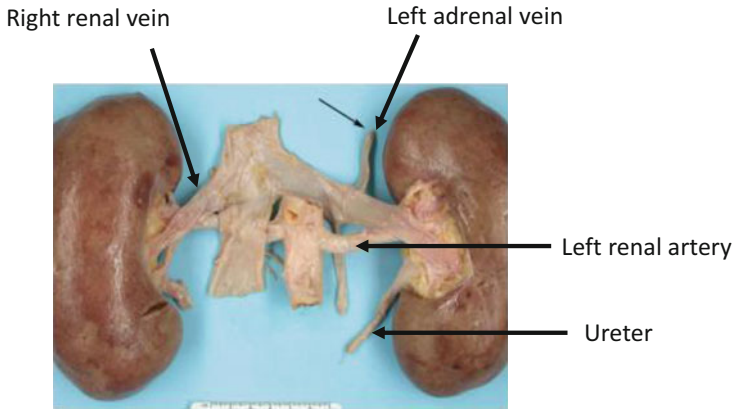

Fig. 7.2 Renal vasculature and external structures. Arrow indicates the left adrenal vein entering the left renal vein. The right adrenal vein drains into the inferior vena cava (IVC) directly and is not shown

smaller kidney. This may be due to congenital abnormalities or reduced blood flow leading to ischemia.

The renal arteries branch off the abdominal aorta (Fig. 7.2), delivering approximately 10% of the cardiac output to each kidney. Inside the kidneys, the renal arteries divide into smaller branches, eventually leading to the glomerular capillaries. These capillaries form part of the glomerular filters within the nephron. After the glomerulus, the non-filtered blood travels within peritubular capillaries then coalesces into the renal veins, eventually leading back into the inferior vena cava.

The nephron is the "working unit" of the kidney, consisting of the glomerular filter leading to an epithelial cell lined tubule (Fig. 7.3). Each kidney has

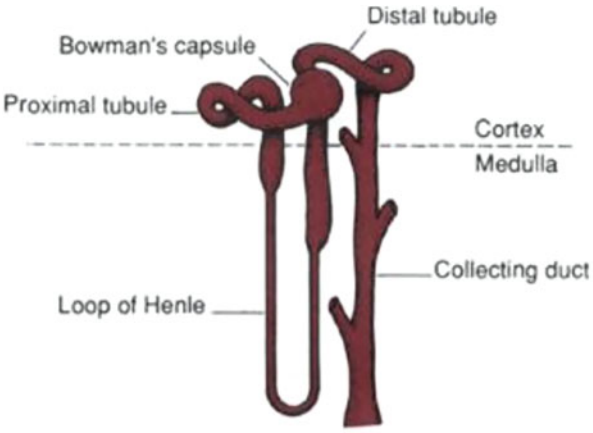

Fig. 7.3 Schematic of a nephron. Note, Bowman's capsule contains the glomerulus

approximately 1 million nephrons though there is wide variability among individuals. The tubule reclaims most of the filtered molecules not destined to leave our body (e.g. water, sodium, potassium, phosphorus, glucose). The tubules are anatomically divided into different segments (proximal tubule, loop of Henle, distal tubule, and collecting ducts) based on their shape and function. Each tubule intertwines with the kidney's microvasculature so water and solutes can be reabsorbed, and additional, protein-bound toxins can be directly excreted from the blood into the tubules, bypassing the glomerular filter. The ultrasound beam cannot distinguish individual nephrons.

Each kidney has an outer cortex (*L.* bark of a tree), which contains the glomerular filters as well as parts of the proximal and distal tubules. The inner medulla (*L.* marrow) contains the loops of Henle and collecting ducts as well as numerous peritubular capillaries. Distal tubules from several different adjacent glomeruli come together to form the collecting ducts, which aggregate within the medullary renal pyramids. There are approximately 7–9 pyramids per kidney (Fig. 7.4). From the major calyces urine flows into the renal pelvis, the ureter, and the bladder.

7.1.1 Renal Structures on Ultrasound

The outer rim of cortex, as well as the division between the cortex and medulla (corticomedullary junction), can generally be visualized. The pyramids contain a greater amount of water within the collecting ducts, and thus are often visible on ultrasound as hypoechoic structures (Fig. 7.5) leading into the minor then major calyxes of the collecting system. The cortical rim should be at least 1 cm and loss of cortex is indicative of chronic kidney disease (CKD). However, formal estimation of cortical depth is often challenging and the corticomedullary junction is generally better visualized in children than adults.

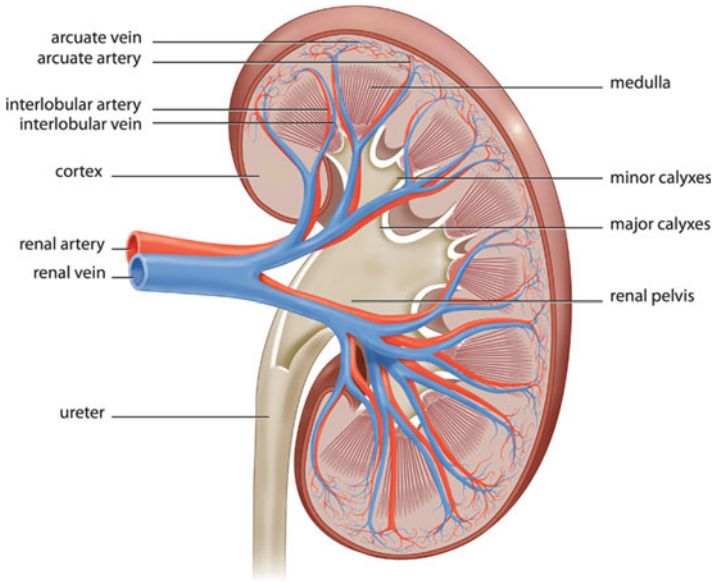

Fig. 7.4 Cut section of kidney demonstrating architecture & blood flow

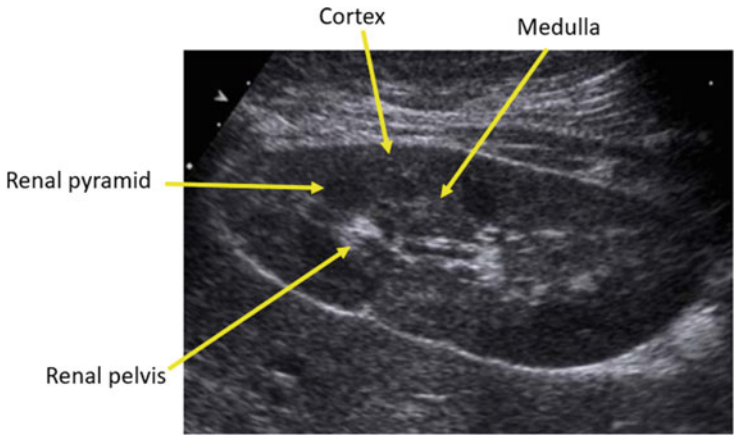

Fig. 7.5 Demonstration of the renal cortex, medulla, pelvis, and a renal pyramid, on the normal kidney of a 17-year-old

A loss of the corticomedullary differentiation seen on ultrasound can indicate chronic kidney disease (CKD) however it is also common with aging. A reduction in renal size (Fig. 7.6), as well as an increase in cortical echogenicity due to the development of kidney fibrosis, are better indicators of CKD.

The renal sinus consists of the collecting system as well as larger renal vessels, lymphatics, nerves, and fat. The sinus fat makes this area echogenic and the sinus

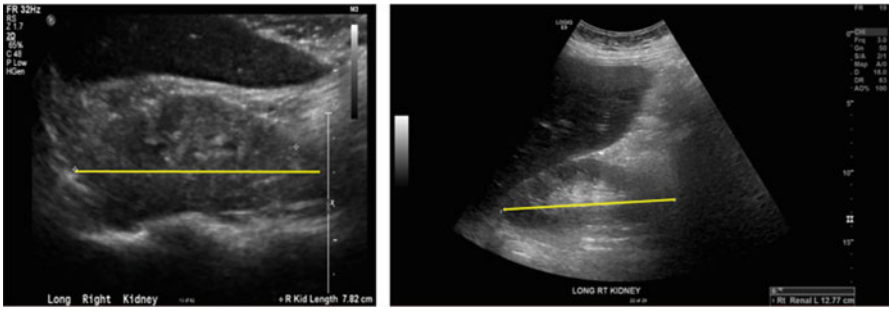

Fig. 7.6 Side by side comparison of small right kidney with poor cortical & medullary differentiation in a patient with end stage renal disease on dialysis (left panel), versus a regular size kidney with good differentiation in a patient with normal renal function (right panel). Yellow line indicates approximate placement of a measurement line to show how measurement helps with size comparison

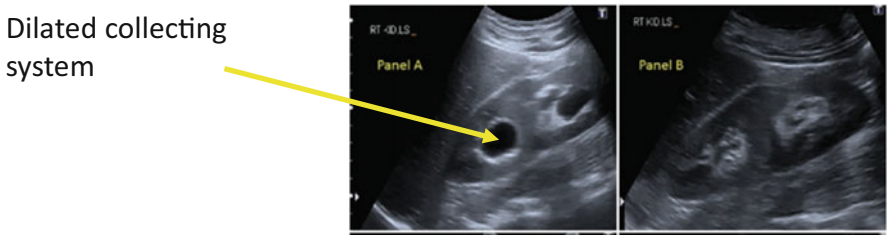

Fig. 7.7 Panel A demonstrates a kidney with hydronephrosis, secondary to bladder outlet obstruction and urinary retention. Panel B demonstrates the same kidney decompressed after the bladder was drained via catheter

should take up approximately 1/3 of the kidney visually. The large renal vessels may be seen, however the smaller vessels, lymphatics and nerves are not appreciated. A shrinking of the renal cortex around the renal sinus, which often makes the renal sinus appear more prominent, can also be indicative of CKD.

Urine formed within the collecting ducts in the renal pyramids empties into the minor then major calyces followed by the renal pelvis and then proximal ureter. The proximal ureter may not be well seen on ultrasound in a healthy kidney. Regular peristaltic contractions drive collected urine down the ureters to the bladder. When this flow is interrupted, for example by a kidney stone lodged in the ureter or a cancerous mass compressing the ureter, urine will back up into the collecting system and eventually into the kidney parenchyma itself, causing hydronephrosis. If the obstruction is not resolved, hydronephrosis can result in pain, infection, and loss of kidney function. This hydronephrosis is often well visualized on ultrasound and this modality is critical for its diagnosis (Fig. 7.7). Sometimes kidney stones (termed nephrolithiasis) can be seen as hyperechoic structures in the ureter, leading to the

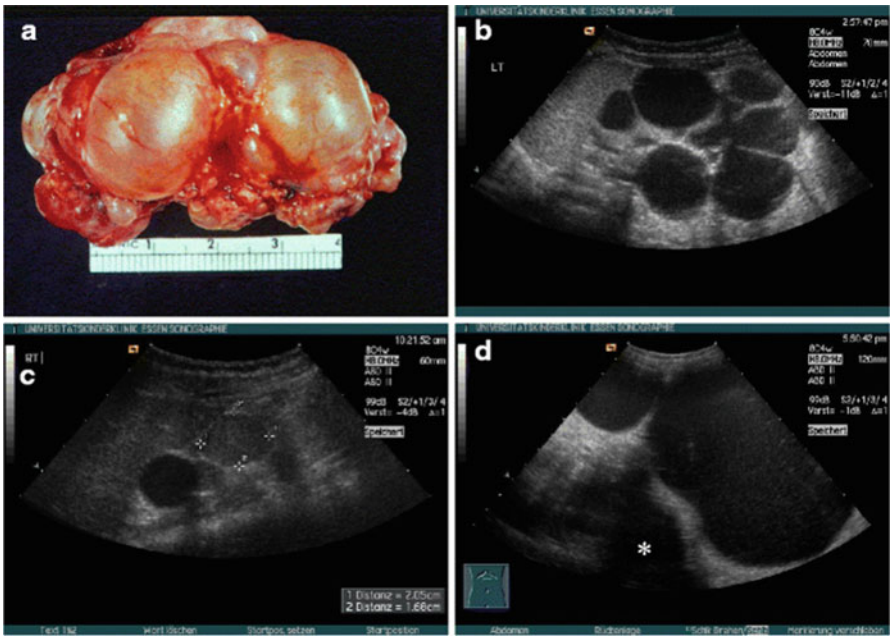

Fig. 7.8 Polycystic kidneys. Panel a is the gross appearance, panel b is a sonographic depiction, panel c contrasts cyst appearance with a tumor (marked with calipers) and panel d represents very large cysts in a polycystic kidney

hydronephrosis. However, not visualizing a stone does not rule out nephrolithiasis as a cause of renal outlet obstruction. For example, while calcium oxalate stones are dense and echogenic on ultrasound, smaller less dense uric acid stones are often not detected by the ultrasound beam.

While ultrasound cannot detect normal tubules, it is very helpful in visualizing renal cysts. These cysts are believed to be derived from abnormal tubule development and given their large size and fluid-filled cavities they are easily seen as hypoechoic smooth walled round structures on ultrasound. "Simple" renal cysts are a normal part of the aging process. Other cysts may be indicative of malignancy, benign tumors, or genetic diseases. For example, adult polycystic kidney disease is a genetic disease where abnormal tubule development leads to the formation of dozens of cysts which grow over decades and reduce kidney function (Fig. 7.8). This causes approximately 5% of kidney failure. Ultrasound is critical for screening for this disease in patients with chronic kidney disease or in relatives of those with known polycystic disease.

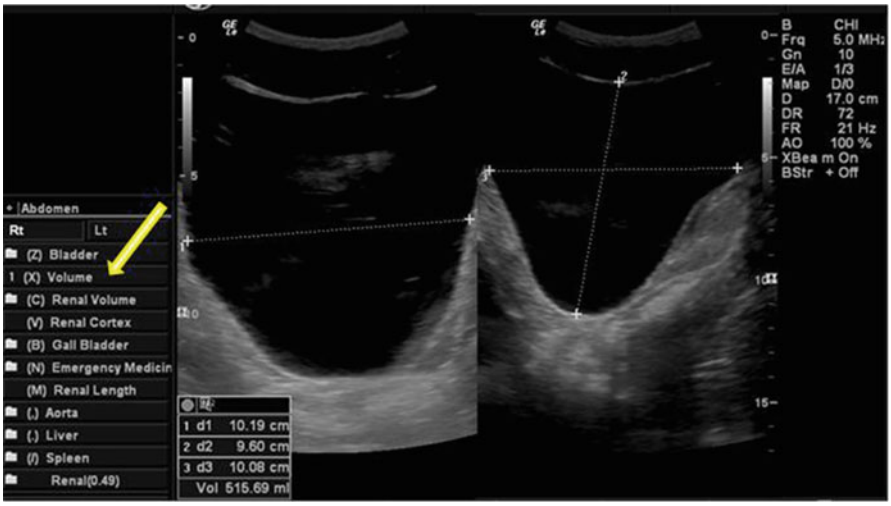

Fig. 7.9 Transverse view of the bladder on the left, mid-longitudinal view of the bladder on the right (in split screen display mode). The automatic volume calculation has been performed after selecting the appropriate calculation (yellow arrow), and the volume of urine in the bladder is displayed at the bottom of the screen

7.1.2 Bladder on Ultrasound

The bladder is designed to store urine until an appropriate time for elimination. Its walls are formed of multilayered weaved muscles that allow muscular contraction from all sides to expel urine when both the internal and external urethral sphincters are relaxed. Ultrasound can be used to evaluate the size and structure of the bladder, look for bladder stones or masses, and evaluate how well a patient empties their bladder (Fig. 7.9).

A post-void residual (PVR) is an estimation (based on measuring the volume of the bladder) of how much urine is left in the bladder after a patient urinates. Elevated PVRs suggest incomplete bladder emptying and can indicate an obstruction to urine flow (such as an enlarged prostate or prostate cancer) or weak bladder contractions (such as from neurologic damage from diabetes or spinal cord injury).

Doppler ultrasound can visualize the movement of urine from the ureters into the bladder (Fig. 7.10). These “ureteral jets” occur up to 4–5 times a minute and if seen, indicate that urine flow is not obstructed from the ipsilateral ureter. This aids in the assessment of hydronephrosis or kidney stones.

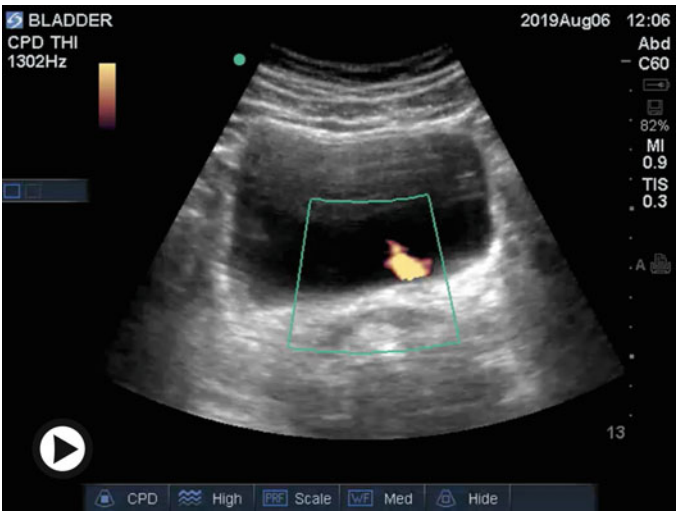

Fig. 7.10 (Video 7.1) Video of a bladder in the transverse plane, with yellow ureteral jets demonstrated with the use of color power Doppler (▶ https://doi.org/10.1007/000-7qd)

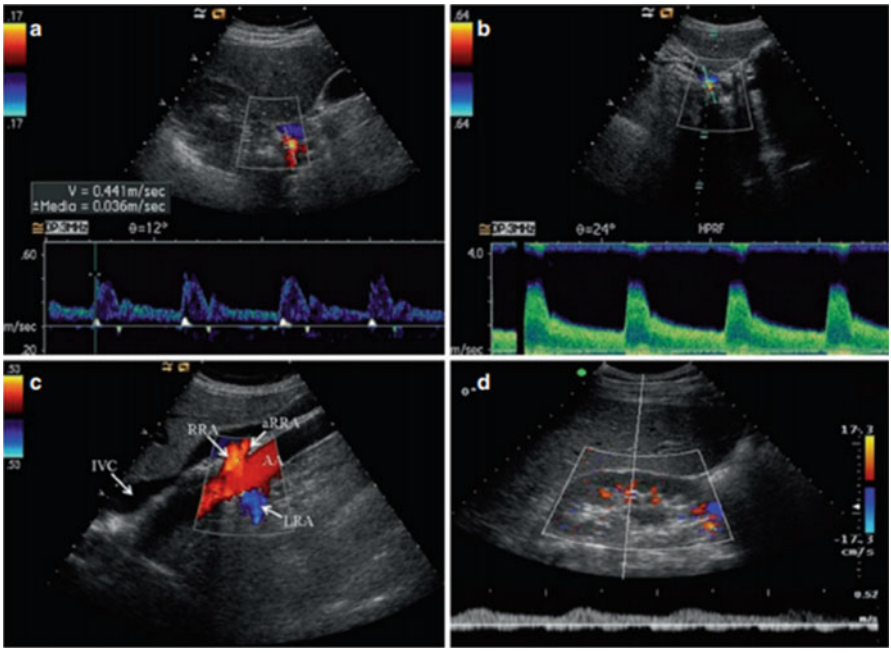

Fig. 7.11 In the vascular lab, Doppler ultrasound can be used to assess flow velocity in the renal arteries, as demonstrated in panels a and b. Panel c demonstrates the inferior vena cava (IVC), abdominal aorta (AA), right renal artery (RRA), left renal artery (LRA), and an accessory right renal artery (aRRA). Trained clinicians at the bedside can easily assess the aorta and inferior vena cava. Panel d shows color and pulsed Doppler imagining of intrarenal arteries

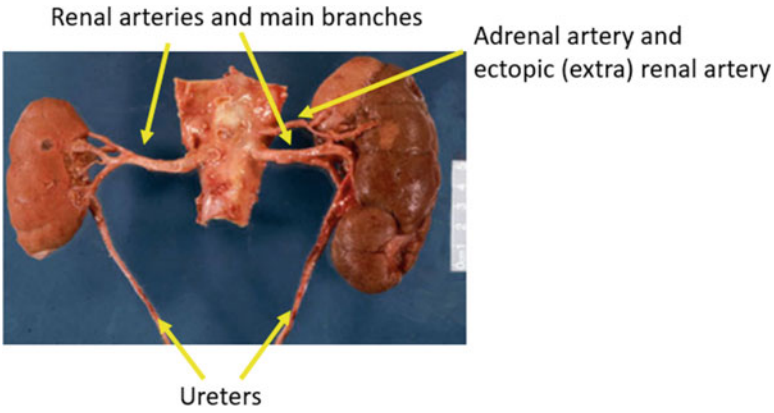

Fig. 7.12 Chronic renal artery stenosis with reduced renal size of the right kidney (*left side of figure*), and also of the superior pole of the left kidney (*right side of figure*), which is being fed by a stenotic polar artery

7.1.3 Renal Vasculature on Ultrasound

Ultrasound can visualize blood flow within the aorta, the main renal arteries and their subsequent larger branches (Fig. 7.11). Ultrasound can also visualize the main renal veins and the inferior vena cava (IVC). Comprehensive ultrasound (usually performed in the radiology department by trained sonographers with advanced machines) can detect clots within the renal veins which are seen rarely in the setting of severe protein loss from the kidneys, malignancy, or hypercoagulable states. With point-of-care ultrasound (POCUS) renal venous ultrasonography is generally limited to volume assessment via the IVC. In the setting of acute kidney injury, the volume assessment is often vital in diagnosis and management.

Clinically, evaluation of the renal arteries is useful in certain patients with hypertension (Zhu et al. 2018). Renal artery stenosis is a condition where reduced blood flow to one or both kidneys, usually due to atherosclerosis causing a narrowing in the artery, can lead to ischemia within the kidney (Fig. 7.12). This can cause chronic kidney disease and activate RAAS leading to hypertension. The elevated blood pressure is an attempt to deliver more blood flow to the ischemic kidney. This process is similar to an atherosclerotic plaque in the coronary arteries leading to a heart attack. Over time the ischemic kidney will reduce in size and become more hyperechoic, eventually progressing to CKD and potentially renal failure. Unfortunately, opening up these blockages in the kidney with a stent to restore blood flow has not proven helpful in preventing CKD or controlling hypertension.

Notably, the sympathetic nerves connecting the brain and kidney run along the renal arteries. These nerves help control renal sodium retention and renin release, contributing to the regulation of blood pressure. Ultrasound and radiofrequency waves can be used to burn these nerves to reduce sympathetic signals to the kidneys

Table 7.1 Clinical applications

Clinical ultrasound application	Value of the ultrasound	Classic image
Assess for hydronephrosis	Detect ureteral or bladder outlet obstruction in cases of pain or acute kidney injury. Arrow demonstrates hydronephrosis.	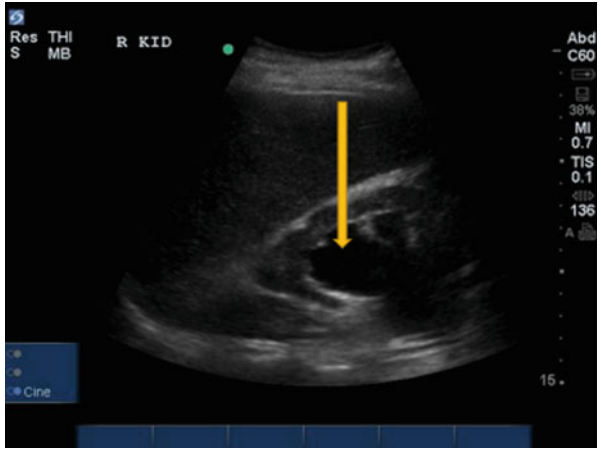

Measurement of kidney size	May help determine if renal injury is acute or chronic	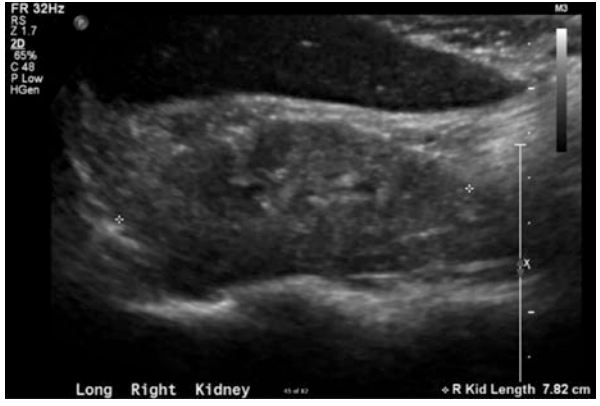
Recognize cysts/masses	Characterize incidental findings (simple cyst pictured here with posterior acoustic enhancement)	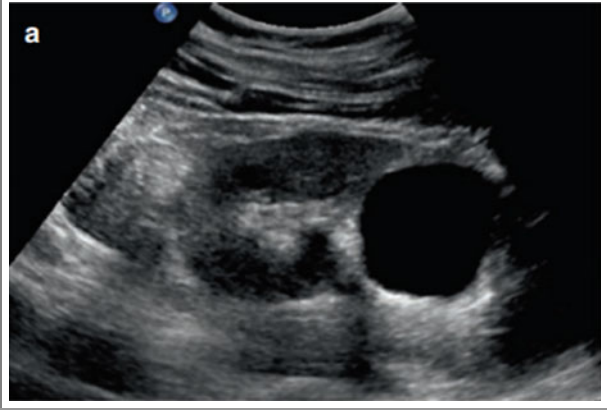

(continued)

Table 7.1 (continued)

Clinical ultrasound application	Value of the ultrasound	Classic image
Recognize kidney stones	Confirm diagnosis when visualized (arrow)	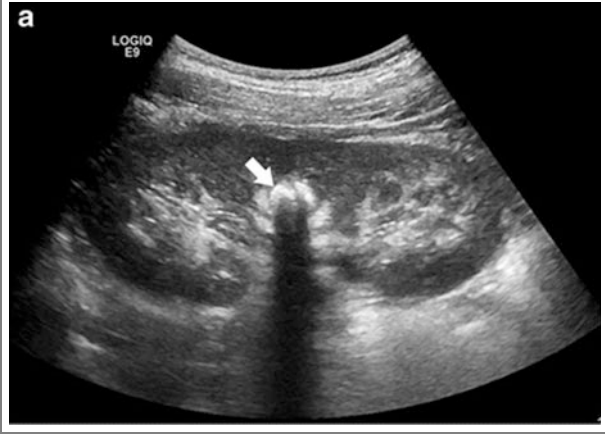

Detect ureteral jets in bladder	Rule out ureteral obstruction	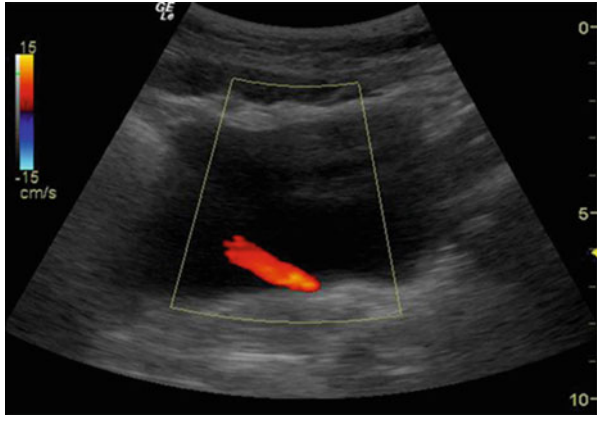

(continued)

Table 7.1 (continued)

Clinical ultrasound application	Value of the ultrasound	Classic image
Determine bladder volume	Rule out bladder outlet obstruction/ incomplete voiding. This picture demonstrates a large prostate (arrow), and urine in the bladder after the patient tried to fully void.	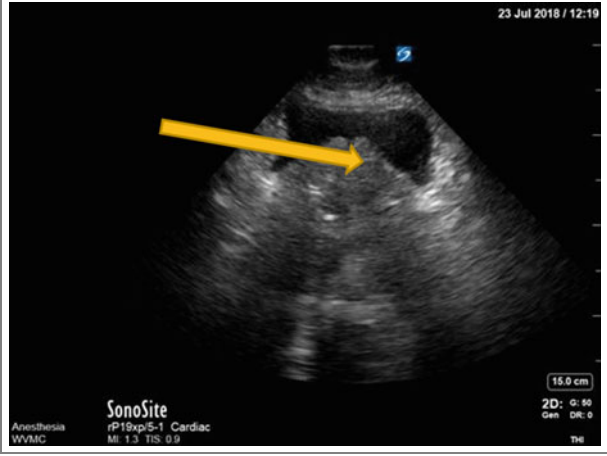

Assess volume status in acute kidney injury	Determine if treatment should include additional fluids	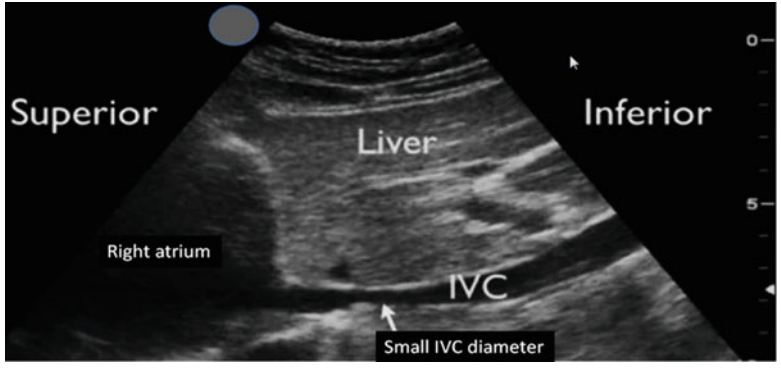

and thereby reduce blood pressure. This is an early but promising potential treatment for hypertension.

7.2 Clinical Topic 1

7.2.1 Urinary Obstruction

Urinary obstruction refers to blockage of the urine produced by the kidney at some point from the collecting ducts to exiting the body via the urethra. This could be congenital, as from a rotated kidney that crimps off the ureter, or acquired from a variety of causes. The obstruction can be intrarenal (within the kidney itself, like a small stone) or extrarenal (from the pelvis to the urethra, like a compression from a neighboring tumor outside the ureter), unilateral (one kidney/ureter is obstructed) or bilateral (both sides obstructed), complete (so no urine able to get through) or partial (with some urine being excreted, like with a large prostate partially blocking the bladder outlet). Finally, as with all things in medicine, it is important to differentiate if the process is acute (new), or chronic (developing over weeks or months).

Urinary obstruction is a problem commonly encountered in the care of adults, and symptoms can include flank or pelvic pain, a reduction in patient-reported urine output, or needing to urinate often or urgently, even while asleep. Obstruction, however, can also cause kidney damage without symptoms. Clinical findings can include blood in the urine, reduced urine output (though there can still be normal urine output with one-sided obstruction), high blood pressure or kidney injury based on laboratory studies. The primary concerns associated with urinary obstruction, regardless of the cause, are kidney failure that can be irreversible if the obstruction is not alleviated, urinary tract infections due to the inability to excrete urine properly, and obstructive symptoms that can be distressing. Renal ultrasound should be performed if there is a clinical concern for urinary obstruction in a patient with acute kidney injury, based on their medical history (Podoll et al. 2013), or if there is no other clear cause for the kidney injury.

7.2.1.1 Hydronephrosis

Normal kidneys will have the central hyperechoic area consistent with the renal sinus (Figs. 7.13 and 7.14). Hydronephrosis is notable for anechoic urine “pushing out” the hyperechoic sinus (Figs. 7.15).

There are grading systems from mild to severe, but for general purposes it is most simple to focus on presence or absence of hydronephrosis. There may be small, central, anechoic areas that are blood vessels, but these will not be “pushing out” the hyperechoic renal sinus, and color Doppler can be applied to demonstrate flow, which rules out hydronephrosis as the cause of these anechoic areas (Fig. 7.16). It is

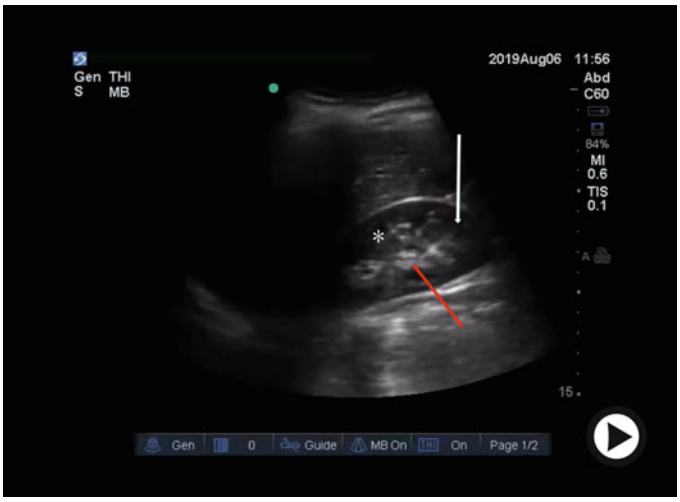

Fig. 7.13 (Video 7.2) This video demonstrates a normal right kidney, with the renal pyramids (white arrow) being hypoechoic to the renal cortex (star). The renal sinus (red arrow) is hyperechoic compared to the renal cortex (▶ https://doi.org/10.1007/000-7qa)

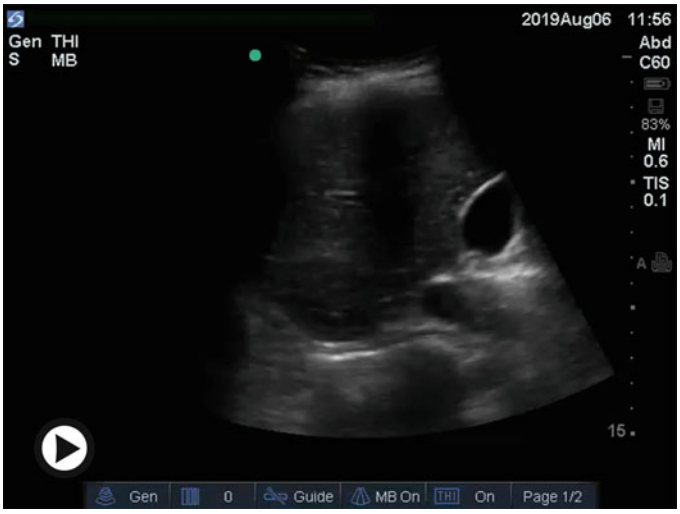

Fig. 7.14 (Video 7.3) The differentiation of kidney structures is less obvious in the transverse plane, as demonstrated in this video. The gallbladder is incidentally noted on the right side of the video as an anechoic structure with a hyperechoic wall (▶ https://doi.org/10.1007/000-7qb)

also important to ensure a cortical renal cyst does not trick you into interpreting an image as hydronephrosis (Fig. 7.8 and Table 7.1). Cysts are round and do not arise from the sinus.

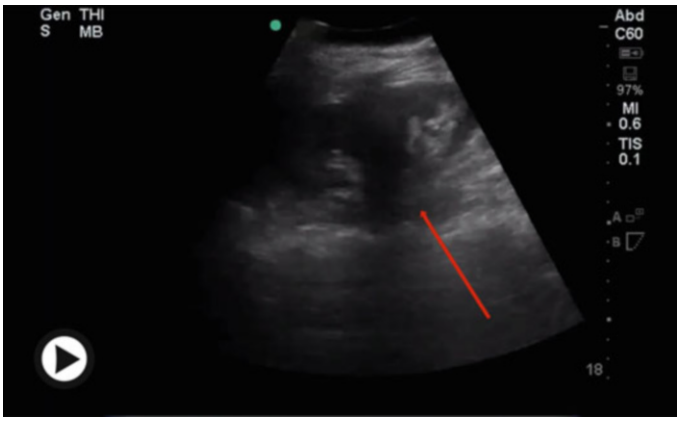

Fig. 7.15 (Video 7.4) This video demonstrates hydronephrosis. The hyperechoic renal sinus is displaced by anechoic retained urine (arrow) (▶ https://doi.org/10.1007/000-7qc)

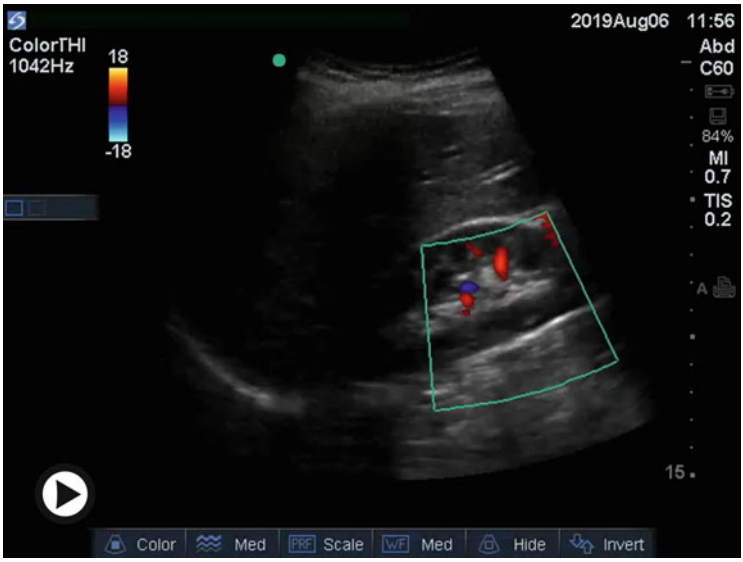

Fig. 7.16 (Video 7.5) In this video, Color Doppler has been applied to demonstrate blood flow in the renal sinus (▶ https://doi.org/10.1007/000-7q9)

Sometimes when the obstruction is further down into the ureter you can see hydroureter if the obstruction is acute, or hydroureteronephrosis if it is present long enough to cause dilation of the renal pelvis and sinus (Fig. 7.17).

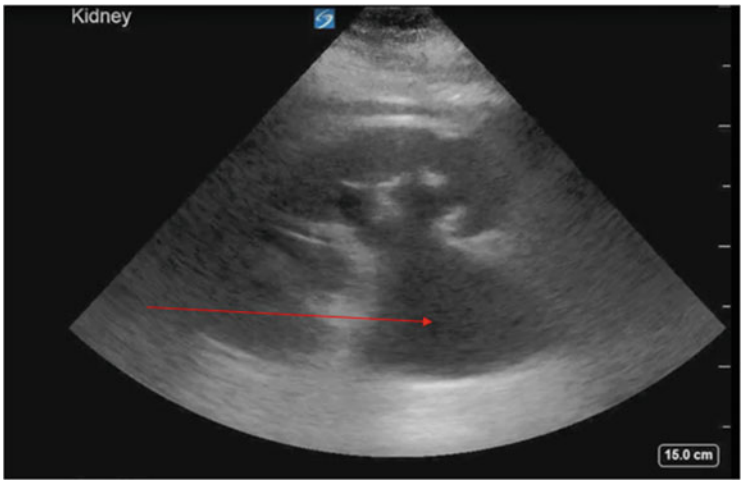

Fig. 7.17 In this kidney the hydronephrosis extends obviously out to the ureter (arrow), in what is called hydroureteronephrosis

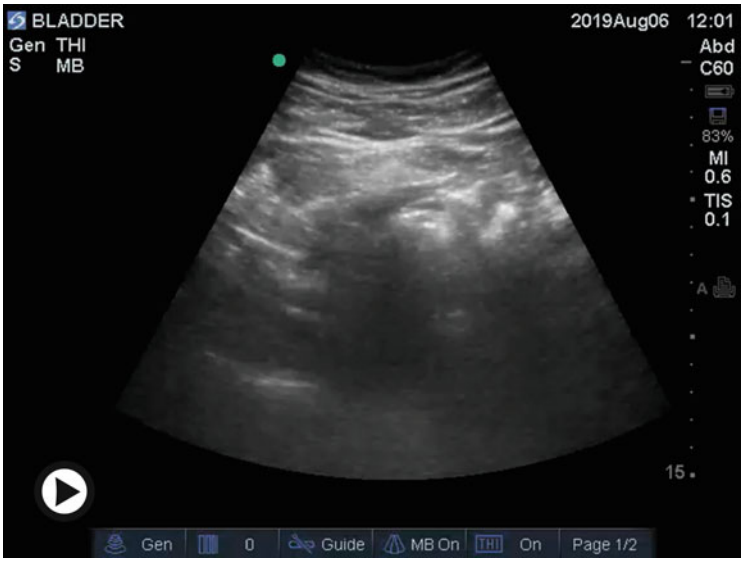

Fig. 7.18 (Video 7.6) This video demonstrates a cranial to caudal sweep through the anechoic bladder in a transverse plane (▶ https://doi.org/10.1007/000-7qe)

7.2.1.2 Bladder Assessment

The bladder varies greatly in appearance depending on the amount of urine it contains. A fully decompressed/empty bladder may be hard to visualize behind the

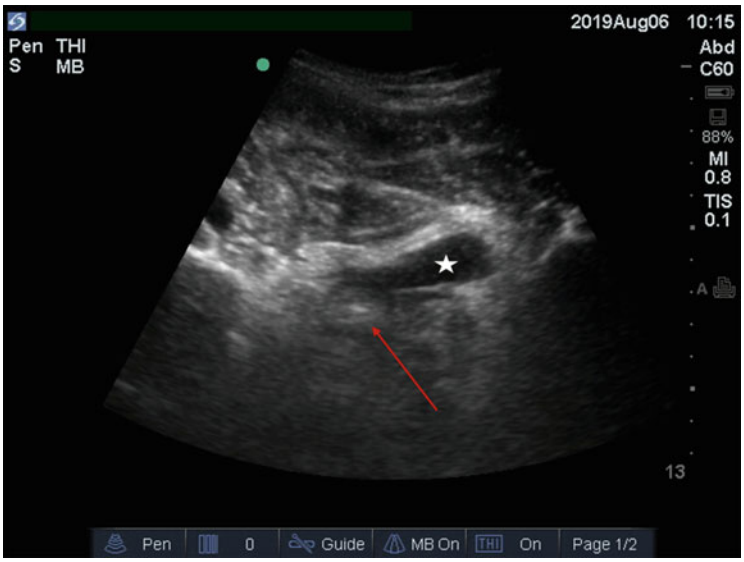

Fig. 7.19 Small, decompressed bladder (star) in transverse plane. The rectum can also be appreciated in this view (arrow)

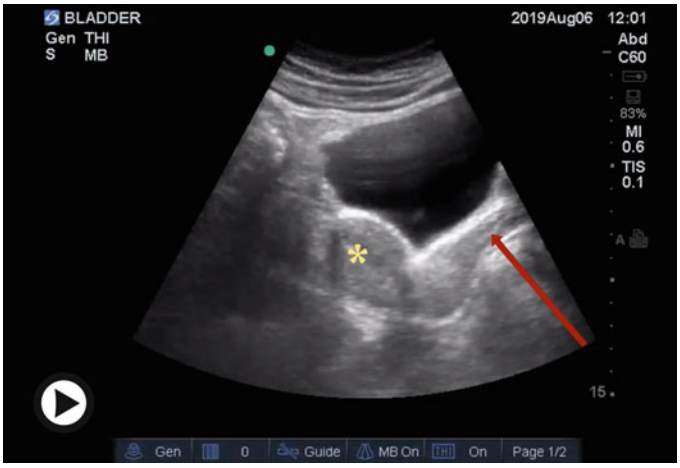

Fig. 7.20 (Video 7.7) In this video an anechoic female bladder is visualized in sagittal plane. Other pelvic organs can be seen, including the vaginal canal (arrow) and uterus (star) (▶ https://doi.org/10.1007/000-7qf)

symphysis pubis. As urine collects the bladder will distend more, increasing in sagittal length, and transverse height & width. The normal bladder contains anechoic urine, and appears almost rectangular in a transverse plane (Fig. 7.18), however when empty may appear more flattened (Fig. 7.19), and with distension may become

more rounded. In a sagittal plane the bladder is irregularly shaped, with a posterior segment that descends more posteriorly in the pelvis (Fig. 7.20).

Measurement of bladder volume is addressed in Exercise 1, and consists of taking diameter measurements in three planes, and multiplying by a correctional factor (Chan 1993). A post-void residual of >100 cc is considered acute urinary retention (Noble & Brown 2004), and volumes >200 cc may warrant catheterization. Other findings such as blood clots, an enlarged prostate, the balloon of a Foley catheter (used to drain urine from the bladder past an obstruction within the urethra such as an enlarged prostrate), bladder stones, and tumor may be seen on bladder ultrasound, but are beyond the scope of this chapter. If ureteral obstruction is suspected, Doppler can be used to assess for ureteral jets of urine emptying into the bladder (Fig. 7.10 and Table 7.1). If present, this rules out complete ureteral obstruction on the side of visualized jet(s).

7.3 Clinical Topic 2

7.3.1 Renal Injury

Renal injury is a state in which the kidneys are not functioning normally. The rate of filtration, otherwise known as glomerular filtration rate (GFR) decreases, which manifests as a rise in serum creatinine measured on basic bloodwork. This decrease in function can be accompanied by severe effects such as fluid retention with volume overload, electrolyte derangements (e.g. elevated potassium, phosphorus), and metabolic acidosis (Hilton 2006). The disease is typically stratified by chronicity, with injuries occurring over days to weeks classified as 'acute' (and potentially reversible) and processes extending past 3 months classified as 'chronic' (generally not reversible).

7.3.1.1 Acute Kidney Injury

Acute kidney injury (AKI) is a common problem that is associated with poor patient outcomes. AKI is frequently classified by the amount of urine output and the presumed location, or source of the kidney injury.

Descriptive terms regarding urine output include anuric (no or minimal urine produced per day), oliguric (less than two cups of urine produced per day), or non-oliguric (regular urine volume produced per day).

The type of injury can be subdivided into pre-renal (problem occurring before the kidney), intrarenal (problem occurring in the kidney parenchyma), or post-renal (problem occurring after the kidney). Pre-renal injuries stem from decreased blood flow to the kidney (e.g. low blood volume, low blood pressure due to infection, or heart failure). Intrarenal injuries involve direct damage to the glomerular filter tubules of the nephrons (e.g. inflammatory disorders or toxic insults like drugs or

products of cell breakdown). Post-renal injuries come from obstruction of the urinary collecting system that drains the kidneys through the ureters to the bladder and subsequently exiting through the urethra (e.g. kidney stones, an enlarged prostate, or cancer).

7.3.1.2 Chronic Kidney Disease

Chronic kidney disease (CKD) is classified as kidney damage that persists for 3 months or more (Singri et al. 2003). It is termed end-stage renal disease (ESRD) if the kidneys are not able to properly meet the body's needs. ESRD patients must receive renal replacement therapy, such as dialysis or a kidney transplant, to survive. CKD is most often caused by diabetes and hypertension, however there are numerous other causes that can lead to CKD.

7.3.2 Ultrasound Assessment in Renal Injury

Point-of-care ultrasound (POCUS) of the urinary system can be helpful in the differentiation of renal injury. Ultrasound is the most useful imaging study in the assessment of renal injury and can separate chronic kidney disease from potentially reversible acute kidney injury by assessing kidney size, echogenicity, and establishing the presence or abscence of hydronephrosis (KDIGO 2012). Furthermore, determination of renal injury etiology may be enhanced by assessment of intravascular volume assessment (e.g. how hydrated is the patient) to determine if low blood flow to the kidneys may be contributing. Both function of the heart and assessment of the lungs can be useful tools to assess hydration status as well. While POCUS should not replace formal sonography, bedside providers are able to replicate some findings that can enhance clinical decision-making at the bedside (Remer et al. 2014; Caronia et al. 2013).

7.3.2.1 Cortical Echogenicity

The renal parenchymal echogenicity increases when there is increased acoustic impedance of tissue, which is directly related to the density of the tissue. In CKD, normal renal parenchyma is replaced by denser fibrous tissue, which increases renal echogenicity (Faubel et al. 2014) (Fig. 7.21). Less commonly, some acute renal disease may cause increased cortical echogenicity, for example inflammatory disease and urinary obstruction. Therefore, echogenicity should be used in combination with kidney size and clinical factors (e.g. evidence of chronicity on laboratory testing) in the assessment for chronic kidney disease.

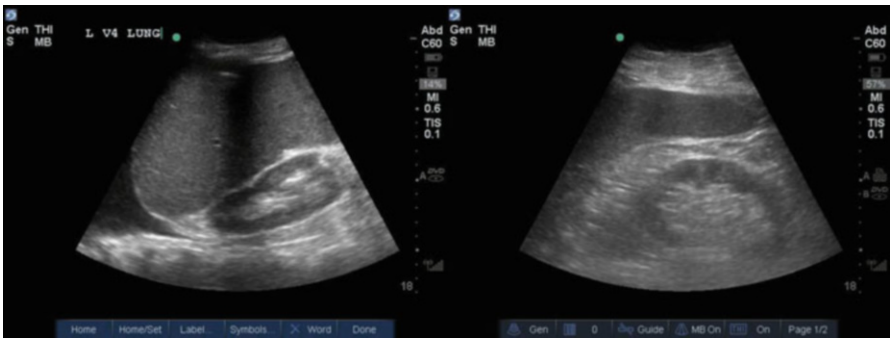

Fig. 7.21 The kidney can be compared to the adjacent solid organ (either spleen or liver) to evaluate echogenicity. Normally, the kidney cortex is hypoechoic relative to the adjacent organ (left). Increased relative echogenicity (seen on right) of the kidney can suggest chronic kidney disease. It is also important to note that in cases where the liver or spleen has increased echogenicity (from scarring or fat deposits), this rule may be invalidated (Faubel et al. 2014)

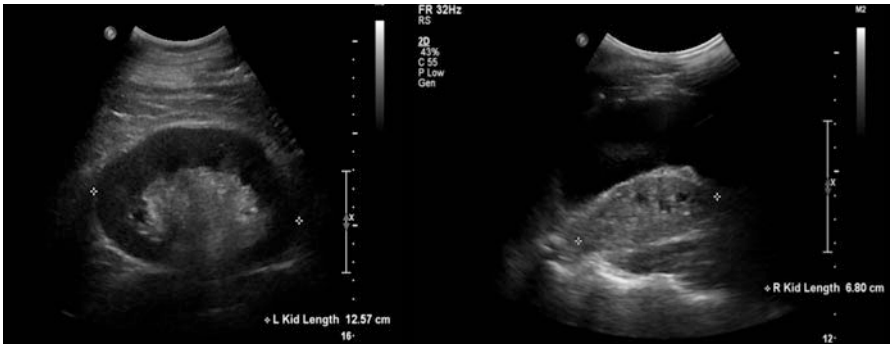

Fig. 7.22 Kidney length is measured in long axis, find the greatest possible length. A normal kidney (left) is contrasted with a small, echogenic kidney (right) suggestive of chronic kidney disease

7.3.2.2 Kidney Size

While renal volume (Volume = Length × Width_1 × Width_2, width is measured in the short-axis view) is the best measure of renal mass as it correlates with GFR, kidney length is a suitable surrogate and is more easily measured (O'Neill 2000) (Fig. 7.22). Kidney length varies with body height and is decreased in children who experience progressive renal growth until roughly 18 years of age. In kidney disease, there may be specific changes affecting the nephron, interstitial tissue, or the vasculature that reflect different disease processes. However, most sustained injuries resulting in CKD lead eventually to the shrunken and atrophied kidneys seen on ultrasound in advanced cases. Renal biopsies in these cases show glomerular scarring, atrophy of the tubules, and interstitial fibrosis (Hricak et al. 1982). Thus,

kidneys that are smaller than the average 9–12 cm length are suggestive of persistently decreased GFR and CKD. Certain pathologies can lead to enlarged kidneys due to either cystic growths or infiltration or swelling of the kidney parenchyma. Pregnancy is another condition where kidneys enlarge from increased interstitial volume and vascularity, and subsequently return to their normal size by 12 weeks postpartum (Cietak & Newton 1985; Cheung & Lafayette 2013). Finally, when there are differences in the size between kidneys by roughly 2 cm, one should consider vascular abnormalities that may cause differences in blood flow to one of the kidneys, such as renal artery stenosis.

7.3.2.3 Volume Assessment

Inferior vena cava (IVC) assessment by POCUS may help the bedside clinician understand blood flow through the kidneys and identify pre-renal kidney injuries (Fig. 7.23). As a reminder, pre-renal injuries stem from decreased perfusion, or blood flow. For the IVC, clinicians are interested in the diameter and amount of collapse (Fig. 7.24). This is used to estimate the central venous pressure (CVP). The CVP is in turn used to estimate the intravascular volume status of the patient. If the IVC is flat or collapses completely, the CVP is felt to be low or <5 mm Hg, and in acute kidney injury this might argue for low blood volume causing a pre-renal or low perfusion state as the cause. If the IVC is dilated to >2.1 cm with <50% collapse, CVP is felt to be elevated. Low intravascular volume is not contributing to a pre-renal kidney injury. However, excessive volume, such as in heart failure, can

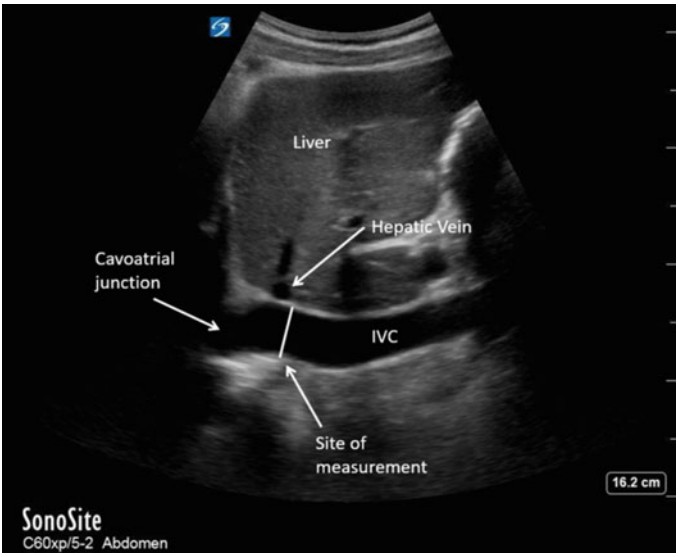

Fig. 7.23 IVC measurement occurs 1–2 cm from cavoatrial junction or immediately inferior to the hepatic vein

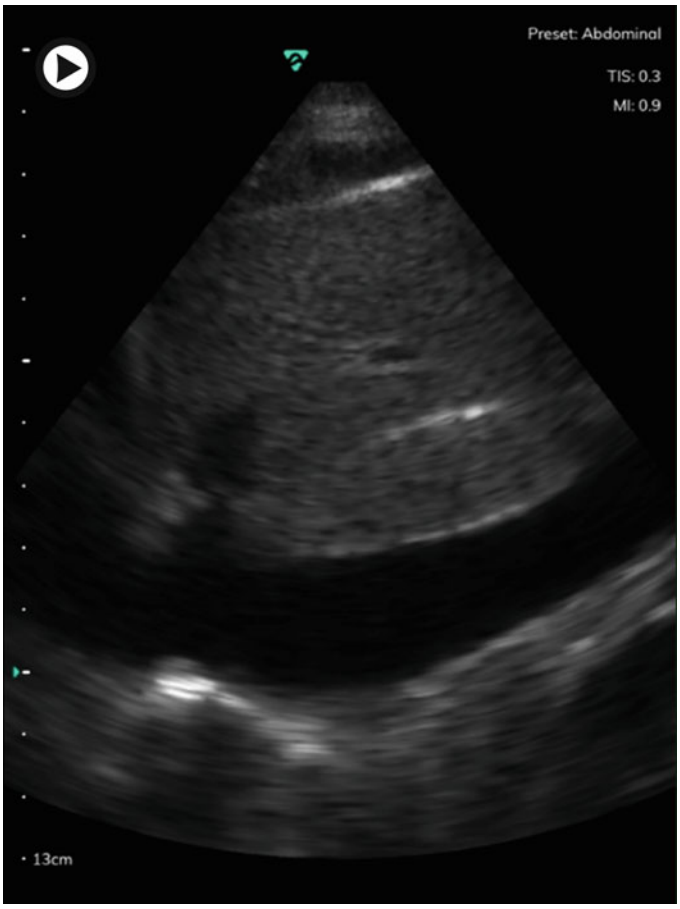

Fig. 7.24 (Video 7.8) This video demonstrates IVC variation with respiration (▶ https://doi.org/10.1007/000-7qg)

cause elevated CVP with renal venous congestion, which is another sort of pre-renal or low perfusion type of acute kidney injury. It should be noted that factors like patients breathing on their own or being ventilated with positive pressure (changes intrathoracic pressure and blood flow return to the heart), abdominal compression from adipose or fluid, or obstruction from clots or tumors might all affect assessment of CVP.

7.3.3 Laboratory Exercises

7.3.3.1 Exercise #1: Focused Kidney & Bladder Assessment

Learning Objectives

Learn to obtain short and long axis views of both kidneys, in addition to sagittal and transverse views of the bladder. Learn to measure kidney length, and calculate bladder volume.

Transducer/Probe

A typical low frequency phased array or curvilinear transducer is recommended for scanning the abdomen including the kidney and bladder. The recommended preset is the abdominal preset, or renal preset if available. A lower frequency probe is necessary given their deeper placement in the retroperitoneal space. If you utilize a phased array transducer, you will need to rock the beam cranially & caudally to interrogate the super & inferior poles of the kidney.

Additional Equipment and Supplies

None, other than those related to performing ultrasound.

Patient Position and Image Orientation

A supine patient position is most common for assessing kidneys and bladder. Select the abdominal preset, or if available, renal preset. In the abdominal preset the orientation marker will be on the top left side of the screen.

Performing the Scan

Assessment of the kidneys and bladder is useful in many scenarios including reduced kidney function detected on random laboratory testing, symptoms such as flank pain, bloody urine, reduced urine output, inability to urinate, discomfort with urination, and more.

1. Apply adequate gel to the probe, then place the probe in the mid-axillary line of the right or left side, with the probe marker directed towards the patient's head. The liver and spleen serve as acoustic windows for the right and left kidneys, respectively (Figs. 7.25 and 7.26).

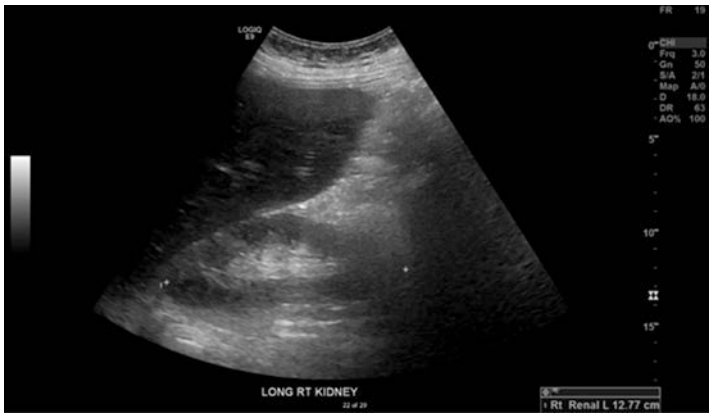

Fig. 7.25 Longitudinal view of the right kidney with the liver on the left (cranial) side of the image. The small crosshairs represent the calipers, and the length is displayed at the bottom right of the image

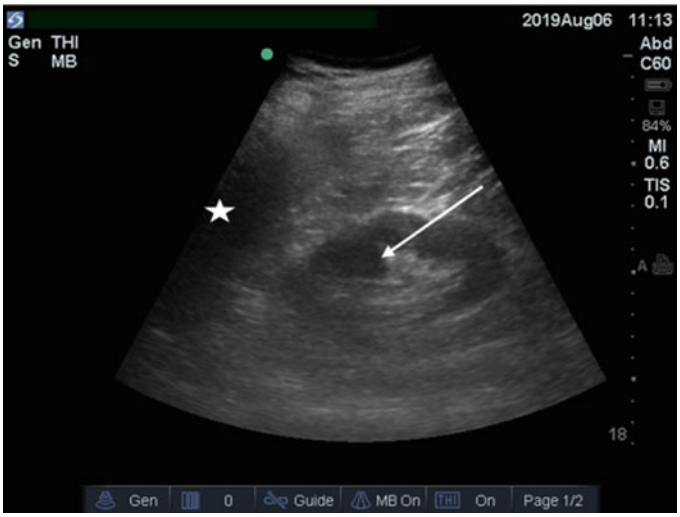

Fig. 7.26 Longitudinal view of the left kidney, with the spleen on the left (cranial) side of the image (star). There is an incidental finding of a cyst as well (arrow). This was a model with more soft tissue between the probe and organs, thus more acoustic attenuation and a less clear image

2. As the kidneys often lie obliquely, the best visualization for a complete longitudinal view (to measure kidney length for example) may be oblique and may require raising the ipsilateral arm above the head, or slight rotation of the probe marker posteriorly.
3. To assess for cortical echogenicity, an image of the left or right kidney should be obtained with the liver or spleen obtained in the same window and at the same focal depth.

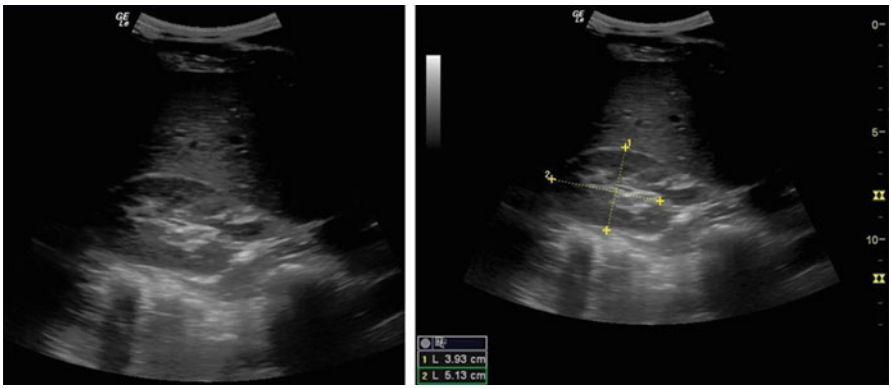

Fig. 7.27 Mid transverse views of the right kidney with the liver on the top of the image. The right image shows the measurement of anterior to posterior diameter and width

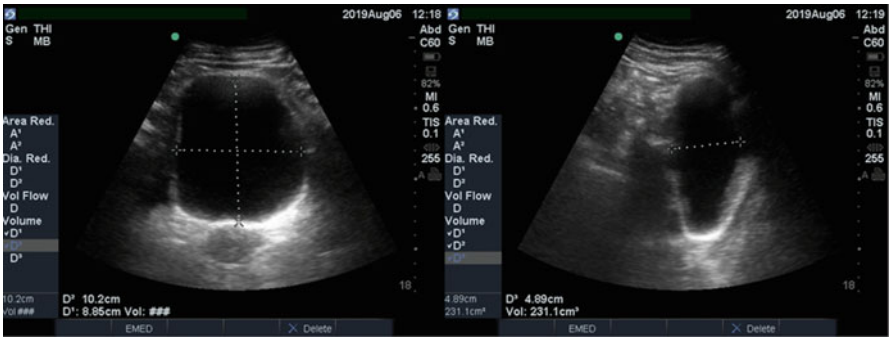

Fig. 7.28 Demonstration of the three planes in which diameter is measured to calculate bladder volume

4. Once the kidney and the liver or spleen are in the same window, renal cortical echogenicity should be carefully compared to the adjacent solid organ. Normal kidneys are isoechoic or hypoechoic in relationship to the liver and spleen.
5. Fan through to find the greatest length, and freeze. The image of the kidney should include both the upper and lower pole of the kidney, and a uniform rim of cortex all around. Failure to demonstrate these features may result in a shorter kidney length measurement, or missing other findings. Measure the maximal diameter of the kidney by placing calipers on the most cranial and most caudal aspect of the kidney.
6. After visualizing the longitudinal view of the kidney, rotating the transducer by 90° gives a transverse view of the kidney (Fig. 7.27). This view allows measurement of the kidney's anterior-posterior thickness and width.
7. To visualize the bladder, move caudally to just above the suprapubic symphysis in the midline, with the probe marker directed to the model's right. If the bladder is empty, it may be more challenging to visualize.

8. Scan the entire bladder by fanning the probe caudally into the pelvic cavity, and rocking side to side. Examine the bladder wall for any mass, thickening, or contained structures besides anechoic urine.
9. Once at widest region of the bladder freeze, and measure the maximal transverse diameter and anterior-posterior diameter.
10. Next unfreeze, rotate the probe marker 90 degrees towards the patient's head. Rock to center the bladder on the screen, and fan side to side until at the image with maximum superior to inferior height. At this point measure the greatest diameter from the superior wall to inferior wall (Fig. 7.28).
11. Calculate bladder volume = L × W × H × 0.75

7.3.3.2 Exercise #2: Inferior Vena Cava (IVC) Assessment

Learning Objectives

Learn to obtain a short and long axis views of the IVC. Learn to differentiate the IVC from the aorta, and to assess for collapse with respiration.

Transducer/Probe

A typical low frequency phased array or curvilinear transducer is recommended for IVC assessment. The recommended preset is the abdominal preset, since we will be scanning the upper abdomen to visualize the IVC.

Additional Equipment and Supplies

None, other than those related to performing ultrasound.

Patient Position and Image Orientation

A supine patient position is recommended. Select the abdominal preset, in which the orientation marker will be on the top left side of the screen. The cardiac exam type can be used if continuing from a cardiac exam, however the screen marker for orientation will be different from the abdominal exam type.

Performing the Scan

Determining the relative "size" of the inferior vena cava (IVC) in the abdomen provides information regarding the volume status of a patient. If the volume status is adequate, then blood volume returning to the heart is likely satisfactory. If the size is

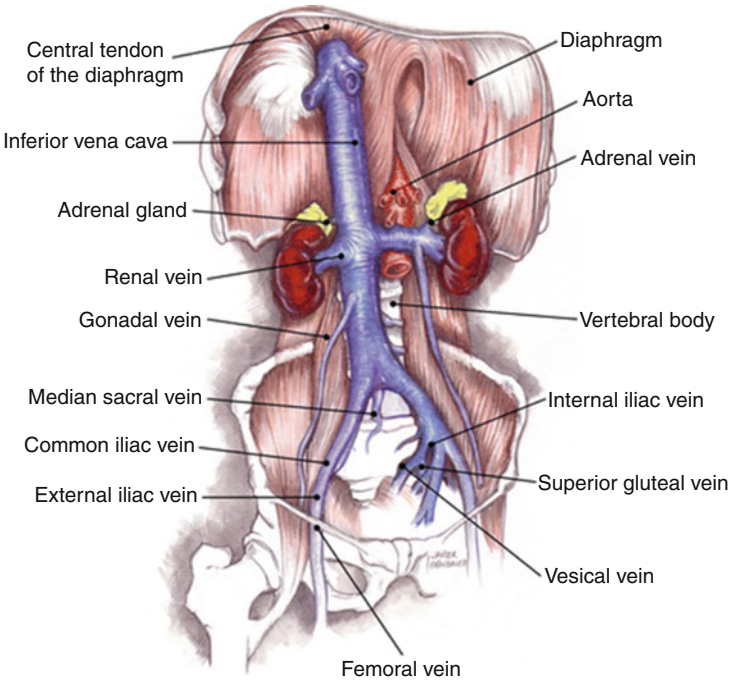

Fig. 7.29 This graphic shows the IVC, which returns blood to the right atrium after crossing the diaphragm. The IVC is just right to the midline and the abdominal aorta is towards the left of the midline

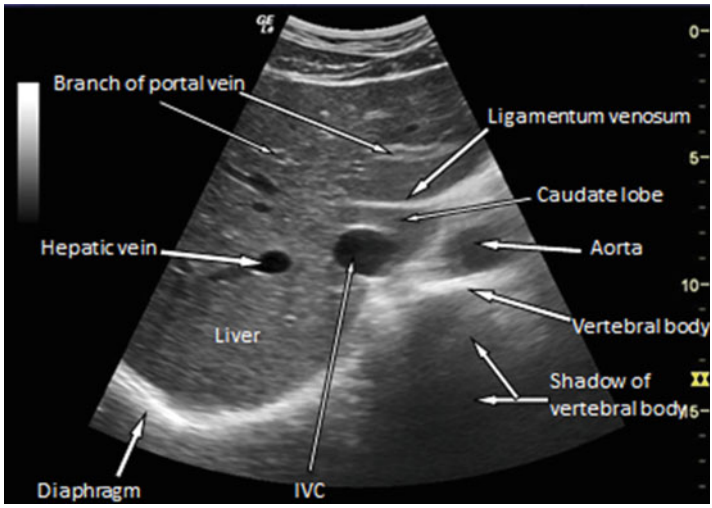

Fig. 7.30 A transverse view of the intrahepatic portion of the IVC. The intrahepatic segment of the IVC is observed to estimate volume status and approximate central venous pressure (CVP)

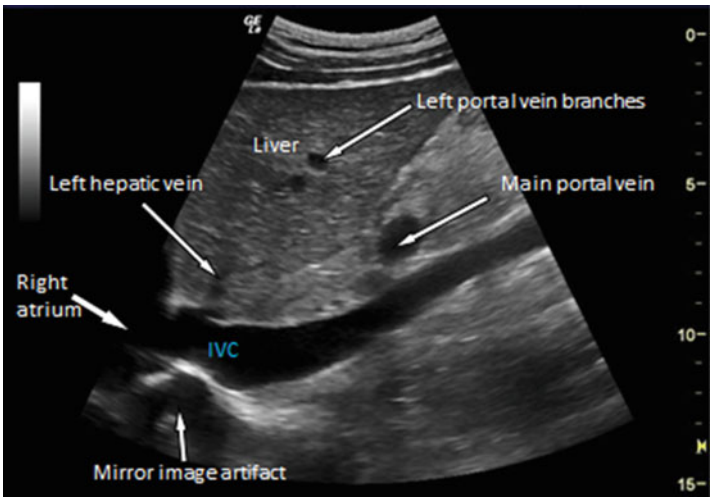

Fig. 7.31 A mid-longitudinal view of the IVC. Note that the IVC is draining straight into the right atrium. The IVC shows normal distension as would be expected in a patient with normal volume status and normal CVP (central venous pressure)

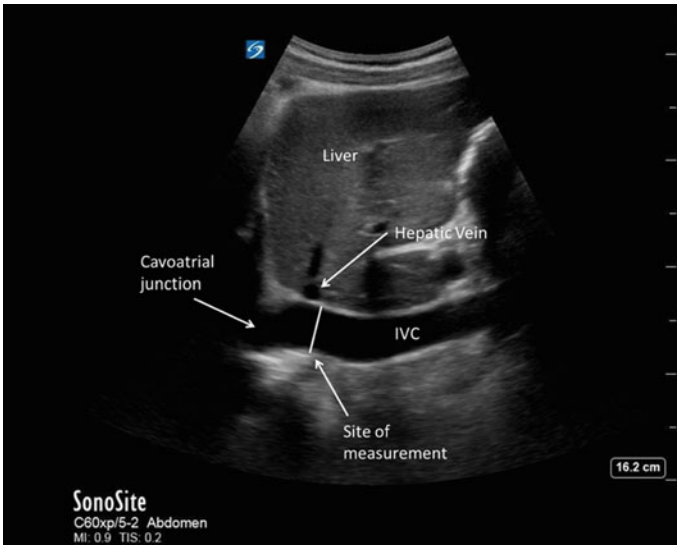

Fig. 7.32 A mid-longitudinal view of the IVC. Note the white bar indicating measurement of the IVC

diminished, then blood volume may be compromised. Figure 7.29 is a sketch illustrating the basic anatomy associated with this procedure.

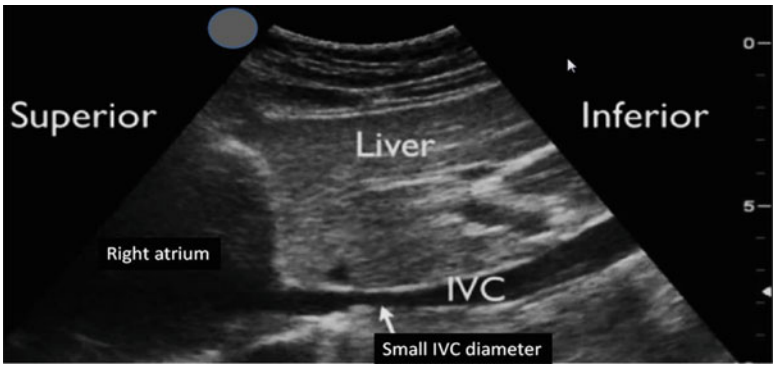

Fig. 7.33 Still image showing a small IVC diameter suggesting hypovolemia or low central venous pressure. See figure below showing a dilated IVC

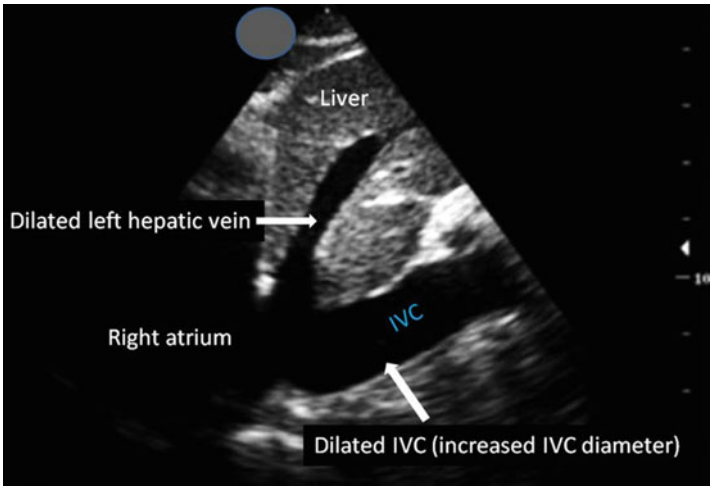

Fig. 7.34 A distended IVC in a patient with markedly elevated CVP. This is suggestive of hypervolemia and/or cardiac failure

1. Apply gel, and place the probe horizontally on the abdomen just below the diaphragm to obtain a transverse view of the intrahepatic IVC and aorta (Fig. 7.30).
2. Slide the probe side to side to position the IVC in the middle of the image and then rotate the probe 90 degrees clockwise (probe marker pointing toward the patient's head) in the sub-xiphoid region to obtain a mid-longitudinal view of the IVC as it connects to the right atrium (Fig. 7.31). Angulate the transducer slightly cephalad to include a segment of the right atrium.
3. Fan the probe to the patient's left to identify the aorta. Fan right and back left to differentiate the IVC and the aorta.

4. Fan back to the IVC. Observe the IVC diameter as it varies with respiration. Use the "Freeze" function of the ultrasound to record a cine of the IVC through the respiratory cycle.
5. Find a part of the cine when the IVC reaches its maximal diameter, then use the calipers function to measure the IVC along its short axis (as pictured in Fig. 7.32) just distal to the hepatic vein or 1–2 cm away from the cavoatrial junction. Record this number.
6. Find a part of the cine where IVC reaches its minimum diameter. Use calipers to measure this diameter.
7. Use the equation $[IVC_{D\ max} - IVC_{Dmin}/IVC_{Dmax}] \times 100\%$ to calculate respiratory collapse. Normal cutoffs for diameter are <2.1 cm and collapse $>50\%$ with respiration (Figs. 7.33 and 7.34).

References

Caronia J, Panagopoulos G, Devita M et al (2013) Focused renal sonography performed and interpreted by internal medicine residents. J Ultrasound Med 32(11):2007–2012. https://doi.org/10.7863/ultra.32.11.2007

Chan H (1993) Noninvasive bladder volume measurement. J Neurosci Nurs 25(5):309–312

Cheung KL, Lafayette RA (2013) Renal physiology of pregnancy. Adv Chronic Kidney Dis 20(3):209–214. https://doi.org/10.1053/j.ackd.2013.01.012

Cietak KA, Newton JR (1985) Serial quantitative maternal nephrosonography in pregnancy. Br J Radiol 58(689):405–413. https://doi.org/10.1259/0007-1285-58-689-405

Faubel S, Patel NU, Lockhart ME, Cadnapaphornchai MA (2014) Renal relevant radiology: use of ultrasonography in patients with AKI. Clin J Am Soc Nephrol 9(2):382–394. https://doi.org/10.2215/CJN.04840513

Hilton R (2006) Acute renal failure. BMJ 333(7572):786–790. https://doi.org/10.1136/BMJ.38975.657639.AE

Hricak H, Cruz C, Romanski R et al (1982) Renal parenchymal disease: sonographic-histologic correlation. Radiology 144(1):141–147. https://doi.org/10.1148/radiology.144.1.7089245

KDIGO (2012) Clinical practice guideline for the evaluation and management of chronic kidney disease. Kidney Int Suppl 3:1–150

Noble VE, Brown DFM (2004) Renal ultrasound. Emerg Med Clin North Am 22(3):641–659. https://doi.org/10.1016/j.emc.2004.04.014

O'Neill WC (2000) Sonographic evaluation of renal failure. Am J Kidney Dis 35(6):1021–1038. https://doi.org/10.1016/S0272-6386(00)70036-9

Podoll A, Walther C, Finkel K (2013) Clinical utility of gray scale renal ultrasound in acute kidney injury. BMC Nephrol 14(1):188. https://doi.org/10.1186/1471-2369-14-188

Remer EM, Papanicolaou N, Casalino DD et al (2014) ACR appropriateness criteria® on renal failure. Am J Med 127(11):1041–1048.e1. https://doi.org/10.1016/j.amjmed.2014.05.014

Singri N, Ahya SN, Levin ML (2003) Acute renal failure. JAMA 289(6):747–751

Zhu R, Xu Z, Qi Z et al (2018) How to diagnose renal artery stenosis correctly using ultrasound? Evaluation of results of renal arteries duplex ultrasonography examinations. Med Ultrason 20(3):298. https://doi.org/10.11152/mu-1341

Chapter 8
Ultrasound of the Musculoskeletal System

Robert M. DePhilip and David P. Bahner

8.1 Anatomy and Physiology of the Musculoskeletal System

Ultrasound imaging provides unique opportunities to study the physiology and pathology of the musculoskeletal (MSK) system. This chapter begins by describing the molecular and histological features that give bones, muscles, tendons, and ligaments their characteristic appearance, or echotexture, in ultrasound imaging. Examples of changes in normal echotexture that indicate pathology are then given. Next, dynamic imaging of structures of the MSK system is described as the capability to observe a body part as it is moved actively by the patient, or passively by the person performing the imaging. The chapter concludes with four laboratory exercises that are examples of how ultrasound imaging can be used to enhance the understanding of concepts underlying the normal physiology of the MSK system: (1) visualization and measurement of the pennation angle in a muscle before and after contraction; (2) demonstration of increased blood perfusion in a muscle after exercise; (3) operation of the calf venous pump; and (4) demonstration of differences in flow patterns in arteries before and after exercise. As the name indicates, the MSK system is composed of the bones and skeletal muscles of the body. It is beyond the scope of this book to name all the bones and skeletal muscles that exist in the human body. Instead, we will focus on the basic physiology of bones and skeletal muscle.

Supplementary Information The online version contains supplementary material available at https://doi.org/10.1007/978-1-0716-1863-9_8. The videos can be accessed by scanning the related images with the SN More Media App.

R. M. DePhilip (✉) · D. P. Bahner
The Ohio State University College of Medicine, Columbus, OH, USA
e-mail: Robert.DePhilip@osumc.edu; David.Bahner@osumc.edu

D. P. Bahner
The Ohio State University College of Medicine, Columbus, OH, USA

L. B. Wilson et al. (eds.), *Understanding Physiology with Ultrasound*, Physiology in Health and Disease, https://doi.org/10.1007/978-1-0716-1863-9_8

8.1.1 Skeleton

The skeleton of the human body is comprised of bones and there are 206 different ones. This skeleton supports the body and protects the internal organs. For example, the heart and lungs are protected by the rib cage and vertebral column. The brain is protected by the bones of the skull. Bones are hard, rigid structures consisting of a matrix. This matrix is primarily composed of hydroxyapatite (mineral form of calcium and phosphate complexed together) and proteins. Within the bone are cells called osteoblasts and osteoclasts. Although it is beyond the scope of this book, there is a complex interplay between these cells resulting in a constant remodeling of bone. In general, osteoblasts "build" and osteoclasts "breakdown" the bone matrix. Until late puberty, bone growth occurs in a linear (grow taller) pattern because specialized regions, called epiphyseal plates, have not closed. Once the plates close though, bones can only grow thicker. Checks and balances of the osteoblastic and osteoclastic activities prevent bones from becoming too thick once they complete their linear growth. However, certain pathologies can result in too much bone growth or too much bone breakdown. One such pathology is excess secretion of growth hormone. Growth hormone stimulates the release of insulin-like growth factor (IGF-1), which in turn causes excess bone growth. If this occurs before closure of the epiphyseal plates, giantism results. If on the other hand, excess growth hormone secretion occurs in an adult, thus after closure of the plates, then the bones grow thicker. Acromegaly is the term for this condition and is characterized by significant increases in the thickness of the skull, widening of the jaw, and longer and wider hands and feet.

On the other hand, conditions exist is which there is excessive bone breakdown. Osteopenia refers to loss of bone, while osteoporosis refers to significant loss of bone. After menopause, the loss of estrogen production puts women at risk for osteopenia and osteoporosis. Also, prolonged treatment with glucocorticoids can result in osteoporosis. In addition to providing structure, bones also produce cells of the blood. The flat bones of the body (specifically, the sternum and the flat parts of the hip bone) are the sites of blood cell formation and are the source of bone marrow transplants. Finally, the bones of the MSK system store minerals, one of the key ones being calcium.

8.1.2 Skeletal Muscle

The skeletal muscle of the body works in conjunction with the bones to provide support. In addition, skeletal muscle is responsible for moving our bodies. Skeletal muscle is also called striated muscle because it is made up of a repeating pattern of thick (myosin) and thin (actin) microfilaments that make up the myofibrils within

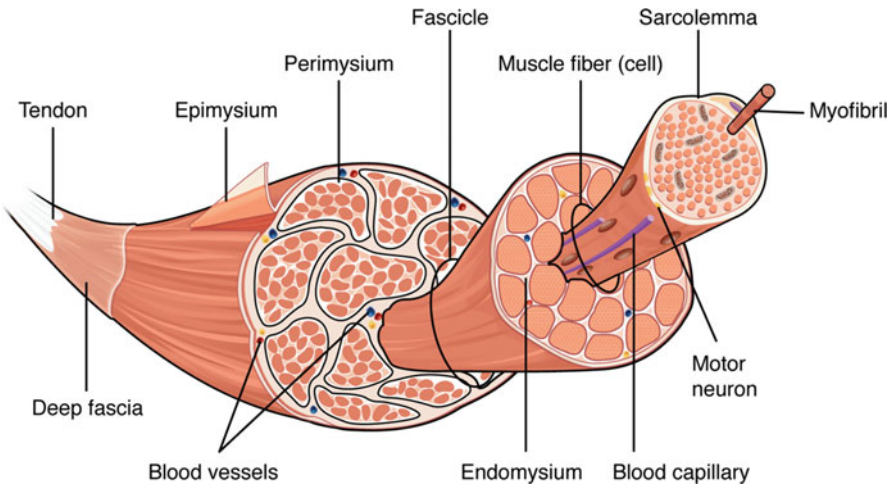

Fig. 8.1 Organization of muscle fibers into fascicles and fascicles into an anatomically-named muscle by layers of connective tissue. Image from: Anatomy & Physiology by Lindsay M. Biga, Sierra Dawson, Amy Harwell, Robin Hopkins, Joel Kaufmann, Mike LeMaster, Philip Matern, Katie Morrison-Graham, Devon Quick & Jon Runyeon and licensed under a Creative Commons Attribution-ShareAlike 4.0 International License, except where otherwise noted. Download for free at https://open.oregonstate.education/aandp

individual muscle cells and that gives skeletal muscle its characteristic striated appearance when viewed with a microscope.

Figure 8.1 highlights the macro–to–microanatomy of skeletal muscle and shows that an anatomically-named muscle, which is attached to bone by a tendon, is made up of a number of fascicles. In turn, fascicles are made up of a number of individual muscle fibers (which are also called muscle cells, or myocytes). Individual muscle fibers are made up of myofibrils. An anatomically-named muscle is wrapped in a connective tissue layer called epimysium. Each individual fascicle is wrapped in a layer of connective tissue called perimysium, and each individual muscle fiber (cell) is wrapped in endomysium. These investments of connective tissue give muscle its characteristic echotexture, as described below.

Figure 8.2 takes one muscle fiber from Fig. 8.1 and shows the molecular anatomy of myofibrils. Each myofibril is composed of regions called sarcomeres (Fig. 8.2). These sarcomeres are the functional unit of skeletal muscle. Within the sarcomeres are 4 key (two are indicated in Fig. 8.2) proteins that interact to cause contraction of skeletal muscle. We will briefly discuss the process of cross-bridge cycling, which is the term used to describe how skeletal muscle contracts.

Actin and myosin are two proteins with high affinity for one another, thus they bind. Myosin has an enzyme, myosin ATPase, that splits ATP (adenosine triphosphate) into ADP (adenosine diphosphate) and phosphate. This splitting of ATP converts the chemical energy associated with the molecule into a mechanical energy for the myosin protein. In other words, splitting ATP allows myosin to "pull" or

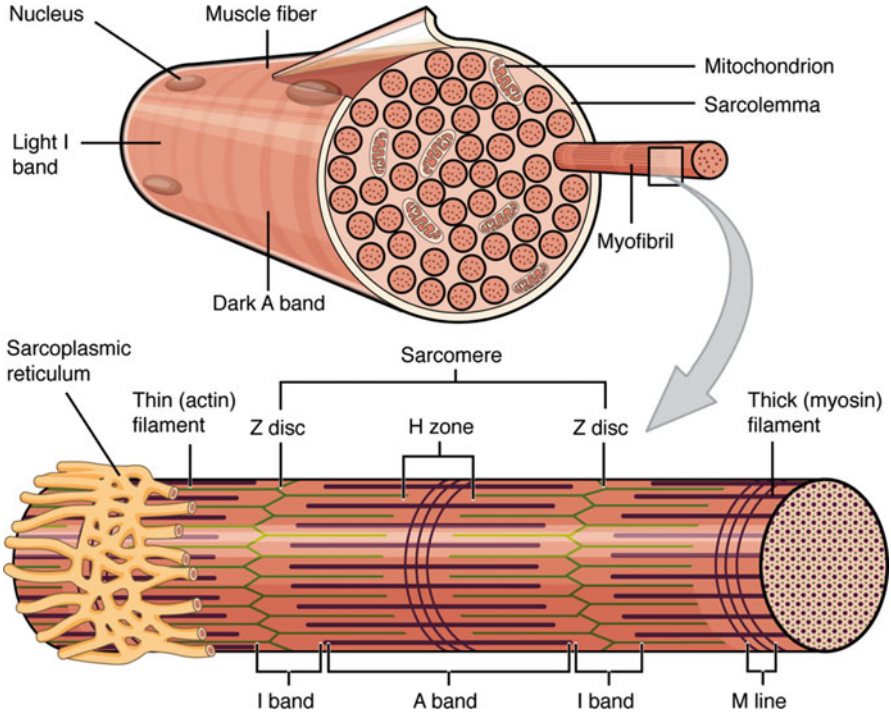

Fig. 8.2 Schematic showing the microanatomy of a single myofibril to illustrate the sarcomere, the functional unit of skeletal muscle. Note the two proteins, actin and myosin, that reside in the sarcomere. Two other proteins that are not pictured, but are functionally important are troponin and tropomyosin. These are discussed in the text. Image from: Anatomy & Physiology by Lindsay M. Biga, Sierra Dawson, Amy Harwell, Robin Hopkins, Joel Kaufmann, Mike LeMaster, Philip Matern, Katie Morrison-Graham, Devon Quick & Jon Runyeon and licensed under a Creative Commons Attribution-ShareAlike 4.0 International License, except where otherwise noted. Download for free at https://open.oregonstate.education/aandp

"move" the actin protein when they bind. This pulling of actin by myosin is called the power stroke and produces tension in the muscle. Depending upon the load on the muscle (imagine lifting a cup, the cup being the load), if the tension produced by the muscle is greater than the load, then the muscle shortens (you move the cup to your mouth to drink). This is called an isotonic (muscle shortens) contraction. If on the other hand, the load is too great for your muscle to move (imagine trying to lift a car), then this "pulling action" that occurs when actin and myosin bind produces a force, but the muscle doesn't shorten. This is called an isometric contraction. The maximal force generated by a muscle occurs when it is contracting isometrically.

The ATP described in the preceding paragraph provides the energy for myosin to pull on actin, but it also plays another crucial role. In general, ATP is plentiful in the cell. ATP (different molecule from the one the myosin splits) causes actin and myosin to dissociate. The myosin ATPase then splits this ATP, and with this energy, it binds and pulls actin again. Another ATP dissociates actin and myosin, the myosin ATPase splits, myosin pulls actin, and the process repeats. This is cross-bridge

cycling and it is how skeletal muscle generates force and can shorten if the load it is working against is not too great. When a person dies, ATP in the cell is depleted. Because there is no ATP in the cell to dissociate actin and myosin, their binding results in muscle stiffness called rigor mortis.

The other two important proteins in the sarcomere are troponin and tropomyosin. In short, these are regulatory proteins that prevent or block the binding of actin and myosin. Troponin has a calcium binding site and thus is influenced by the amount of calcium in the cytosol of the cell. In the uncontracted state, cytosolic calcium is very low and the cross-bridge cycling does not occur because troponin and tropomyosin prevent or block myosin from binding to actin. However, when cytosolic calcium rises, it binds to troponin, causing the troponin and tropomyosin proteins to move away from the binding site on actin for myosin. Thus, a high cytosolic calcium, with its subsequent binding to troponin, results in cross-bridge cycling and the consequent contraction of the muscle. The details regulating cytosolic calcium are beyond the scope of this book, but the rise occurs in response to an action potential in the neuron innervating the muscle.

8.2 US Imaging of the MSK

Ultrasound is a high-resolution modality for imaging the MSK system that is convenient, economical, and avoids ionizing radiation. Ultrasound imaging of the MSK system follows all the principles of echo generation by tissues in other body systems and uses the same conventions for correlating transducer position with orientation of the image on the screen that are basic to imaging elsewhere in the body.

There are unique features of MSK ultrasound imaging that are due to the physical properties and tissue structure of muscle, tendon, and bone. Interpretation of MSK ultrasound images depends on recognizing the normal echotexture of these tissues, so that changes from normal can be identified as injury or disease. In certain instances, the resolution of ultrasound imaging of the MSK system rivals that of more expensive and less accessible modalities, such as magnetic resonance imaging (MRI). However, ultrasound stands alone in its ability to perform dynamic imaging—imaging of a muscle or its tendon as a patient actively moves a body part, or has a body part moved passively by the examiner.

There are also technical aspects of MSK ultrasound imaging that make it different than ultrasound imaging of other body systems. Because most of the structures being imaged are relatively close to the body surface, usually within a depth of 5 cm, a high-resolution, linear transducer is used most often. Images, thus, have very good resolution, but limited depth. Bones, which are usually avoided in imaging of other body systems because they cast a posterior shadow, are an important part of MSK imaging, and one learns to gain useful information from the surface of bones that

serve as landmarks to surrounding structures. Finally, ultrasound imaging of the MSK system is subject to an artifact called **anisotropy** that is described below.

The most easily recognized parts of the MSK system are the bones of the skeleton and the skeletal muscles that move these bones. However, the bones and muscles are supported by various connective tissues—ligaments that connect bone to bone, tendons that connect muscle to bone, cartilages between bones, and fascia that forms muscle compartments—and all these connective tissues are important parts of the MSK system. Finally, the nerves that control muscle movement and signal position and pain, and the arteries and veins that circulate blood to bones, muscles, and connective tissues must be included in the MSK system.

This next portion of this chapter begins with a description of the echotexture of tissues in the MSK system and then describes dynamic imaging, using examination of the shoulder joint as an example. Examples of clinical uses of ultrasound imaging are then given, followed by examples of laboratory exercises using ultrasound imaging to demonstrate concepts of MSK physiology.

8.2.1 Echotexture of the Tissues in the MSK System

8.2.1.1 Skeletal Muscle

Muscle fibers have high water content and by themselves are hypoechoic and appear dark or black. The key to recognizing the echotexture of skeletal muscle in ultrasound images is to understand that muscle echogenicity is derived from the layers of connective tissue that organize muscle. Individual muscle fibers are wrapped in a layer of connective tissue called endomysium (Fig. 8.1). Many muscle fibers are grouped together in fascicles and these fascicles are wrapped in a layer of connective tissue called perimysium. It is this perimysial layer of connective tissue that has sufficient structure to produce an echo. For this reason, descriptions of muscle in ultrasound involve descriptions of its muscle fascicles. Finally, fascicles are grouped together and wrapped in epimysium to form the anatomically-named muscles.

The perimysial layers are aligned with the long axis of the muscle fascicles so that the echoes produced by the perimysial layers provide an orientation to the muscle itself. When the long axis of the transducer is aligned with the long axis of a muscle, it is also aligned with the perimysial layers, which give a linear pattern of echoes in the image (Fig. 8.3a). When the transducer is rotated 90 degrees, so that the beam images a cross-section of the muscle and its fascicles, the perimysial reflections appear as echogenic dots (Fig. 8.3b). When the long axis of the transducer is in an oblique position—between its long and trans positions—the perimysial reflections are short lines (Fig. 8.3c). It is important to begin scanning with an understanding of the orientation of fascicles in the muscles to be examined and anticipate the orientation of fascicular echoes.

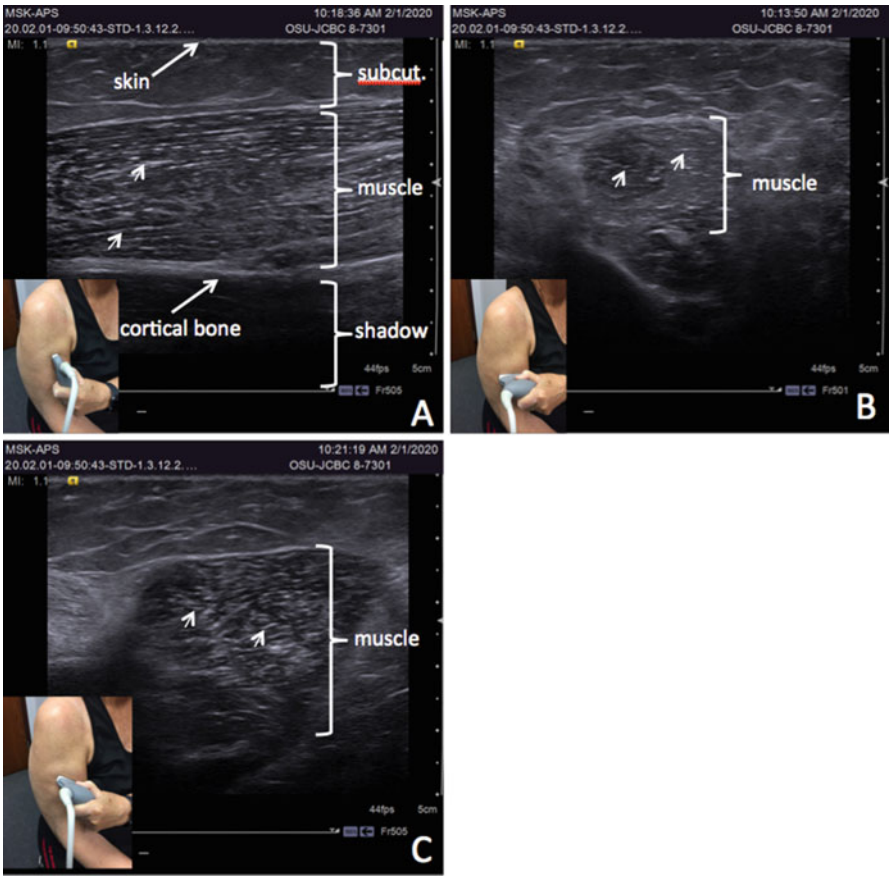

Fig. 8.3 Changing pattern of perimysial echoes in longitudinal (**a**), transverse (**b**), and (**c**) oblique views of the biceps brachii muscle. In **a**, the long axis of the transducer is aligned with the long axes of the muscle fascicles and the perimysial reflections are seen as long echogenic lines (examples at short arrows). In **b**, the long axis of the transducer is at 90 degrees to the long axes of the muscle fascicles and many of the perimysial reflections appear as faint dots (examples at short arrows). In **c**, the long axis of the transducer is oblique to the long axis of the muscle and the perimysial reflections appear as short lines (examples at short arrows), intermediate between the long lines seen in **a** and the dots seen in **b**. In **a**, reflections corresponding to the surface of the skin and the cortical surface of the humerus are indicated, as are the subcutaneous tissue, the biceps brachii muscle, and the acoustic shadow deep to the cortex of the humerus. Only the muscle is indicated in (**b**, **c**). The insets in the lower left of (**a**–**c**) show the transducer orientations used to acquire each ultrasound image

8.2.1.2 Tendons and Ligaments

Tendons and ligaments are both made up of collagen fibers, and the more ordered and linear these fibers are arranged, the greater the reflection of the ultrasound beam

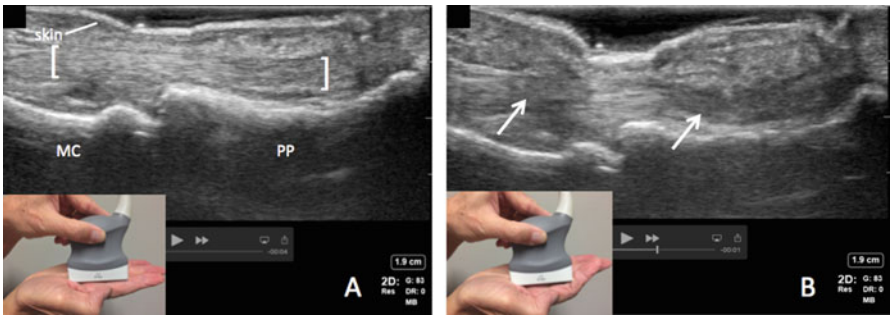

Fig. 8.4 Demonstration of anisotropy in the long flexor tendons of a digit of the hand. In the fully extended digit (**a**), maximal reflection of the flexor tendon is seen because the ultrasound beam strikes the tendon at near 90 degrees. In a slightly flexed digit (**b**), the beam strikes parts of the tendon at less than 90 degrees, producing areas of anisotropy (arrows). The skin is in the near field. The tendon is shown between the brackets in (**a**). MC, metacarpal bone; PP, proximal phalanx. Note the shadows in the far field due to the bones. The insets show the transducer positioned over the metacarpophalangeal joint

to produce an echo. In general, the ordered structure of fibers in tendons is greater than the ordered structure of fibers in ligaments, making tendons more echogenic than ligaments.

Tendons can have a round, flattened, or sheet-like form. The tendon of the long head of the biceps brachii muscle and the tendon of the semitendinosus muscle are round and cord-like. The tendons of the long flexor tendons of the wrist and digits are flattened and have an oval profile in cross-section. Sheet-like tendons form the attachment of the flat abdominal muscles to bone.

Ligaments are fibrous tissues that connect bone to bone. In general, ligaments get their strength from the amount of collagen fibers and from the linear arrangement of these collagen fibers. The more collagen fibers and the more aligned these fibers are, the stronger the ligament will be. Ligaments can be relatively discrete structures, such as the anterior and posterior cruciate ligaments of the knee, but often, named ligaments are simply thickenings of the fibrous joint capsule, as is the medial collateral ligament of the knee. Joint capsules have a rich supply of proprioceptive and pain fibers that provide positional sense and awareness of pain.

MSK ultrasound imaging is subject to a unique artifact called **anisotropy**, defined as angle-dependent echogenicity. In other words, the strength of the echo produced by a structure, particularly a tendon, is dependent on the angle that the ultrasound beam strikes the structure (angle of insonation). Figure 8.4 shows an example of anisotropy. When the ultrasound beam strikes the long flexor tendons of the digits of the hand at 90 degrees, the tendons produce a continuous, strong reflection. If the digit is flexed slightly, so that the ultrasound beam strikes parts of the tendon at an angle that is several degrees less than 90, the echo is much weaker, and areas of hypogenicity appear in the tendon. A tear or rupture in a tendon is also hypoechoic, and operators must manipulate the transducer and interrogate any hypoechoic area in

a tendon thoroughly to determine whether it is a true defect or whether it is an anisotropic artifact.

8.2.1.3 Bone and Cartilage

There are two types of bone in the adult human skeleton: compact bone and spongy bone. Compact bone is dense and made up of layers of organic material and inorganic salts with little space between the layers. Compact bone is often called cortical bone because it is found on the outermost part of the bone. (Cortical bone is the outermost part of a bone in the same way as the cortex of the kidney is the outermost part of that organ.) Spongy bone has relatively large spaces between its bony components. The bony components are called trabeculae and the spaces between trabeculae are filled with bone marrow, or often later in life, with fat. Spongy bone is also called cancellous bone and is found at the ends of long bones and between two layers of compact bone, as in the flat bones of the skull bones, sternum, and flat portions of the hip bones. Blood cell formation occurs in the spongy bone of flat bones, making spongy bone the source of cells for bone marrow transplants.

Bone has such a large acoustic impedance mismatch with adjacent muscles, tendons, and ligaments that only the cortical surface of bones can be visualized with ultrasound, and this cortical surface is seen a strong reflection. Posterior to the strong reflection from the surface of the bone is always a shadow.

Cartilage contains the same organic and inorganic components that are found in bone, but in different proportions and in different structural arrangements and, thus, its echogenic appearance is different. The organic part of cartilage contains more protein, specifically, proteoglycans, that hold water. The high water content of cartilage gives it an anechoic (black) appearance in ultrasound images. The inorganic part of cartilage contains less calcium and phosphate. The result being that cartilage is strong and resilient, like bone, but not brittle. There are three types of cartilage: hyaline cartilage, fibrocartilage, and elastic cartilage. Hyaline cartilage is found on the articulating surfaces of bones (the surfaces of bones that touch each other at a joint). Hyaline cartilage is also found at the growth plate of long bones and at the junction of the first rib and the sternum. Fibrocartilage contains more collagen fibers than hyaline cartilage and gives fibrocartilage a bit more flexibility than hyaline cartilage. Fibrocartilage is found in the symphysis pubis and in the intervertebral disks. Elastic cartilage contains an abundance of elastic fibers, giving elastic cartilage even more flexibility than fibrocartilage. Elastic cartilage is found in the outer ear, in the nasal cartilages, and in the epiglottis.

8.2.1.4 Joints, Joint Capsules, and Bursae

Movement of the bones occurs where one bone is connected to another at a joint, or articulation. There are three types of joints in the body: synovial joints that allow a high degree of freedom of movement, fibrous joints that allow a very limited amount of movement, and cartilaginous joints that allow no movement at all. Most of the focus in the MSK system is on movements that occur at synovial joints and it is important to know the parts of a synovial joint because each component can be imaged with ultrasound and each is the site of unique pathology (Fig. 8.5). A synovial joint has a fibrous joint capsule that encloses the joint and attaches one bone to another. The fibrous joint capsule is lined by a synovial membrane that produces synovial fluid that lubricates the joint. The ends of the bones in the joint are

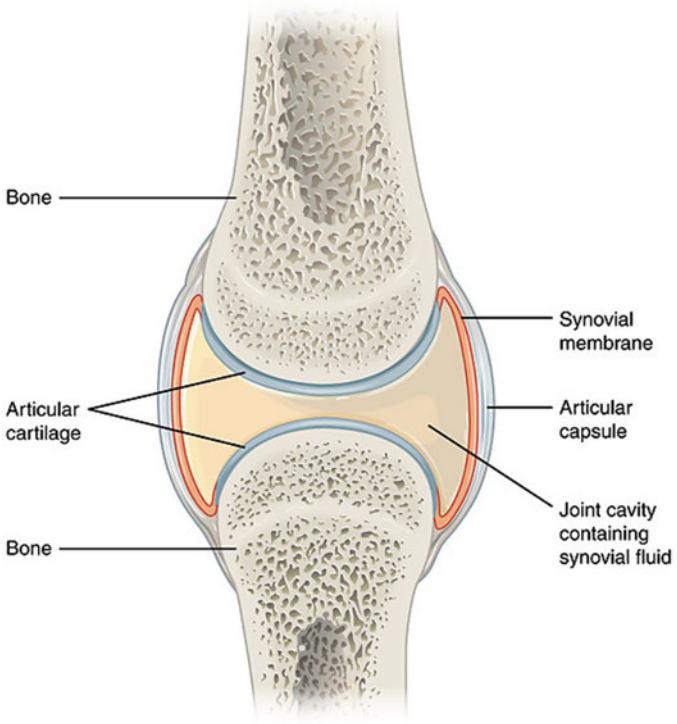

Fig. 8.5 The parts of a synovial joint have different echogenicity in ultrasound images. Bone, specially the surface of bone, is highly echogenic and has a posterior shadow. The articular cartilage, made up of hyaline cartilage, is anechoic. The articular (fibrous) capsule is relatively echogenic. The joint cavity (here, greatly exaggerated in size) usually contains a very small amount of synovial fluid for lubrication, which is anechoic. Image from: Anatomy & Physiology by Lindsay M. Biga, Sierra Dawson, Amy Harwell, Robin Hopkins, Joel Kaufmann, Mike LeMaster, Philip Matern, Katie Morrison-Graham, Devon Quick & Jon Runyeon and licensed under a Creative Commons Attribution-ShareAlike 4.0 International License, except where otherwise noted. Download for free at https://open.oregonstate.education/aandp

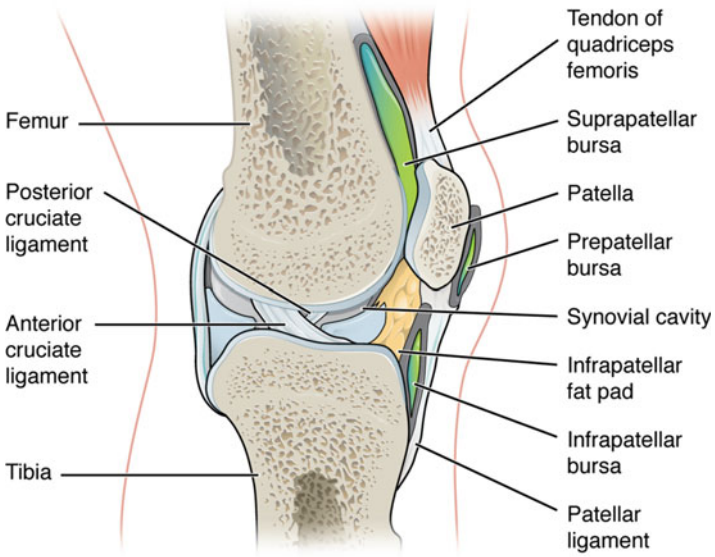

Fig. 8.6 Bursae associated with the knee joint. The suprapatellar bursa is between the tendon of quadriceps femoris and the femur. The infrapatellar bursa is between the patellar ligament and the tibia. The prepatellar bursa is between the skin and the patella. Bursae reduce the friction between structures rubbing against each other. Image from: Anatomy & Physiology by Lindsay M. Biga, Sierra Dawson, Amy Harwell, Robin Hopkins, Joel Kaufmann, Mike LeMaster, Philip Matern, Katie Morrison-Graham, Devon Quick & Jon Runyeon and licensed under a Creative Commons Attribution-ShareAlike 4.0 International License, except where otherwise noted. Download for free at https://open.oregonstate.education/aandp

lined with hyaline cartilage that provides a smooth gliding surface for one bone to move on another and that prevents erosion of the bony surface.

A bursa (pl., bursae) is a closed sac of synovial membrane that reduces the friction as one structure moves over another. There often is a bursa between a tendon and the bone it passes over, as there is between the quadriceps tendon and the distal end of the femur (Fig. 8.6). Bursae are also found between the skin and the bone deep to the skin. Bursae are important structures to recognize because they can become inflamed and painful and irritated with repeated muscle and tendon movement. When bursae become inflamed, they can accumulate large amounts of fluid, echogenically dark, within them that is produced by the synovial membrane.

Two other features of muscle structure of interest: the attachment of muscle fibers to tendons, the myotendinous junction, and the attachment of tendon to bone, because both are susceptible to injury when an unusual force is applied to them. Both of these sites can be imaged with ultrasound.

8.2.2 Dynamic Imaging

Simply stated, dynamic imaging is visualization of anatomical structures as they are moving. Movement is accomplished by the patient actively moving a body part, or the examiner moving the part passively for them. In either case, the patient can report on discomfort or pain elicited by the movement, and the structures associated with the pain can be identified and investigated further. Pain may be associated with a tendon passing through a narrow region between two bones (an impingement syndrome), or a nerve passing through a similarly constricted area between muscles or created by bones (a compression neuropathy).

The rotator cuff of the glenohumeral (shoulder) joint consists of the tendons of four muscles (subscapularis, supraspinatus, infraspinatus and teres minor) that have their proximal attachments on the scapula and their distal attachments on the humerus. As the tendons of these muscles cross the shoulder joint, they reinforce the thin, fibrous capsule of the joint. Because of the extensive mobility of the shoulder joint, the rotator cuff is often injured and dynamic imaging with ultrasound can be used to diagnosis the source of pain.

Dynamic imaging of the rotator cuff follows a protocol of specific limb positions and movements (Jacobson 2011). Figure 8.7 shows one part of the full protocol, a transverse view of the anterior humeral head. Imaging begins with the limb in a "neutral" position (hand on the ipsilateral knee in a relaxed position with palm up in supination). The probe is placed in a transverse position with the probe marker facing laterally. The tendon of the long head of the biceps brachii muscle is seen between the greater and lesser tuberosities of humeral head. The humeral head continues to be imaged as the patient rotates the humerus externally (laterally), and in the end position, the greater tuberosity has rotated out of view, while the tendon of the subscapularis muscle has been drawn into view.

This simple maneuver provides information about (1) the stability of the tendon of the long head of the biceps brachii muscle in the bicipital groove, (2) the attachment of the tendon of the subscapularis muscle to the lesser tuberosity, and (3) the smooth movement of the head of the humerus against the undersurface of the deltoid muscle that is due to the functioning of the subdeltoid bursa. Pain elicited at any point during the maneuver can be correlated with specific structures that can then be investigated more closely.

8.2.3 Examples of Clinical Applications of MSK Ultrasound Imaging

The number of clinical applications of ultrasound imaging continues to grow (Forney and Delzell 2018). Figure 8.9 shows the identification of tears in the Achilles tendon. In this example, tears appear as hypoechoic regions that are filled with clotted blood. Any hypoechoic region of a tendon must be investigated with

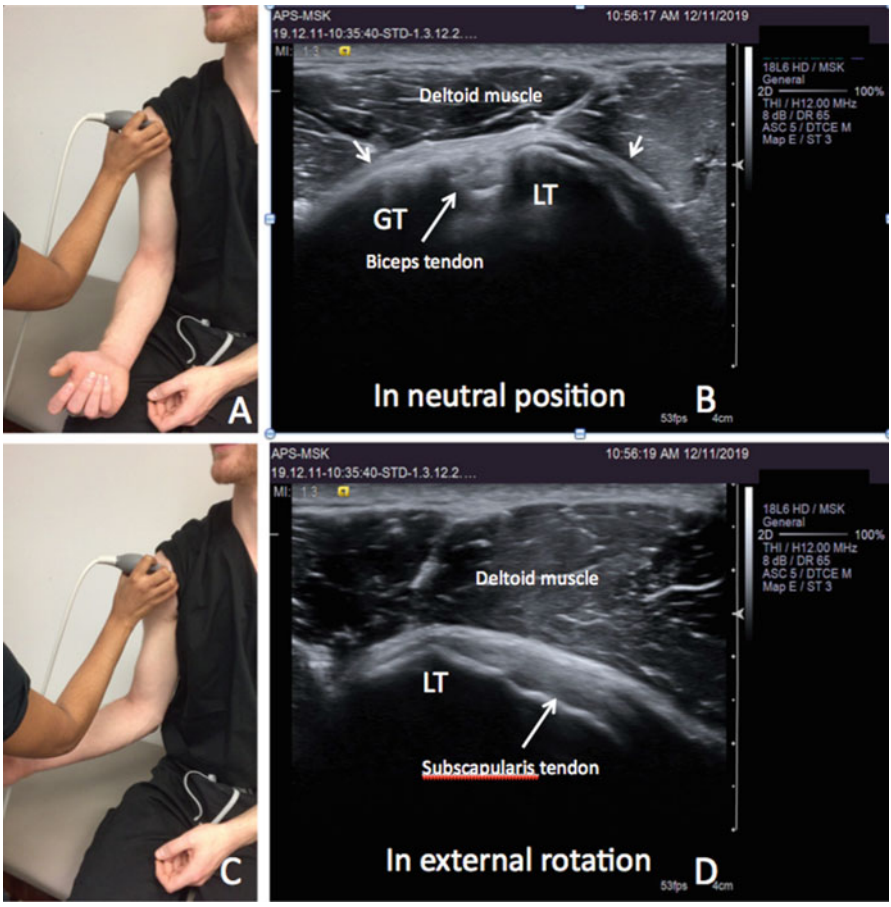

Fig. 8.7 Position of the upper limb and corresponding images of the humeral head acquired with ultrasound. In (**a**) the upper limb is in a "neutral" position and the transducer is in a transverse position over the proximal humeral head with probe marker pointing laterally. Panel (**b**) shows the corresponding ultrasound image with the biceps tendon in the bicipital groove, deep to the deltoid muscle and between the greater tuberosity (GT) and the lesser tuberosity (LT). The position of the subdeltoid bursa is indicated by two unlabeled arrows in **b**. The bursa lies between the deltoid muscle and the head of the humerus and is only seen in pathological conditions when the bursa is filled with large amounts of synovial fluid that is anechoic. In (**c**) the humerus has rotated externally (laterally) and the corresponding ultrasound image (**d**) shows that the greater tuberosity has rotated laterally out of view and the lesser tuberosity has rotated from medial to lateral, drawing the tendon of the subscapularis muscle into view. Panels **b** and **d** are still images taken from the video clip in Fig. 8.8

multiple angles of insonation, to rule out an anisotropy artifact. Figure 8.10 shows a rupture in the attachment of the distal end of the biceps brachii muscle to the radius. Here the tendon has retracted into the arm due to the contraction of the muscle, and the space normally occupied by the tendon is filled with a blood clot. Figure 8.11

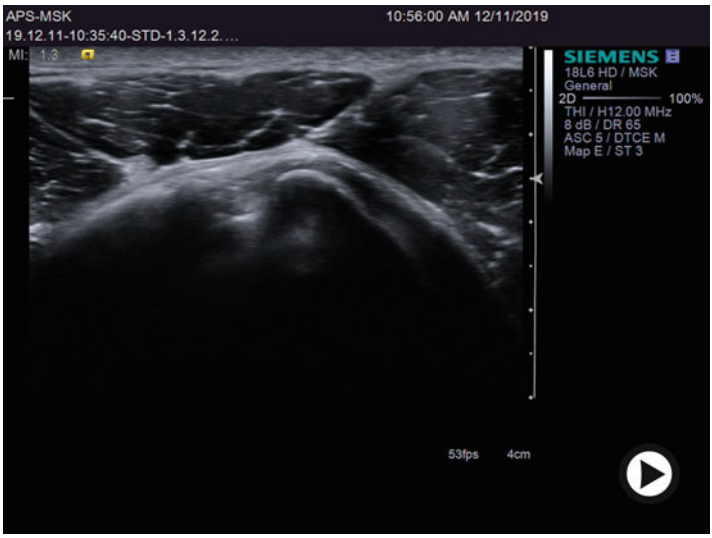

Fig. 8.8 (Video 8.1) Video clip showing external rotation of the humerus beginning in the neutral position, moving to external rotation, and returning to the neutral position. Double-click on figure to start video or click on the icon in the lower-left corner of the figure to show the video controller (▶ https://doi.org/10.1007/000-7qj)

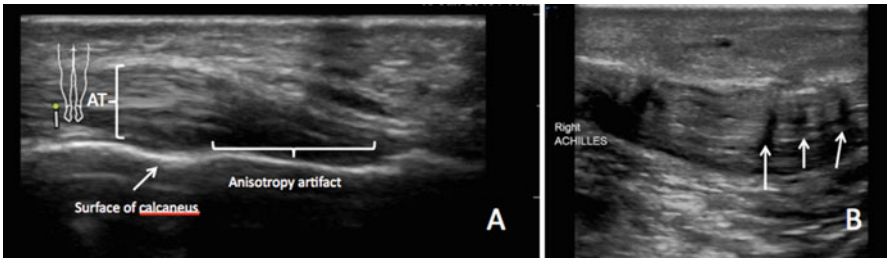

Fig. 8.9 Long view of a normal (**a**) and ruptured (**b**) Achilles tendon. In A, as the Achilles tendon inserts into the calcaneus, the tendon fibrils are not visualized because of anisotropy. Visualizing these fibrils can be achieved by rocking the probe, so that the tendon is perpendicular to the ultrasound beam (in this example, by rocking the probe toward the head). In (**b**) the fibers of a ruptured Achilles tendon are loosely associated and true defects in the tendon (arrows) are seen as hypoechoic areas filled with hematoma (clotted blood). The width of the ruptured tendon is wider and retracted into the calf because it is not tightly attached to the calcaneus. *AT* Achilles tendon

shows a large effusion (accumulation of fluid) in the suprapatellar bursa. In this example, the fluid was removed by arthrocentesis (insertion of a needle into the joint). The insertion of the needle into the bursa was performed under ultrasound guidance, so ultrasound was involved in both the identification and removal of excess fluid.

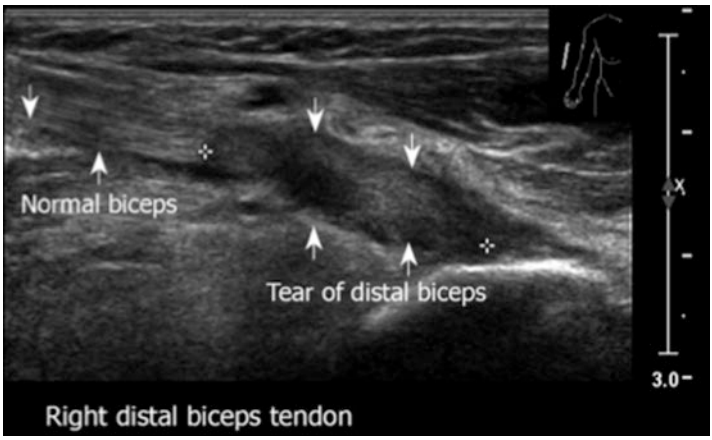

Fig. 8.10 A portion of the normal biceps tendon that has retracted into the arm is seen on the left side of this image. The position of the tear demonstrates loss of fibrillary echotexture, thickening, and evidence of hematoma

Doppler imaging is used to investigate any anechoic structure that is discovered during a scan. Anechoic structures can be cysts, effusions, or lymph nodes. Of these three, only lymph nodes have blood supply that can be visualized with color flow Doppler. Figure 8.12 is a gray scale image of an anechoic region that was also examined using color flow Doppler. The presence of blood vessels within the anechoic region identifies it as a lymph node. A cyst or an abscess would not have internal blood vessels.

8.2.4 Laboratory Exercises That Demonstrate Concepts of Physiology of the MSK System

This ability of ultrasound to perform dynamic imaging in real time can be utilized to study the physiology of the MSK system. For example, ultrasound can be used to visualize and measure the change in the pennation angle in a muscle before and after contraction. The pennation angle is that angle formed between the long axis of the muscle fascicles and the long axis of their tendon of insertion. Ultrasound can also be used to demonstrate the increased perfusion of a muscle after exercise and the function of the calf muscle pump that begins the return of venous blood from the lower limb to the heart. As a final example, ultrasound imaging can demonstrate changing flow patterns in arteries before and after exercise.

These exercises use a range of imaging modes and not all modes are available on all ultrasound instruments. Gray scale mode (also called B-mode or real-time imaging) is the most basic mode and is available on all instruments. Gray scale imaging alone provides a wealth of information on the physiology of the MSK

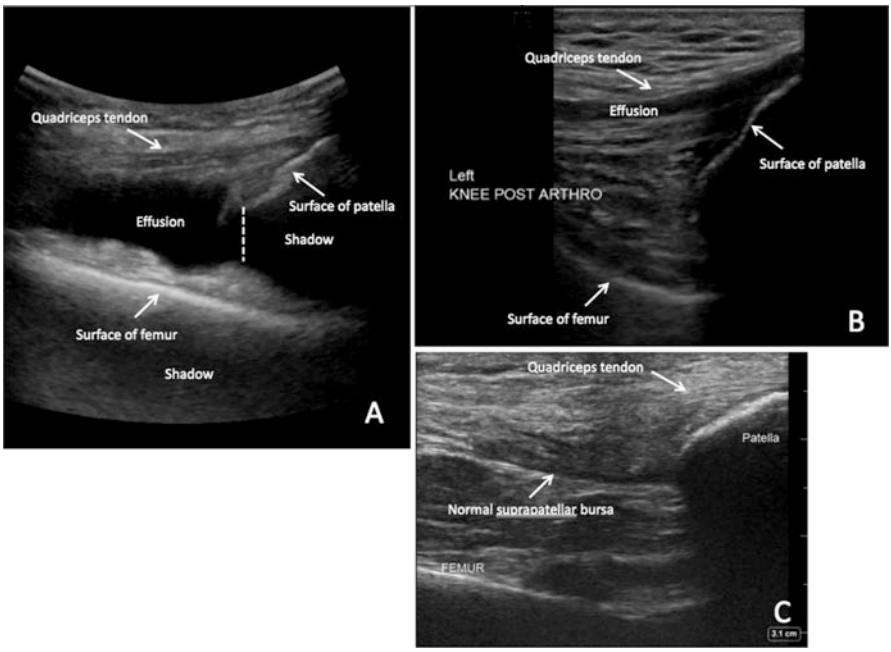

Fig. 8.11 Longitudinal view of the suprapatellar bursa before (**a**) and after (**b**) removal of an effusion. In (**a**) a curved probe is used to obtain a larger field of view and to visualize more of the effusion. The quadriceps tendon is seen inserting into the superior pole of the patella. Both the patella and the femur cast posterior shadows. A dashed line separates the effusion within the suprapatellar bursa from the shadow that is posterior to the patella. In (**b**) (post–arthrocentesis), the volume of the effusion is markedly reduced. In (**c**) the slit-like appearance of the suprapatellar bursa in a normal knee is shown

system, e.g., on changes of muscle and tendon positions during joint movement (Figs. 8.7 and 8.8), on changes of muscle dimensions during contraction (Figs. 8.14 and 8.15), and even the movement of valve leaflets in a venous valve (Figs. 8.20 and 8.21). Color flow Doppler mode provides information on the direction of blood flow (Fig. 8.18) and a qualitative assessment of flow velocity. Power Doppler mode, used in Fig. 8.16, is 3–5 more sensitive than color flow Doppler mode, but does not provide information on the direction of blood flow. Color flow Doppler can be used if power Doppler is not available. Spectral Doppler mode, used in Figs. 8.19 and 8.22, may not be available on all instruments, but provides a spectrum of blood flow velocity vs. time, from which a quantitative assessment of velocity in arteries and veins can be made. The spectral waveform also provides characteristic patterns that indicate changes in peripheral resistance after exercise (Fig. 8.22) or in arteries with pathological stenosis.

The term "patient" is used in the following exercises to emphasize their clinical application, but can be replaced by "model", "subject", or "volunteer" when used in a non-clinical, educational setting. In addition, valuable practice and information can

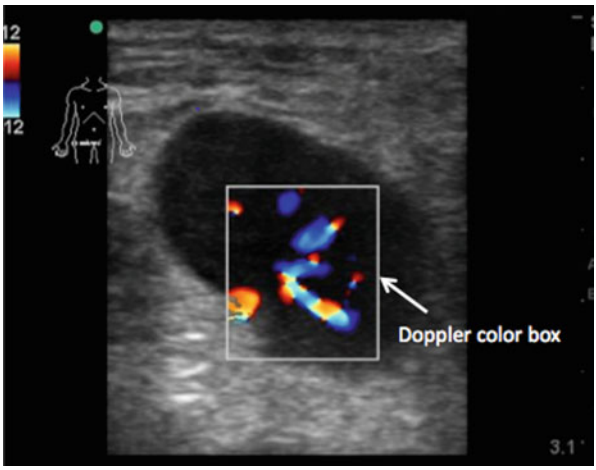

Fig. 8.12 Combined gray scale and color flow Doppler image of a lymph node. Blood flow is only detected within the area of the Doppler color box. Anechoic structures are frequently seen during an ultrasound examination. Color flow Doppler allows the operator to demonstrate whether there is any blood flow in the structure. In the image below, a lymph node demonstrates internal flow compared to an abscess, which can be more irregularly shaped and does not exhibit any color flow

be obtained when these exercises are be performed by an operator on themselves (self-scanning).

8.2.4.1 Exercise 1: Ultrasound Imaging of Muscle Architecture During Contraction

Learning Objectives To explore the sonographic architecture of the tibialis anterior muscle, a muscle with bipennate fiber orientation, and to measure the change in its pennation angle during muscle contraction.

Skeletal muscle can be divided into different types based on overall, gross architecture (Fig. 8.13) and this architecture is related to muscle function. Muscles like the biceps brachii have a fusiform pattern in which fascicles extend the length of the muscle. This pattern allows a longer range of contraction, but at the expense of strength of contraction. Pennate muscle structure has more limited range of contraction, but can develop greater strength because muscle fascicles attach along a longer length of the tendon.

The tibialis anterior muscle is an example of a bipennate muscle that has muscle fascicles inserting into two sides of a central tendon. In the tibialis anterior muscle, one set of fascicles arises from the upper 2/3 of the lateral surface of the tibia, the interosseous membrane between the tibia and fibula, and the fascia covering the extensor digitorum longus muscle. A second set of fascicles arises from the deep

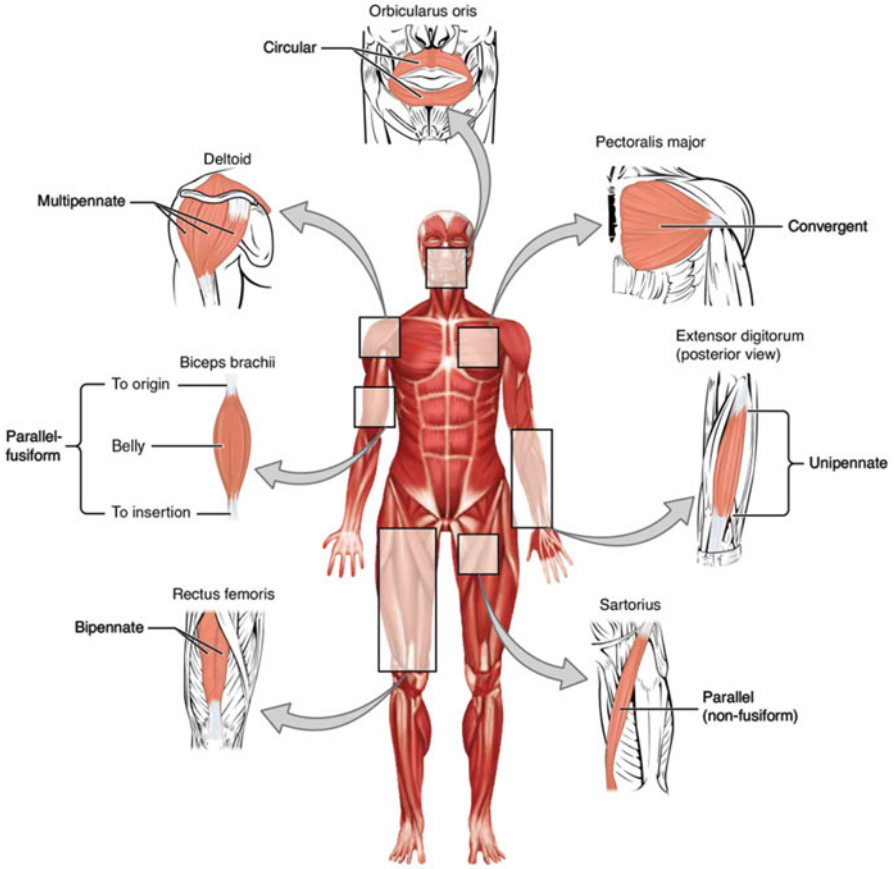

Fig. 8.13 Different types of muscles based on overall fascicle organization. Image from: Anatomy & Physiology by Lindsay M. Biga, Sierra Dawson, Amy Harwell, Robin Hopkins, Joel Kaufmann, Mike LeMaster, Philip Matern, Katie Morrison-Graham, Devon Quick & Jon Runyeon and licensed under a Creative Commons Attribution-ShareAlike 4.0 International License, except where otherwise noted. Download for free at https://open.oregonstate.education/aandp

surface of the deep fascia of the leg. Both sets of fascicles insert into the central tendon of the muscle.

Transducer A linear, high-frequency (e.g., 5–12 MHz) transducer provides the best resolution of superficial structures (within 1–5 cm of the skin surface).

Patient Positioning and Surface Anatomy Patient should be seated on the edge of an examining table or on a stool with leg hanging freely.

The upper part of the tibialis anterior can be palpated immediately lateral to the bony anterior border of the tibia. To activate the muscle, dorsiflex the foot (raise the top of the foot towards the shin). When activated, the tibialis anterior is easily palpated.

Protocol

1. Select the "MSK" or "Small Parts" preset on the instrument, which automatically sets the frequency, depth, and gain for scanning superficial structures
2. Apply a generous amount (10–15 ml) of gel to the faceplate of the transducer and place its long axis over the tibialis anterior muscle where you feel its contraction, with the transducer marker oriented to the patient's head (see inset in Fig. 8.14). Have the patient relax the muscle by letting the foot hang freely and "go limp". While keeping the faceplate of the transducer flat on the patient's skin, slide the transducer toward the knee and then, toward the foot, and sweep the transducer laterally and medially until you acquire the image shown in Fig. 8.14a.
3. Keeping the transducer in the same position used to obtain an image of the resting muscle, ask the patient to slowly, but completely, dorsiflex the foot (raise the top of the foot towards the shin), and thus, contract the tibialis anterior. Observe the change in muscle pattern during contraction, and at the end of contraction, obtain the image shown in Fig. 8.14b.
4. The hyperechoic reflections seen within the substance of the muscle are produced by the perimysial coverings of the muscle fascicles and are indirect indicators of the linear arrangement of the component muscle fibers. Note how these perimysial reflections converge on a central tendon. In the image of the resting muscle, measure the pennation angles formed between well-resolved perimysial reflections on both sides of the muscle's central tendon. Do the same in the image of the contracted muscle. Compare the pennation angles in resting and contracted muscle. An inexpensive, plastic protractor can be used to measure pennation angles on "frozen" images of resting and contracted muscles directly on the display screen of the ultrasound instrument. Alternatively, a protractor can be used to measure pennation angles on printed images that are downloaded from the instrument.
5. Finally, obtain a short (3–5 s) video clip of the muscle contracting, beginning in the resting state and ending in the contracted state.

Extension of the Exercise and Clinical Correlation This simple exercise provides powerful visual evidence of the changing pennation angle during muscle contraction. If these images are studied carefully, one also sees that the central tendon moves from right to left in the images (better seen in the video clip of contraction), which is a distal to proximal movement of the tendon, an indication that the tendon is pulling the foot superiorly. An obvious extension of this exercise is to study other bipennate muscle (e.g., the rectus femoris and the first dorsal interosseous muscle of the hand). In addition, one can measure the increase in cross-sectional diameter of the tibialis muscle (and others), by rotating the transducer 90 degrees to obtain a transverse view of the muscle. In the research setting, Bland et al. (2011) used ultrasound imaging techniques to examine the relationship between tibialis anterior muscle architecture (muscle thickness, cross-sectional area, pennation angle, and fascicle length) and strength and ankle function in ambulatory patients with cerebral palsy and unilateral foot drop.

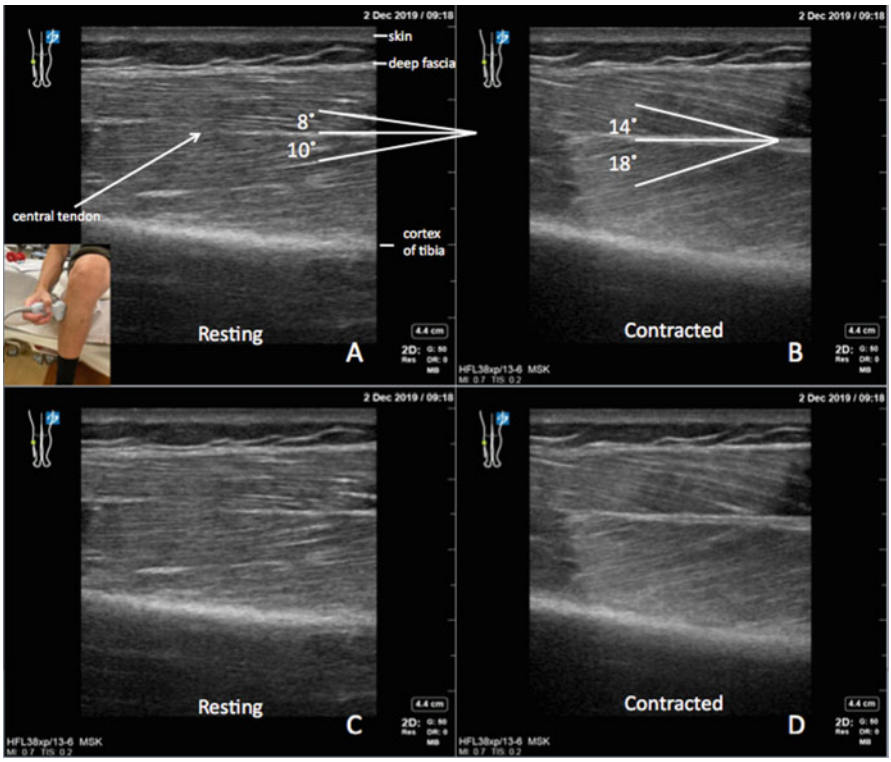

Fig. 8.14 Long view of tibialis anterior muscle in resting (**a**, **c**) and contracted (**b**, **d**) states. In each panel, the skin is at the top of the image (labeled in **a**). Between the skin and the deep fascia is the superficial fascia (not labeled). The cortex of the tibia and its posterior shadow are in the far field. Note the central tendon and the linear, hyperechoic reflections produced by the perimysial connective tissue enclosing muscle fascicles. In the resting muscle (**a**), fascicles originating from the deep fascia attach to the central tendon at a pennation angle of 8 degrees, while fascicles originating from the tibia attach to the central tendon at a pennation angle of 10 degrees. In the contacted muscle (**b**), fascicles originating from the deep fascia attach at a pennation angle of 14 degrees, and fascicles from the tibia attach at a pennation angle of 18 degrees. Panels **c** and **d** are the same images shown in **a** and **b**, but without labels. The inset in **a** shows the position of transducer used to obtain a long view of tibialis anterior muscle. The probe is placed over the part of the muscle that makes a noticeable bulge when it is activated by dorsiflexing the ankle (raising the top of the foot towards the shin). The probe marker is oriented toward the patient's head. Panels **a**–**d** are still images taken from the video clip in Fig. 8.15

8.2.4.2 Exercise 2: Use Power Doppler to Observe Differences in Blood Perfusion of Muscle at Rest and After Exercise

Learning Objectives In this exercise, power Doppler is used to assess the blood flow in the biceps brachii muscle before and after exercise. The blood flow to be measured here is in very small vessels that are small branches of the brachial artery. These blood vessels are contained within the perimysial layers of connective tissue

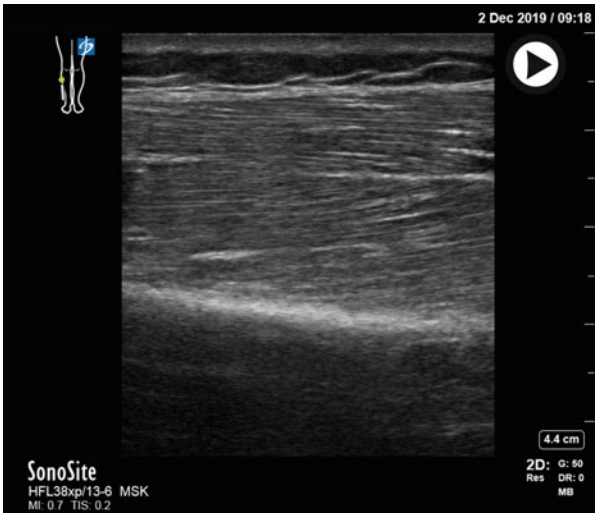

Fig. 8.15 (Video 8.2) Video clip showing changes in pennation angles of the tibialis anterior muscle beginning with the resting state and moving to the contracted state (▶ https://doi.org/10.1007/000-7qh)

shown in Fig. 8.1. Because blood flow in these arteries is so low, power Doppler—with its high sensitivity—is used here, rather than color flow Doppler, though color flow Doppler could also be used. Power Doppler images can be identified because blood flow is presented in hues of yellow and orange, rather than the red and blue hues of color flow Doppler.

Transducer A linear, high-frequency (e.g., 5–12 MHz) transducer provides the best resolution of superficial structures (within 1–5 cm of the skin surface).

Patient Positioning Patient should be seated comfortably on the edge of an examining table or stool with the open hand (palm up) resting on their lap.

Protocol

1. Select the "MSK" or "Small Parts" preset on the instrument, which automatically sets the frequency, depth, and gain for scanning superficial structures.
2. Apply a generous amount (10–15 ml) of gel to the transducer and acquire a long view of the biceps brachii muscle using the transducer orientation shown in Fig. 8.16a. The transducer should be aligned with the long axis of the muscle with the transducer indicator pointing to the patient's head. Take note of the position of the transducer on the skin so that this position can easily be relocated and the same portion of the muscle can be re-imaged multiple times.
3. Activate the power Doppler function and a color box will appear superimposed on the gray scale image. Adjust the color gain and the pulse repetition frequency

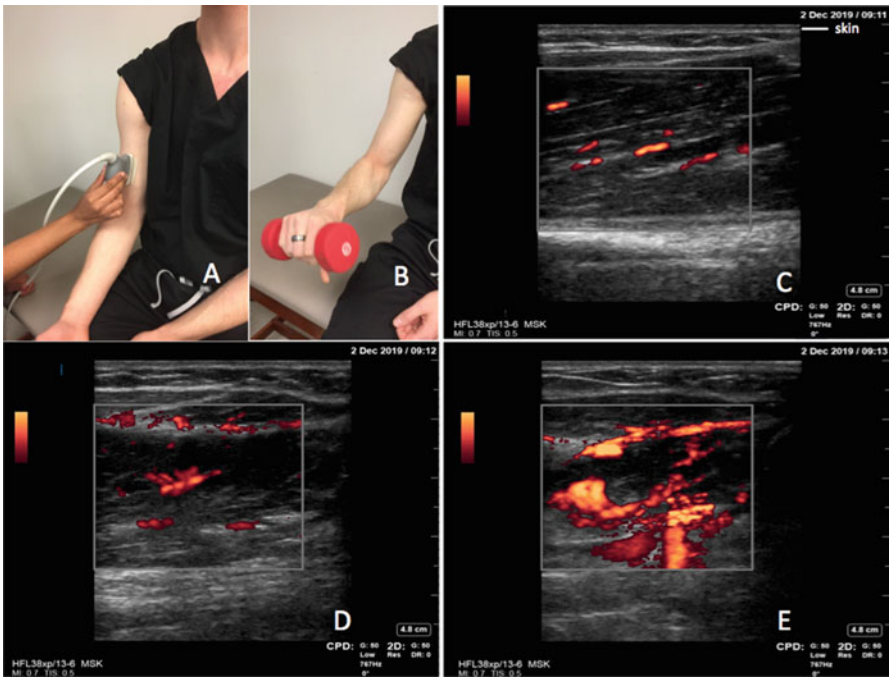

Fig. 8.16 The position of the transducer used to acquire a longitudinal view of the biceps brachii muscle is shown in (**a**). In (**b**) the forearm is shown while completing a cycle of supination-pronation with the hand holding a 5 lb. weight. Combined gray scale—power Doppler images of the biceps brachii muscle (long view) at rest (**c**), and after 25 (**d**) and 50 (**e**) cycles of pronation and supination

(PRF) to a setting that will just detect blood flow (seen as orange color) in the muscle (Fig. 8.16c). Once this baseline setting of PRF is made, all parameters of the ultrasound instrument that control color (specifically, PRF, color gain, and size of the color box) should be held constant. Capture a short (10 s) video clip to assess blood flow in the resting muscle. Typically, after a splash of color due to movement of the transducer, there should be little or no flow detected in the resting muscle tissue. Because power Doppler is sensitive to any motion, it is important that the patient be as still as possible, and that the examiner hold the transducer as still as possible as the power Doppler video clip is captured. A still image displaying a baseline level of blood perfusion can be selected from the video clip.

4. Remove the transducer and ask your patient to exercise the biceps brachii muscle by performing 25 cycles of pronation and supination of the forearm, while holding an appropriate weight—a 2 or 5 lb. dumbbell, or a book of similar weight (Fig. 8.16b). Re-acquire a combined gray scale–power Doppler image of the same area of the biceps and record a second, 10 s video clip (Fig. 8.16d).

Qualitatively compare the blood perfusion in the video clip of the resting muscle with perfusion in the exercised muscle.

5. Ask the subject to perform an additional 25 cycles of pronation-supination of the forearm, while holding the weight, and acquire a third combined gray scale–power Doppler image (Fig. 8.16e). Compare resting levels of blood perfusion with increased perfusion after exercise.

Extension of the Exercise and Clinical Correlation This exercise can be extended by examining other muscles using an appropriate exercise. It is also valuable to compare local effects of exercise on muscle perfusion with systemic effects by comparing the level of perfusion in an exercised muscle with perfusion in the contralateral muscle that was not exercised. Newman et al. (1997) were among the first to show the ability of power Doppler ultrasound imaging to evaluate exercise-induced changes in muscle blood volume.

8.2.4.3 Exercise 3: Use Ultrasound Imaging to Explore Venous Return in the Popliteal Vein

Learning Objectives Demonstrate augmented (increased) venous return using both passive externally applied pressure on the calf and active contraction of calf muscles. Demonstrate the action of valves in peripheral veins.

When blood appears on the venous side of a capillary bed in the lower limb, the pressure moving blood back to the heart is close to zero. Venous return in the lower limb is initiated as muscles in the calves contract, and squeeze the deep veins. Blood in the veins is forced centrally because the valves in the veins are designed to allow one-way flow of blood toward the trunk. Blood flow away from the trunk is prevented by the design of the valves. The intermittent contraction of calf muscles moves the blood centrally by forcing the blood through an opened, proximal valve and preventing back flow through a closed, distal valve (Fig. 8.17). The most proximal venous valve in the lower limb is in the common iliac veins, near the point where the two common iliac veins join to form the inferior vena cava. Proximal to this point, there are no valves, and blood is propelled to the heart primarily by changes in intrathoracic pressure that occur during respiration, aided by contraction and relaxation of the abdominal wall muscles.

Transducer A linear, high-frequency (e.g., 5–12 MHz) transducer provides the best resolution of superficial structures (within 1–5 cm of the skin surface).

Patient Positioning Ask your subject to take a prone position on an examining table, and then, to take tension off the skin and deep fascia, keep the knee is a slightly flexed position by placing a rolled towel under the ankle (Fig. 8.18a).

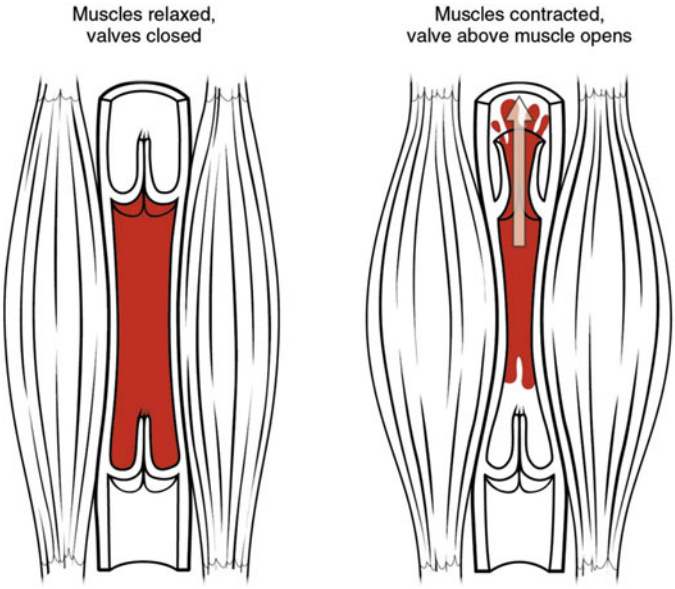

Fig. 8.17 Action of the muscle pump in the calf. Blood in a deep vein of the calf is forced toward the body trunk through an opened, proximal valve in the vein by muscle contraction. Flow away from the trunk is prevented due to the closed, distal valve. Image from: Anatomy & Physiology by Lindsay M. Biga, Sierra Dawson, Amy Harwell, Robin Hopkins, Joel Kaufmann, Mike LeMaster, Philip Matern, Katie Morrison-Graham, Devon Quick & Jon Runyeon and licensed under a Creative Commons Attribution-ShareAlike 4.0 International License, except where otherwise noted. Download for free at https://open.oregonstate.education/aandp

Protocol

1. Select the "MSK" or "Small Parts" or "Vascular" preset on the instrument, which automatically sets the frequency, depth, and gain for scanning superficial structures.
2. Begin by identifying the popliteal vein at the back of the knee. Apply a generous amount (10–15 ml) of gel to the transducer and with the transducer in a transverse position, explore the popliteal fossa (Fig. 8.18a), a diamond-shaped area at the back of the knee formed superiorly by the semitendinosus and semimembranosus muscles, medially, and by the biceps femoris muscle laterally. Inferiorly, the popliteal fossa is formed by the medial and lateral heads of the gastrocnemius muscles. The popliteal vein lies in the fossa between the tibial nerve and the popliteal artery. Acquire the transverse view of the popliteal fossa shown in Fig. 8.18b.
3. Confirm the identity of the popliteal vein by putting enough pressure on the skin with the transducer that the vein collapses and the opposite walls of the vein touch each other. Acquire the image shown Fig. 8.18c. This collapse of the vein with

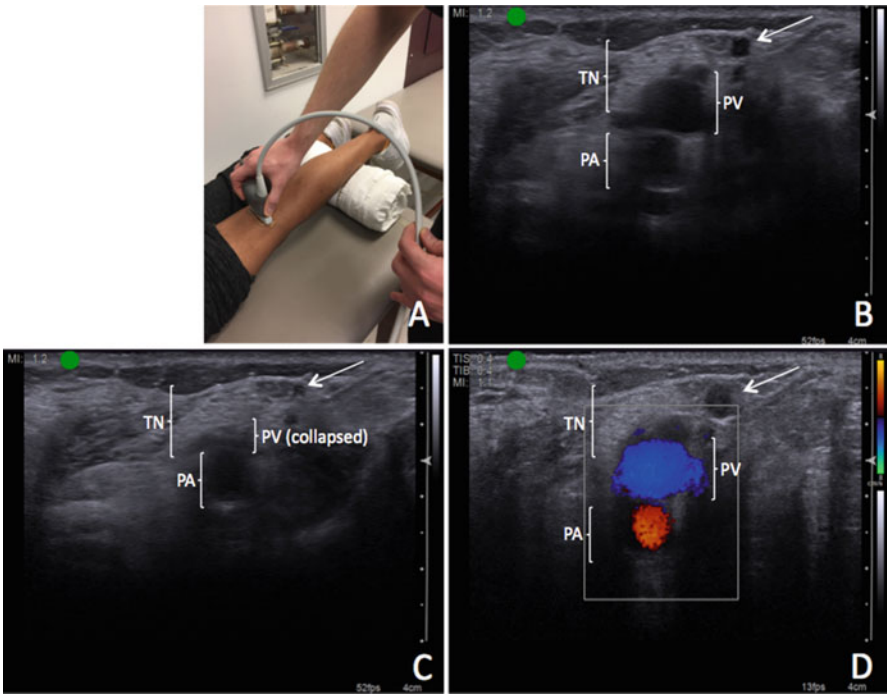

Fig. 8.18 Identification of the popliteal vein and artery in the popliteal fossa and demonstration of coaptation in the popliteal vein. The position of the transducer used to acquire a transverse view of the popliteal fossa is shown in (**a**). The transducer marker is pointing laterally. The corresponding gray scale image is shown in (**b**). The popliteal vein (PV) and popliteal artery (PA) are indicated. The tibial nerve (TN) appears as a crescent–shaped, hyperechoic structure superficial to the popliteal vein. In (**c**) compression of the popliteal fossa with the transducer has collapsed the lumen of the popliteal vein. The opposing walls of the vein are touching each other (demonstrating coaptation) and the vein seems to disappear in the soft tissue. In (**d**) color flow Doppler is used to confirm identification of the uncompressed popliteal vein, shown in blue, and popliteal artery, shown in red. The arrows in (**b**–**d**) point to the same superficial vein, which like the deeper popliteal vein, collapses with compression by the transducer (shown in **c**)

compression so that the opposite walls of the vessel touch each other is called **coaptation** and is used throughout the body to distinguish veins from arteries. The higher pressure within the arteries and their stronger walls prevent their collapse.

4. Additional confirmation of the identity of the popliteal vein and artery is obtained by using color flow Doppler. With the transducer still in the transverse position, activate the color flow Doppler function and fan the faceplate of the transducer slightly toward the thigh. Blood flow in the popliteal vein will be color-coded, blue, indicating flow away from the transducer, and blood in the popliteal artery will be coded, red, indicating flow toward the transducer (Fig. 8.18d).

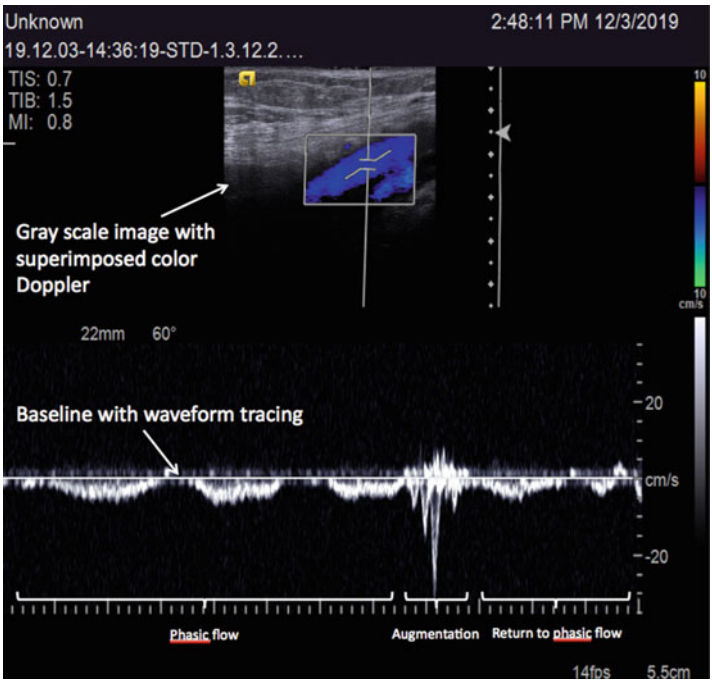

Fig. 8.19 Evidence for augmentation of venous return in the popliteal vein obtained with spectral Doppler. The gray scale image of the popliteal vein with superimposed color flow Doppler appears in the top half of the image. The position of the gate in the lumen of the vein shows where the velocity measurement is made. Blood flow is shown as a waveform tracing relative to the baseline (lower half of the image). The waveform tracing below the baseline indicates flow away from the transducer and towards the heart. A waveform tracing above the baseline would indicate retrograde flow toward the transducer. The waveform tracing plots blood flow velocity in cm/sec on the y-axis and time on the x-axis. Blood in the popliteal vein is returned to the trunk at a low velocity (about 5 cm/s) in a waveform depicting phasic flow. During augmentation, there is a rapid increase in velocity to 25 cm/s, followed by a return to phasic flow

5. Once the popliteal vein is identified, slowing rotate the transducer 90 degrees to obtain a longitudinal, gray scale view of the popliteal vein. It may take a few attempts to distinguish the popliteal vein from the closely related popliteal artery. Once a long view of the vein has been acquired in gray scale mode, activate color flow Doppler mode. Obtain a gray scale image with superimposed color flow Doppler, as shown in the upper half of Fig. 8.19. Now, activate spectral Doppler mode (also called "pulsed wave Doppler mode" on some instruments). Position the sampling gate in the center of the lumen of the vein. Obtain a spectral waveform of the venous flow in the popliteal vein as shown in the lower half of Fig. 8.19.
6. Now, keeping the transducer positioned over the vein and the spectral mode function on, briskly squeeze the calf causing increased blood flow toward the heart. A spectrum of a normal vein with competent valves will display phasic

blood flow before the brisk squeeze of the calf (Fig. 8.19). During the squeeze, there will be a short burst of increased blood flow (augmentation), indicated by the spike in the tracing below the baseline, followed by a return to phasic flow. If the ultrasound instrument is equipped with audio, there will be increased audio signal when the spike of flow is being displayed.

In the clinical setting, if augmentation does not produce a proximal rush of venous blood, as indicated by a spike in venous return on the spectral waveform, one would suspect a proximal blockage of the vein. This would most likely be due to a thrombus (clot) located more proximally in the vein than the position being examined by the transducer. The thrombus prevents normal forward flow. There is also the case where the augmented rush of venous blood proximally is accompanied by a nearly equivalent wave of reversed flow, indicated by a spike above the baseline). In this case, one would be suspicious of an incompetent valve that is allowing regurgitation of venous blood.

In review, augmentation of venous return in the calf involves:

(A) Identification of the popliteal vein in a transverse view of the popliteal fossa;
(B) Confirmation of identification of the popliteal vein by coaptation and by color flow Doppler;
(C) Acquisition of a "long" view of the popliteal vein;
(D) Acquisition of a waveform of the popliteal vein by using spectral Doppler and squeezing the calf to observe a short burst of increased venous return.

7. Complete this exercise of the lower limb veins by demonstrating the action of valves in the vein. Again, acquire a long view of the popliteal vein using gray scale mode. Slide the transducer over the popliteal vein and locate a venous valve. Valves occur where there are slight bulges in the diameter of the vein. Find such a slight bulge in the vein and adjust the gain so that the blood in the vein is anechoic and look for any echogenic tissue, indicating a cusp of the valve that projects from the inner wall of the vein toward the lumen. Capture a short video clip of the valve and study its action by adjusting the playback speed of the replay.

   An example of a valve in its closed (A) and its open position (B) is shown in Fig. 8.20. When exploring for the valves, be sure to use light pressure with the transducer because firm pressure will partially collapse the vein and obscure the valve. Also, use plenty of gel to ensure that there are no air gaps between the transducer and the skin when using such light pressure.

Extension of the Exercise and Clinical Correlation In the clinical setting, the demonstration of coaptation in the popliteal vein is strong evidence that there is not a clot in the vein. Presence of a clot would prevent the opposite walls of the vein to come in contact with each other with pressure applied by the transducer. Examination of the popliteal vein is part of a two-point clinical examination for thrombi in the lower limb. The second part of the two-point examination is assessment of compressibility in the femoral vein in the femoral triangle. The same steps of identification of the femoral vessel, test of compression of the femoral vein, and assessment

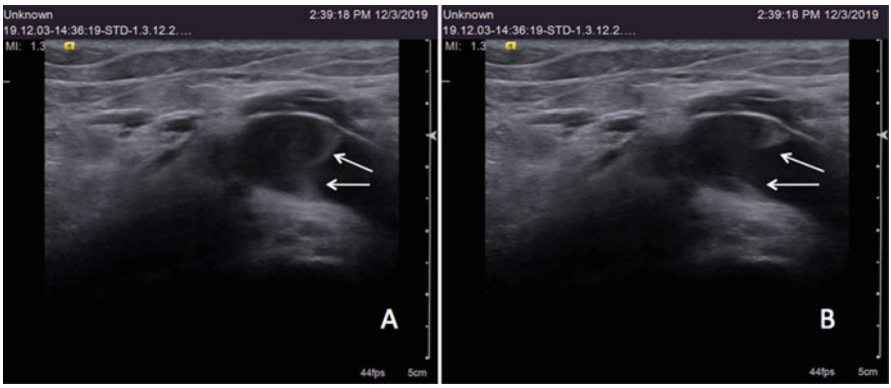

Fig. 8.20 Long views of the popliteal vein showing a valve in its closed (**a**) and open (**b**) positions. Each arrow points to a cusp in the bicuspid valve. Panels A and B are still images taken from the video clip in Fig. 8.21

with color flow Doppler and spectral Doppler can evaluate the femoral vein for presence of thrombus and competency of proximal valves.

In a clinical examination of venous return in the lower limb, augmentation of venous return is performed by the sonographer, or by an assistant, by applying a brisk squeeze of the calf. This calf squeeze can be replaced in the physiology laboratory by asking the individual being examined to quickly dorsiflex their ankle (raise the top of the foot towards the shin), and then relax their calf. The calf muscle contractions that produce dorsiflexion of the ankle are sufficient to squeeze the deep veins of the calf that drain into the popliteal vein and augment venous return. This demonstration of augmenting venous return by simply contracting the calf muscles provides powerful evidence for the importance of exercise in producing venous return and preventing stasis of blood in the leg that, under certain circumstances, can produce clots.

8.2.4.4 Exercise 4: Use Spectral Doppler to Demonstrate the Change from a High Resistance Waveform to a Low Resistance Waveform in an Artery Supplying Exercising Muscles

Learning Objectives The objective here is to demonstrate how flow in a large to medium diameter artery changes with physiologic demands of muscle for oxygen. Arteries can be classified as either low or high resistance based on the blood flow needs of the organs they supply. A low resistance artery supplies organs, such as the brain and the kidneys, which require continuous blood during both systole and diastole. A high resistance artery is one whose smaller branches create a high resistance by constricting, thus, reducing blood flow when not required. Large and

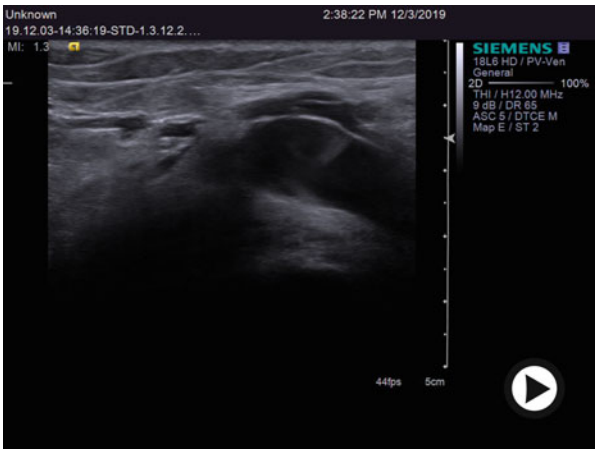

Fig. 8.21 (Video 8.3) Video clip showing the movements of the cusps of a valve in the popliteal vein during valve opening and closure (▶ https://doi.org/10.1007/000-7qk)

medium-sized arteries that supply the limbs are high resistance arteries that have low flow during diastole that can increase to higher flow during muscle activity.

The spectral Doppler mode (also called pulsed wave Doppler) can be used to obtain waveforms of arteries that identify them as either low resistance or high resistance. Moreover, spectral Doppler can record the change of a high resistance artery to a low resistance type with changing blood flow demands.

The spectral waveform of a high resistance artery is shown in Fig. 8.22a and consists of a peak systolic velocity, corresponding to the arterial pulse, and a return to baseline levels (no flow) during diastole. Between the peak systolic velocity and no flow during diastole, there may be a momentary reversal of flow due to the elasticity in the walls of these large arteries. (This momentary reversal in the direction of flow is indicated by the spectral line dipping below the baseline.) The spectral waveform of a low resistance artery is shown in Fig. 8.22b. The peak systolic velocity is followed by a flow rate that stays above baseline during diastole. Flow is maintained to the exercising muscle during diastole because of oxygen demands.

Transducer A linear, high-frequency transducer provides high resolution of structures that are superficial (within 1–5 cm of the skin surface). Use the "MSK", "Small Parts", or "Vascular" preset on the ultrasound instrument.

Patient Positioning To collect images, ask your patient to take a prone position on an examining table, and then keep the knee is a slightly flexed position by placing a rolled towel under the ankle (Fig. 8.18a). The patient can perform toe raises while standing.

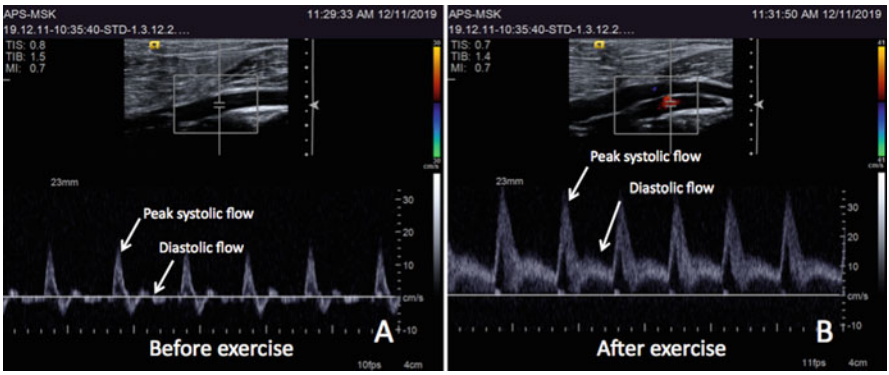

Fig. 8.22 Spectral waveform in the popliteal artery before (**a**) and after (**b**) exercise. Before exercise, diastolic flow returns to baseline levels after peak systolic flow. After exercise, diastolic flow does not return to baseline levels. In addition, peak systolic flow is higher after exercise (30 cm/s) than before (14 cm/s)

Protocol

1. The steps in acquiring images of the popliteal artery follow the steps used to image venous blood flow in the popliteal vein in Exercise 3 above, but this time, focus on the artery. Obtain a transverse view of the popliteal fossa as shown in Fig. 8.18a, and verify the identity of the popliteal artery by using color flow Doppler (Fig. 8.18d).
2. With color flow Doppler mode activated, acquire a long view of the popliteal artery by slowly rotating the transducer from a transverse orientation to a longitudinal one (transducer marker toward the patient's head), always keeping the popliteal artery in view. The combine gray scale–color flow Doppler image to be acquired is shown in the upper half of both A and B in Fig. 8.22.
3. Activate spectral flow Doppler mode, also designated "pulsed wave (PW) Doppler" on some instruments. Position the gate of the spectral Doppler mode in center of the lumen of the artery. Record the waveform, as in the lower half of Fig. 8.22a.
4. The patient is then asked to stand and perform 25 toe raises. The patient again assumes a prone position, the popliteal artery is imaged again, and a second spectral waveform is recorded (lower half of Fig. 8.22b).
5. Compare the spectral waveforms of the artery before and after exercise (see below).

Extension of the Exercise and Clinical Correlation After exercise, the vascular fields to the limb muscles are opened, resulting in lower peripheral resistance. An indication of lower peripheral resistance is shown on the spectral waveform by flow in the artery during diastole. Low resistance flow during diastole is indicated by the fact that the velocity of blood flow remains above the baseline (Fig. 8.22b). In

addition, a comparison of the two waveforms shows that the peak systolic velocity has increased from 14 to 30 cm/s. This simple exercise shows the dramatic change in blood flow due to exercise and stimulates other questions. Is the increased blood flow in the popliteal artery due to a local or a systemic event, a question that can be answered by examining the same artery in the opposite, unexercised limb. Which arteries in the body are low and which are high resistance? Is there a corresponding increase in venous return from the limb?

8.3 Summary

Ultrasound imaging is a low cost, high-resolution technique that can be used to image many parts of the MSK system. Ultrasound imaging can be performed dynamically to visualize muscles and tendons as they move, and can be used to image structures serially, allowing comparisons between different experimental conditions. Ultrasound imaging of the MSK system depends on understanding the unique echotexture of muscle, tendon, and connective tissue and being aware of anisotropic artifacts. Finally, ultrasound imaging provides visual data obtained non-invasively from the living body that powerfully reinforces the understanding of physiological concepts.

References

Bland DC, Prosser LA, Bellini LA, Alter KE, Damiano DL (2011) Tibialis anterior architecture, strength and gait in individuals with cerebral palsy. Muscle Nerve 44(4):509–517

Forney MC, Delzell PB (2018) Musculoskeletal ultrasound basics. Cleveland Clin J Med 85(4): 283–300

Jacobson JA (2011) Shoulder US: anatomy, technique and scanning pitfalls. Radiology 260(1): 6–16

Newman JS, Alder RS, Rubin JM (1997) Power Doppler sonography: use in measuring alterations in muscle blood volume after exercise. Am J Radiol 168:1525–1530

Chapter 9
Ultrasound of the Endocrine System

David Resuehr and J. Michael Wyss

9.1 Anatomy and Physiology of Endocrine System

The endocrine system provides a major mechanism by which the nervous system regulates homeostasis and many body functions, including growth, development, reproduction, blood pressure, blood ion concentrations, and even certain aspects of behavior. The endocrine system effects its actions by the secretion of hormones that affect target tissue functions, but unlike most neurons, which alter the activity of neurons and other targets by releasing neurotransmitters directly onto the target tissue, the neural control of the endocrine system acts by inducing endocrine glands throughout the body to alter their release of hormones into the blood supply, thus affecting the function of widespread organs.

Hormones are peptides, proteins, steroids and amines that are released in small amounts into the blood and delivered to target tissues, where they elicit physiologic responses. Hormones are synthesized and secreted by specialized endocrine cells, usually found in endocrine glands, e.g., *the hypothalamus, anterior and posterior lobes of the pituitary, thyroid, parathyroid, adrenal cortex, adrenal medulla, gonads, placenta, and pancreas*. The kidney also is considered to be an endocrine gland, and endocrine cells are found throughout the gastrointestinal tract. Figure 9.1, is a diagrammatic summary of the endocrine glands with a highlight of those that can be relatively easily examined with ultrasound.

Supplementary Information The online version contains supplementary material available at https://doi.org/10.1007/978-1-0716-1863-9_9. The videos can be accessed by scanning the related images with the SN More Media App.

D. Resuehr (✉) · J. Michael Wyss
University of Alabama at Birmingham, Birmingham, AL, USA
e-mail: resuehr@uab.edu; jmwyss@uab.edu

L. B. Wilson et al. (eds.), *Understanding Physiology with Ultrasound*, Physiology in Health and Disease, https://doi.org/10.1007/978-1-0716-1863-9_9

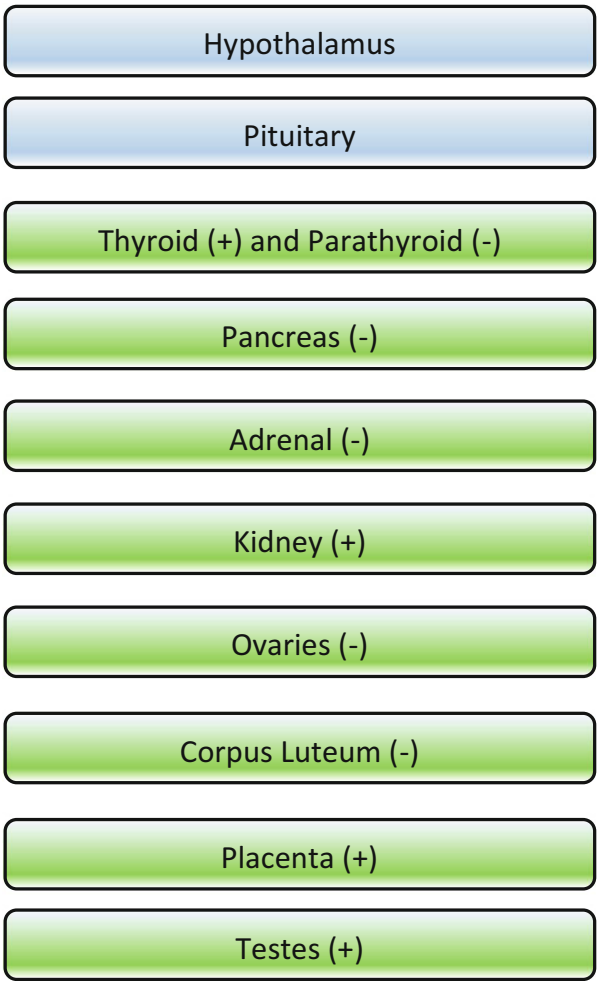

Fig. 9.1 Endocrine glands with those amendable to ultrasound exam highlighted green and the "ease of scanning" indicated with "+" or "-"respectively

Due to its location in the anterior neck, the thyroid is easily accessible for ultrasound scanning. Other glands that can be assessed with ultrasound are the parathyroid, adrenal, pancreas, gonads and the placenta; however, some of these glands are quite difficult to visualize with the current ultrasound methodology. As indicated in Fig. 9.1, the ease of scanning varies tremendously between endocrine glands, with some being best visualized with a special endocavity probe, and thus, these are rated as more difficult to scan (−). Increasingly, ultrasound (US) provides endocrinologists with tools that can give diagnostic confidence, improve efficiency, and decrease overall medical costs for many conditions. Skilled sonographers can confidently perform diagnostic exams, locate masses, guide biopsies, and help initiate a proper course of treatment for patients. The thyroid gland is especially amenable to sonography, and it has thus been integrated into history and physical

exams and other tests (especially needle biopsy) to provide valuable information that has improved patient care. As the thyroid is a commonly scanned endocrine gland that offers a lot of insight into metabolic functioning and regulation, especially when combined with its hormone levels, we will use it as an instructional model for the endocrine system in this chapter.

9.2 Hormone Synthesis

The three classes of hormones are peptides and proteins, steroids, and amines. The biosynthetic pathway of each class of hormones differs. Most hormones are peptide and protein hormones, these are synthesized from amino acids; steroid hormones are derivatives of cholesterol; and amine hormones are derivatives of tyrosine.

9.3 Mechanisms of Hormone Action

Hormones exert their actions on target cells by binding to specific receptors (membrane bound, cytosolic or nuclear), forming a hormone-receptor complex. In turn, this hormone receptor complex activates/generates "signaling molecules or second messengers" (cAMP being an example) that elicit physiological responses within the cell. Proteins and amines work this way and the receptor is on the cell membrane.

Steroid and thyroid hormones act by binding to their receptors inside of target cells (cytosolic or nuclear), which are then activated to alter responsive genes, either stimulating or sometimes inhibiting gene transcription and the associated synthesis of proteins. These changes in protein synthesis produce the physiologic changes. For example, thyroid hormone affects a variety of cells in the body, thereby regulating the basal metabolic rate. Details of the precise mechanistic alterations are beyond the scope of this book.

9.4 The Hypothalamus: The single Most Important Orchestrator of Hormones in the Body

The single most important orchestrator of hormones in the body is the hypothalamus, which acts via both the autonomic control of hormones (e.g., epinephrine release) and through direct release of hormones and hormone controlling substances (called releasing hormones). The hypothalamus (see Fig. 9.2) releases several hormones that in turn regulate the release of different hormones from the anterior pituitary. Consequently, this orchestrates an array of physiological responses, the details of which are beyond the scope of this book. Since we are focusing on the thyroid gland, we

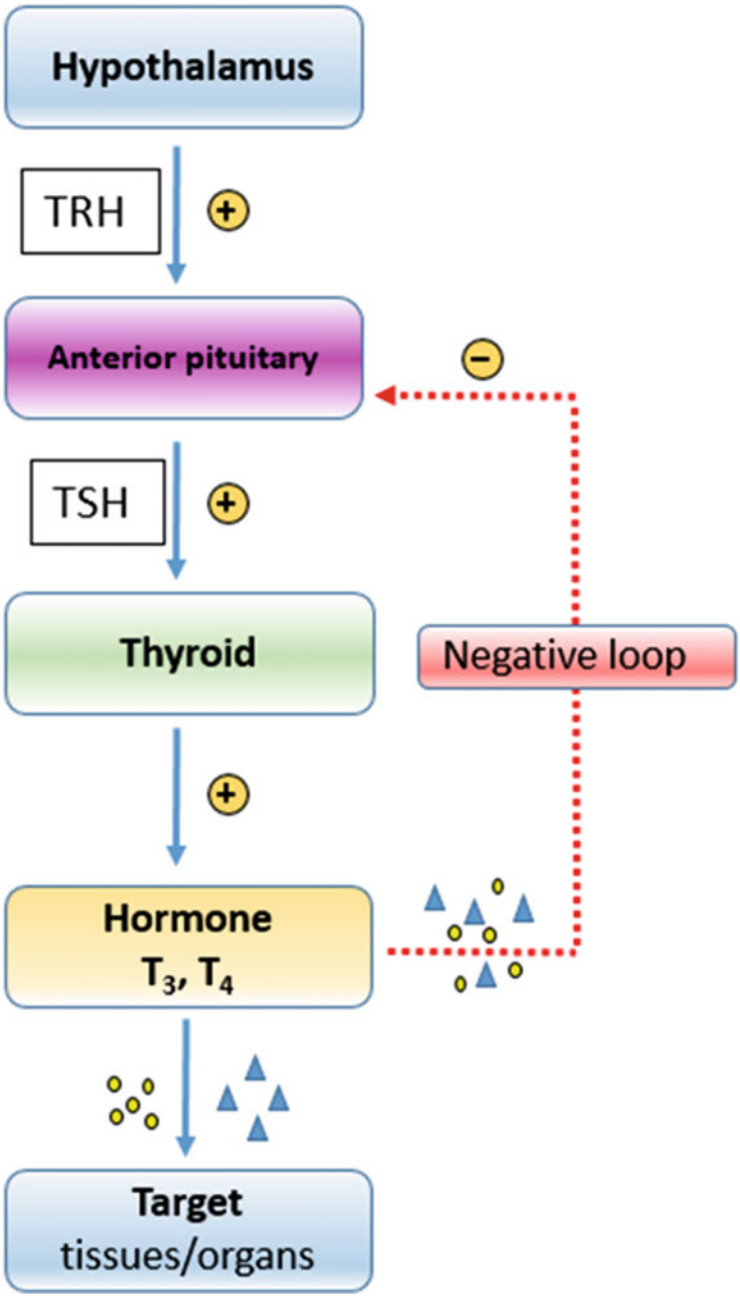

Fig. 9.2 Thyroid hormone regulation. The hypothalamic-pituitary axis controls the synthesis and secretion of thyroid hormones. The hypothalamus releases TRH, which causes release of thyroid stimulating hormone (TSH) from the anterior pituitary. In turn, TSH stimulates the release of TH, which exert their effects on many organs of the body

will limit most of the following discussion to it. Secretion of thyroid hormones (TH) begins in the hypothalamus with the release of thyroid releasing hormone (TRH; Fig. 9.2), one of the "releasing" factors from the hypothalamus indicated above.

Like the thyroid system, other hypothalamic neurons release activating and inhibiting hormones into a specialized vascular system referred to as the hypothalamic hypophyseal portal system. In short, these hypothalamic hormones enter this vascular portal system and are then carried to the anterior pituitary where they cause the release (or inhibition) of hormones from the anterior pituitary gland. In all cases, the release of hormones is in areas in which the blood brain barrier is disrupted, allowing peptides to pass directly into the portal and circulating blood. Using TH as our example, TRH is released from hypothalamic neurons into the portal system where it causes the release of thyroid stimulating hormone (TSH) from the anterior pituitary (Fig. 9.2). Other hormones released by the anterior pituitary include growth hormone (stimulating growth) and adrenocorticotrophin (stimulating glucocorticoids), and the release of these is stimulated by the hypothalamic hormones (released into the same portal system) growth hormone releasing hormone (GHRH) and corticotrophin releasing hormone (CRH).

In contrast to the hormone regulation described above, the largest hypothalamic neurons that communicate with the pituitary (magnocellular neurons) send axons down through the posterior pituitary and release peptides (i.e., oxytocin and vasopressin) directly into the blood. In turn, these hormones directly regulate several organs including the kidney (water retention), breasts (milk ejection in nursing mothers), and brain (learning and memory).

9.5 Hormone Receptor Regulation

The circulating hormone levels are important, however, they are not the only factor determining the response of a target tissue. The target tissue needs to express receptors that are specific to the respective hormone.

Altering either the number or the affinity of receptors is called down-regulation or up-regulation. Down-regulation means that the number of receptors or the affinity of the receptors for the hormone has decreased. Up-regulation means that the number or the affinity of the receptors has increased. Hormones can down-regulate or up-regulate their own receptors in target tissues and even may regulate receptors for other hormones.

Quick facts
Hormones exert their actions on target cells by binding to specific receptors (membrane bound, cytosolic or nuclear)
In many hormonal systems, the hormone-receptor complex is coupled to effector proteins
When the effector proteins are activated, a second messenger (e.g. cAMP) is produced.
These *second messengers amplify the original hormonal signal* and orchestrate the physiologic actions.

9.6 The Thyroid: A Model for Using of Ultrasound to Probe Hormonal Physiology

The thyroid gland regulates the release of three hormones that regulate the body's metabolism, i.e., the rate at which the body produces energy from nutrients and oxygen. It also affects critical body functions, such as energy level and heart rate. The thyroid gland, which is located in the neck, consists of two lobes connected by small bridge of thyroid tissue called the isthmus (Fig. 9.3). It is found at the front of the neck, below the thyroid cartilage (aka Adam's apple). Its three hormones, i.e., thyroxine (T4), triiodothyronine (T3) and the peptide hormone calcitonin are secreted into the blood. T3 and T4 contain large amounts of iodine, which must be

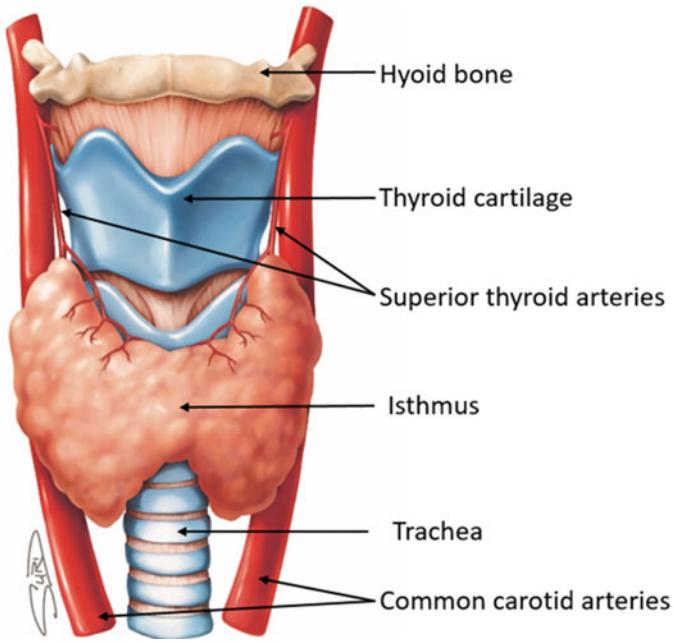

Fig. 9.3 Location and gross anatomy of the thyroid gland

adequately supplied in the diet. These thyroid hormones affect virtually every organ system in the body, including those involved in normal growth and development. Calcitonin is a 32 amino acid peptide hormone that is secreted by parafollicular cells of the thyroid gland in both humans and many other animals. Its release reduces blood calcium (Ca^{2+}), opposing the effects of parathyroid hormone (PTH) which is secreted from the parathyroid glands. The thyroid gland was the first of the endocrine organs that was found to be the cause of a hormone deficiency disorder. In 1850, patients without thyroid glands were describe as having cretinism causing cognitive impairment.

9.7 Scanning the Thyroid Gland

Fortunately, the thyroid gland is relatively easy to scan, and thyroid US has proven to be a very effective and frequently useful tool in the evaluation and management of thyroid disorders. An experienced sonographer can differentiate several common disease states. To scan the thyroid gland, a high frequency linear array probe with a range of 5–13 MHz is typically used. The supine patient should be positioned with the head slightly extended. Both lobes of the thyroid gland can then be systematically scanned in both the transverse and longitudinal planes. Images of both lobes should be obtained in mid longitudinal and mid transverse views to document height and width of the gland, respectively. The isthmus should also be imaged in transverse view (Fig. 9.4).

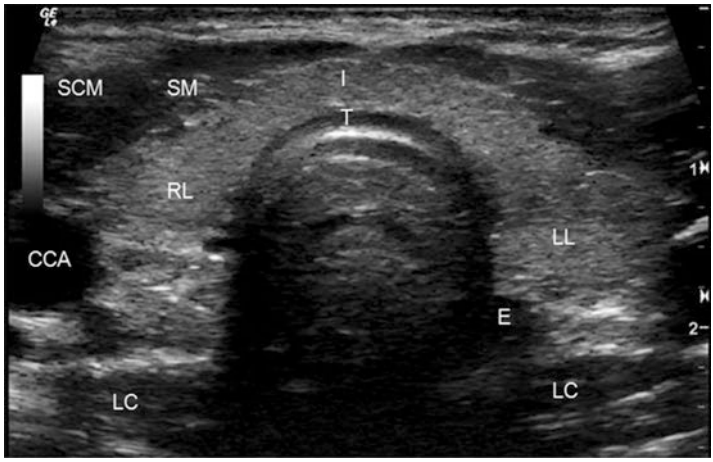

Fig. 9.4 Mid transverse view of a healthy thyroid gland. This midline view shows an acoustic shadow of the trachea (T) and the isthmus (I) of the thyroid anterior to the trachea. Other structures: strap muscles (SM), common carotid artery (CCA), sternocleidomastoid muscle (SCM), longus colli muscle (LC), and esophagus (E). The internal jugular vein (IJV) is too lateral to be captured in this image. The IJV can be seen in Fig. 9.14

The thyroid is bordered anteriorly by the (infrahyoid) strap muscles (SM), laterally by the common carotid artery (CCA), internal jugular vein, and sternocleidomastoid muscle (SCM), and posteriorly by the longus colli muscle (LC). The esophagus (E) may also appear behind and to the right of the trachea and can be confirmed by asking the patient to swallow some food or water. The CCA is round and incompressible in the transverse plane. On the other hand, the IJV is further anterolateral, and is compressible when gentle pressure is applied with the transducer. If unsure about the vasculature, the patient should be asked to do a Valsalva maneuver by briefly bearing down or pressing with the mouth closed. This will result in venous backup which distends the IJV (sometimes very impressively) and clearly identifies the vessel. The normal thyroid parenchyma is a bit more hyperechoic than the surrounding infrahyoid muscles anterior to it. Thyroid nodules are quite common and can range from cystic to solid in appearance. Distinguishing between benign and malignant nodules based on ultrasound features is beyond the scope of this book.

Volume of a lobe and total volume of the thyroid gland (volume of left and right lobes) can be calculated by measuring the height, width, and depth of the lobes (Figs. 9.5 and 9.6) and using the ellipse formula as shown in Table 9.1. Normal total thyroid volume is between 6.6 and 14.9 cc.

Four parathyroid glands (PARA is derived from a Greek for beside/alongside) are at the posterior aspect of the thyroid gland and secrete parathyroid hormone (PTH), which is essential to life. It regulates the concentration of Ca^{2+} in the blood, being secreted into the blood when the circulating Ca^{2+} concentration decreases. Via the blood, it can act on bone, kidney, and intestine (indirectly via vitamin D), to increase the plasma Ca^{2+} concentration into the "normal" range.

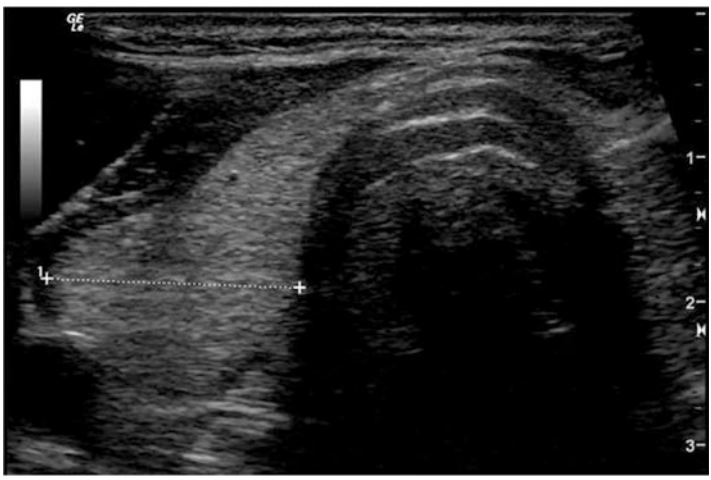

Fig. 9.5 Mid-transverse view of the right lobe of the thyroid gland. The calipers (+) are placed to measure the transverse /width of the right lobe

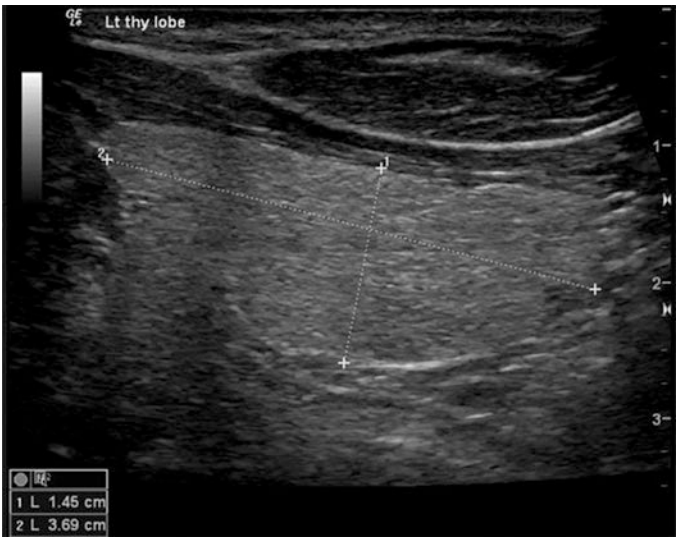

Fig. 9.6 Showing a mid-longitudinal view of the left lobe of the thyroid gland. The calipers are placed to measure the height and the AP dimension of the left lobe

Table 9.1 Quick reference for ultrasound thyroid examination. Following volumetric calculation, if there are nodules, these should be documented accordingly

Thyroid volume calculation
• Total volume of thyroid = volume of left lobe + volume of right lobe
• Volume calculation of a single lobe of the thyroid gland: Thyroid lobe volume (cc) = height × width × depth × 0.523 (ellipse formula) • Normal thyroid volume (both left + right lobe) range is 6.6–14.9 cc
For thyroid nodule analysis, the following should be noted: • Number • Location • Size • Calcifications • Halo • Margin disruption • Aspect ratio • Solid, cystic or complex?

Assessment of the thyroid has become common due to improvements in US technology and the availability of more healthcare providers trained in US.

Some common endocrinology applications for point-of-care ultrasound
• Identification of thyroid nodules (and determination of vascularity of lesions)
• Guide fine needle aspiration of nodules

9.8 Diseases of the Thyroid Gland

Thyroid disorders are very common and tend mainly to occur in women, although men, teenagers, children and babies can be affected. According to the American Thyroid Association (ATA), more than 12 percent of the U.S. population will develop a thyroid condition during their lifetime, and ~20 million Americans have some form of thyroid disease. The relative frequency of thyroid disorders and its relatively easy imaging by ultrasound make it an ideal candidate for ultrasound assessment.

Females have a higher incidence of all thyroid diseases than males. The most common cause for thyroid enlargement is nodular thyroid disease that frequently presents with a midline neck swelling and can cause dysphagia (difficulty in swallowing) and hoarseness of the voice. There are three general categories that can be applied to thyroid disease: (a) benign masses, (b) malignant tumors and (c) diffuse enlargement of the thyroid (Fig. 9.7).

9.9 Hyperthyroidism

Graves' disease (thyrotoxicosis) is the most common form of *hyperthyroidism* in the USA (~1 in 200 adults). It is an autoimmune disorder characterized by increased circulating levels of thyroid-stimulating immunoglobulins that are antibodies to TSH receptors on thyroid follicular cells. When present, the antibodies intensely stimulate the thyroid gland, resulting in increased secretion of thyroid hormones and

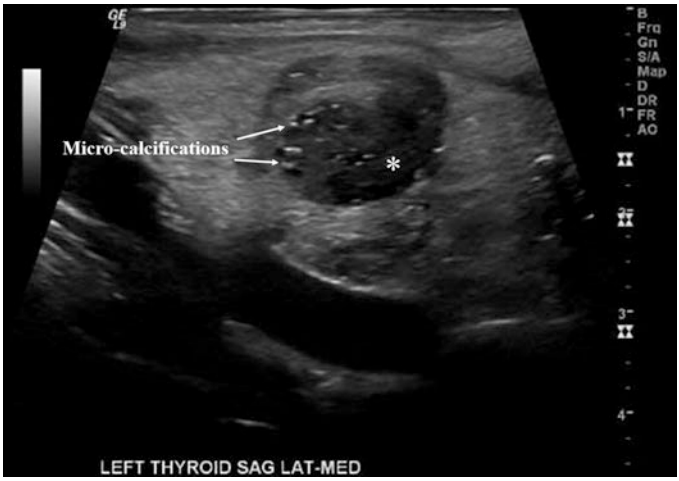

Fig. 9.7 Sagittal view of the left lobe of the thyroid gland. Note the nodule (*). This nodule presents as hypoechoic (blacker) compared to the surrounding thyroid gland. Also present are micro-calcifications within the nodule

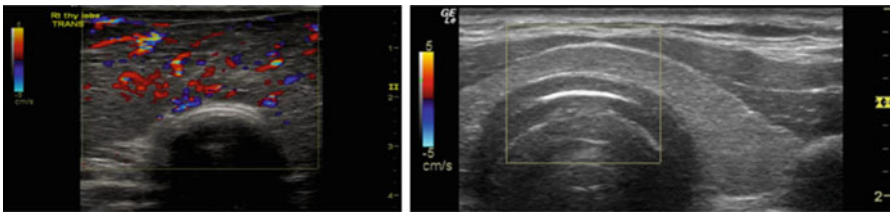

Fig. 9.8 Side-by side comparison of a thyroid gland of a patient with Grave's disease (left) and a healthy thyroid gland (right). Color Doppler was used in both images to illustrate hypervascularity in Grave's disease and no identifiable vascular flow in the normal thyroid. Note also the thickening of the thyroid isthmus in the diseased gland

hypertrophy of the gland. Other causes of hyperthyroidism are thyroid neoplasm, excessive secretion of TRH or TSH, and administration of excessive amounts of exogenous thyroid hormones.

The **diagnosis of hyperthyroidism** is based on symptoms and the detection of increased levels of T3 and T4. TSH levels may be decreased or increased, depending on the cause of the hyperthyroidism. If the cause of hyperthyroidism is Graves' disease, then TSH levels are decreased by negative feedback onto the anterior pituitary from the high levels of T4 being converted to T3 in the hypothalamus and pituitary. The increased activity of the thyroid gland causes it to enlarge (called goiter), and goiter may compress the esophagus and cause difficulty in swallowing (dysphagia).

The hypertrophied thyroid gland can easily be identified and its size and volume calculated with US. On gray-scale US, the thyroid looks heterogeneous and hypoechoic and is diffusely enlarged up to 3 times is normal size. Color flow Doppler imaging shows a hypervascularity (Fig. 9.8 and 9.9), which demonstrates extensive intra-thyroid flow in systole and diastole. Contrary to Hashimoto's thyroiditis (see below), it is possible for the thyroid appearance to return to normal during periods of remission.

Treatments for hyperthyroidism include administration of drugs such as propylthiouracil (which inhibits the synthesis of thyroid hormones), surgical removal of the gland, or radioactive ablation of the thyroid gland with iodine-131.

9.10 Hypothyroidism

Hypothyroidism is a common condition, present in about 5% of the adult population. As might be expected, its symptoms are nearly opposite of those associated with hyperthyroidism and Grave's disease and include decreased metabolic rate and weight gain without increased food intake, decreased heat production and cold intolerance, decreased heart rate, slowing of movement, slurred speech, slowed mental activity, lethargy, and somnolence, periorbital puffiness, constipation, hair loss, and menstrual dysfunction. When the cause of hypothyroidism is a defect in the

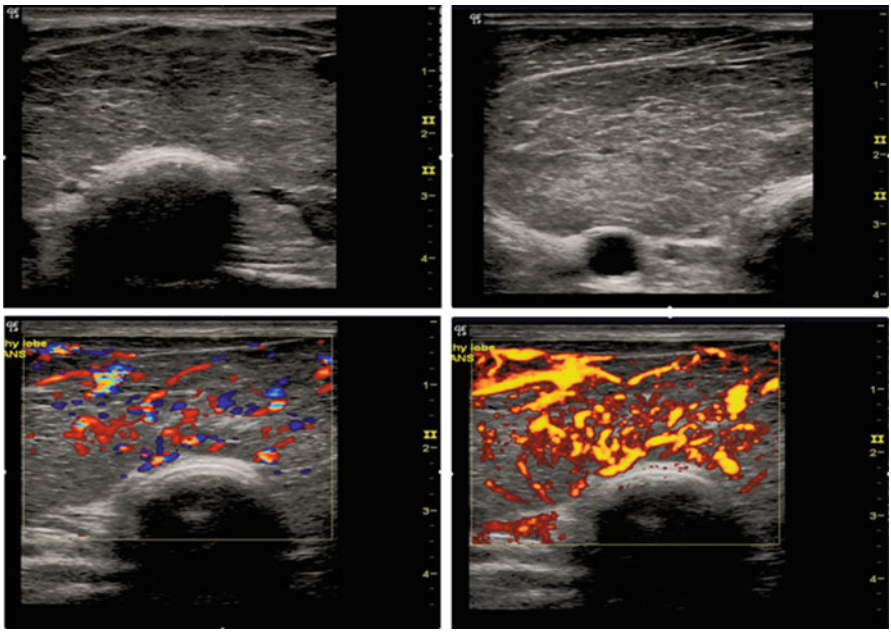

Fig. 9.9 Thyroid gland of a patient with Grave's disease. Top: B-mode midline-transverse (left) view and right lobe (right). Bottom left: color flow Doppler, right: power Doppler. Color flow Doppler imaging shows marked hyper vascularity

thyroid, a goiter develops from the unrelenting stimulation of the thyroid gland by the high circulating levels of TSH. Finally, and of critical importance, if hypothyroidism occurs in the perinatal period and is untreated, it results in congenital iodine deficiency syndrome (previously known as cretinism) an irreversible form of growth restriction and cognitive impairment.

The most common cause of hypothyroidism is an autoimmune destruction of the thyroid gland (thyroiditis) in which antibodies either destroy the gland or block thyroid hormone synthesis, such as *Hashimoto's thyroiditis* (see below). Other causes of hypothyroidism are surgical removal of the thyroid as treatment for hyperthyroidism, hypothalamic or pituitary failure, and iodine deficiency.

The diagnosis of hypothyroidism is based on symptoms and a finding of decreased levels of T3 and T4. Hashimoto's thyroiditis predominantly occurs in females >40 years of age.

Treatment of hypothyroidism involves thyroid hormone replacement therapy, usually T4. Like endogenous T4, exogenous T4 is converted to its active form, T3, in the target tissues.

On ultrasound, *Hashimoto's thyroiditis* is characterized by focal or diffuse glandular enlargement with coarse, heterogeneous and hypoechoic parenchymal echo pattern of the normally hyperechoic thyroid parenchyma (Fig. 9.10) as a result of chronic lymphocytic infiltration. In contrast to Grave's disease, this

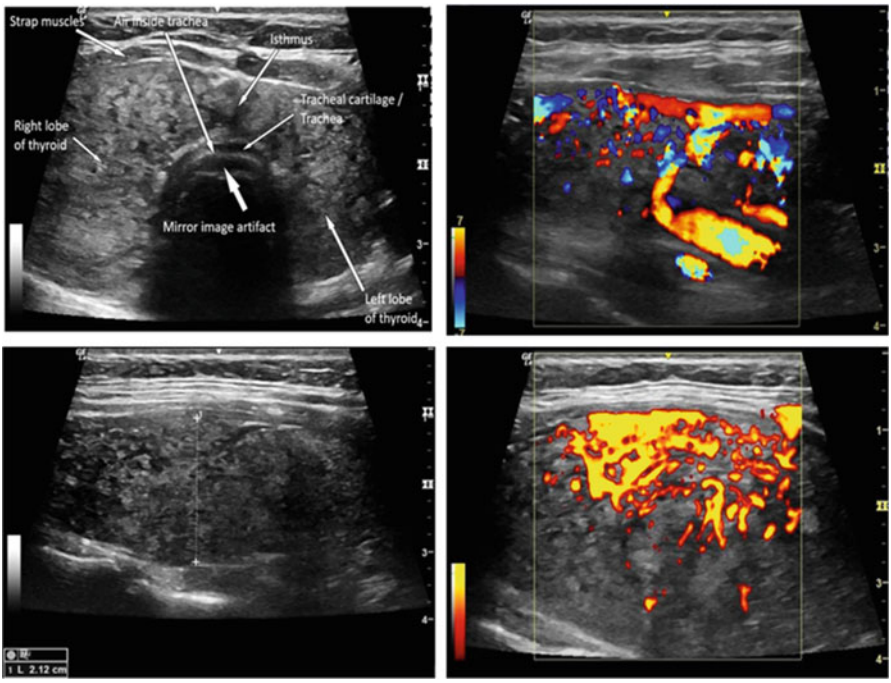

Fig. 9.10 Thyroid gland of a patient with Hashimoto's thyroiditis. Top: B-mode midline-transverse (left) view and long axis color flow Doppler (right). Bottom left: long axis of left lobe with measurement calipers, right: power Doppler. Color and power Doppler imaging shows marked hypervascularity

hypoechogenicity persists for life. The thyroid parenchyma may appear pseudolobulated due to the presence of fibrous septae. Color Doppler may show increased vascularity of the parenchyma (Fig. 9.10, right top and bottom) likely due to TSH actions. A small and atrophic gland represents the end stage of Hashimoto's thyroiditis, due to the destructive nature of the disease. Other findings include a coarse and heterogeneous internal structure containing a proliferation of hyperperfused vessels.

9.11 Goiter

Goiter is an enlargement of the thyroid that is associated with hyperthyroidism, but perhaps surprisingly, also associated with certain forms of hypothyroidism and euthyroidism. The terms hyperthyroid, hypothyroid, and euthyroid describe, respectively, the clinical states of excess thyroid hormone, deficiency of thyroid hormone, and normal levels of thyroid hormone. Thus, they describe blood levels of thyroid hormone, not the size of the thyroid gland. Goiter can be definitively diagnosed only

by analyzing the etiology of the various thyroid disorders. The central principle in understanding goiter is that high levels of TSH and substances that act like TSH (e.g., thyroid-stimulating immunoglobulins) have a trophic (growth) effect on the thyroid and cause it to enlarge.

Worldwide, the most common cause of goiter is lack of iodine in the diet; however, in the USA, where the standard use of iodized salt greatly decreases iodine deficiency, goiter is more often associated with the over- or under-production of thyroid hormones or nodules that develop in the gland itself. Both lead to a diffuse enlargement and thickening of both lobes of the thyroid gland including the connecting isthmus (Fig. 9.11). As a consequence of iodine deficiency, isoechoic nodules are frequently found within the goiter, and cysts or regressive calcifications often develop in these nodules, which if they are large and form on the surface of the gland, may be palpable and visibly protrude on the organ surface. As degeneration of thyroid parenchyma progresses, the cysts can grow very large and display central hyperechoic hemorrhages. It is noteworthy that less than 1% of these patients display malignant degeneration of hyper- or isoechoic nodules. Note that the US picture of Graves' disease may be indistinguishable from Hashimoto's thyroiditis (Fig. 9.10), but the clinical picture varies significantly. In addition, the US findings for the diseases can vary and may or may not be present in individual patients (Table 9.2).

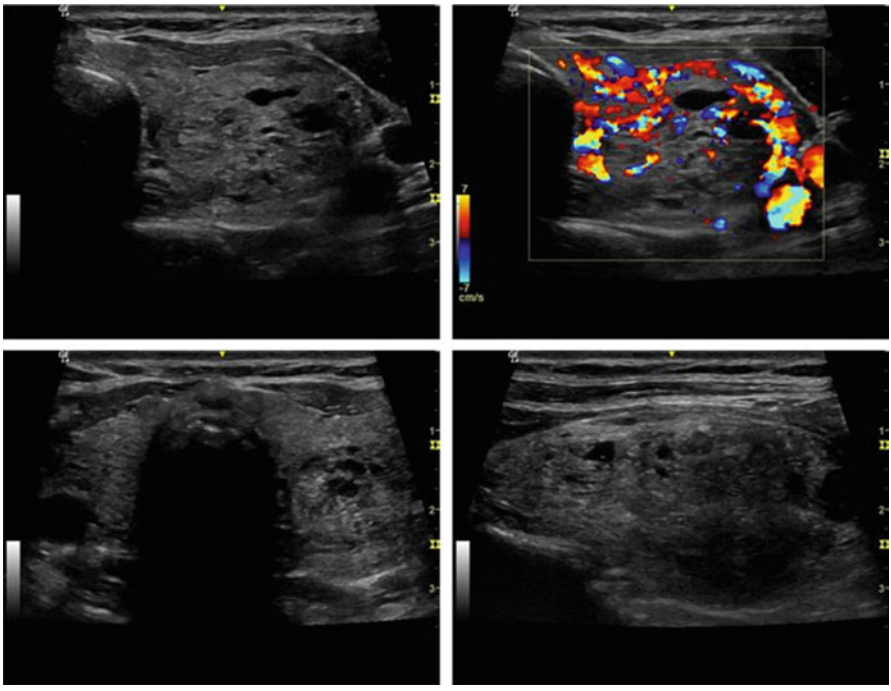

Fig. 9.11 Thyroid gland of a patient with a goiter. Top left: left lobe transverse, same lobe with color Doppler (top right), bottom left entire gland transverse, bottom right longitudinal

Table 9.2 Thyroid Hormone Pathology and US appearance

	Hyperthyroidism	Hypothyroidism
Symptoms	Increased basal metabolic rate Weight loss Negative nitrogen balance Increased heat production Sweating Increased cardiac output Dyspnea (shortness of breath) Tremor, muscle weakness Exophthalmos Goiter	Decreased basal metabolic rate Weight gain Positive nitrogen balance Decreased heat production Cold sensitivity Decreased cardiac output Hypoventilation Lethargy, mental slowness Drooping eyelids Myxedema Growth restriction Cognitive impairment (perinatal) Goiter
Causes/diseases	Graves' disease (increased thyroid-stimulating immunoglobulins) Thyroid neoplasm Excess TSH secretion Exogenous T_3 or T_4 (factitious)	Autoimmune or Hashimoto thyroiditis Surgery for hyperthyroidism I^- deficiency Congenital (cretinism) Decreased TRH or TSH
TSH levels	Decreased (feedback inhibition of T_3 on the anterior lobe) Increased (if defect is in anterior pituitary)	Increased (by negative feedback if primary defect is in thyroid gland) Decreased (if defect is in hypothalamus or anterior pituitary)
US appearance (only frequently observed findings)	Diffusely enlarged gland (~2–3×), hypoechoic and heterogeneous, hyper vascularity on color Doppler "thyroid inferno"	Focal or diffusely enlarged gland, coarse heterogeneous and hypoechoic parenchymal echo pattern, multiple hypoechoic micronodules (1–6 mm), fibrous echogenic septae can create a pseudolobulated appearance of the parenchyma, increased vascularity on color Doppler
Treatment	Propylthiouracil (inhibits peroxidase enzyme and thyroid hormone synthesis) Thyroidectomy $^{131}I^-$ (destroys thyroid) β-Adrenergic blocking agents (adjunct therapy)	Thyroid hormone replacement therapy

Quick facts
The thyroid gland is located in the middle of the lower neck.
Although the thyroid gland is relatively small, it produces a hormone that influences almost every cell, tissue and organ in the body.
Hypothyroidism is a condition where the thyroid gland does not produce enough thyroid hormone. Symptoms include extreme fatigue, depression, forgetfulness, and some weight gain.
Hyperthyroidism, another form of thyroid disease, is a condition causing the gland to produce too much thyroid hormone. Symptoms include irritability, nervousness, muscle weakness, unexplained weight loss, sleep disturbances, vision problems and eye irritation.
Graves' disease is a type of hyperthyroidism; it is an autoimmune disorder that is genetic and estimated to affect one percent of the population.

9.11.1 Exercise 1: Midline Transverse View of the Thyroid Gland and the Surrounding Structures

9.11.1.1 Learning Objectives

Identify the thyroid gland and surrounding structures in the transverse plane. The midline transverse view enables you the opportunity to compare both lobes in the same image.

9.11.1.2 Type of Transducer/Probe

The high frequency linear probe is used due to the thyroid gland lying shallow to the neck's surface.

9.11.1.3 Patient Position and Image Orientation

Supine, neck extended with chin lifted (Fig. 9.12).

An orientation marker, usually the company logo, will be on the top left side of the ultrasound screen. The logo matches up with the probe marker, often a palpable ridge on one side of the probe.

On a transverse view, structures on the left side of the screen are closer to the patient's right side. On a longitudinal view, structures on the left side of the screen are closer to the patient's head. The top of the screen is always superficial or where the probe makes contact with the body surface.

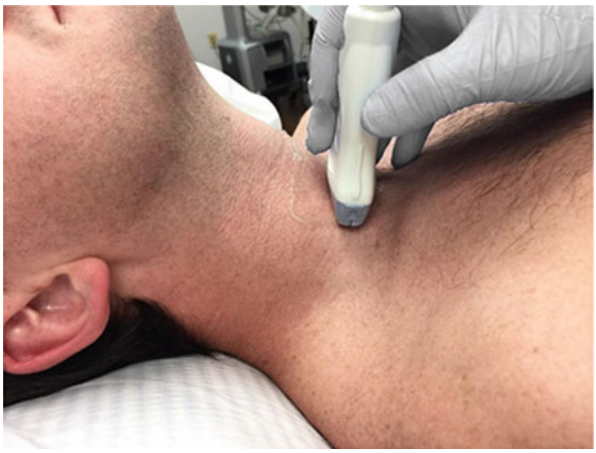

Fig. 9.12 Transverse scan of the thyroid gland in the midline of the neck with the probe marker pointing toward the patient's right side

9.11.1.4 Performing the Transverse View of the Thyroid Gland

1. Place the probe in the transverse position by pointing the probe marker towards the patient's right.
2. Place the probe on the neck midline. Sweep and fan the probe inferior and superior until you can identify thyroid tissue.
3. In the midline transverse view, you should be able to identify the isthmus and both the right and left lobes.
4. Once you have the isthmus and both lobes in view, freeze the image. Identify the surrounding landmarks as shown in Fig. 9.13. Compare the size and appearance

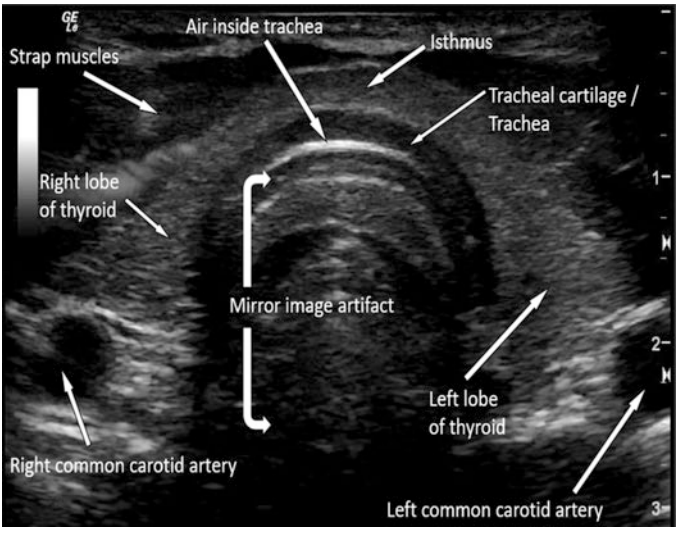

Fig. 9.13 Transverse view of the thyroid gland in the midline of the neck

of the right and left lobes. The isthmus and both lobes of the thyroid gland have a uniform/homogenous echotexture and have smooth margins. The thyroid tissue is slightly more echogenic (brighter) as compared to the overlying strap muscles due to higher iodine content.
5. Note the mirror image of the thyroid isthmus and the tracheal cartilage deep to the strong reflector of air in the trachea.
6. With the subject in a sitting position, capture a good transverse view of the thyroid gland and ask the subject to swallow. You will note that the thyroid gland moves superiorly out of ultrasound view with swallowing and returns after the swallowing. Swallowing is often part of the physical exam of the neck as it helps identify the thyroid tissue when it slides under the examiner's fingers.

9.11.2 Exercise 2: Using Ultrasound to Observe and Obtain Thyroid Volume

9.11.2.1 Learning Objectives

Identify the thyroid gland and obtain left and right lobe measurements for a volume calculation.

9.11.2.2 Type of Transducer/Probe

The high frequency linear probe is used due to the thyroid's superficial position in the neck.

9.11.2.3 Patient Position and Image Orientation

Supine, neck extended. While scanning one side of the thyroid gland, it may be helpful for the patient's head to be tilted towards the opposite side ~45°.

On a transverse view, structures on the left side of the screen are closer to the patient's right side. On a longitudinal view, structures on the left side of the screen are closer to the patient's head. The top of the screen is always superficial or where the probe makes contact with the body surface.

9.11.2.4 Calculating Thyroid Volume

1. Place the probe in the transverse position by pointing the probe marker towards the patient's right.

2. Place the probe on the neck, midline. Sweep and fan the probe inferior and superior until you identify thyroid tissue.
3. Once you identify the thyroid slide the probe lateral to the patient's left to visualize the left lobe. Once you are directly on the left lobe fan or sweep the probe superior and inferior to visualize the entire left lobe in the transverse plane.
4. Adjusting the Gain may help bring the image into view more clearly. The lumen of the blood vessels should appear black (anechoic). Note that the internal jugular vein (IJV) is generally located just lateral and slightly anterior to the common carotid artery and is deep to the sternocleidomastoid (SCM) muscle but the position may show considerable individual variation.
5. Stop in the widest area of the left thyroid lobe and freeze your image.
6. Activate the measuring tool on the machine and place the calipers on the lateral and medial edges of the thyroid to acquire the left thyroid lobe width measurement as in Fig. 9.14.
7. While in the transverse plane, rotate the transducer clockwise until the transducer marker is pointing superior while trying to keep the thyroid tissue in view.
8. Sweep or fan the transducer medial and lateral to observe all the thyroid tissue of the left lobe.
9. Obtain a longitudinal mid left lobe image (when you can see the most thyroid tissue). Once you freeze the image, activate the measurement tool. You will do two measurements in the longitudinal plane. Place the calipers on the superior and inferior edges of the thyroid to obtain the thyroid height/length measurement. Place the calipers on the anterior and posterior edges to obtain the thyroid anterior-posterior measurement or depth (Fig. 9.15).

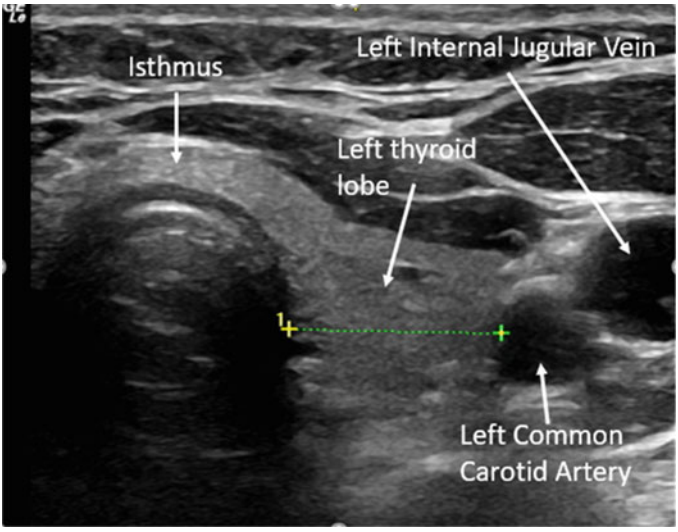

Fig. 9.14 Mid-transverse view of the left lobe of the thyroid gland. The calipers are placed to measure the width of the left lobe

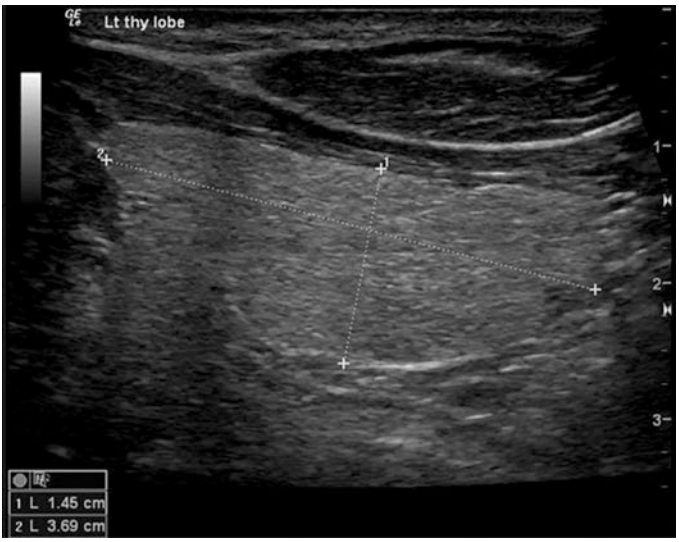

Fig. 9.15 Mid-longitudinal view of the left lobe of the thyroid gland. The calipers are placed to measure the height and the AP (depth) dimension of the left lobe

10. If time permits, repeat the above procedure on the patient's right side to obtain measurements of the right lobe.

Each lobe has a smooth globular-shaped contour and should be no more than **3–4 cm in height, 1–1.5 cm in width, and 1 centimeter in depth (AP)**. The isthmus is identified anterior to the trachea as a uniform structure that is approximately **0.5 cm in height and 2–3 mm in depth.** The small depth of the isthmus of the thyroid can make it quite difficult to feel on physical examination.

Volume Calculation of a Lobe of Thyroid Gland

$$\text{Thyroid Lobe Volume (cc)} = \text{Height} \times \text{Width} \times \text{Depth} \times 0.523 \text{ (ellipse formula)}.$$

Thyroid Volume Calculation

$$\text{Total thyroid volume} = \text{Volume of left lobe} + \text{Volume of right lobe}.$$

Normal Range

$$\text{Normal thyroid volume (both left} + \text{right lobe) range is } \mathbf{6.6 - 14.9\ cc}.$$

Further Reading

American Thyroid Association. https://www.thyroid.org/media-main/press-room/
Chaudhary V, Bano S (2013) Thyroid ultrasound. Indian J Endocrinol Metab 17(2):219–227
Holmes D (2016) Thyroid cancer: incidence trends in the USA. Nat Rev Endocrinol 12(6):312
Lyu YJ et al (2019) Ultrasound-guided fine-needle aspiration biopsy of thyroid nodules <10 mm in the maximum diameter: does size matter? Cancer Manag Res 11:1231–1236
Mao Y, Xing M (2016) Recent incidences and differential trends of thyroid cancer in the USA. Endocr Relat Cancer 23(4):313–322
Solbiati L et al (2001) Ultrasound of thyroid, parathyroid glands and neck lymph nodes. Eur Radiol 11(12):2411–2424

Chapter 10
Ultrasound of the Reproductive System

Marlene A. Wilson, Dina Brown, and Lauren Castleberry

10.1 Anatomy and Physiology of Reproductive System

10.1.1 Male Reproduction

The function of the male reproductive system is to continuously produce viable, mature sperm (spermatozoa) and to deliver those sperm to a female's reproductive tract. The first part of this function is accomplished through spermatogenesis (see Fig. 10.1), which occurs continually in males from puberty well into senescence. This process entails mitotic divisions of male germ (stem) cells called spermatogonia into spermatocytes, followed by meiosis to half the number of chromosomes and create haploid spermatids. Spermatids then develop into spermatozoa (sperm) through a process called spermiogenesis. This process causes morphological changes that include a decrease in cytoplasm, an increase in mitochondria, and development of a flagellum for motility. The full process of spermatogenesis and sperm maturation takes ~64–70 days, and it is estimated that adult men produce about 128 million sperm each day after puberty until andropause. The basic anatomy of the male reproductive system is illustrated in Fig. 10.1.

Supplementary Information The online version contains supplementary material available at https://doi.org/10.1007/978-1-0716-1863-9_10. The videos can be accessed by scanning the related images with the SN More Media App.

M. A. Wilson (✉) · D. Brown
University of South Carolina School of Medicine, Columbia, SC, United States
e-mail: Marlene.Wilson@uscmed.sc.edu; Dina.Brown@uscmed.sc.edu

L. Castleberry
Lexington Medical Center, West Columbia, SC, USA
e-mail: lxcastleberry@lexhealth.org

L. B. Wilson et al. (eds.), *Understanding Physiology with Ultrasound*, Physiology in Health and Disease, https://doi.org/10.1007/978-1-0716-1863-9_10

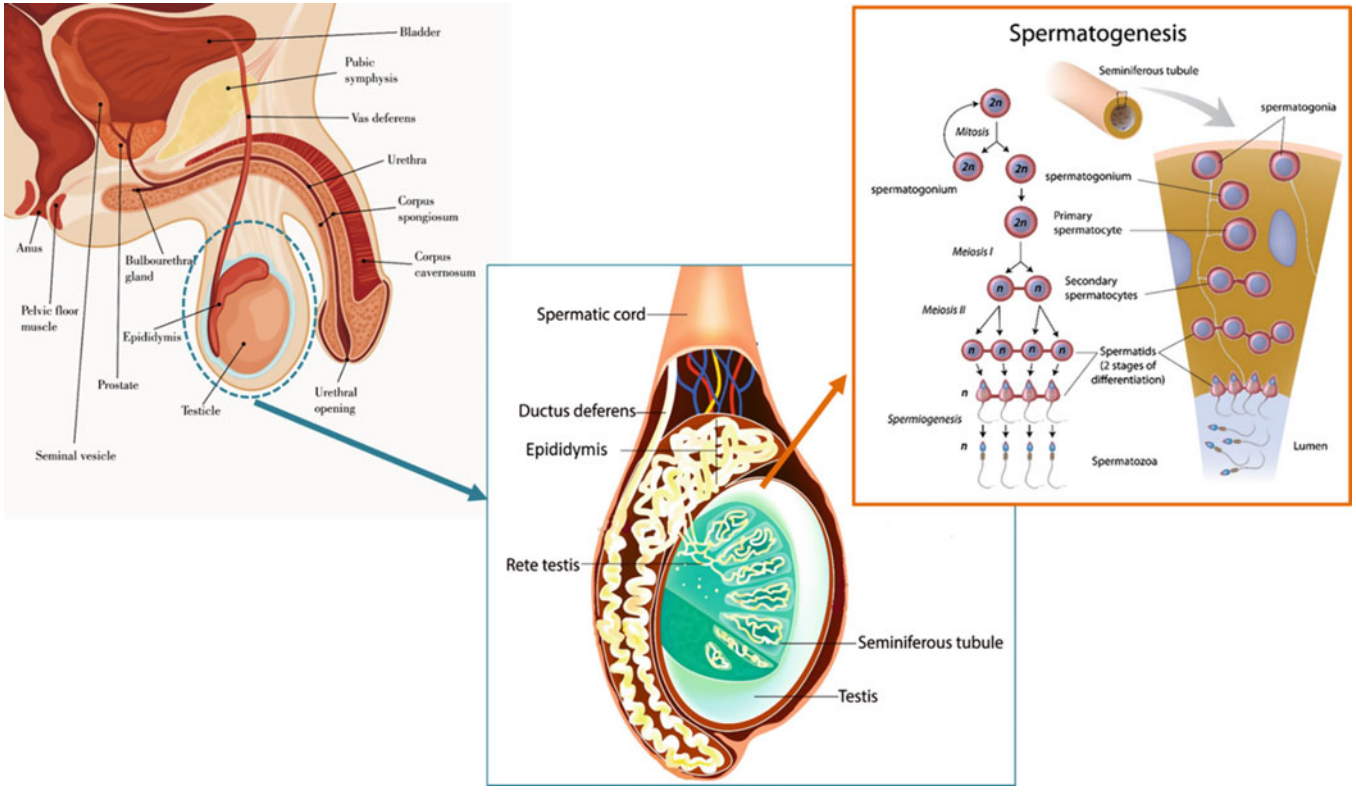

Fig. 10.1 Male reproductive system. The male reproductive tract includes the male gonads or testes, plus the epididymis, vas deferens, and penis, as well as several male accessory glands such as the prostate gland and seminal vesicles. Spermatogenesis takes place in the seminiferous tubules of the testes, and motile spermatozoa (sperm) are collected through the rete testes for storage in the epididymis. Sertoli cells in the seminiferous tubules of the testis surround and support spermatogenesis, while Leydig cells of the testes produce testosterone. During the ejaculatory process, sperm travel through the vas deferens, then the ejaculatory ducts, and into the urethra

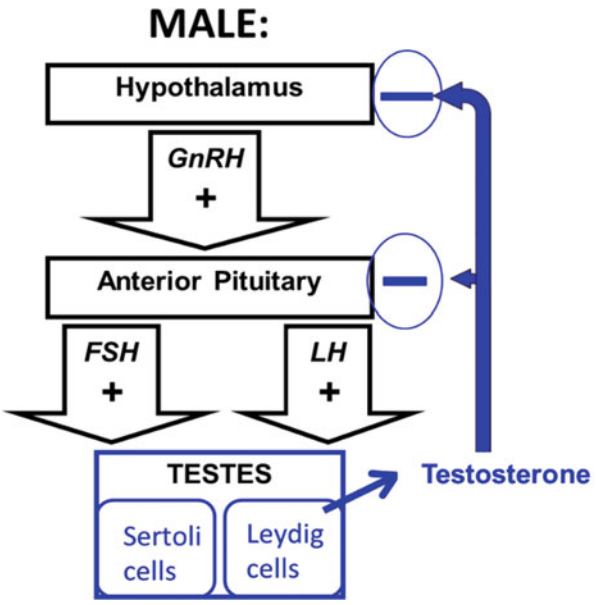

Fig. 10.2 Hypothalamic-Pituitary-Gonadal (HPG) axis in males. The hypothalamus secretes gonadotropin releasing hormone (GnRH) into the hypophyseal portal system to stimulate the anterior pituitary gland to secrete luteinizing hormone (LH) and follicle stimulating hormone (FSH) into the circulation. LH and FSH act on the testes to simulate production of the gonadal steroid hormone testosterone, as well as support spermatogenesis in males. The testosterone secreted from Leydig cells of the testes controls GnRH, LH, and FSH release through negative feedback regulation at the hypothalamus and pituitary

The Male Hypothalamic-Pituitary-Gonadal (HPG) Axis The two primary functions of the male testes, which are spermatogenesis and secretion of the male androgenic steroid hormone testosterone, are regulated by the hypothalamic-pituitary-gonadal (HPG) axis. As seen in Fig. 10.2, in this neuroendocrine feedback system, the hypothalamus produces a peptide hormone called gonadotropin releasing hormone (GnRH) and secretes it into the hypophyseal portal system, which carries GnRH to the anterior pituitary gland. GnRH stimulates the anterior pituitary cells (called gonadotrophs) to produce and secrete the two gonadotropic hormones, luteinizing hormone (LH) and follicle stimulating hormone (FSH) from the anterior pituitary. After puberty, GnRH secretion from the hypothalamus occurs in a pulsatile manner to regulate pituitary release of these two glycoprotein hormones. Luteinizing hormone stimulates testosterone production from Leydig cells of the testes, while FSH stimulates spermatogenesis and supports Sertoli cell function. The high local concentration of testosterone produced from Leydig cells in the testes is critical for maintaining spermatogenesis. Testosterone, which is a steroid hormone derived from cholesterol, is secreted from the testes into the bloodstream where it can influence cells throughout the body and the brain. In some tissues, like the prostate gland and corpora cavernosa, testosterone is converted to an even more potent

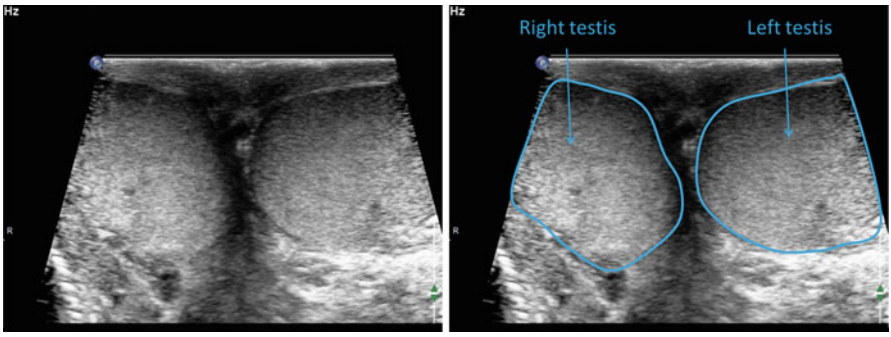

Fig. 10.3 Ultrasound of both right and left testes in adult male. The testes are located outside the body cavity in the scrotum to maintain a lower temperature and promote spermatogenesis

androgen dihydrotestosterone (DHT). These androgens support male reproductive functions by not only maintaining spermatogenesis in the testes, but also male accessory gland function and erectile function required for delivering sperm to the female. In the brain, testosterone feeds back onto the hypothalamus and pituitary gland in a negative feedback loop to regulate GnRH and LH secretion. Therefore, if testosterone levels fall too low, this negative feedback loop increases GnRH and LH secretion to enhance testosterone secretion (see Fig. 10.2).

The Testes and Spermatogenesis The process of spermatogenesis takes place in the male gonads or testes. In humans, as seen in Fig. 10.1, the testes are located outside the body cavity in the scrotum to maintain the temperature in the testes 1.5–3 °C below body temperature. Both testes can be seen using ultrasound (Fig. 10.3). The reduced temperature of the testes is essential for the normal process of spermatogenesis to occur. Spermatogenesis in the testes takes place in loops of seminiferous tubules that contain not only the spermatogonia and spermatocytes, but support cells called Sertoli cells. Sertoli cells provide nutrients to differentiating sperm, secrete fluid into the lumen of the seminiferous tubules for sperm storage and transport, and create the blood-testes barrier by forming tight junctions that protect the developing sperm from the male's immune system and other insults. Located outside the seminiferous tubules is the other major cell type of the testes called Leydig cells. Leydig cells play a critical role in male reproductive physiology since they synthesize and secrete the primary male sex steroid hormone testosterone.

Erection, Emission and Ejaculation The second primary function of the male reproductive system is the delivery of viable spermatozoa (sperm) into the female reproductive tract through the processes of erection, emission, and ejaculation. The sperm exit the seminiferous tubules via ducts and are stored in the epididymis (see Fig. 10.1), where they can remain viable for several months. Figure 10.4 shows an ultrasound image of a testis and the associated epididymis (note epididymal head) where sperm storage occurs. The male reproductive glands, including the seminal vesicles and prostate gland, add enzymes and secretions, such as fructose, citrate, prostaglandins, fibrinogen, and calcium, to the seminal fluid to provide nourishment

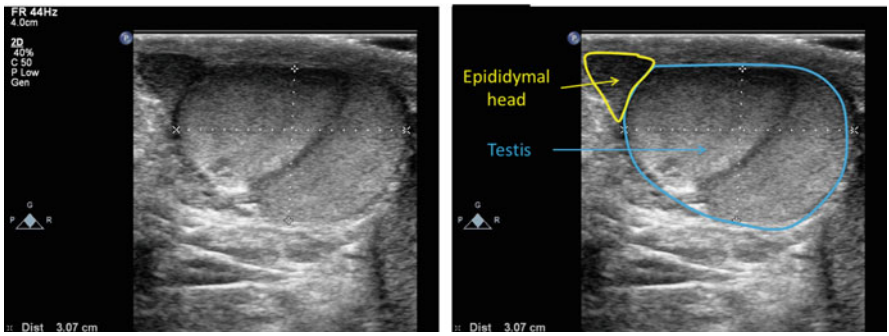

Fig. 10.4 Ultrasound of testis showing head of the epididymis. Sperm are produced in the seminiferous tubules of the testes and are stored in the epididymis

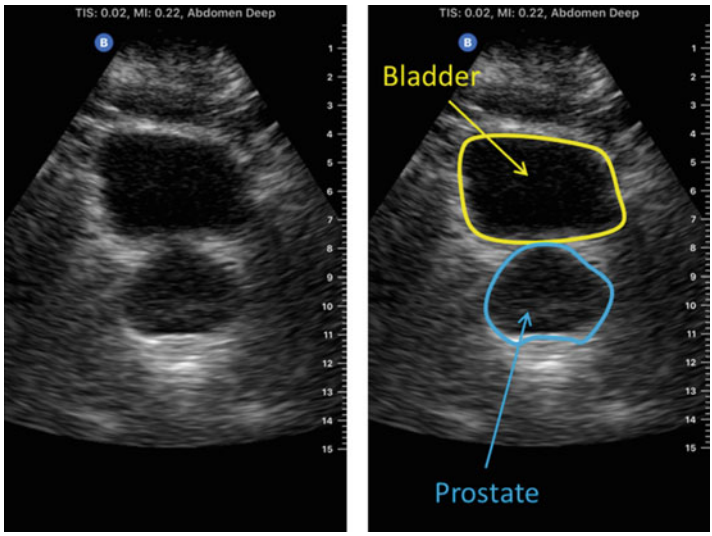

Fig. 10.5 Ultrasound of prostate gland situated below the urinary bladder. The prostate gland adds enzymes and other secretions to the seminal fluid providing nourishment and energy for the sperm during transit to the female reproductive tract. Prostate function is supported by conversion of testosterone secreted from the testes into dihydrotestosterone (DHT), a more potent androgen

and an energy source, as well as enhance sperm motility thereby promoting fertilization. The prostate also secretes prostate specific antigen (PSA), which can be measured in blood; high levels suggest a patient may have prostate hypertrophy. As seen in the ultrasound image in Fig. 10.5, the prostate gland is located near the urinary bladder (also see diagram in Fig. 10.1). Upon sexual arousal, the sperm are moved from the epididymis, along the male reproductive tract through the vas deferens, and into the urethra by smooth muscle contractions. Penile erection is the result of blood filling the corpora cavernosa due to vasodilation induced by

activation of the parasympathetic nervous system. Emission refers to the movement of sperm and seminal fluid into the urethra, and this is mediated by activation of the sympathetic nervous system. This sympathetic activation also closes the internal sphincter of the bladder, thereby preventing the ejaculate from entering the bladder. Activation of motor nerves cause rhythmic contractions and ejaculation of sperm.

10.1.2 Some Common Clinical Ultrasound Applications for Male Reproductive Physiology

Ultrasonography is used in many clinical applications, as well as in training health professionals. A few of the more common clinical uses are listed below.

Male Ultrasonography-Testes

- Testicular torsion (rotation of the testicles that twists the spermatic cord bringing blood to the scrotum, causing pain and swelling).
- Abnormal collection of peri-testicular fluid.
- Evaluation of trauma or hematoma.
- Testicular infection or inflammation.
- Testicular neoplasms and tumors.
- Varicocele (enlarged veins in the scrotum).
- Cryptorchidism (undescended testicles).

Male Ultrasonography-Prostate Gland

- Prostate hypertrophy and cancer.

10.2 Female Reproduction

In contrast to male reproductive physiology, the female reproductive process orchestrates a variety of hormonal and physiological changes to produce one mature ovum during every reproductive cycle or menstrual cycle (typically around 28 days), to promote successful implantation of a fertilized ovum in the uterus and maintain the developing fetus during pregnancy until parturition. In females, oogonia (germ cells) are only produced during gestation, and the oogonia begin meiosis and become oocytes up until 6 months after birth. They will not complete meiosis to become haploid until after fertilization. In addition, there is significant loss of oocytes during a woman's life, with ~2 million at birth, 400,000 at puberty and only a few remaining at menopause.

The female reproductive tract consists of the female gonads or ovaries, the fallopian tubes, the uterus, the cervix, and the vagina (see Fig. 10.6). As seen in this figure, the uterus also consists of several layers, including the inner endometrium and the outer muscle layer or myometrium that can be distinguished using

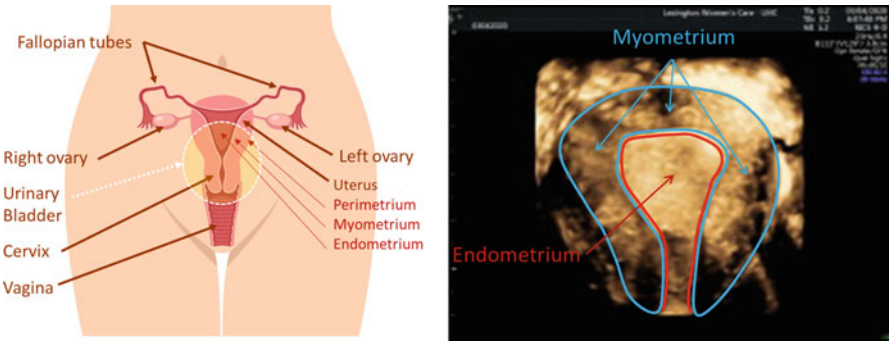

Fig. 10.6 The female reproductive system. The female reproductive tract includes the female gonads or ovaries, the fallopian tubes, the uterus, the cervix, and the vagina. The uterus consists of several layers, including the inner endometrium and the outer muscle layer or myometrium. The endometrium and myometrium can be distinguished using either two-dimensional or three-dimensional coronal ultrasound imaging. 3D imaging helps provide an optimal image of the uterus contour

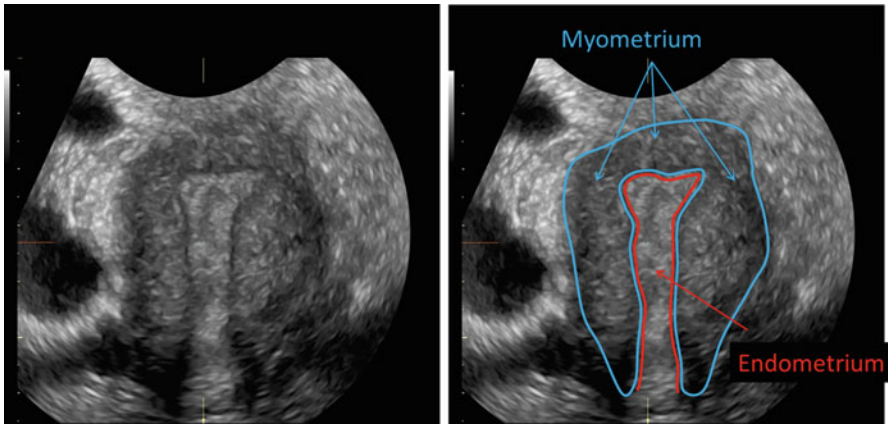

Fig. 10.7 Three-dimensional coronal ultrasound image of normal female uterus. The outer uterine myometrium has a hypoechoic appearance and contrasts with the inner hyperechoic appearance of the endometrial cavity and cervical canal

ultrasound. As seen in Figs. 10.6 and 10.7, using three-dimensional (3D) coronal imaging, the outer uterine muscle layer or myometrium has a hypoechoic appearance, which contrasts with the inner hyperechoic appearance of the endometrial cavity and cervical canal. The normal myometrium has a homogenous echogenicity with smooth outer margins.

The Hypothalamic-Pituitary-Gonadal (HPG) Axis The regulation of oogenesis and ovarian secretion of estrogen and progesterone fluctuate over the menstrual cycle, and this is controlled by the hypothalamic-pituitary-gonadal (HPG) axis. As

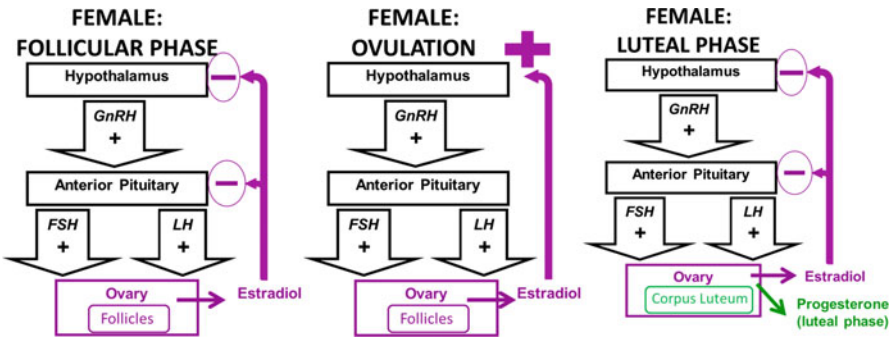

Fig. 10.8 Hypothalamic-Pituitary-Gonadal (HPG) axis in females at different stages of the reproductive cycle. The hypothalamus secretes gonadotropin releasing hormone (GnRH) into the hypophyseal portal system to stimulate the anterior pituitary gland to secrete luteinizing hormone (LH) and follicle stimulating hormone (FSH) into the circulation. LH and FSH act on the ovaries to stimulate production of ovarian steroid hormones (testosterone, estradiol, and progesterone) as well as support follicular development in females. Throughout most of the cycle (follicular phase, luteal phase) estradiol secreted from developing follicles exerts negative feedback regulation of GnRH, LH and FSH release from the hypothalamus and pituitary. Just before ovulation at mid-cycle, estradiol exerts positive feedback regulation at the hypothalamus to trigger the LH surge leading to ovulation of the mature ovum from the Graafian follicle. After ovulation, the negative feedback exerted by estradiol returns, similar to what is seen in the follicular phase

seen in Fig. 10.8, this neuroendocrine feedback system is similar to that seen in the male. The hypothalamus secretes GnRH into the hypophyseal portal system, where GnRH stimulates the production and secretion of luteinizing hormone (LH) and follicle stimulating hormone (FSH) from the anterior pituitary. After puberty, GnRH secretion from the hypothalamus occurs in a pulsatile manner to regulate pituitary release of LH and FSH, although the amplitude and frequency of these pulses shift over the menstrual cycle. Luteinizing hormone stimulates androgen (such as testosterone) production in theca cells of the ovaries, and these androgen precursors are aromatized to estrogens in the granulosa cells of the developing follicles. FSH stimulates follicular development to support oogenesis, as well as stimulating the enzyme that converts androgens to estrogens in granulosa cells. As a steroid hormone, estrogen circulates throughout the body and brain to influence many physiologic functions. For most of the female reproductive cycle, the HPG axis operates in a negative feedback loop, where estrogen secreted from the ovaries feeds back onto the hypothalamus and pituitary gland to regulate GnRH and LH secretion, respectively. Unlike the male, however, during sexual differentiation the female hypothalamus develops the ability to switch into a positive feedback mode. This switch to positive feedback occurs during the late follicular phase just before ovulation, and the increasing levels of estrogen produced from the large, mature (or Graafian) follicle (see below) stimulate GnRH secretion from the hypothalamus to induce a surge in LH. This LH surge is the trigger for ovulation, and once the ovum is expelled, LH induces luteinization of the ruptured follicle into the corpus

luteum. Without this positive feedback loop, estrogens are unable to induce an LH surge and ovulation cannot occur.

The Ovaries and Oogenesis The female gonad is the ovary, which is an oval shaped solid structure found inside the abdominal cavity (see Fig. 10.6). As seen in Fig. 10.9, within the ovary, developing oocytes surrounded by granulosa cells are called an ovarian follicle. Surrounding the follicle are theca cells, which are the female counterpart of male Leydig cells, since they secrete androgen precursors that can be converted to estrogen by the follicle. In the ovary, follicles of different sizes are seen that are at different stages of development (Fig. 10.9, discussed below). Following ovulation of the mature ovum, the follicles transform into the corpus luteum that synthesizes not only estrogen, but the other major feminine gonadal steroid hormone progesterone. After ovulation, the ovum is ready for fertilization by male sperm and is taken into the fallopian tubes to travel to the uterus. If fertilization is successful, the developing fetus implants in the uterine cavity several days later.

The Female Menstrual Cycle By convention, as seen in Fig. 10.9 the female reproductive cycle or menstrual cycle is 28 days, with day 1 being the onset of menstrual bleeding. The reproductive cycle is further divided into the follicular or proliferative phase during days 1–14, and the luteal phase during days 15–28 of the cycle. Ovulation of the mature ovum, ready to be fertilized, occurs at mid-cycle during the transition between the follicular and luteal phases. During the 28-day reproductive cycle, there are fluctuations in the secretion of both estrogen and progesterone, as well as the gonadotropic hormones LH and FSH. As seen in Fig. 10.9b, estrogen and progesterone levels are lowest at menses (early days of the cycle). Estrogen levels increase during the follicular phase causing proliferation of theca and granulosa cells, resulting in growth of the follicle. The follicular phase is also called the proliferative phase because the increases in estrogen also cause thickening of the uterus, as seen in the bottom of Fig. 10.9, as well as cornification of the vaginal epithelium in preparation for coitus. In the late follicular phase, just before ovulation, the hypothalamus switches into positive feedback regulation, and the increasing estrogen levels induce an increase in GnRH release which leads to the LH surge (see Fig. 10.8 and LH surge Fig. 10.9b). This LH surge is the trigger for ovulation of the dominant Graafian follicle, releasing the mature ovum into the peritoneal cavity near the fallopian tubes (Fig. 10.6). After ovulation, the ovum is ready for fertilization by sperm and if fertilization occurs, the second meiotic division occurs. The ruptured follicle transitions to the corpus luteum initiating the luteal or secretory phase of the menstrual cycle, and the corpus luteum begins secreting not only estrogen but progesterone as well. The luteal phase is characterized by high circulating levels of both estrogen and progesterone. Progesterone acts on the uterus to enhance vascularization, and it decreases uterine contractions to allow implantation of the blastocyst in the uterine cavity should successful fertilization occur. The corpus luteum lasts ~14 days, and if fertilization and implantation do not occur it regresses to become the scar-like corpus albicans. Without the corpus luteum, both estrogen and progesterone levels fall rapidly, and without this

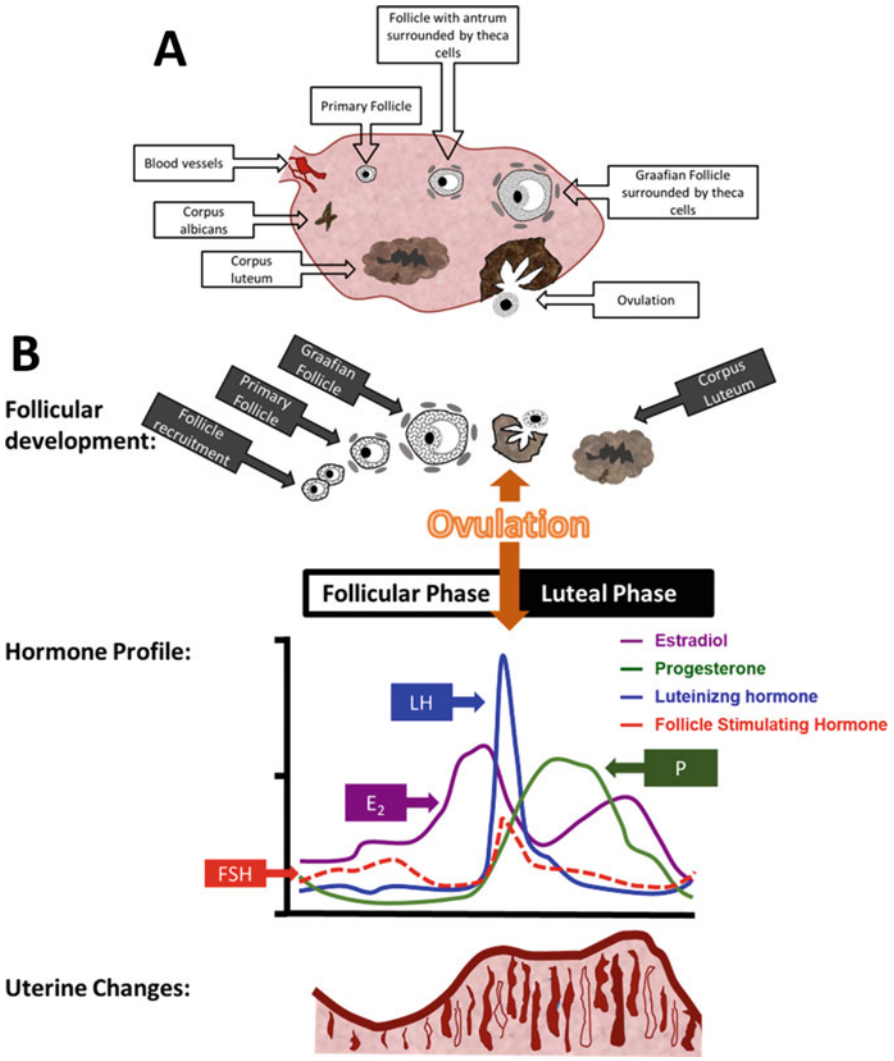

Fig. 10.9 Female follicular development in the ovary and during the reproductive (menstrual) cycle: Panel A (top) diagrams different stages of follicular development seen in the ovary. Each follicle contains a maturing oocyte surrounded by granulosa cells that proliferate as follicles grow and mature. In large Graafian follicles, the ring of granulosa cells is called a cumulus oophorus that will be released with the ovum during ovulation. The follicles are surrounded by theca cells responsible for producing the androgen precursors for estradiol synthesis by the follicle. The 28-day reproductive or menstrual cycle (right panel) is divided into the follicular or proliferative phase (days 1–14) and the luteal or secretory phase (days 15–28), which are separated by ovulation. Panel B (bottom) shows different stages of follicle development, ovulation, and induction of the corpus luteum. The Hormone Profile panel shows changes in estradiol (E_2), progesterone (P), luteinizing hormone (LH), and follicle stimulating hormone (FSH) over the cycle. Note the increase in estradiol during the follicular phase, as the follicle grows, which also leads to the LH surge just prior to ovulation. The increase in estradiol during the follicular phase and progesterone during the luteal phase causes thickening and vascularization of the uterus (bottom panel). As estradiol and progesterone levels decrease at the end of the luteal phase, the uterine lining is sloughed off and menses occurs

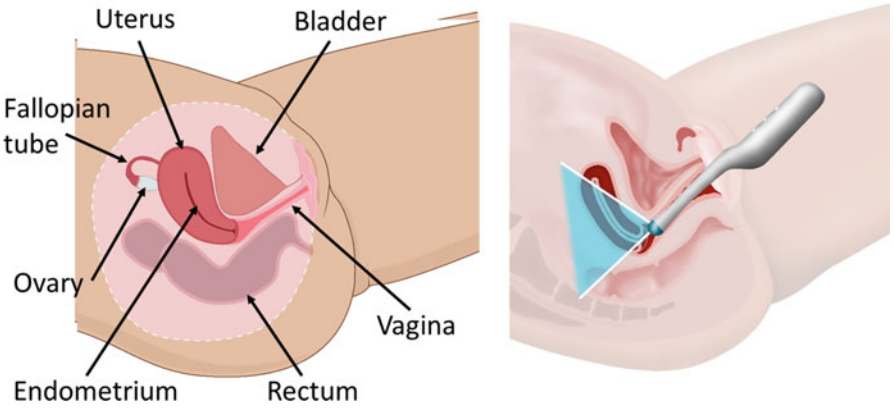

Fig. 10.10 Female reproductive system with endovaginal transducer placement. When placed endovaginally, the ultrasound probe is placed directly against the cervix, preventing interference from any other tissue and allowing for a clearer imaging of female reproductive system changes compared to trans-abdominal imaging

hormonal support, the uterine endometrium is sloughed off and menses occurs to begin the cycle again.

Menstrual Cycle: Uterine Changes Uterine changes over the reproductive cycle can also be seen using ultrasonography, and endovaginal transducer placement illustrated in Fig. 10.10. Endovaginal ultrasound reduces interference from other tissues and allows for a clearer imaging of female reproductive system changes when compared to trans-abdominal imaging. Figures 10.11 and 10.12 show images of normal uteri in the longitudinal plane using endovaginal ultrasonography. The normal uterus during female reproductive years is pear shaped and has a body twice the size of the cervix. The outer contour is flat or slightly convex and the inner endometrial cavity contour is flat. Figure 10.11 shows both anteverted (angles anterior, top panels) and retroverted (angles posterior, bottom panels) uteri, while Fig. 10.12 illustrates the hypoechoic area that is known as the junctional zone of the uterine myometrium. As seen in Fig. 10.13, the normal uterine changes occurring during the reproductive cycle can been seen using endovaginal ultrasonography. During the follicular (proliferative) phase the endometrial uterine lining is mildly echogenic. Due to the effects of increasing estrogen levels from the ovary during the follicular phase, the endometrial lining undergoes gradual thickening from about 4 mm post-menstruation to 12 mm on the day of the LH surge (~day 14). After ovulation, the influences of estrogen and progesterone secreted from the corpus luteum cause the endometrium to maintain thickness and increase vascularization, creating a homogeneous echogenic appearance. If fertilization and implantation do not occur, the corpus luteum regresses, estrogen and progesterone levels fall rapidly, the blood (fluid) can be seen in the endometrial cavity with the onset of menses (see video in Fig. 10.14), starting a new reproductive cycle. Post-menstruation in the early follicular phase the endometrial lining is thin since estrogen levels have not yet

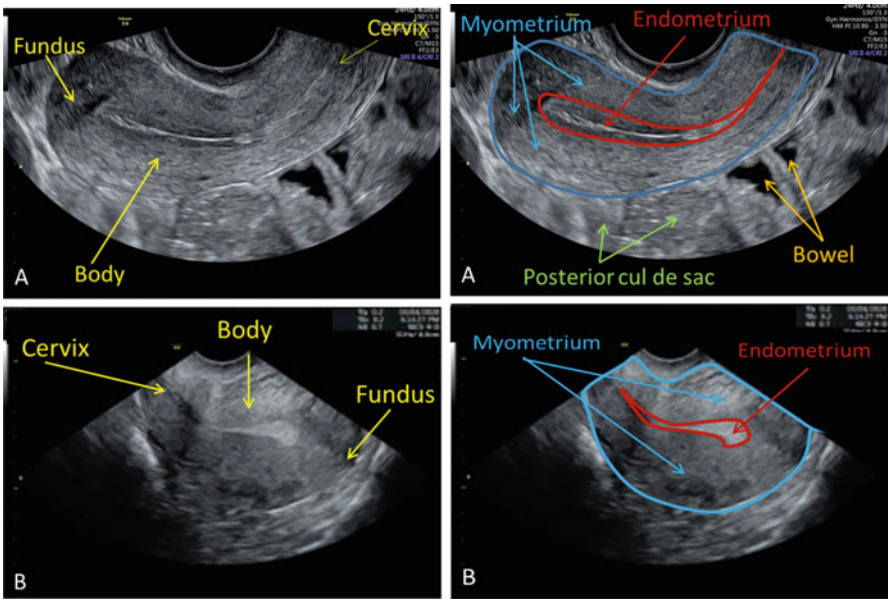

Fig. 10.11 Ultrasound of normal uterus in the longitudinal plane using endovaginal transducer placement. The normal uterus during female reproductive years is pear shaped and has a body twice the size of the cervix. The outer contour is flat or slightly convex and the inner endometrial cavity contour is flat. The top panels (A) show an anteverted uterus (angles anterior), while bottom panels (B) show a retroverted uterus (angles posterior)

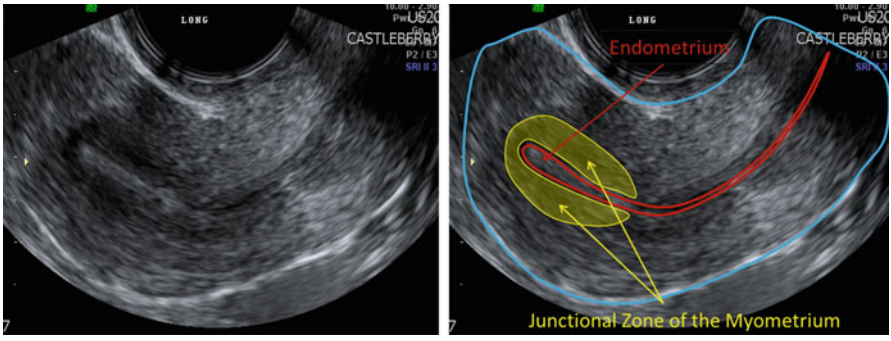

Fig. 10.12 The junctional zone of the uterine myometrium using endovaginal transducer placement. The endometrium is surrounded by a hypoechoic area that is known as the junctional zone. This should not be mistaken for the endometrial echo. Here, the junctional zone of the myometrium is highlighted to demonstrate its distinction from the endometrial echo

increased and you can sometimes see fluid within the endometrial cavity (typically blood; Fig. 10.13, Days 1–4 Menses). This ultrasonography approach can also be used to assess abnormal uterine changes (see below).

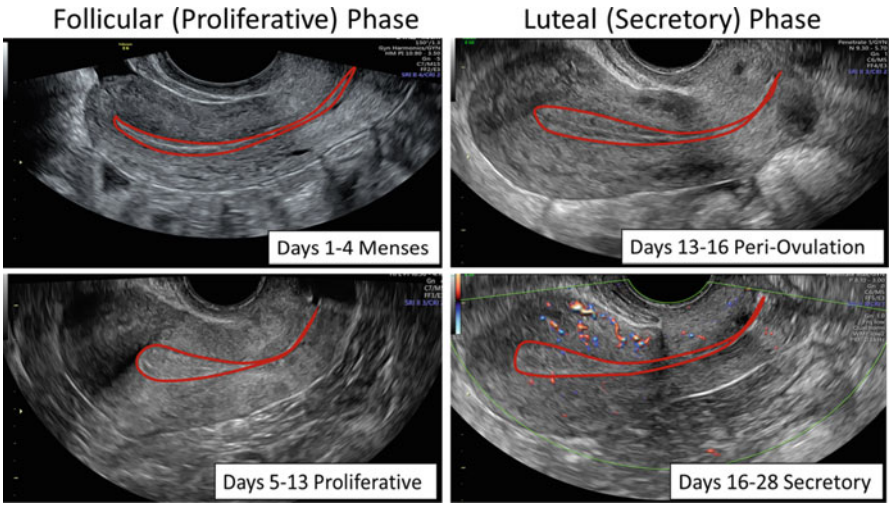

Fig. 10.13 Uterine changes during the female menstrual cycle seen using endovaginal transducer placement. Early in the menstrual cycle during menses (Days 1–4) the thinned endometrial lining appears hyperechoic and fluid (blood) can be seen within the cavity. Later during the follicular or proliferative phase (Days 5–13; bottom left) the endometrial cavity has a mildly echoic appearance and begins to thicken due to increasing estrogen levels. Around ovulation and during the early luteal phase (Days 13–16) the endometrial lining now has a striated appearance, with an inner layer that is relatively hyperechoic surrounded by a more hypoechoic peripheral layer. During the late luteal (secretory) phase (Days 16–28) the endometrial lining becomes more homogenously echoic in response to rising progesterone levels secreted from the corpus luteum. This is just before the beginning of menstruation

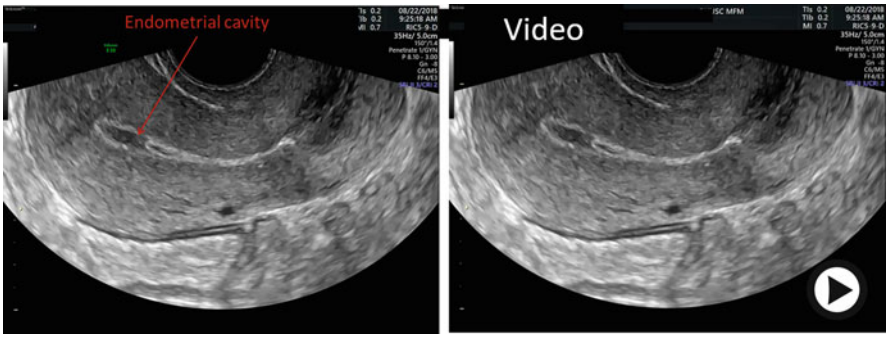

Fig. 10.14 (Video 10.1) Dynamic imaging of endometrial fluid moving in the endometrial cavity. Using cine clips, the intra-cavitary fluid (including blood) is often visible moving within the endometrial cavity at the level of the fundus. This can occur during the menstrual cycle (blood) or as a result of cervical stenosis (narrowed cervical opening) (▶ https://doi.org/10.1007/000-7qq)

Menstrual Cycle: Ovarian Changes After menarche, a few ooctyes in the small, primary follicles begin the process of oogenesis (see Fig. 10.9). During the final stage of follicular development one single follicle becomes a dominant, Graafian follicle that progresses on to ovulation, while the other follicles regress. Since the full maturation of an oocyte and development of a mature follicle requires ~70 days, this indicates that oogenesis spans more than two reproductive cycles. During the follicular phase, as estrogen levels increase, granulosa cells proliferate and the follicle grows in size and develops a fluid filled cavity or antrum. Ultrasonography of the ovary can detect follicles of different sizes and stages of maturation as seen in Fig. 10.15. For example, the dominant Graafian follicle becomes prominent during the late follicular phase when estrogen levels are high just before ovulation, and the oocyte surrounded by granulosa cells (called the cumulus oophorus) can be seen within the growing follicle (see Figure 10.15c and video in Fig. 10.16). After ovulation, the corpus luteum, which is responsible for secreting high levels of both estrogen and progesterone during the luteal phase, is seen in Figure 10.15d.

Pregnancy Once in the vagina, the spermatozoa travel up the female reproductive tract aided by contractions of the uterus, and successful fertilization of the ovum usually occurs within ~24 h of ovulation near the fallopian tubes. The fertilized ovum begins dividing and the blastocyst of ~100 cells arrives in the uterine cavity about 4 days after fertilization, where it typically implants, as seen in the ultrasound images in Fig. 10.17. This is dependent upon high levels of progesterone secreted from the corpus luteum, and a high progesterone/estrogen ratio. The outer rim of cells called trophoblasts invade the endometrium and becomes the placenta, which provides nutrients, oxygen/carbon dioxide exchange, disposal of waste, and hormones for the developing fetus. By convention, gestation is 40 weeks, and divided into three trimesters of fetal development. Progesterone levels rise significantly during pregnancy, and are responsible for sustaining the fetus in the uterine cavity by decreasing myometrial (muscle) contractions. Once implantation occurs, the developing fetus secretes the hormone human chorionic gonadotropin (hCG) which prevents the corpus luteum from regressing and maintains progesterone levels during the first trimester. The placenta is the source of progesterone during the second and third trimester. Ultrasonography is widely used to assess fetal development in the uterine cavity. Figure 10.18 shows an ultrasound image of a first trimester fetus and a 4D video of fetal movements *in utero*.

10.2.1 Some Common Clinical Ultrasound Applications for Female Reproductive Physiology

Female Ultrasonography: Uterine

- Transvaginal transducer placement can be used to detect endometrial polyps (Fig. 10.19), fibroids, or evaluate post-menopausal bleeding.

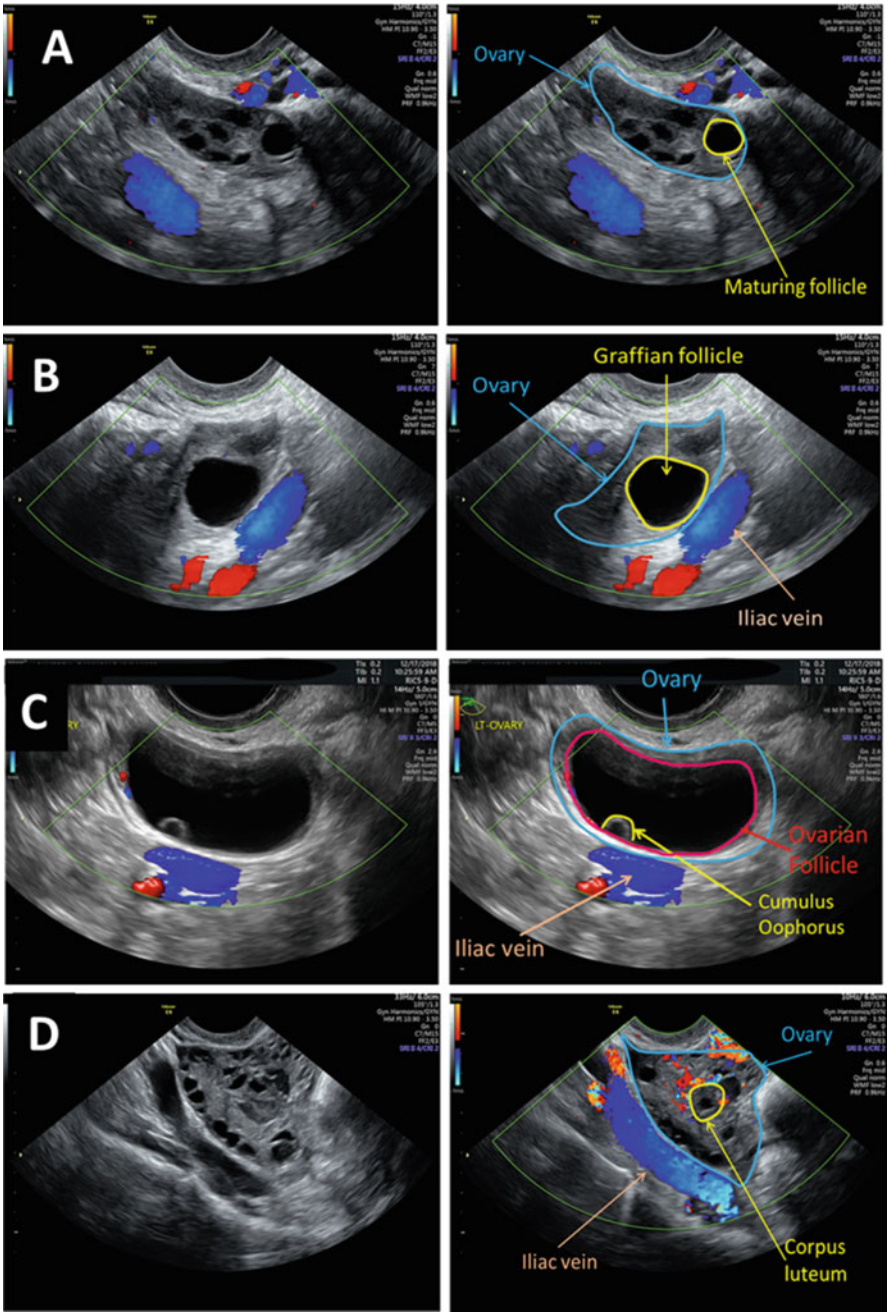

Fig. 10.15 Ovarian follicular changes over the female reproductive cycle. As the follicle grows due to granulosa cell proliferation, the follicle also develops a fluid filled sac called an antrum (Panels A and B). The oocyte with its surrounding granulosa cells, called a cumulus oophorus, can be seen protruding into the large follicle (Panel C). After ovulation, the follicle becomes the corpus luteum (Panel D) and starts secreting both estradiol and progesterone

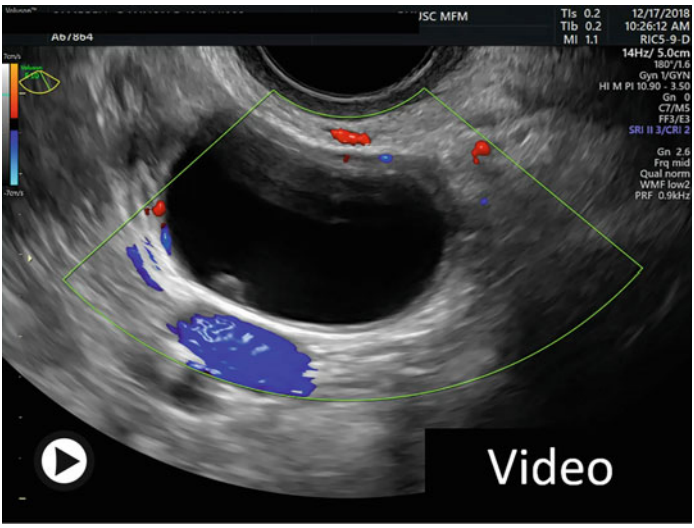

Fig. 10.16 (Video 10.2) A cine clip video demonstrating the oocyte surrounded by granulosa cells, called a cumulus oophorus, seen within the large ovarian follicle. The ovum and cumulus oophorus is released from the Graafian follicle at ovulation (▶ https://doi.org/10.1007/000-7qp)

- Endometrial hyperplasia can also be observed using ultrasonography, which is seen as a thickened endometrium and often has a "swiss cheese" appearance (Fig. 10.20).
- 3D-coronal imaging is used to assess uterine congenital anatomical malformations such as a bicornuate, arcuate, or septate uteri.
- Ultrasound can detect uterine fibroids or adenomyosis (endometrium invades uterine wall).
- Ultrasound is used to check placement of intrauterine devices (IUDs) used for birth control.
- Hydrosalpinx, which is fluid in the fallopian tubes that can impair fertility, can be seen using ultrasonography.

Female Ultrasonography: Ovarian

- Ultrasonography of the ovaries can be used to detect cysts or masses.
- Analysis of follicles or corpus luteum appearance is used to detect polycystic ovarian syndrome (PCOS).
- Evaluation of the number of follicles is used for fertility treatment or assessment.

Female Ultrasonography during Pregnancy

- Determine intra-uterine versus ectopic pregnancy.
- Ultrasound is used to assess fetal development and health.

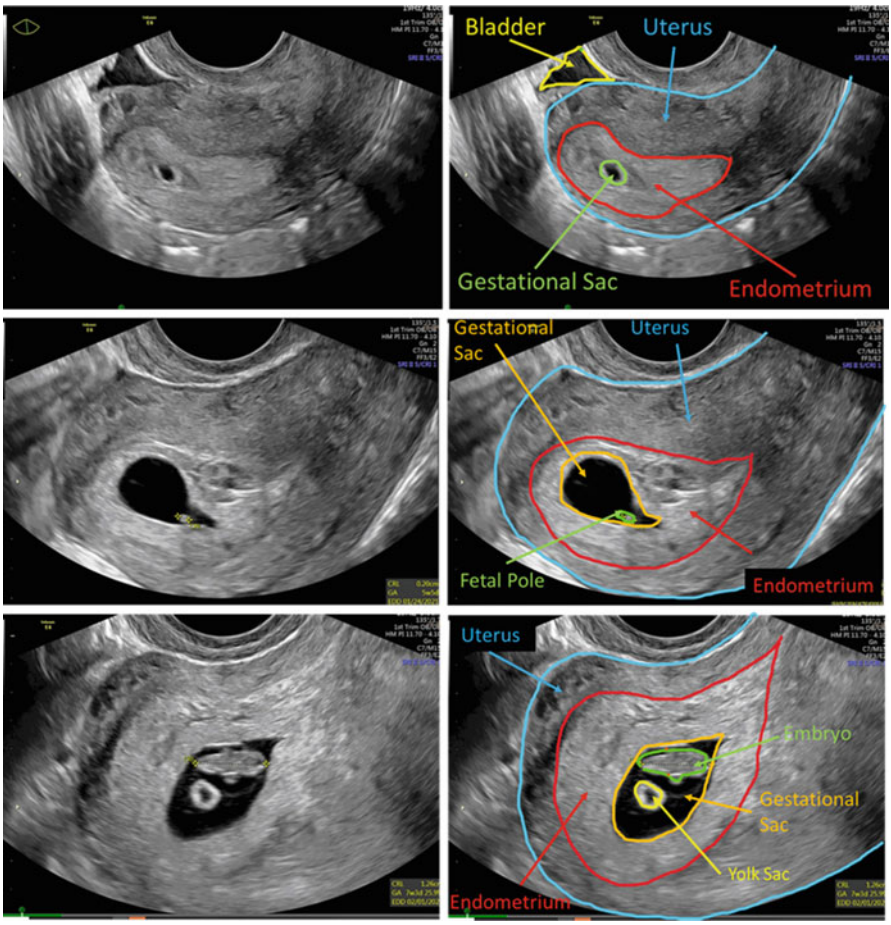

Fig. 10.17 Ultrasound images of the dividing cells of the blastocyst implanted in the uterus (top) and the development of the embryo during early stages of gestation (bottom)

10.3 Laboratory Exercises in Reproductive Physiology

10.3.1 Exercise 1: Observing the Male Pelvis with the Abdominal Approach

10.3.1.1 Learning Objectives

Identify the prostate with the abdominal ultrasound approach.

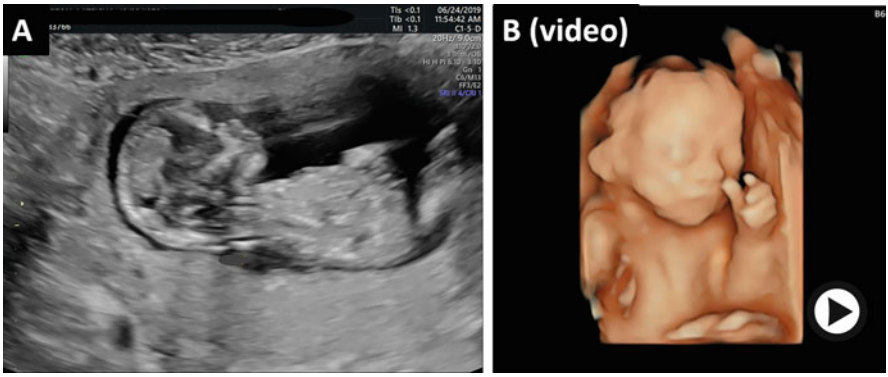

Fig. 10.18 (Video 10.3) Panel A shows ultrasound image of a first trimester fetus. Panel B shows 4D video imaging in real-time of a 20 week fetus performed at the time of an anatomy survey. This video demonstrates the *in utero* fetal movements that make it challenging to obtain measurements of fetal structures and evaluate for fetal anomalies (▶ https://doi.org/10.1007/000-7qr)

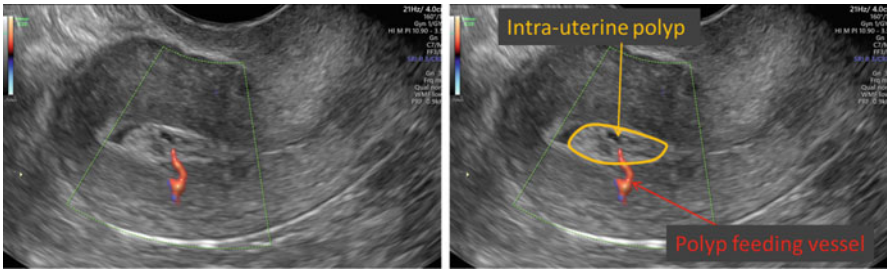

Fig. 10.19 Ultrasound of intra-uterine (endometrial) polyps. Polyps can be distinguished by their hyperechoic appearance that often distorts the endometrial echo. The presence of intra-cavitary fluid can help to further solidify the diagnosis of endometrial polyps. An endometrial polyp with a finger-like projection in the cavity is outlined above. Using color Doppler, as many as half of endometrial polyps will demonstrate a solitary feeding vessel

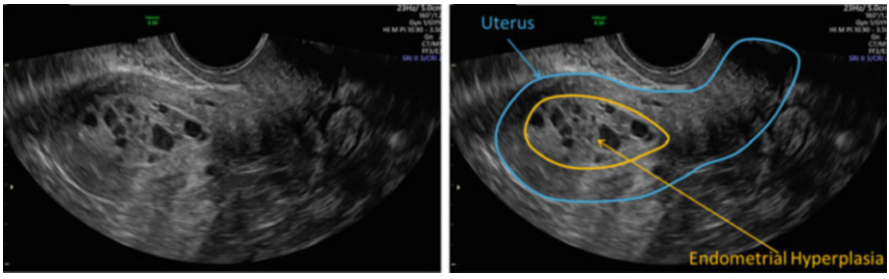

Fig. 10.20 Ultrasound of endometrial hyperplasia. A "swiss cheese" appearance is commonly seen with endometrial hyperplasia, though a tissue diagnosis is required to confirm the diagnosis. The diagnosis of endometrial hyperplasia is also suggested when the endometrial echo is thickened ($\geq$ 4 mm) in the postmenopausal patient

10.3.1.2 Transducer/Probe

Pelvic imaging abdominally is best performed with a low frequency curvilinear probe.

10.3.1.3 Additional Equipment and Supplies

None, other than those related to performing ultrasound.

10.3.1.4 Patient Position and Image Orientation

The patient position should be supine. It is recommended the patient have a full bladder to improve the visualization of the prostate. The full bladder acts as an acoustic window allowing the ultrasound beam to travel well and enhances visualization of the structures deep to the bladder.

An orientation marker, usually the company logo, will be on the top left side of the ultrasound screen. The logo matches up with the probe marker, often a palpable ridge on one side of the probe. On a transverse view, structures on the left side of the screen are closer to the patient's right side. On a longitudinal view, structures on the left side of the screen are closer to the patient's head. The top of the screen is always superficial or where the probe makes contact with the body surface.

10.3.1.5 Performing the Male Abdominal Pelvic Ultrasound

1. Chose a general abdomen preset in the ultrasound settings. Apply adequate gel to the probe.
2. Place the transducer in the suprapubic region just above the drape as shown in Fig. 10.21. The probe marker should point toward the patient's right. Fan the ultrasound beam toward the patient's feet until you visualize the bladder. The bladder appears anechoic (black) on ultrasound.
3. It may be necessary to apply a little pressure to obtain a good image. The prostate will appear hypoechoic and deep to the bladder on this approach. See Fig. 10.22.
4. Most ultrasound evaluation of the prostate is accomplished with transrectal ultrasound. However, you can observe the approximate size of the prostate with the abdominal approach. You can also determine the amount of residual urine in the bladder after voiding. Prostatic enlargement can impair emptying of the bladder and lead to larger residual volumes after voiding.

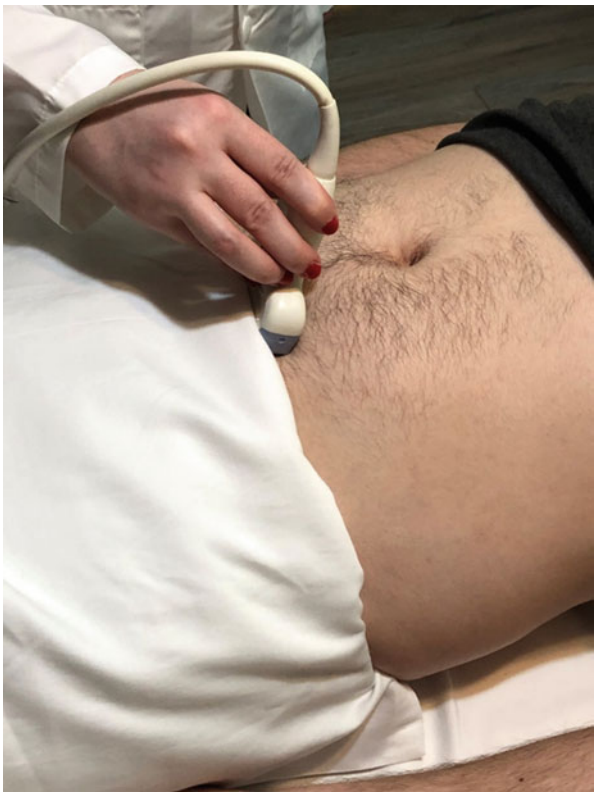

Fig. 10.21 Abdominal Transducer placement for visualizing male prostate gland

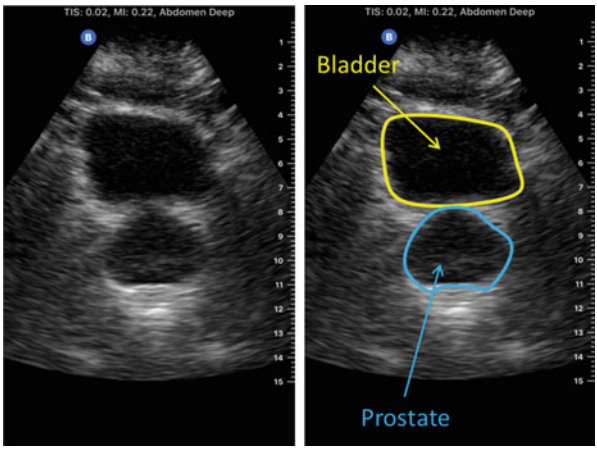

Fig. 10.22 The normal male prostate gland in transverse ultrasound plane. A full urinary bladder will provide an acoustic window to help visualized the prostate abdominally. The prostate is the hypoechoic (darker grey) area inferior to the anechoic (black) bladder

10.3.2 Exercise 2: Observing the Female Pelvis with the Abdominal Approach

10.3.2.1 Learning Objectives

Identify the uterine structures with the abdominal ultrasound approach.

10.3.2.2 Transducer/Probe

Pelvic imaging abdominally is best performed with a low frequency curvilinear probe.

10.3.2.3 Additional Equipment and Supplies

None, other than those related to performing ultrasound.

10.3.2.4 Patient Position and Image Orientation

The patient position should be supine. It is recommended the patient have a full bladder to be able to visualize the uterus. The full bladder acts as an acoustic window allowing the ultrasound beam to travel well and enhances visualization of the structures deep to the bladder.

An orientation marker, usually the company logo, will be on the top left side of the ultrasound screen. The logo matches up with the probe marker, often a palpable ridge on one side of the probe. On a transverse view, structures on the left side of the screen are closer to the patient's right side. On a longitudinal view, structures on the left side of the screen are closer to the patient's head. The top of the screen is always superficial or where the probe makes contact with the body surface.

10.3.2.5 Performing the Female Abdominal Pelvic Ultrasound

Uterus in the Longitudinal Plane

1. Choose a general abdomen preset in the ultrasound settings. Apply adequate gel to the probe.
2. Place the transducer in the suprapubic region just above the drape as shown in Fig. 10.23. The probe marker should be pointed toward the patient's head for the longitudinal view. Rock the ultrasound beam toward the patient's feet until you visualize the bladder and uterus.

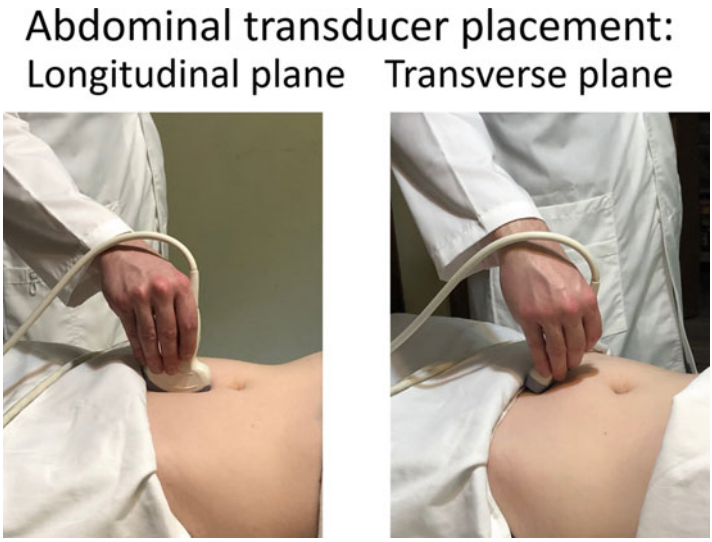

Fig. 10.23 Abdominal Transducer Placement for longitudinal (LEFT) and transverse (RIGHT) imaging of the female uterus

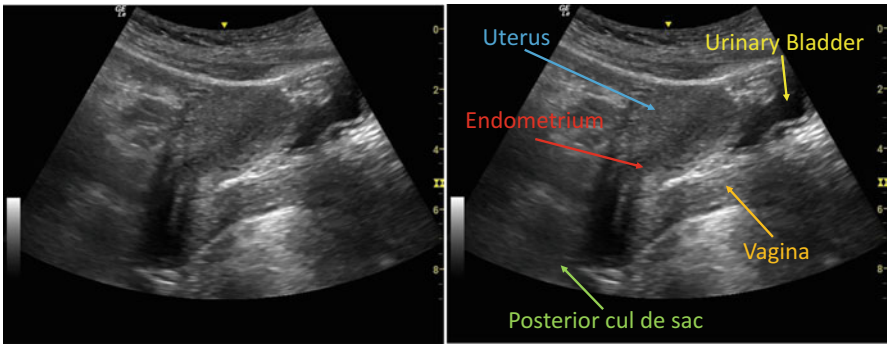

Fig. 10.24 Normal female uterus in the abdominal longitudinal plane. A full urinary bladder will provide an acoustic window to help visualize the uterus abdominally. The uterus appears hypoechoic (darker grey) to the surrounding tissue. Area containing fluid appears anechoic or black on ultrasound. Therefore, the fluid filled urinary bladder appears anechoic (black). The normal uterus during reproductive years is pear shaped and has a body twice the size of the cervix. The outer contour is flat or slightly convex and the inner endometrial cavity contour is flat

3. It may be necessary to apply a little pressure to obtain a good image.
4. Evaluate if the uterus is anteverted or retroverted. With an anteverted uterus the fundus will tilt anteriorly. A retroverted uterus the fundus will tilt posteriorly. See Fig. 10.24 for representative images of an anteverted uterus.

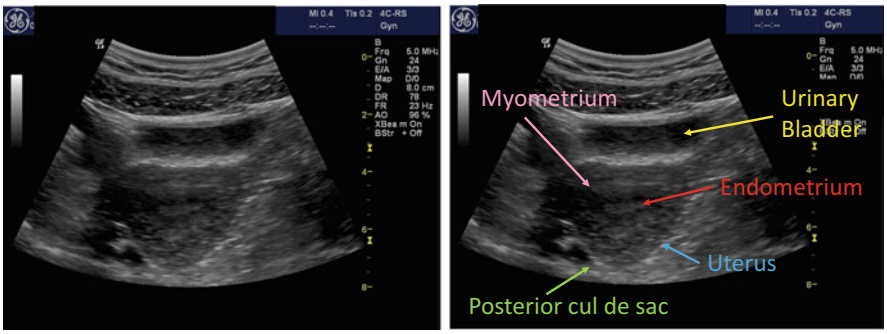

Fig. 10.25 The normal female uterus in the abdominal transverse plane. A full urinary bladder helps provide an acoustic widow to visualize the uterus. The hypoechoic (darker shade of grey) uterus is posterior to the anechoic (black) urinary bladder

5. Observe the uterus and the thickness of the endometrium. Can you identify which phase of the menstrual cycle the endometrium resembles?
6. Identify the posterior cul-de-sac/rectouterine pouch.

Uterus in the Transverse Plane

1. Once you have obtained the uterus in the longitudinal plane, rotate the transducer counter-clockwise until the probe marker is pointing to the standardized patient's right. See Fig. 10.23 regarding position of the probe for this transverse view.
2. Fan the ultrasound beam inferiorly and superiorly until you can visualize the bladder and uterus.
3. It may be necessary to apply a little pressure to obtain a good image.
4. Identify the uterus, endometrium and posterior cul-de-sac/rectouterine pouch. See Fig. 10.25 for a representative transverse view of the uterus.

Ovaries

1. Identify the uterus in the transverse plane as described above. It may be possible to identify the ovaries and uterus in the same transverse image as you fan the ultrasound beam through the uterus (see Fig. 10.26). If you are unable to visualize the ovaries with the uterus in transverse slide the probe toward the patient's right or rock the ultrasound beam toward the patient's right. Then fan the ultrasound beam superiorly and inferiorly to try to locate the right ovary. Repeat the same process for the left ovary.
2. The ovaries typically appear hypoechoic to surrounding structures and depending on the age of the patient may contain follicles that appear, on ultrasound, as small anechoic (black) circular areas. See Fig. 10.27 for an image showing these follicles.
3. The ovaries typically lie close to the iliopsoas muscles and near the iliac vessels. However, they are mobile and can be displaced due to surrounding conditions. This, along with similar echogenicity of the surrounding structures, can make it difficult to identify the ovaries.

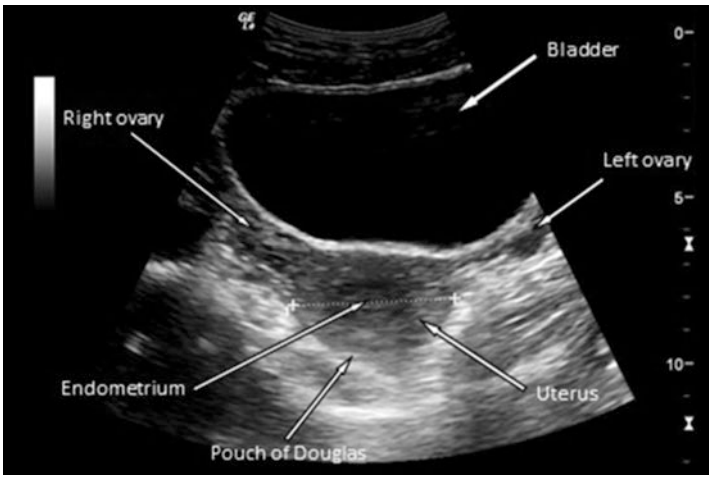

Fig. 10.26 Transverse view of a female pelvis showing the uterus and both ovaries. Note that the urinary bladder serves as a window to help better see these structures

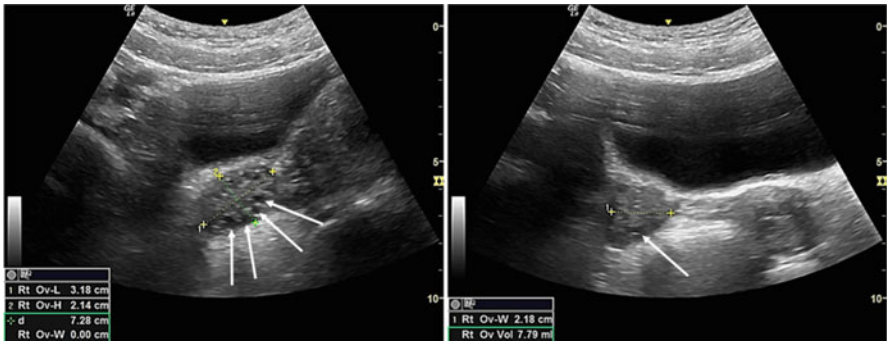

Fig. 10.27 Longitudinal (left image) and transverse (right image) views of a right ovary. Note the anechoic follicles (white arrows) on both images

Further Reading

Costanzo LS (2018) Chapter 10, Reproductive physiology. In: Physiology, 6th edn. Elsevier, Philadelphia, PA, pp 461–482

Molina PE (2018a) Chapter 8: Male reproductive system. In: Molina PE (ed) Endocrine physiology, 5th edn. McGraw-Hill Education, New York

Molina PE (2018b) Chapter 9: Female reproductive system. In: Molina PE (ed) Endocrine physiology, 5th edn. McGraw-Hill Education, New York

Parikh T, Czuzak M, Bui N et al (2018) Novel use of ultrasound to teach reproductive system physical examination skills and pelvic anatomy. J Ultrasound Med 37(3):709–715. https://doi.org/10.1002/jum.14408

Chapter 11
Ultrasound of the Nervous System

Jongyeol Kim and Thomas Pressley

11.1 Anatomy and Physiology of the Nervous System

The nervous system is vast, complex, and impacts all parts of our bodies. Because of our nervous system, we can walk, talk, see, smell, think, laugh, and a whole host of other things. The nervous system begins with neurons, which are specialized cells designed to conduct electrical impulses and typically, to release specific compounds (neurotransmitters and neuromodulators) that act on other cells, e.g., other neurons or cells within various organs. Because of this, neurons represent the basic functional component of the nervous system. Groups of neurons arrange together to form nerves, the sciatic nerve being a well-known example. Although other functional cells exist in the nervous system that are important for its function, astrocytes for example, this chapter will only discuss neurons.

The nervous system is divided into two major components (Fig. 11.1): (1) The central nervous system (CNS), and (2) The peripheral nervous system (PNS). The CNS is composed of the brain and spinal cord and it sends and receives information to the various tissues and organs of the body via the PNS. The PNS is subdivided into the somatic nervous system (innervation of skin and muscle primarily), autonomic nervous system (internal organs and tissues of the body), and the enteric nervous system (nervous system that regulates gastrointestinal function, see Chap. 6 of this book). In general, only the somatic nervous system (portions of it) is under voluntary control. A good example is movement. We can voluntarily activate neurons to cause skeletal muscle to contract (see also Chap. 8 of this book). As its

Supplementary Information The online version contains supplementary material available at https://doi.org/10.1007/978-1-0716-1863-9_11. The videos can be accessed by scanning the related images with the SN More Media App.

J. Kim (✉) · T. Pressley
Texas Tech University Health Sciences Center School of Medicine, Lubbock, TX, USA
e-mail: jongyeol.kim@ttuhsc.edu; thomas.pressley@ttuhsc.edu

L. B. Wilson et al. (eds.), *Understanding Physiology with Ultrasound*, Physiology in Health and Disease, https://doi.org/10.1007/978-1-0716-1863-9_11

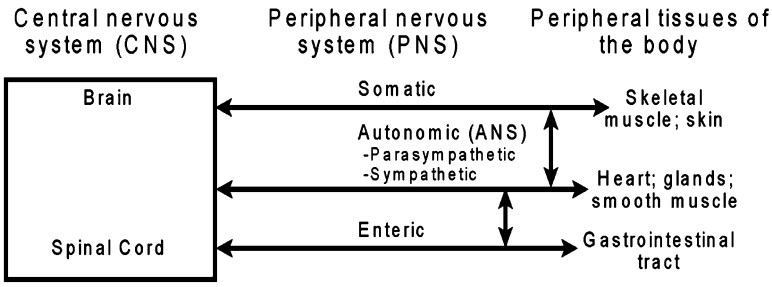

Fig. 11.1 A basic schematic of the nervous system. See text for details

name implies, the autonomic nervous system is automatic and not typically under voluntary control. Headway has been made over the years with biofeedback techniques that may allow some individuals to modify autonomic activity, but in general, the activity is not under voluntary control. The autonomic nervous system has two branches, the parasympathetic and sympathetic nervous systems. In general, the parasympathetic nervous system (PSNS) is involved in normal, resting functional aspects. For example, activation of the PSNS increases gastrointestinal activity and slows heart rate. So, in a nutshell, the PSNS is about "resting and digesting." The reverse of this is the sympathetic nervous system (SNS). In general, this is the body's "alarm" system. It is activated by stress or threats in the environment (seeing a bear in the woods). Activation of the SNS increases heart rate, decreases gastrointestinal motility, dilates pupils, and releases epinephrine (adrenaline) from the adrenal cortex. Although activation of the SNS is critically important when confronted with stressful situations, it should be appreciated that basal activity of the SNS is critically important for normal function. For example, basal sympathetic activity is critically important for maintaining blood pressure. Pathologically, dysautonomias represent altered function of the autonomic nervous system, and this can lead to a variety of problems: Altered blood pressure regulation being one of these problems. Diabetes mellitus is one condition that can damage neurons of the autonomic nervous system resulting in dysautonomia.

As illustrated in Fig. 11.1, there is bidirectional signaling between the CNS and the PNS (note arrows in the figure). Efferent neurons from the CNS evoke responses in the body, e.g., contraction of muscle to move a limb. Afferent neurons from all regions of the body send signals into the CNS. Most of this afferent signaling goes into the spinal cord, but some goes directly into the brain (pupillary light reflex described below). This afferent input to the CNS is critically important for normal physiological function. Some of the input we perceive, however, a significant amount is below the level of perception. A host of reflex responses are elicited and required to maintain normal function and these occur without any conscious awareness. The pupillary light reflex and myotatic stretch reflex are good examples and these will be explored in this chapter.

Afferent neurons sending signals to the CNS contain specialized regions called receptors. Activation of these receptors results in an action potential in the afferent neuron traveling to the CNS. The activation of these receptors and the resultant

action potential in these afferent neurons provides the CNS with information regarding the internal environment via interoreceptors, or the external environment via exteroreceptors. For example, if a weight is placed on your hand, you "feel" the pressure of this weight. This is an external stimulus activating exteroreceptors in your skin and muscle that sends signals (action potentials of neurons) to your brain telling you that "something is on my hand." Although this is an example of an external stimulus activating exteroreceptors that is felt (perceived), one should appreciate that there is a constant barrage of sensory input from interoreceptors to the CNS that is not perceived. It is critically important that the CNS send efferent signals, primarily via the autonomic nervous system, to adjust organ function to appropriately respond to this information.

Exteroreceptors and interoreceptors comprise an overview classification regarding the source of the stimulus. On a cellular level, most sensory receptors are specialized to respond to a specific stimulus. They respond to changes in: (1) temperature (thermoreceptors), (2) pressure/force/position/stretch (mechanoreceptors), (3) chemicals (chemoreceptors), (4) tissue damage or possible tissue damage (nociceptors), and (5) light (photoreceptors). Some receptors are less specialized and can respond to two or more of the above stimuli, chemical and mechanical changes for example. These are often referred to as polymodal receptors and they often fall within the nociceptor category. As an aside, because nociceptors respond to tissue damage or potential tissue damage, these are the receptors that are believed to trigger the perception of pain.

Unfortunately for this book, much of the nervous system is hidden from ultrasound (US). An individual neuron is far too small to visual via US. Even advanced tools such as the CT scan or MRI do not have resolution to detect pathologies in individual neurons. Although individual nerves may be visualized to some degree, the resolution is not such that functional changes can be captured. The action potential that is so crucial to nervous system physiology involves the flow of ions across the neuronal membrane; sodium, potassium, calcium, and chloride being the keys ones. Currently, nothing can visualize individual ions, thus US cannot. There are tools to assess electrical activity of the nervous system, the electroencephalogram (EEG) being a good example. Thus, nervous system physiology cannot be captured visually. However, US can be used to assess responses that we know involve neural components. The remainder of this chapter describes some exercises that can be done to assess reflex responses driven by nervous system physiology.

11.2 Pupillary Light Reflex

The movie, Jurassic Park, contains one of the most memorable depictions of the pupillary light reflex in popular culture. A recreated Tyrannosaurus rex is stalking two children, who are in a sport utility vehicle. As the dinosaur looks into a window, one of the children accidentally shines a flashlight into its eye, causing a dramatic decrease in pupil size. Unfortunately, this also encourages the predator to attack with determination.

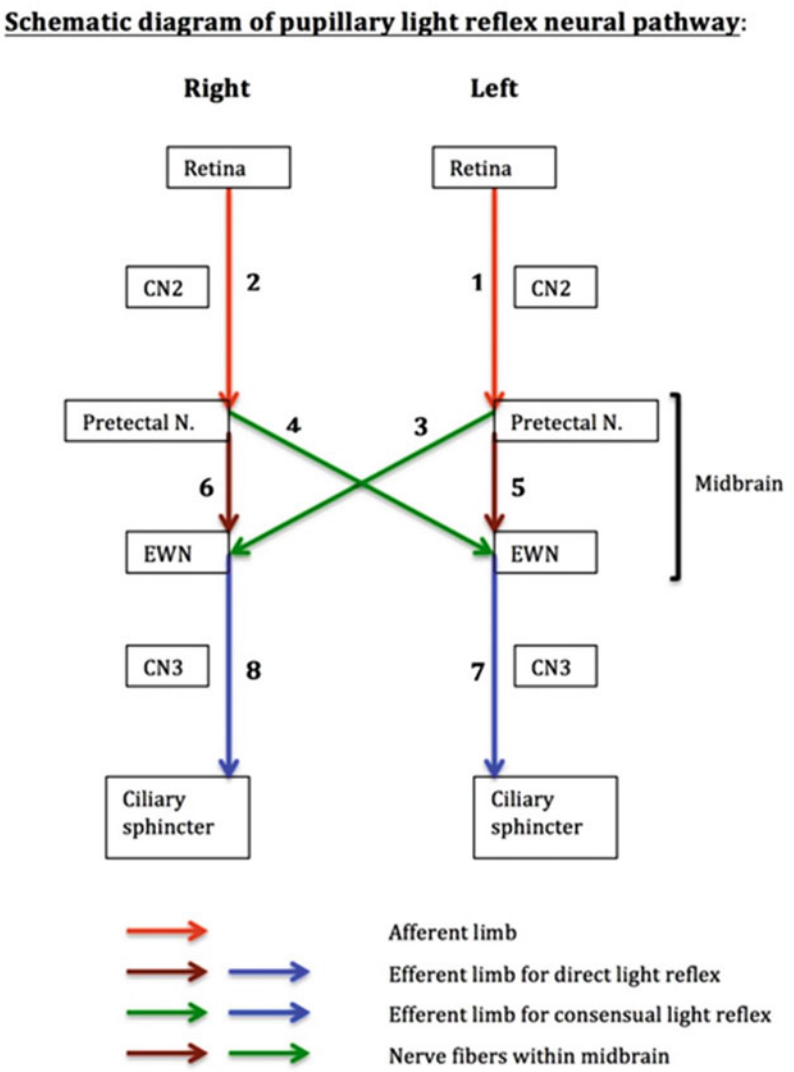

Fig. 11.2 Schematic diagram of light reflex neural pathway. *CN* cranial nerve; *N* nucleus; *EWN* Edinger-Westphal Nucleus. Source: Wikipedia

Most of us are familiar with the reflex. Despite the fact that it is best observed in a darkened room, we can easily see a partner's pupil contract in the presence of a bright light. Light striking the retina activates photoreceptors in the retina, the afferent neuron travelling in cranial nerve II fibers to the brain (Fig. 11.2). Once in the central nervous system, neurons in a part of the brain known as the Edinger-Westphal nucleus (EWN) process the signal and activate the oculomotor fibers of cranial nerve III, which, in turn, evoke constriction of the pupillary constrictor muscles.

What is less well known and observable is the consensual reflex. Because of cross talk between the two sides of the head, both eyes respond to the light, even though only one may be illuminated. This reflex is easily documented with ocular ultrasonography.

11.3 Myotatic Stretch Reflex

Muscle stretch reflex (or deep tendon reflex) is a monosynaptic reflex between sensory afferent nerves (group Ia afferents, mechanoreceptors) and motor efferent nerves (α motoneurons). When the muscle is stretched, group Ia afferent fibers in the muscle spindle are activated and their firing rate increases. These group Ia afferents enter the spinal cord and synapse directly on and activate α motoneurons. These α motoneurons innervate the muscle that was originally stretched (homonymous muscle) and when they are activated, they cause contraction of the homonymous (Fig. 11.3). When the muscle contracts, it shortens and decreases stretch on the muscle spindle. The muscle spindle returns to its original length, and the firing rate of the group Ia afferents returns to baseline. Simultaneously, information is sent from the spinal cord to cause contraction of synergistic muscles and relaxation of antagonistic muscles.

The stretch reflex is illustrated by the knee-jerk reflex, which is initiated by tapping the patellar tendon, causing the quadriceps muscle to stretch (Figs. 11.3 and 11.4 Video). When the quadriceps and its muscle spindles are stretched, group Ia afferent fibers are stimulated. These group Ia afferent fibers synapse on and activate α motoneurons in the spinal cord. These α motoneurons innervate and cause contraction of the quadriceps (the muscle that originally was stretched). As the quadriceps muscle contracts and shortens, it forces the lower leg to extend in the characteristic knee-jerk reflex.

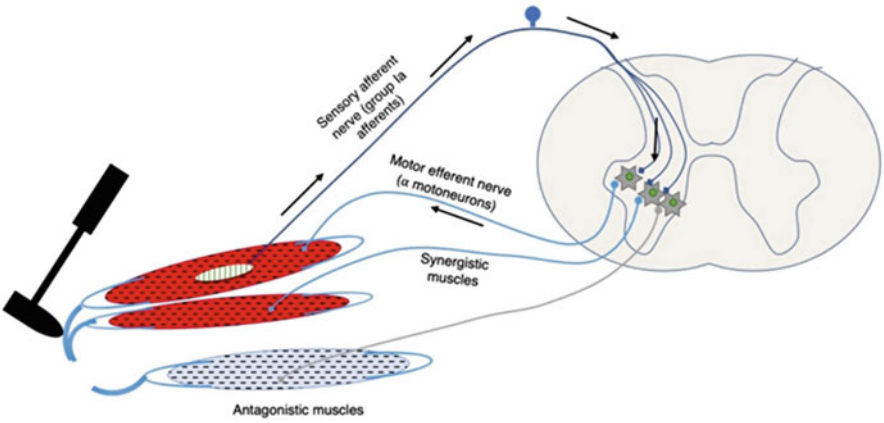

Fig. 11.3 The various components of the myotatic stretch reflex with knee jerk

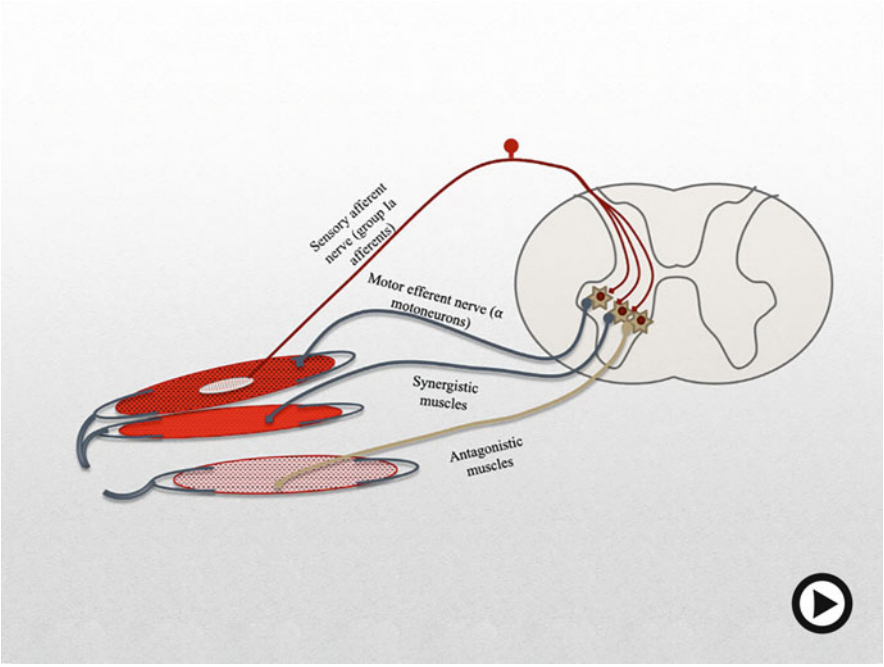

Fig. 11.4 (Video 11.1) Video illustrating the various components of the myotatic stretch reflex (▶ https://doi.org/10.1007/000-7qv)

11.3.1 Exercise 1: Ultrasonography of the Consensual Reflex

11.3.1.1 Learning Objectives

Learn to ultrasound the pupil of the eye and identify the consensual reflex when light is shined in the contralateral eye.

11.3.1.2 Transducer/Probe

A high frequency linear probe is used to image the eye. Particular care must be taken when scanning the eye (see below).

11.3.1.3 Additional Equipment and Supplies for Exercise and Optional Assessment

1. Flashlight or penlight
2. Various neutral optical filters with different transmittance

3. Various colored optical filters
4. Rulers for measuring distance

Working near the eye requires care to avoid pain and injury. Caution needs to be taken when performing ophthalmic ultrasound exams. In keeping with safety recommendations by the American Institute of Ultrasound in Medicine (AIUM) only equipment specifically approved by the US Food and Drug Administration (FDA) for ophthalmic indications should be used to scan the eye. This is due to sensitivity of the eye to heating. The thermal index (TI) should not exceed 1.0 and the mechanical index (MI) should not exceed 0.23. The appropriate ophthalmic preset on an FDA cleared ultrasound machine should be used to keep these output settings below those maximum levels. Scan time should be kept as low as possible. Many students may prefer to handle the probe placement and manipulation themselves while a partner controls the ultrasound machine. Sufficient gel should be used to minimize transmitting pressure to the eye. After the exam, a soft cloth or gauze can be used for clean-up, followed by gentle washing in the sink with plenty of water to remove the last of the soluble gel.

11.3.1.4 Patient Position and Image Orientation

The patient may be sitting upright in a chair or lying supine on an exam table.

For this exercise, ultrasound imaging for the eye will be used. In this application the orientation marker, usually the company logo, will be on the top left side of the screen. The logo matches up with the probe marker which is most often a palpable ridge on one side of the probe. Whichever side of the target organ the probe marker is on, that side of the target organ will match up with the orientation marker on the screen. The top of the screen is always superficial or where the probe makes contact with the body surface.

11.3.1.5 Performing the Pupillary Eye Examination

1. Position the volunteer and ultrasound machine in a dimly-lit room. Chairs for both the volunteer and the operator will facilitate a steady use of the ultrasound probe or the volunteer can be supine on the exam table.
2. Turn on B-mode and select the linear probe and the ophthalmic preset.
3. Following gel application, gently place the probe below the orbit (Fig. 11.5). The probe is then directed about 45° upwards until an interpretable image is visualized. It should be straightforward to identify the circular, fluid-filled eyeball.
4. Ask the volunteer to look upwards at a fixed object and hold a steady gaze. The probe is manipulated to create a fold of skin just beneath the orbit, and the probe is adjusted gently to a near-coronal plane near the front of the eyeball. The pupil should become visible as a small, circular structure (Figure 11.6). The volunteer

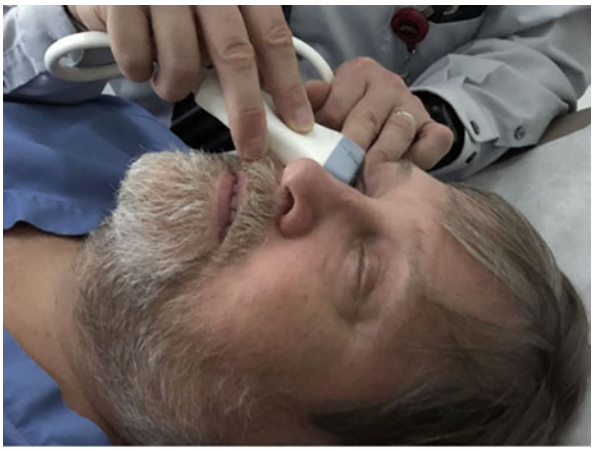

Fig. 11.5 Positioning of the ultrasound probe for visualization of the pupil

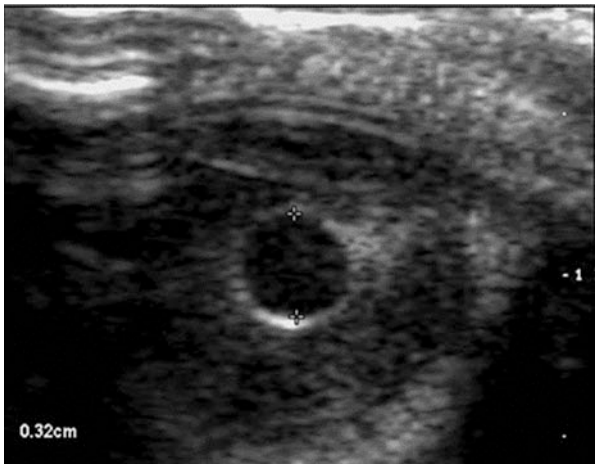

Fig. 11.6 B-mode imaging of the pupil in a near-coronal plane. The pupil is demarcated by the + signs

can assist you in producing an image by looking at various heights upon request. Once an image is obtained, ask the volunteer to avoid any additional eye movement.

5. Holding the probe in position, shine the flashlight or penlight into the other, open eye, taking care that the beam does not impinge on the closed eye. An immediate pupillary light reflex will be elicited in the open eye. The ultrasound coronal image will enable you to watch the pupil of the closed eye as it contracts in a consensual reflex. Multiple attempts are very convincing that the pupil of the closed eye is indeed contracting, despite the lack of stimulating light. A very bright light may be uncomfortable for the volunteer. In this situation, closing both eyes may help. The light will probably be bright enough to elicit the reflex even after passing through the eyelid.

11.3.1.6 Optional Assessment of the Pupillary Response

M-mode Measurements Switching the machine to M-mode allows the students to be more quantitative. The pixel scan can be adjusted such that the diameter of the pupil is readily visualized (Fig. 11.7). The magnitude of the contraction can now be measured. Admittedly, the use of M-mode requires that both the eye and the probe remain immobile, which requires some practice. Shifting of the image to the left or right in response to inadvertent rocking of the probe will introduce an artifact as the scan line moves more tangential to the pupil. This might be misinterpreted as a contraction.

With some practice, the quantitative capabilities of M-mode provide the opportunity for a more inquiry-based, student-designed activity. Students can time the duration of the reflex and the rates of contraction and dilation when the light is presented and removed. Students can evaluate the effects of light intensity if various neutral filters are available to control the brightness of the light. Alternatively, the light can be placed at fixed distances from the eye using a ruler to achieve a similar variety of intensities. Colored filters would allow an exploration of wavelength and its influence. Of course, any student-developed experimental design should be approved by the responsible educator before the students can proceed.

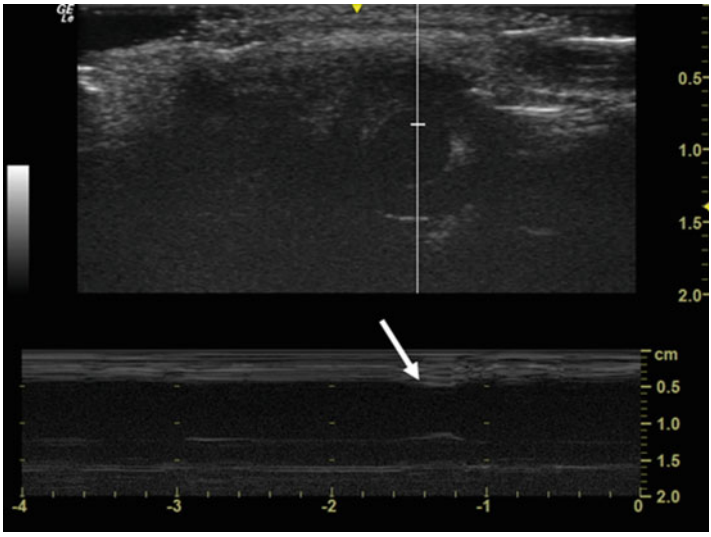

Fig. 11.7 M-mode imaging of a pupil contraction upon illumination of the opposite eye. The arrow indicates the contraction

11.3.2 Exercise 2: Ultrasonography of Stretch Reflex

11.3.2.1 Learning Objectives

Learn to obtain ultrasound views of the knee-jerk reflex and recognize relevant anatomical structures and the normal physiological reflex response.

11.3.2.2 Transducer/Probe

This exercise is best performed with a high-frequency linear probe.

11.3.2.3 Additional Equipment and Supplies

Reflex hammer.

Volunteer or subject (optional).

11.3.2.4 Patient Position and Image Orientation

The subject (or yourself) is sitting on a chair or bed for knee jerk reflex as seen in Fig. 11.8.

For this exercise, the ultrasound imaging for the musculoskeletal system will be used and musculoskeletal imaging uses the same screen orientation with other ultrasound imaging. An orientation marker, usually the company logo, will be on the top left side of the screen. The logo matches up with the probe marker which is most often a palpable ridge on one side of the probe. Whichever side of the target organ the probe marker is on that side of the target organ will match up with the

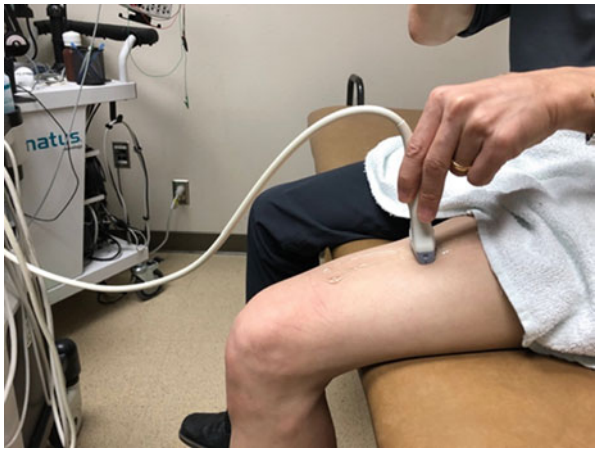

Fig. 11.8 The subject is sitting on a bed or (on a chair) for knee jerk

orientation marker on the screen. The top of the screen is always superficial or where the probe makes contact with the body surface.

11.3.2.5 Performing the Stretch Reflex with B-mode: Transverse View

1. Use the musculoskeletal (MSK) preset.
2. Apply adequate gel to the middle of the thigh and place the probe on the middle of the thigh with the probe marker pointed toward the subject's right side (Fig. 11.8).
3. Identify the rectus femoris muscle (beneath the subcutaneous tissue) and vastus intermedius (just above the femur) on the transverse view and observe the morphologic change of muscles when the subject flexes (contracts) the muscles (Fig. 11.9)
4. Tap or percuss the patellar tendon with a reflex hammer and note the muscle contraction and change in muscle size.

11.3.2.6 Optional Assessment of the Stretch Reflex Response

Stretch Reflex with B- and M-Modes: Transverse View

1. Use musculoskeletal (MSK) preset.
2. Apply adequate gel to the middle of the thigh and the probe on the middle of the thigh with the probe marker pointed toward the subject's right side (Fig. 11.8).
3. Identify the rectus femoris muscle (beneath the subcutaneous tissue) and vastus intermedius (just above the femur) on the transverse view and observe the morphologic change of muscles when the subject flexes (contracts) the muscles.
4. Turn on M-mode.
5. Tap or percuss the patellar tendon with a reflex hammer.

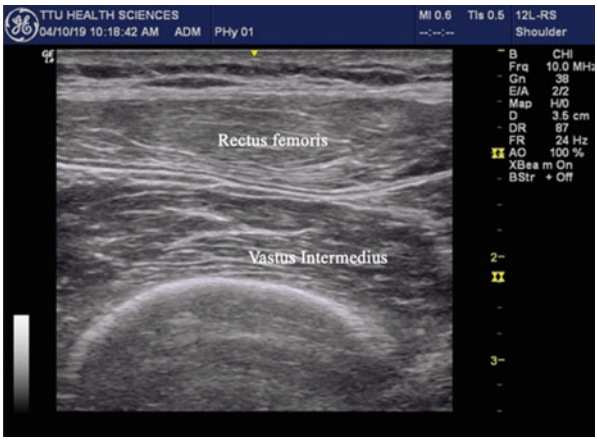

Fig. 11.9 Transverse view of B-mode identifying rectus femoris and vastus intermedius

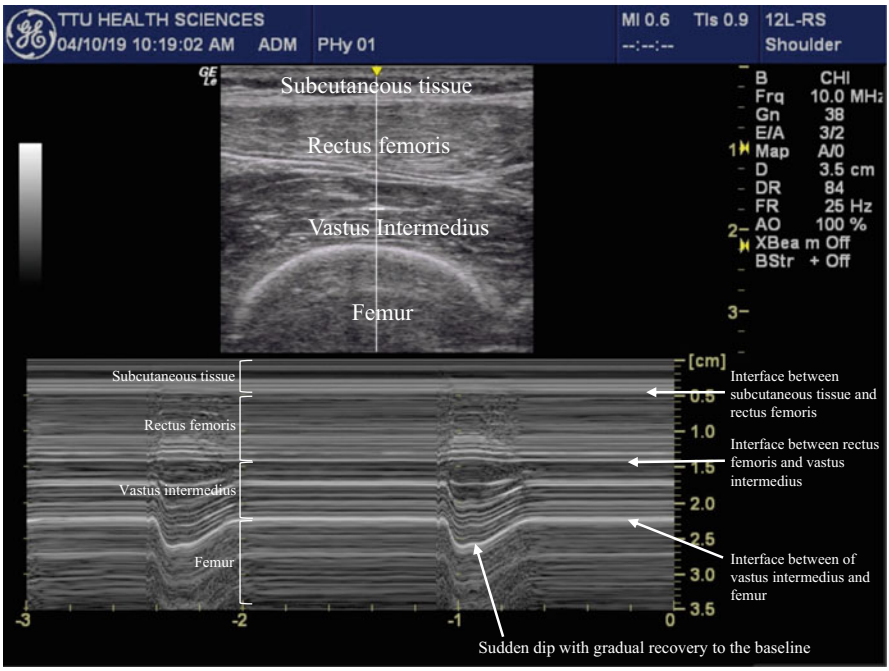

Fig. 11.10 M-mode: Putting the scan line in the middle of vastus intermedius; dipping with gradual return to the baseline due to contraction of muscle

6. Transverse view on B-mode will demonstrate enlargement of the rectus femoris and vastus intermedius secondary to the stretch reflex.
7. M-mode (on rectus femoris, vastus intermedius, or surface of femur) will show the sudden dip with gradual recovery to the baseline. (Fig. 11.10 and Video Fig. 11.11)
8. Calculate the speed of contraction of muscles. (Fig. 11.12): Activate "measurement control" by pressing a designated button or knob on the ultrasound machine to control a measurement caliper. Place the first caliper (1+) at the onset of contraction of muscle for the first reflex and fix it. Move the second caliper (2+) at the peak of the contraction of muscle, fix it and the automatically calculated speed (13.95 cm/s) of the contraction will display in a small box in the screen. Move the third caliper (+) at the end of muscle relaxation, fix it and the automatically calculated speed (2.15 cm/s) of the relaxation will display in a small box.
9. Measure the total duration of contraction and relaxation of muscles during the second reflex (Fig. 11.12): Place the fourth caliper (4+) at the onset of the contraction and fix it. Place the fifth caliper (+) at the end of the relaxation of the muscle, fix it, and the automatically measured time (0.320 s or 320 ms) will display in a small window.

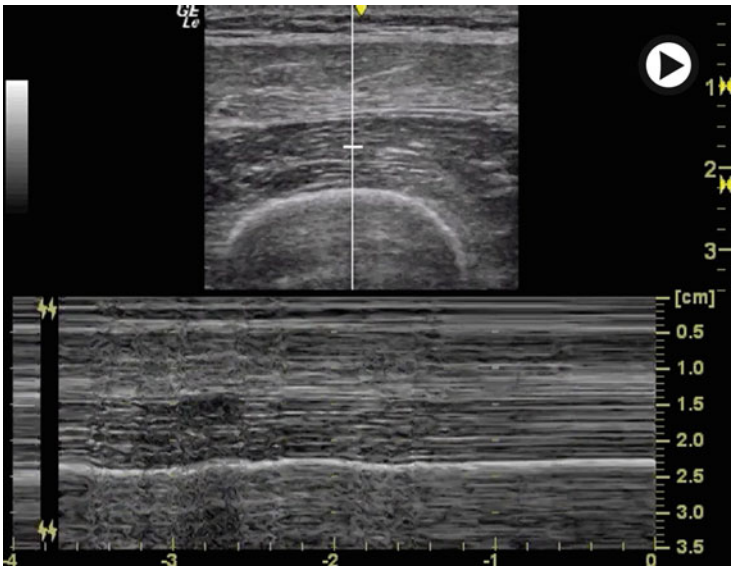

Fig. 11.11 (Video 11.2) Stretch reflex with M mode (transverse view) insonating the vastus intermedius (▶ https://doi.org/10.1007/000-7qt)

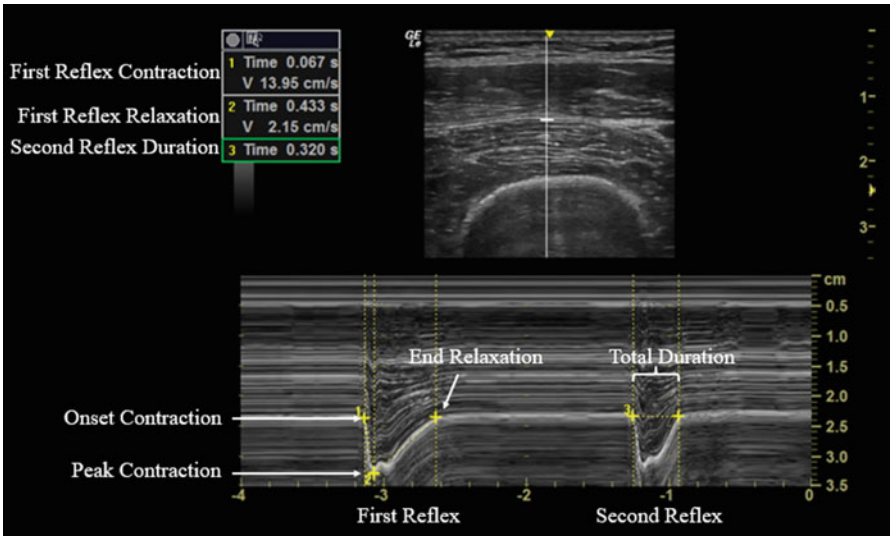

Fig. 11.12 M-mode: Calculating the speed of contraction and relaxation of muscles during two separate reflexes

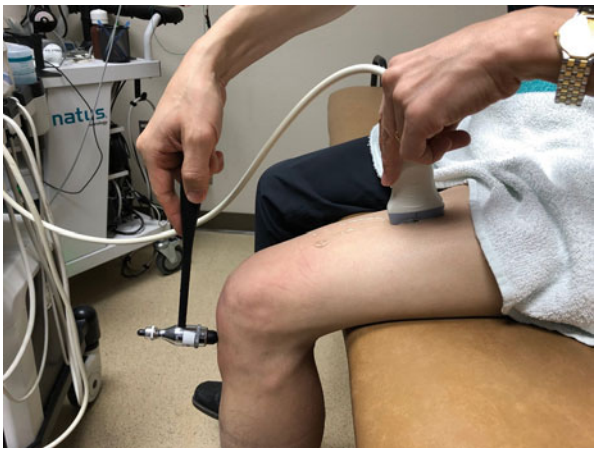

Fig. 11.13 Stretch reflex with probe in the longitudinal position with probe marker pointing toward the hip

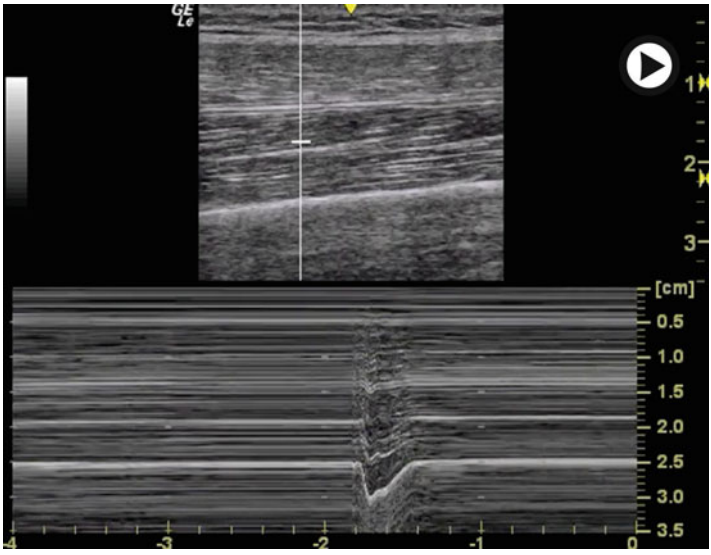

Fig. 11.14 (Video 11.3) Stretch reflex with M-mode (longitudinal view) insonating the vastus intermedius (▶ https://doi.org/10.1007/000-7qs)

10. The above steps can be repeated with the probe in the longitudinal position and the probe marker pointed toward the hip (Figure 11.13). A similar M-mode respond will be elicited but in the longitudinal orientation (Figure 11.14 video).

Stretch Reflex with B- and Doppler (Spectral) Modes: Transverse View

1. Turn on Doppler-mode with audio (duplex mode or simultaneous mode).
2. Tap or percuss the patellar tendon with a reflex hammer.

3. Transverse view on the B-mode will demonstrate thickening of the rectus femoris and vastus intermedius due to contractions secondary to the stretch reflex.
4. Doppler-mode on either the rectus femoris or vastus intermedius will demonstrate sharp biphasic or triphasic waveform with chirping sound due to contraction of muscles secondary to the stretch reflex. (Fig. 11.15 image and Fig. 11.16 video).

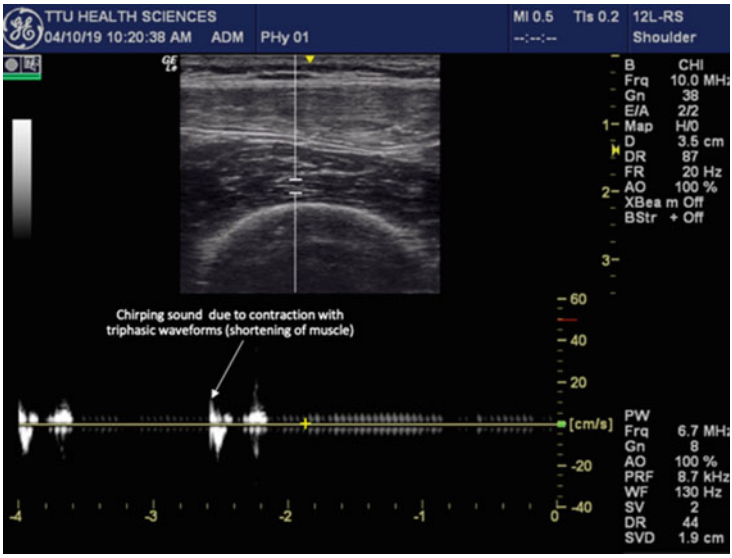

Fig. 11.15 Doppler mode: insonating the vastus intermedius; a chirping sound with biphasic or triphasic waveform

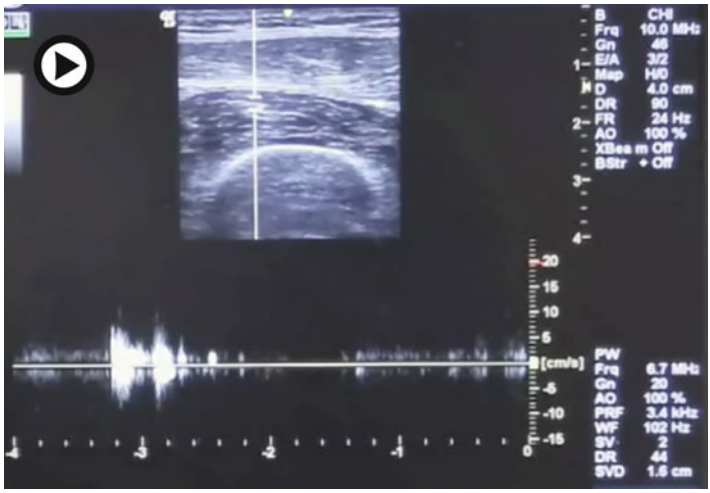

Fig. 11.16 (Video 11.4) Stretch reflex with B mode (transverse view) and Doppler mode insonating the vastus intermedius (▶ https://doi.org/10.1007/000-7qw)

5. The above steps can be repeated with the probe in the longitudinal position and the probe marker pointed toward the hip. Still image (Figure 11.17). A similar Doppler-mode response will be elicited but just in a different orientation (Figure 11.18 video).

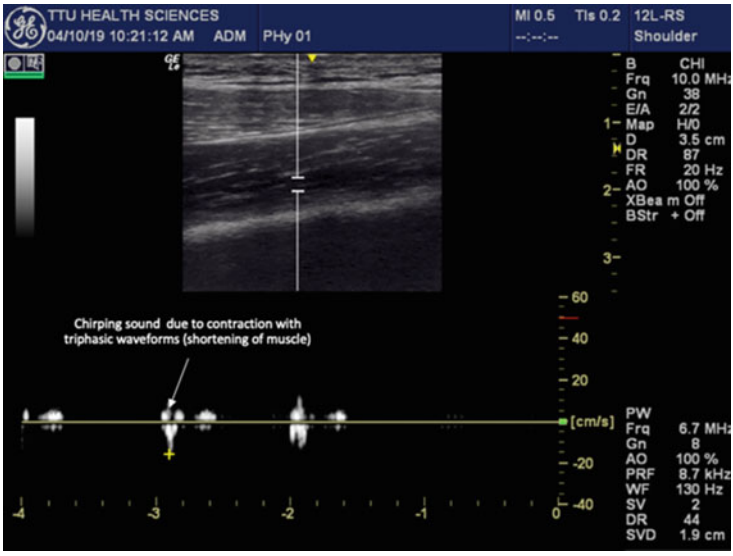

Fig. 11.17 Doppler mode: insonating the vastus intermedius in the longitudinal view; a chirping sound with biphasic or triphasic waveform which can be seen and heard in the video Fig. 11.18

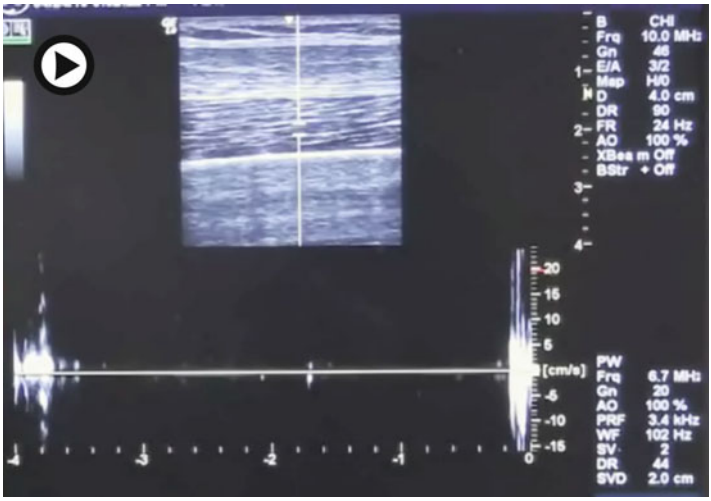

Fig. 11.18 (Video 11.5) Stretch reflex with B mode (longitudinal view) and Doppler mode insonating the vastus intermedius (▶ https://doi.org/10.1007/000-7qx)

These exercises can be performed for other reflexes as well such as the biceps, triceps, and ankle reflexes.

Further Reading

Costanzo LS (2014) Pupil. In: Autonomic nervous system, physiology, 6th edn. McGraw Hill, New York

Costanzo LS (2018) Stretch reflex. In: Neurophysiology, physiology, 6th edn. Elsevier, Philadelphia, PA

Sargsyan AE et al (2009) Ultrasonic evaluation of pupillary light reflex. Crit Ultrasound J 1:53–57

Silverthorn DU (2004) Light enters the eye through the pupil. In: The eye and vision, human physiology: an integrated approach, 3rd edn. Pearson, New York

Chapter 12
Introducing Ultrasound into a Physiology Course from A to Z

Richard Hoppmann, L. Britt Wilson, Keith Barron, and Paul Bornemann

Introducing ultrasound into a course is no longer the daunting task it was a decade ago. The major challenges to incorporating ultrasound into education have largely been addressed: cost, difficulty of learning to perform ultrasound, incorporating ultrasound into a course without adding excessive contact hours, and lack of evidence of the value-added of ultrasound in education.

Advances in ultrasound technology have resulted in laptop and handheld ultrasound devices that are smaller, more powerful, and much less expensive than in the past. With the addition of artificial intelligence (AI), students and teachers alike can more easily learn ultrasound to capture quality images and determine physiological measurements such as cardiac ejection fraction. With the use of artificial intelligence, online learning resources, and the adoption of a more self-directed learning model, ultrasound can be incorporated into courses without a significant increase in contact hours. With the emergence of evidence in the literature on the value of ultrasound as a teaching tool and clinical practice tool, it has become more broadly accepted in academia and more schools are incorporating ultrasound into their curricula.

This chapter will present important topics to be considered when making plans to introduce ultrasound into a physiology course but many of the topics are also applicable to introducing ultrasound into other courses and even entire curricula and clinical training programs. Some thoughts on funding options of ultrasound programs will be included. In addition, a scaled-down approach to introducing

R. Hoppmann (✉) · K. Barron · P. Bornemann
University of South Carolina School of Medicine, Columbia, SC, United States
e-mail: Richard.Hoppmann@uscmed.sc.edu; Keith.Barron@uscmed.sc.edu; Paul.Bornemann@uscmed.sc.edu

L. B. Wilson
Department of Pharmacology, Physiology, and Neuroscience, University of South Carolina School of Medicine, Columbia, SC, USA
e-mail: Britt.Wilson@uscmed.sc.edu

L. B. Wilson et al. (eds.), *Understanding Physiology with Ultrasound*, Physiology in Health and Disease, https://doi.org/10.1007/978-1-0716-1863-9_12

ultrasound into a physiology course will be presented for those with very limited resources. A practical checklist for introducing ultrasound into a physiology course is also provided.

Below is a list of important topics for consideration when introducing ultrasound into a physiology course.

1. Purchase of ultrasound equipment
2. Models and standardized patients
3. Trained instructors
4. Student contact hours
5. Ultrasound educational materials and student assessment
6. Student feedback
7. Space and additional equipment for ultrasound scanning stations
8. Potential sources of funding

12.1 Purchase of Ultrasound Systems

When ultrasound education was first being introduced into medical student education in the 1990s and early 2000s, a major challenge was the cost of the ultrasound equipment. At that time, portable laptop-sized machines were available and even though they were much less expensive than the large ultrasound systems used by radiology, they were still in the $40–60K range for a machine and several ultrasound probes. This made purchasing an adequate number of systems for hands-on learning for a large class of students an almost unsurmountable barrier for most programs.

As the market for portable devices expanded and more manufacturers entered the market place, the cost of systems began to drop and the quality of the portable systems improved. Presently, the quality of laptop systems rivals the larger more expensive systems and the price has dropped into the $20–40K range including 3 probes to cover the spectrum of scans necessary for multiple organ system instruction. A typical laptop system and probes can be seen in Fig. 12.1.

In 2007, the first hand-held ultrasound device was introduced and many manufacturers have since followed suit. The cost of hand-held ultrasound devices, like laptop systems, has come down over time while the quality and functionality of these devices have increased. There are now a broad array of hand-held devices available from ones that are self-contained to those that consist of an ultrasound probe that plugs into a smart tablet or phone or connects wirelessly. Some of these devices are cloud-based and have incorporated artificial intelligence to assist in capturing images, evaluating images, and computing physiological measurements. There is also a device that adds electronic stethoscope sounds and an electrocardiogram to the ultrasound image to produce a 3-signal physiological assessment. The cost of handheld ultrasound devices is in the $2K to $10K range. An array of hand-held ultrasound devices can be seen in Fig. 12.2.

Although purchasing basic ultrasound equipment for a course has become less of a financial challenge, there are still several important issues to consider when buying

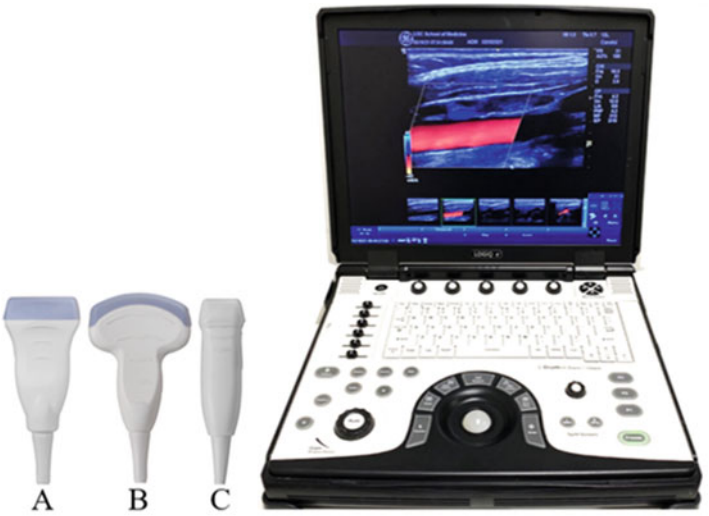

Fig. 12.1 A portable laptop ultrasound system consisting of display screen, console control panel, power source, and storage space for captured images. Also shown are three ultrasound probes that attach to the system and allow scanning of all organ systems relevant to the study of human physiology. (**a**) Linear array probe. (**b**) Curvilinear probe. (**c**) Sector probe

ultrasound systems, such as the number and type of systems needed. Meeting with regional company representatives to try out the systems and discuss purchase options and support services is highly recommended prior to purchase.

12.1.1 Number of Ultrasound Systems

The number of ultrasound systems needed for effective hands-on learning sessions can be based on an approximate teaching ratio of four to five students per scanning station. With six scanning stations, 24–30 students can be scheduled for each scanning session which typically lasts 45 to 50 minutes. Thus, for a class of 100–120 students, four laboratory sessions can be scheduled over a four-hour block to give all students adequate time to scan and cover the content objectives for the session. If space, equipment, and number of instructors permit, additional scanning stations can be added so more students can be accommodated for each session.

12.1.2 Type of Systems

Laptop ultrasound systems will generally have more functionality, larger screens, and produce higher quality images than hand-held ultrasound devices making them

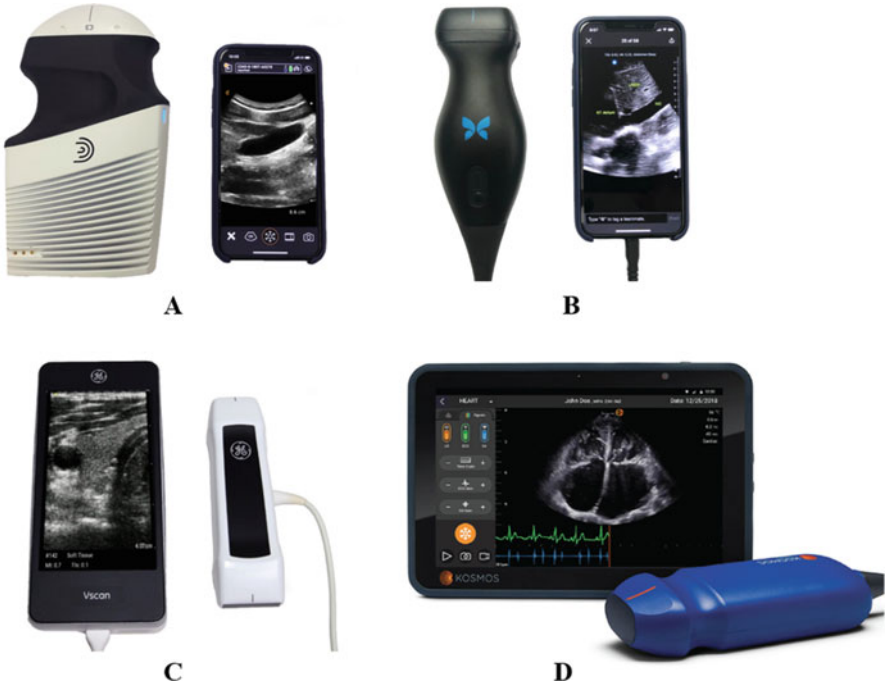

Fig. 12.2 Hand-held ultrasound devices: (**a**) Wireless probe. (**b**) Single broad-frequency probe with phone plug-in. (**c**) Dual-frequency probe. (**d**) 3-Signal (ultrasound, e-stethoscope, ECG) probe with tablet

better for the new learner. However, most hand-held devices are adequate for learning basic ultrasound skills and meet the needs of student physiology laboratory sessions. In addition, transitioning from a laptop to the hand-held device is relatively easy. Thus, a combination of laptop-sized ultrasound systems and hand-held devices will generally work well and provide a varied scanning experience for students while also decreasing total cost over using laptop systems only.

When possible, purchase ultrasound devices that have image mirroring or casting capabilities to a large screen. A large viewing screen at each ultrasound station is preferable to just using the small ultrasound system monitor or hand-held device screen so all learners can stay engaged and learn as others in the group are scanning. See Fig. 12.3.

12.1.3 Demonstration, Testing, and Purchase Options

Before making a final purchase decision, explore several laptop and hand-held ultrasound systems. Most companies are happy to come to your institution to provide that opportunity and it is also a chance to get to know the regional company

Fig. 12.3 Students during an ultrasound laboratory session. All are engaged in the learning process

representative who can serve as a great resource if questions arise in the future. The faculty who will be involved in ultrasound education should be invited to try out the equipment, especially faculty who have experience teaching with ultrasound. Faculty can help assess the ease of use of the machine and if it has the ultrasound applications that will be needed for the various ultrasound laboratory sessions that are planned as well as anticipate future scanning needs. Prior to company demonstrations and testing, it is helpful to develop a list of questions and issues for discussion during their visit as follows:

1. Educational discounts and company sponsored in-service training for faculty.
2. Availability of cloud-based image storage and automated image evaluation services and the cost of such services.
3. Warranties, upgrades, and the cost of maintenance contracts. These additional costs can vary considerably among manufacturers.
4. Availability of ultrasound systems designed specifically for education as opposed to clinical practice. These educational ultrasound systems are usually less expensive than the clinically designed systems and even though they may not be as technically advanced as those for making clinical decision, they are generally more than adequate for teaching purposes.
5. Reduced rates based on volume of purchase. If volume purchases are possible, the institution might consider a joint purchase order with a simulation center, residency training program, or another institutional entity that may be interested in purchasing ultrasound equipment.

12.2 Models and Standardized Patients

Depending on institutional policy, students can scan each other but no student should be required to be a scanning subject. All findings on students should be considered confidential. If something of concern is discovered in a student, the student should be informed and consultation should be made with a clinical faculty member if available and a decision made as to whether referral should be made for follow-up evaluation. If a clinical faculty member is not available, the student should be encouraged to discuss the issue with his/her parents, private physician, or the student health center.

In general, standardized patients for ultrasound labs can be drawn from the institution's standardized patient program if one exists. It is advised to use easy to scan male models who are relatively thin and healthy when students are first being introduced to ultrasound scanning. The difficulty level of scanning models should be gradually increased over time. Some patients can be quite difficult to scan even for an experienced physician or sonographer, especially those who are obese or have medical conditions like emphysema, which can make capturing a good image of the heart quite difficult. Trying to scan these difficult patients early in the learning process can be quite discouraging for students and the inability to capture quality images diminishes learning the physiology subject content.

Undergraduate pre-medical and other health professions students often make great models and are excited to be involved in the ultrasound program. Children of faculty are usually a good source of models for pediatric scanning. Having several models available for ultrasound demonstrations with chronic stable diseases such as mild congestive heart failure and interesting findings like gallstones can add significantly to the ultrasound learning experience for the students.

Ultrasound models, who are not volunteers, are generally paid $15 to $25 per hour for their service. When possible, models should be briefly scanned prior to starting a laboratory session to assess difficulty level of scanning and to ensure that pathology unknown to the model is not present. If pathology is identified, it should be discussed with the model privately and a decision made on how to proceed.

12.3 Trained Instructors

All faculty with ultrasound training and expertise can be invited to help teach the physiology hands-on ultrasound labs and help train other faculty who would like to learn to perform basic ultrasound. There are faculty across many medical specialties and subspecialties who use ultrasound regularly in their clinical practices. These include radiologists, cardiologists, hospitalists, intensivists, obstetricians and gynecologists, emergency medicine physicians, surgeons, endocrinologists, and rheumatologists. Other specialties are beginning to incorporate ultrasound into their practices, especially primary care providers in family medicine, internal medicine,

and pediatrics and can be invited to participate as well. All instructors should be given ultrasound learning material that will be used in the student scanning session as well as the objectives for the laboratory sessions. Short instructional scanning videos to view prior to the laboratory sessions are particularly helpful for students and instructors.

In addition to physician faculty, sonographers have extensive training and experience in ultrasonography and are an excellent resource to assist with student labs and train faculty. Resident physicians in training with ultrasound experience can also assist with teaching ultrasound laboratory sessions.

Faculty training in ultrasound can be accomplished with online learning material, in-house hands-on workshops, and ultrasound industry sponsored in-service workshops. When possible, faculty should be supported to attend ultrasound workshops offered regionally or nationally with the understanding that they will assist in teaching future student labs. In addition, the opportunity for faculty to sign out an ultrasound device to practice scanning can significantly accelerate their ultrasound learning curve and is much appreciated by faculty. This option is easier to offer now that hand-held ultrasound devices are available.

Peer and near-peer student teaching of ultrasound labs have been successfully introduced into a number of ultrasound programs. These have been particularly successful when the student teachers have received specific laboratory scanning instructions prior to the scheduled class laboratory sessions.

With the advent of AI assisted self-directed ultrasound learning applications such as real-time automatic labeling of anatomical structures, display of probe position directions, and grading of the quality of the images, learning to scan has become much easier for students and faculty. AI assisted learning applications on ultrasound systems also means fewer faculty may be needed for scheduled student laboratory sessions.

12.4 Student Contact Hours for Ultrasound

Finding time in a course to add new material has been a challenge in most areas of education for many years but is especially challenging in the life sciences and medicine. Discoveries and the accumulation of new information continue to mount in these areas and is doing so at an accelerating rate. At most institutions, course directors are required to limit the number of student contact hours as institutional oversight committees and accrediting bodies have become quite sensitive to the detrimental effects of heavy student course requirements that do not leave adequate time for independent learning and flexible study time.

Development of an overall strategy to introduce ultrasound into a course should begin with a review of course material by the course director and those providing ultrasound assistance to determine which topics can best be taught with ultrasound. Starting with just a few relevant topics that can be covered well is recommended. Neither the students nor the faculty should feel overwhelmed with the number of

topics initially introduced into the course. Three topics in which ultrasound is used to complement learning is a very reasonable starting point. The scheduling of the ultrasound labs should be coordinated with when relevant physiology content is being covered in the course by other instructional formats such as didactic presentations. Laboratory sessions should be relatively short and easy to implement. More ultrasound can be added to the course over time based on learner outcomes and feedback from the students and faculty.

It should not be the intent of introducing ultrasound into a physiology course to replace important physiological content but to primarily use ultrasound as an effective and engaging way to teach subject content already in a course. However, time will be needed for students to learn to use ultrasound in the course to maximize teaching efficacy and active participation in the laboratory scanning sessions. Much of this can be accomplished in ways that utilize self-directed learning and minimize scheduled contact hours. This approach can include online ultrasound learning modules and scanning videos, open laboratory scanning sessions with students scanning each other or models, ultrasound simulation, and using ultrasound devices with instructional artificial intelligence.

Open laboratory sessions deserve a special note of emphasis as these sessions are consistently highly rated by students on course feedback and evaluation forms. These are voluntary sessions offered in addition to required scheduled laboratory sessions. They add scheduling flexibility and more time for self-directed learning opportunities for students. Over the years, it has become clear that not all students learn how to scan at the same pace. The more relaxed pace of open labs is particularly suited to students who need more time to practice hand-eye coordination tasks and work on image orientation of anatomical structures. During open labs with students scanning each other or models, an instructor should be available for questions and help with scanning skills when needed but no formal teaching is scheduled.

12.5 Ultrasound Educational Materials and Student Assessment

This textbook should provide most, if not all, of the educational materials in the form of text, images, videos, and laboratory exercises that a physiology course director will need from introductory courses to some of the more advanced physiology courses. The ultrasound basics and organ systems material were selected by those experienced in using ultrasound to teach physiology and pathophysiology to a broad group of learners, including those new to ultrasound. The format and content were also developed to encourage self-directed learning, which has become such an important approach to education at all levels today. If needed, additional resources can be found through ultrasound organizations such as the Society of Ultrasound in

Medical Education (SUSME) and the American Institute of Ultrasound in Medicine (AIUM).

In addition, SUSME together with the World Interactive Network Focused on Critical Ultrasound (WINFOCUS) holds an annual World Congress on Ultrasound in Medical Education where ultrasound educators from around the world gather to share the latest advances in ultrasound technology and education. The World Congress also offers a number of ultrasound workshops specifically designed for those using ultrasound to teach. The World Congress offers a great opportunity to network with colleagues and participate in collaborative efforts to advance the field of ultrasound education, which is rapidly developing into an academic niche for faculty that includes research, grants, publications, intellectual property, and leadership opportunities.

12.5.1 Student Assessment

It is generally a good strategy to include graded assessment of basic ultrasound knowledge and skill as well as the physiology material of the course to help ensure adequate student engagement and that learning objectives are being met. Student assessment can be in the form of multiple-choice questions on exams, assessment of images captured in lab, data from simulation exercises, and an objective structured clinical examination (OSCE). Some combination of these assessment methods generally works well.

Multiple choice questions, especially clinical cases incorporating ultrasound images related to the physiology content of the course, can be an easy and effective way to assess knowledge of both ultrasound and physiology. Ultrasound images obtained during laboratory sessions can be saved to a USB drive or directly uploaded to a cloud-based image archive system for assessment and feedback. Several medical imaging archiving companies offer these cloud-based services. Recently, ultrasound manufacturers have begun offering cloud-based platforms with the purchase of their ultrasound systems that provide these services, including grading of image quality and tracking of the progress of individual learners in their ultrasound skills.

Asynchronous use of a cloud-based review portal for image assessment and instructor feedback can add flexibility to the assessment process for students and faculty. An example of assessment of a student image obtained during an ultrasound laboratory session can be seen in Fig. 12.4. The image review includes both feedback annotations on the image itself, as well as completion of a standardized scoring sheet with additional comments. In this image, the reviewer felt the depth of the image should have been decreased to the level of the arrow to provide better assessment and measurement of the heart, which was the objective of the laboratory session.

Simulation can be used to not only help students learn ultrasound, but can also be used to assess student performance over time. Simulation also adds flexibility of time and self-directedness to learning the ultrasound component of the course. As with

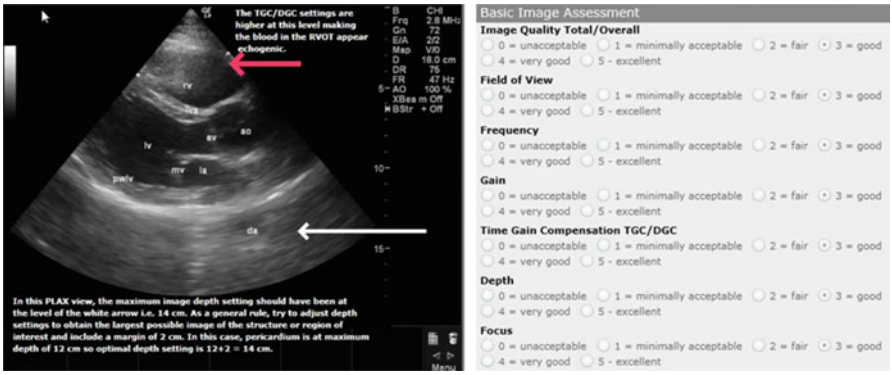

Fig. 12.4 Image assessment. Left panel: a student ultrasound image from a laboratory session in which the student was required to acquire an image of the heart. The reviewer has provided feedback directly on the image. Right panel: a completed standardized image scoring sheet

ultrasound system purchases, simulator purchases should include trying out various simulators and meeting with company representatives to discuss services provided and purchase options.

Objective structured clinical examinations can be used to assess a student's ability to correctly use the ultrasound equipment, capture a pre-determined series of images, and identify structures in the images. A standardized evaluation form and OSCE station can be used like that in Fig. 12.5. Oral or written questions on physiological principles can be included in the examination as well. Students can also be evaluated on their professional interaction with the standardized patient. During the OSCE, students are expected to introduce themselves to the patient, explain what will be performed, be attentive to the comfort and modesty of the patient, and thank the patient for his/her participation.

12.5.2 Estimated Student Time for Ultrasound When Initiating a Program

An estimate of student time associated with the introduction of three ultrasound related topics into a physiology course would be approximately 2.75 h of contact time and 2.0 h of independent study time. This estimate is based on three 50-minute ultrasound labs and one 15-min OSCE for scheduled contact time. Two hours of independent study would be required for online learning material, reviewing scan videos prior to lab, and reviewing image feedback for the three topics. Viewing the scan video before lab minimizes the time needed to explain the laboratory exercise in detail at the start of the lab and thus provides more time for actual hands-on scanning, much like a "flipped classroom" approach.

M1 ULTRASOUND OSCE CHECKLIST (Fall Semester)

Student Name _____ Date _____
Student ID Number _____ Start time _____
Observer _____ End Time _____

Point of care ultrasound view	Adequate image obtained?		Structure Identified?	
	YES	NO	YES	NO
1. Right Upper Quadrant view showing Morisons pouch and right CP angle				
a. Right kidney-longitudinal view				
b. Liver - right lobe				
c. Right hemidiaphragm				
d. Morison's pouch/hepatorenal fossa				
e. Right costophrenic angle				
2. Longitudinal view of left lobe of Liver (mid IVC plane)				
a. Liver- left lobe				
b. Ligamentum venosum				
c. Caudate lobe				
d. IVC				
3. Urinary Bladder - Mid transverse view				
a. Urinary bladder-mid transverse view				
4. Echocardiography-Parasternal Long axis (PLAX) view				
a. Left atrium				
b. Left ventricle				
c. Anterior mitral valve leaflet				
d. Interventricular septum (IVS)				
e. Right ventricular outflow tract/RV				
f. Aortic valve				
g. Pericardium				
5. Neck Ultrasound (Thyroid - Right lobe - mid transverse view with landmark structures)				
a. Right lobe of Thyroid- mid trans view				
b. Right common carotid artery				
c. Tracheal cartilage				
6. Knee Ultrasound (mid longitudinal-suprapatellar) - view should be without anisotropy				
a. Patella				
b. Quadriceps tendon				

7. Miscellaneous Observations	YES	NO
a. Did student introduce herself/himself to the patient?		
b. Did student drape or offer to drape the patient?		
c. Able to select and change probes for each exam ?		
d. Was probe orientation marker pointing in correct direction?		
e. Was proper preset selected for each view?		
f. Was focus position acceptable?		

Fig. 12.5 Left panel: a standard grading sheet for an ultrasound objective structured clinical exam (OSCE). Right panel: A faculty member evaluating a student during an OSCE

Thus, a total of 4.75 h would be associated with the introduction of three ultrasound related topics in this example. Preferably, some of these laboratory sessions would simply replace previous physiology labs of the same or similar topics taught without ultrasound. Thus, the net student time added to the course would actually be less than 4.75 h.

Open laboratory sessions would be optional but most students would likely spend a total of 1–2 h in the lab scanning at various times during the course. The open laboratory sessions can also include time using an ultrasound simulator if one is available.

12.6 Student Feedback

Feedback from students is important in developing the ultrasound component of a course. Students provide valuable input for improvement of the course and also take greater ownership in the course and their learning when actively engaged in program development and evaluation.

The literature shows that the vast majority of students are very happy with ultrasound offered in a course and often request additional ultrasound be added to the course. Feedback should be captured regularly as it can play an important role in

determining when and how much to change or expand the ultrasound component of the course over time. Student feedback also provides important information that can be provided to institution education oversight committees such as the curriculum committee. Below is a sample list of questions for an end-of-course student evaluation for ultrasound in a physiology course. A Likert scale from one to five (strongly disagree to strongly agree) can be used and the evaluation can end with a request for comments on how to improve the course.

1. The use of ultrasound in physiology has enhanced my ability to learn basic physiology concepts.
2. The use of ultrasound has allowed for increased clinical correlation with basic science instruction.
3. I found the online learning modules helpful in learning ultrasonography.
4. I found the online scanning videos helpful in learning ultrasonography.
5. I found scheduled hands-on laboratory sessions helpful in learning ultrasonography.
6. I found open laboratory sessions helpful in learning ultrasonography.
7. I found the ultrasound simulation exercises helpful in learning ultrasonography.
8. I found the overall educational experience in ultrasound enhanced my medical education.
9. I would like to see more ultrasound in the curriculum.
10. Please comment on the ultrasound curriculum, especially your thoughts on how the course can be improved. (open comments section)

12.7 Space and Equipment for Ultrasound Laboratory Sessions

Now with small portable ultrasound systems including handheld devices with good functionality and image mirroring/casting capability, most ultrasound physiology laboratory sessions can be conducted in traditional laboratory space or open multifunctional rooms. An ultrasound scanning room that would work well for laboratory exercises would include multiple ultrasound scanning stations with a portable ultrasound device, a stretcher or exam table for the model, and a large viewing screen. See Fig. 12.6.

If a stretcher or exam table is not available, a sturdy table with an egg-crate mattress, sheet, and pillow can be used. In addition, some laboratory exercises can be modified to scan the model in the sitting position if necessary.

Capability to save images to a USB drive or preferably to save directly to a cloud-based archive system for assessment and feedback is a good feature to have in the laboratory space, especially wireless capability. Other materials needed for scanning stations include ultrasound gel, paper towels, probe disinfectant, trash cans, and power outlets. More specialized space arrangements such as observation rooms and

Fig. 12.6 Basic elements of a laboratory scanning station: stretcher, portable ultrasound device, and a large viewing screen

ultrasound simulation rooms can be explored with a simulation or clinical skills center if one exists on campus.

12.8 Residency Ultrasound Training

Ultrasound training is becoming more important in the Graduate Medical Education (GME) setting in Primary Care specialties. The American Academy of Family Physicians published a curriculum guideline for point-of-care ultrasound in residency training in 2017. A survey of Family Medicine residency directors in 2020 found that nearly 90% of programs had, or were developing, point-of-care ultrasound curricula.

Curricula in GME generally focus more on application of ultrasound in evaluating and treating patients. However, medical school ultrasound education is still variable and medical school graduates will arrive at their residency programs with varying degrees of basic knowledge of physiology as it relates to ultrasound. For this reason, it will be important for residency directors to consider having components of their residency curriculum dedicated to various aspects of ultrasound and physiology. This approach is also consistent with the goal for medical education to be developed as a continuum throughout health professions training. Having residents uniformly trained in ultrasound also strengthens the medical student ultrasound

educational experience as students spend a good deal of time on their clinical clerkships working directly with residents.

12.9 Ultrasound Fellowship

Ultrasound fellowship training after residency, first pioneered by emergency medicine in the late 1990s and early 2000s to provide post-graduate training in clinical ultrasound skills, education, and research, has since expanded to the primary care specialties. The first of these was the Primary Care Ultrasound Fellowship at the University of South Carolina School of Medicine. Fellows provide a valuable source of teaching for students and other learners and can assist with developing and implementing innovative curricula. As fellows investigate the pathophysiology and ultrasonographic manifestations of various disease states during training, they are contributing to the advancement of our understanding of medicine through ultrasound while making significant contributions to individual ultrasound programs. Fellows often remain on faculty after completion of their fellowships. Thus, initiation of an ultrasound fellowship can be considered a good long-term investment in the individual and the institution's ultrasound program.

12.10 Potential Sources of Funding for Ultrasound

Financial support for an ultrasound component to a course or curriculum is necessary to get an ultrasound program started and help ensure a high-quality experience for the learners and sustainability of the program over time. Ultrasound offers multiple potential funding sources to accomplish these goals and will be discussed in this section.

Below is a list of potential funding sources that will be considered.

1. Institutional support
2. Industry partnerships and grants
3. Development efforts and donors
4. Educational grants
5. Training revenue streams
6. Patents and licenses
7. Student technical fees

12.10.1 Institutional Support

Institutional support for introducing ultrasound into a physiology course can be sought from the appropriate department and/or from the office of medical education and curricular affairs in accordance with institutional processes for budget requests. Budgetary decisions are usually made on the basis of the value-added of the request to the size of the request and the mission of the institution. Therefore, when requesting financial resources, it is essential to prepare information on the value-added of ultrasound and the estimated cost of the request as well as the role ultrasound can play in fulfilling the institution's mission.

Some of the value-added aspects from a student education perspective would include data supporting enhanced learning of physiology content, documented high degree of student satisfaction using ultrasound, enhanced curricula integration with ultrasound, compliance with and enhancement of accreditation standards, and preparation of students for additional educational opportunities and career options.

Ultrasound also offers opportunities for research, grants, publications, intellectual property, and fund raising as will be discussed. Thus, when one considers the value-added or the return on the investment, ultrasound can be considered not only a good educational investment for students and faculty but also a good financial investment. Many of these same value-added aspects are consistent with the mission of most academic institutions to provide high quality education, advance research, and prepare students for future careers.

12.10.2 Industry Partnerships and Grants

Ultrasound manufacturers have been supportive of efforts to promote ultrasound as both educational and clinical practice tools. If your institution allows research partnerships with industry, it would be worth exploring special reductions or even equipment donations as part of an agreement to perform educational research with their product. The research agreement should be approved by your institution and should give full control over the research design and decisions on publishing outcomes to the institution. Unrestricted education grants from industry are uncommon today but are worth discussing with companies, especially if there are companies in your region of the country that have manufacturing ties to your community.

12.10.3 Donations

Ultrasound is very attractive to donors primarily because it is visual and donors can more easily appreciate its value. In education, ultrasound is also new and different and donors like that. At many institutions, donor solicitation must go through the

office of development so you should check your institution's policy prior to initiating fund raising efforts. The office of development can help you identify potential donors in the community, donors among your alumni, and other potential sources of donors.

An ultrasound demonstration is a great way to inform the development office and potential donors of the power of ultrasound for education and clinical practice. A color Doppler scan of the carotid artery is a great ultrasound application to demonstrate. When possible, have one of your students participate in the demonstration and also share their experiences with the development office and donor. If you can identify a student to participate from the donor's hometown that immediately helps connect the donor to the institution's efforts.

You should develop an engaging presentation and a short "elevator talk" to pitch your ideas to potential donors about advancing the education programs and raising the profile of the institution with ultrasound. A number of institutions have used "crowdfunding" to raise funds for small ultrasound projects. This form of fund raising is generally handled by your development office as well.

12.10.4 Grants

Ultrasound is a rapidly growing area of interest in education and clinical practice and funding for ultrasound projects is increasing. Educational grants are being funded for teaching at all levels, including STEM grants to help young students learn the life sciences, learn more about their bodies and health, and stimulate interest in life science careers. There is also interest in using ultrasound as teaching tools for the public so they can better understand their diseases and address the health literacy issues we face today. Ultrasound is an excellent tool to teach patients about such conditions as hypertension and heart failure and why it is so important to control their blood pressure. There are numerous other examples of the ultrasound picture being "worth a thousand words".

Traditional national science funding agencies as well as private foundations that have a history of funding innovative educational projects can be pursued for grant support. In addition, local and regional organizations that support community efforts in education are good sources of funding. Your development office will be aware of these.

12.10.5 Training Revenue Streams

Ultrasound training for groups outside of your own institution can produce revenue streams to support ultrasound efforts through online learning material and workshops. For medical institutions, continuing medical education courses on ultrasound have increased in demand and conducting courses and workshops can develop into a

steady revenue stream for the program while also providing an important service to the community.

12.10.6 Patents and Licenses

Because of the broad interest in ultrasound for education and clinical practice, there are many opportunities for inventions and patent licenses. There exists a robust ultrasound market that is fueling research and development, which creates many opportunities for inventors. A good source of information about inventions and the patent process would be your institution's intellectual property office or office of innovation.

12.10.7 Student Fees

Some schools are considering small student fees to help fund ultrasound education components of their curricula. Student fees are not particularly popular in these times of high tuition but are worth considering due to the value-added of ultrasound as previously presented. In addition, a small student fee across hundreds of students can result in sufficient funds to initiate a limited ultrasound program while providing time to develop other financial sources to grow and sustain the program. Technical fees are not uncommon in higher education, especially those related to technology and technology support services. However, an additional note of caution is probably warranted as student fees are such a sensitive topic in academia and any plans to institute such fees should be thoroughly vetted with department and institution leadership.

12.11 A Scaled-Back Model to Introduce Ultrasound into Physiology Courses with Limited Resources

For faculty who have very limited resources but desire to introduce ultrasound into their physiology courses, several options exist. The simplest is to introduce ultrasound images and video loops into didactic lectures, course online learning material, or as a supplement to laboratory material already being used. Images and loops can come from colleagues, open access websites, and this textbook with permission.

To better capture the educational value and dynamic nature of ultrasound, live demonstrations in the classroom can be performed by a clinician or sonographer while the course instructor points out important physiological aspects of the ultrasound scan. This approach is also a good way to engage students in an interactive

discussion based on the ultrasound images being viewed in real-time. Clinical faculty can often make arrangements to bring a portable ultrasound system to class and students are usually quite happy to volunteer as models.

To get the full experience of ultrasound, hands-on scanning can be included in a classroom or laboratory setting using a small number of handheld ultrasound devices (5–10) with mirroring or casting capability to a large screen at the front of the classroom or lab. Students sitting in small clusters can take turns scanning each other. A short video and/or live demonstration of the scan to be performed can be shown at the start of class. Prior to physiology class, a small group of students who are particularly interested in ultrasound can be scheduled for a scanning session that covers specific instructions on the designated scanning exercises for class. These students can then be divided among the student clusters during the large classroom scanning session and serve as peer-peer instructors.

Each small cluster of students can be charged with capturing their best video loop and then mirror it to the large screen for discussion and evaluation by the other clusters. The cluster with the best image can be recognized for their scanning "expertise". A handout with scanning instructions and questions related to the physiology content can be made available to all students online prior to the class. Ultrasound physiology questions can be discussed at the end of class or assigned for the next classroom session.

This hands-on activity can be conducted with relatively little financial investment and could possibly be supported by clinical departments making handheld devices available for the teaching sessions. Two scanning exercises that work particularly well for this approach are scanning the carotid artery and internal jugular vein in the neck (male or female student models) and scanning the parasternal long axis view of the heart (male models). Both views are relatively easy to capture and are great for discussing the physiology of the cardiovascular system.

Introducing ultrasound into a physiology course and looking inside the body to see human physiology at work can be a great learning experience for students and faculty alike. Below is a summary checklist of things to consider prior to introducing ultrasound into a course.

12.12 Ultrasound Initiation Checklist

1. Ultrasound systems—enough for an adequate hands-on experience for all learners.
2. Scanning laboratory needs—stretchers, exam tables, or tables with egg-crate mattresses, pillows, sheets, pillowcases, extension cords, tables for laptop ultrasound systems, ultrasound gel, paper towels, probe disinfectant, and trash cans.
3. Standardized patients with varying degrees of levels of scanning difficulty.
4. On-line learning material: learning modules, "how to" scanning videos, and laboratory handouts.
5. Student assessment—multiple choice questions, image reviews, and OSCEs

6. Instructors—faculty, sonographers, student-peers, residents.
7. Instructor training—in-house, support for attendance at workshops, check out ultrasound devices.
8. Large viewing screen for each ultrasound station with mirroring capability from ultrasound devices.
9. Student policy regarding scanning each other and all findings treated confidentially.
10. Student online feedback opportunities.
11. Additional equipment and resources for a more comprehensive program: ultrasound simulators and a cloud-based image review portal.

Further Reading and Resources

Journal Articles

Barron KR, Wagner MS, Hunt PS et al (2019) A primary care ultrasound fellowship: training for clinical practice and future educators. J Ultrasound Med 38(4):1061–1068

Bell F, Wilson B, Hoppmann R (2015) Using ultrasound to teach medical students cardiac physiology. Adv Physiol Educ 39:392–396

Bornemann P (2017) Assessment of a novel point-of-care ultrasound curriculum's effect on competency measures in family medicine graduate medical education. J Ultrasound Med 36(6):1205–1211

Hall JW, Holman H, Barreto TW, Bornemann P et al (2020) Point-of-care ultrasound in family medicine residencies 5-year update: a CERA study. Family Med 52(7):505–511

Hoppmann R, Rao V, Bell F et al (2015) The evolution of an integrated ultrasound curriculum (iUSC) for medical students: 9-year experience. Crit Ultrasound J 7(1):18–33

Online Resources

American Academy of Family Physicians Guidelines for Point-of-Care Ultrasound. https://www.aafp.org/dam/AAFP/documents/medical_education_residency/program_directors/Reprint290D_POCUS.pdf

American Institute of Ultrasound in Medicine. https://www.aium.org/

Society of Ultrasound in Medical Education. https://www.susme.org/

World Interactive Network Focused on Critical Ultrasound. https://www.winfocus.org/